Qin Fang *Editor*

Aquareovirus

Aquareovirus

Qin Fang

Editor

Aquareovirus

Editor
Qin Fang
State Key Laboratory of Virology
Wuhan Institute of Virology
Chinese Academy of Sciences
Wuhan, Hubei, China

Preface

Aquareoviruses cause infection in bony fish and shellfish and are a significant threat to aquaculture industries worldwide. Golden shiner virus, the first aquatic reovirus, was isolated from the golden shiner by John Plumb et al. in 1979. Since then, a massive number of reovirus-like agents have been identified in fish and shellfish. Moreover, for approximately 40 years, aquareoviruses have been isolated from a wide variety of aquatic animals of freshwater and saline water origins.

Aquareovirus, a member of the family *Reoviridae*, is a nonenveloped viral particle with multiple shelled layers surrounding a genome comprising 11 segments of double-stranded RNA. Aquareoviruses replicate efficiently at extensive temperature ranges in cell cultures of poikilotherm origin, including marine and freshwater piscine cell cultures, as opposed to other reoviruses that replicate in homoiothermous mammalian hosts. Seven *Aquareovirus* species (*Aquareovirus A–G*) and several other tentative species have been recognized by the International Committee on Taxonomy of Viruses. Furthermore, aquareoviruses are closely related to each other and consistently share nine homologous proteins with members of the genus *Orthoreovirus* having ten segments of double-stranded RNA. In addition, substantial progress in aquareovirus genome characterization coupled with single-particle cryo-electron microscopy and three-dimensional image reconstruction confirmed that aquareoviruses not only share the highest amino acid sequence identity with mammalian orthoreoviruses (MRVs) but also highly resemble MRVs in particle structure and conserved functional protein conformation and domains, thereby suggesting a common evolutionary origin between aquareoviruses and orthoreoviruses. Despite striking parallelisms in the molecular interactions necessary for essential functions, such as reovirus entry, transcription and replication, and assembly and release, they display a remarkable diversity in the evolution and virulence of surface proteins with respect to the host species.

Striped bass reovirus (SBRV), a member of the *Aquareovirus-A* species, has been well studied at the molecular level. Most aquareovirus isolates are nonpathogenic or show low virulence in their host species. However, grass carp reovirus (GCRV or GCRV-I, an approved member of the species *Aquareovirus-C*), causing severe

hemorrhagic disease in fingerling and yearling populations, is an exception and appears to be the most pathogenic aquareovirus. Thus far, three types of GCRVs (GCRV-I, -II, and -III) have been genetically identified from infected grass carp in China. GCRV-II is currently an epidemic strain harboring a gene encoding MRV-σ1 cognate cell attachment protein on the particle surface instead of a fusion-associated small transmembrane protein, as observed for most aquareoviruses. Furthermore, GCRV-I has been a major focus for the molecular understanding of aquareoviruses. Molecular characterizations indicate that the 11 genomic segments of GCRV encode at least 12 proteins. Moreover, an intact virion is composed of seven structural proteins: five inner shell proteins (VP1–VP4, VP6) and two outer capsid proteins (VP5 and VP7). Notably, these seven structural proteins and their localization in the particle have been resolved via cryo-electron microscopy and three-dimensional image reconstruction. The inner core proteins include all the endogenous enzymes responsible for viral transcription and replication, while the outer capsid proteins are critical for cellular entry. In addition, great efforts have been made to enhance our knowledge of the molecular background of the nonstructural proteins involved in GCRV infection. Collectively, most of our understanding of the molecular biology and processes involved in virus replication and pathogenesis of the members of the genus *Aquareovirus* has been generated from the SBRV and GCRV studies. As such, clinical diagnostic tools and prevention and control strategies based on the genome sequence and particle structure have become available.

Therefore, this book reviews our current understanding of the basic and molecular biology, protein structure and function, infection and replication, epidemiology and diagnosis, immunological prevention and control, medical treatment of aquareoviruses, and the immune response to aquareovirus infection. Nine chapters are contained in this book. The first chapter (by Q. Fang et al.) provides an overview of aquareoviruses. The following two chapters (by Q. Fang et al.) cover general and molecular characteristics, particle structure and protein function of aquareovirus. The fourth chapter by L. Lu focuses on the current understanding of GCRV infection and replication. And then, subsequent two chapters (Chapter 5 by Y. Fan et al. and Chapter 6 by W. Zeng et al.) mainly deal with the epidemiology of GCRV and the progress in research on diagnostic strategies for detecting aquareoviruses. In addition, the Chapter 7 (by Q. Wang et al.,) and Chapter 8 (by H. Wang) summarize current strategies on prevention and control of grass carp hemorrhagic disease by vaccination and medical treatment. The last chapter (Chapter 9 by J. Su) discusses host immunity against the aquareovirus infection, including the innate and adaptive immunities. Although major progress has been made in our understanding of aquareoviruses, many aspects remain unresolved, such as the underlying mechanism of the interaction between virus infection and host immune defense and the improvements necessary for establishing effective and stable immune prevention strategies. This book, thus, encompasses the basic knowledge and recent progress in research on aquareoviruses, especially GCRV, and discusses some key problems that need to be addressed in future studies.

I am grateful to each of the contributors for writing their various chapters with great effort and enthusiasm and their excellent contributions, especially during the

difficult times of the SARS-CoV-2 pandemic. Despite being preoccupied with their respective research work, they have supported me immensely. In addition, this work was supported by grants from the National Foundation of Natural Science of China (31972838, 31672690, 32030112, 31372561, 31772894) and grants from National Key R&D Program of China (2019YFD0900101, 2019YFD0900103, 2019YFD0900104). Without their support, this book would not have been published. Furthermore, I would like to take this opportunity to thank the State Key Laboratory of Virology for providing regular annual operating funds. Finally, I sincerely hope that this book will help curious graduate students or interested researchers to attain an overall picture of aquareovirus infection and pathogenesis and yield benefits in fisheries concerning better prevention and control of diseases caused by aquareoviruses infection.

Wuhan, China   Qin Fang
December, 2020

Contents

Contributors

Qin Fang State Key Laboratory of Virology, Wuhan Institute of Virology, Chinese Academy of Sciences, Wuhan, China

Yuding Fan Yangtze River Fisheries Research Institute, Chinese Academy of Fishery Sciences, Wuhan, China

Yingying Li Pearl River Fisheries Research Institute, Chinese Academy of Fishery Sciences, Guangzhou, China

Liqun Lu National Pathogen Collection Center for Aquatic Animals, Shanghai Ocean University, Shanghai, China

Jie Ma Department of Fish and Wildlife Sciences, University of Idaho, Moscow, ID, USA

Jianguo Su Department of Aquatic Animal Medicine, College of Fisheries, Huazhong Agricultural University, Wuhan, China
Laboratory for Marine Biology and Biotechnology, Pilot National Laboratory for Marine Science and Technology, Qingdao, China

Hao Wang National Pathogen Collection Center for Aquatic Animals, Shanghai Ocean University, Shanghai, China

Qing Wang Pearl River Fisheries Research Institute, Chinese Academy of Fishery Sciences, Guangzhou, China

Yahui Wang Pearl River Fisheries Research Institute, Chinese Academy of Fishery Sciences, Guangzhou, China

Yingying Wang Pearl River Fisheries Research Institute, Chinese Academy of Fishery Sciences, Guangzhou, China

Jiyuan Yin Pearl River Fisheries Research Institute, Chinese Academy of Fishery Sciences, Guangzhou, China

Weiwei Zeng Guangdong Provincial Key Laboratory of Animal Molecular Design and Precise Breeding, School of Life Science and Engineering, Foshan University, Foshan, China

Pearl River Fisheries Research Institute, Chinese Academy of Fishery Sciences, Guangzhou, China

Fuxian Zhang College of Animal Science, Yangtze University, Jingzhou, Hubei, China

Jie Zhang State Key Laboratory of Freshwater Ecology and Biotechnology, Institute of Hydrobiology, Chinese Academy of Sciences, Wuhan, China

Ke Zhang Yangtze River Fisheries Research Institute, Chinese Academy of Fishery Sciences, Wuhan, China

National Demonstration Center for Experimental Fisheries Science Education, Shanghai Ocean University, Shanghai, China

Chapter 1
Aquareovirus: An Overview

Qin Fang, Jie Zhang, and Fuxian Zhang

Abstract Viruses in the family *Reoviridae* can infect a wide range of hosts, including humans, vertebrates, invertebrates, fungi, bacteria, and plants. They form a diverse group, harboring particular 9–12 segmented double-stranded RNA genomes contained within icosahedral, nonenveloped, multilayered protein capsids. Aquareovirus, a recently classified member of the *Reoviridae* family, has been isolated from aquatic animals of freshwater and saline water origins worldwide. Generally, aquareoviruses exert low pathogenicity in their natural hosts. However, some isolates are highly virulent in cultured fish species. Aquareovirus particles physically resemble orthoreoviruses, and the enclosed 11-segmented genome is similar to that of rotaviruses; however, no antigenic relationship has been detected. An increasing number of genome sequence- and particle structure-based evolutionary analyses suggest that the genus *Aquareovirus* shares a sister-like relationship with members of the genus *Orthoreovirus*. This new molecular evidence indicates that the peculiar endogenous transcription and cell penetration-related characteristics are attributed to uniformly conserved protein and functional domains encoded by the genome segments 1–6 (S1–S6) of aquareoviruses. In contrast, proteins encoded by smaller class gene segments (S7–S11) that are involved in cell-receptor attachment and replication-related events are largely divergent. Therefore, our current understanding of aquareovirus infection and pathogenesis provides significant insights into the fundamental mechanisms involved in the molecular evolution of the 11 genomic segments and, in general, functions of the encoded proteins, thereby leading to the development of better prevention and control strategies for diseases caused by aquareovirus infection.

Q. Fang (✉)
State Key Laboratory of Virology, Wuhan Institute of Virology, Chinese Academy of Sciences, Wuhan, China
e-mail: qfang@wh.iov.cn

J. Zhang
State Key Laboratory of Freshwater Ecology and Biotechnology, Institute of Hydrobiology, Chinese Academy of Sciences, Wuhan, China

F. Zhang
College of Animal Science, Yangtze University, Jingzhou, Hubei, China

Abbreviations

AGCRV	American grass carp reovirus
AHRV	Atlantic halibut reovirus
AqRV	Aquareovirus
ARV	Avian reovirus
BF-2	Bluegill fry
BRV	Baboon orthoreovirus
CCRV	Channel catfish reovirus
CHSE	Chinook salmon embryo
CIK	*Ctenopharyngodon idella* kidney
CoSRV	Coho salmon reovirus
CPE	Cytopathic effect
Cryo-EM	Cryo-electron microscopy
CSRV	Chum salmon reovirus
EPC	Epithelioma papillosum cyprinid
FAST	Fusion-associated small transmembrane
FCRV	Fall chinook reovirus
FHM	Fathead minnow
GCF	Grass carp fin
GCHD	Grass carp hemorrhage disease
GCHV	Grass carp hemorrhage virus
GCRV	Grass carp reovirus
GSRV	Golden shiner reovirus
Mr	Relative molecular mass
MRV	Mammalian orthoreoviruses
MsReV	*Micropterus salmoides* reovirus
PRV	Piscine orthoreovirus
RdRP	RNA-dependent RNA polymerase
SBRV	Striped bass reovirus
SMReV	Turbot *Scophthalmus maximus* reovirus
TEM	Transmission electron microscopy
TFV	Threadfin reovirus
TRV	Turbot reovirus
TSRV	Tasmanian Atlantic salmon AqRV
VIBs	Virus inclusion bodies

1.1 Introduction

Double-stranded RNA (dsRNA) viruses infect a wide variety of host species, ranging from fungi, plants, and insects to mollusks, fish, reptiles, birds, and mammals (including humans). The family *Reoviridae* is the largest and most diverse group of dsRNA viruses [42]. Currently, 15 recognized genera are included in this giant family, mainly based on their respective host range and genome segment components [4]. In addition, according to the particle configuration, such as the presence or absence of a turret protein structure located on the 12 icosahedral vertices of the virion or core particle, the *Spinareovirinae* (turrets) and *Sedoreovirinae* (non-turrets) subfamilies have been classified within this family. The *Spinareovirinae* subfamily includes nine members, and the remaining members of the family belong to the *Sedoreovirinae* subfamily [4].

Reovirus is the first dsRNA virus described. The mammalian orthoreoviruses (MRVs) are the prototype species in the *Reoviridae* family, including serotype 1 (strain Lang, T1L), serotype 2 (strain Jones, T2J), and serotype 3 (strain Dearing, T3D), which were initially described and recognized based on the virus neutralization and hemagglutination inhibition profiles [58]. MRVs are a well-studied prototype of reoviruses; therefore, they are also called reoviruses in a general sense. Reovirus infection in humans usually involves the respiratory and intestinal tracts, with no clinical symptoms or minimal associated disease. In contrast, the well-characterized non-turreted rotaviruses and bluetongue viruses are highly pathogenic to their host species. Rotaviruses are important pathogens responsible for gastroenteritis in juvenile animals and humans. Bluetongue virus is a major threat to livestock in cases of transmission by blood-feeding insects and causes hemorrhagic diseases in livestock. Coltivirus, which is another non-turreted virus of the *Sedoreovirinae* group, contains 12 genomic segments, and it is transmitted by arthropod vectors; it causes neurological disease in humans [42]. Notably, baboon reovirus (BRV), one of the five species recognized in the genus *Orthoreovirus* (subfamily *Spinareovirinae*), can cause severe clinical signs of progressive meningoencephalomyelitis as well as provide histopathological evidence for the disease [43]. Moreover, BRV under natural circumstances may potentially emerge as a serious human pathogen [42, 43]. *Aquareovirus* (AqRV), a newly defined genus in the *Reoviridae* family, infects aquatic organisms and seldom causes clinical symptoms [27]. Furthermore, an increasing number of reovirus pathogens have been isolated from various cultured aquatic animal species with serious macroscopic petechial hemorrhagic syndrome, which leads to high mortality, and thus pose a serious threat to the fishery industry [45, 71, 76]. It appears that the pathogenicity of the different reovirus isolates to their host remains largely distinct.

AqRVs constitute species that are isolated from various aquatic animals and are classified mainly based on their water-linked natural host species and 11-segmented dsRNA genome. Since the first isolation of reovirus-like or rotavirus-like agents from aquatic animals in the late 1970s [52, 60], hundreds of AqRV species have subsequently been identified in a wide variety of aquatic animals, including bony

fish, finfish, and crustaceans [45, 49, 65, 76]. Although these viruses are often isolated from apparently healthy individuals during routine examination, they can cause significant clinical symptoms or severe disease and lead to high mortality [1, 45]. Seven species (*AqRV A* to *AqRV G*) and some other unassigned species have been recognized, mainly based on the classical RNA-RNA hybridization analyses. In addition, sequence analysis and antigenic properties are often used to define newly isolated AqRVs [4]. Among the identified AqRVs, most have been isolated from fish and shellfish with 11 dsRNA genomic segments. Some reovirus species harboring 10, 12, or more genome segments have also been identified from infected aquatic animal hosts in recent years. Piscine orthoreoviruses (PRVs, including PRV-1, PRV-2, and PRV-3), which are prevalent in farmed Atlantic salmon and considered important for the emergence of heart and skeletal muscle inflammation, have been classified into the genus *Orthoreovirus* because of their 10 genomic segments and predicted encoded protein characteristics [41, 42]. Some other reovirus species isolated from diseased crabs with 12 genomic segments have been grouped into the genera *Cardoreovirus* [42]. This book mainly reviews AqRV species isolated from fish and shellfish species with 11-segmented dsRNA genomes.

AqRVs belong to the *Spinareovirinae* subfamily in the family Reoviridae based on their particle structure. A great number of genome sequence analyses reveal a close evolutionary relationship between AqRVs and orthoreoviruses, which represent two different genera in the *Reoviridae* family [3, 42, 57, 58]. Furthermore, the progress achieved by cryo-electron microscopy (cryo-EM) and three-dimensional image reconstruction of single AqRV particles discloses more detailed particle structure information on protein folding and overall similarities in structural proteins between AqRV and MRV [12, 13, 25, 56, 75, 83, 94]. Although our current knowledge is insufficient to understand the pathogenesis of AqRV in host cells thoroughly, it is important to look back upon the progress in research on the general and molecular characteristics of AqRV over the past three decades. Therefore, it will be beneficial to propose effective strategies to better prevent and control AqRV-related diseases in the future. This chapter mainly provides an overview of AqRVs, and the following chapters of the book are devoted to describing the detailed characteristics and functions, general and molecular biology, particle-based structural biology, replication, epidemiology and diagnosis, and medical and immunological prevention and control of AqRV; additionally, it reviews the research progress on the host immune response to AqRV infection.

1.2   Origin of AqRV

The first AqRV was found in North America in the late 1970s [60]. One reo-like virus was isolated in 1977 from the moribund golden shiner (*Notemigonus crysoleucas*) with macroscopic petechial hemorrhagic symptoms; however, the mortality of the diseased golden shiners is relatively low. The virus isolated from

the golden shiner is named the golden shiner reovirus (GSV or GSRV). Nearly around the same time, another virus named 13p2 was isolated in 1977 from juvenile American oysters (*Crassostrea virginica*) reared in Long Island, USA, hatcheries [52, 53]. During the 1980s, some other aquatic reoviruses, such as chum salmon *(Oncorhynchus keta)* reovirus (CSR or CSRV) and channel catfish reovirus (CRV or CCRV), were isolated from young diseased aquatic animals, and apparently healthy adults were examined by routine examination [2, 45, 84]. The morphological and biochemical properties of the four members of a novel group of reovirus isolates from aquatic animals were reported by Winton in 1987 [85]. In addition, a serious grass carp (*Ctenopharyngodon idella*) hemorrhage disease (GCHD) occurred frequently in many freshwater fishery farms in southern China. The epidemic outbreak of GCHD led to a high mortality of up to 85% of fingerlings from an aquaculture-farmed grass carp, causing great economic loss. Based on the typical hemorrhagic syndrome observed in the fish viscera and other tissues, the causative agent that leads to the hemorrhage disease and the significantly high mortality were believed to be of viral origin; however, the pathogen that causes GCHD was not identified as a new member of the family *Reoviridae* until 1983 [10, 30, 70]. Moreover, another rotavirus-like agent, striped bass reovirus (SBRV), which is isolated from diseased fish collected from the Chesapeake Bay, Maryland, USA, has been reported [45, 68]. Thereafter, an increasing number of important viral pathogens have been isolated and identified globally from poikilothermic vertebrates and invertebrates, including fish and shellfish obtained from both freshwater and seawater [4, 45, 49, 55]. Among the reoviruses identified in aquatic animals, most AqRVs are isolated from fish and shellfish and contain 11 dsRNA genomic segments [4]. Based on previously established reovirus identification criteria, the viruses isolated from aquatic animals have the following three basic common characteristics. (1) All virus particles are of icosahedral symmetry and nonenveloped, are approximately 75 nm in diameter, and have double- or multiple-layered protein capsids (outer protein shell and inner capsids or core). (2) The purified particles are ether- and heat-resistant, stable at pH 3, 7, and 10, and remain infectious after RNase or DNase treatment. (3) Acridine orange staining demonstrates a typical greenish-yellow fluorescence in reovirus-like cytoplasmic inclusion bodies and viral replication in the presence of 5-iododeoxyuridine (5-IUdR), suggesting that the virus has a dsRNA genome and is not inhibited by 5-IUdR [42]. Although the majority of AqRVs have been isolated during routine examination of asymptomatic fish and shellfish, some have also been isolated from fish co-infected with bacteria or fish populations undergoing chronic or high mortality [44, 45].

1.3 Characteristic Features of AqRV

As a member of the *Reoviridae* family, AqRV is nonenveloped with two concentric protein shells encapsulating the central dense segmented dsRNA genome. In general, nearly all of the AqRV genomes isolated from fish and shellfish consist of
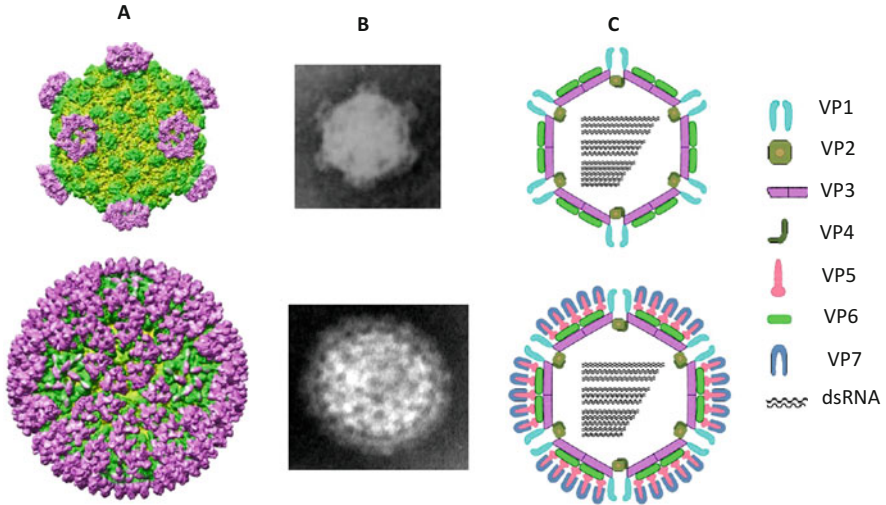
Fig. 1.1 Image of intact virion and core particle of aquareovirus. Cryo-electron microscopy and three-dimensional reconstruction image (**a**), negatively stained TEM image (**b**), and diagram of single aquareovirus core and intact particle (**c**). The nomenclature of proteins is representative of the fusogenic aquareoviruses. The three-dimensional reconstruction image of aquareovirus core and virion in A is modified from reference [12]

11 discrete dsRNA segments. The virus particles are approximately 75 nm in diameter, present an icosahedral symmetry, and have the outer and inner (also termed as the core shell) protein layers with $T = 13$ and $T = 1$ symmetries, respectively (Fig. 1.1).

An intact AqRV virion has a relative molecular mass (Mr) of approximately 120×10^6, a buoyant density in CsCl of approximately 1.37 g/cm³, and a sedimentation coefficient of about 550S [4, 42, 45]. Due to the absence of a lipid envelope, the virions are ether and chloroform resistant. The virions exhibit wide ranges of endurance under acidic and basic conditions (resistant to pH 3–pH 11). Moreover, they are relatively stable under heat; however, the infection stability depends on the isolated species. The infectivity of most of the AqRV particles can be rapidly eliminated by heating at 56 °C for 30 min. However, some AqRV particles remain infectious after incubation at 45 °C for several days or stable at 56 °C for 3 h [71]. In addition, exposure to UV irradiation reduces infectivity [45].

In contrast to orthoreoviruses or other reoviruses, AqRVs have a broad cultivation temperature range and can generally replicate well at temperatures ranging from 15 to 28 °C depending on the host species. Generally, temperatures of 15–25 °C are suitable for cold-water fish and 25–30 °C for warm-water fish. Interestingly, AqRVs can also establish stable replication at 4 °C or below 4 °C, such as at 2.5 °C [67, 94]. Indeed, under proper growth conditions, no significant reduction in infectivity has been found in AqRVs proliferating in minimal essential medium (MEM) with 5% fetal bovine serum (FBS) over a period of 28 days [4].

The AqRV genome is composed of 11 dsRNA segments. The Mr. of their genomic segments ranges from 0.2 to 3.0×10^6, and the total Mr. is approximately $12–20 \times 10^6$ (about 23,500–24,500 bp), which constitutes about 15–20% by weight of the virus particle. Based on gel electrophoretic resolution of their genome, the electrophoretic patterns of almost all the isolated AqRVs are very similar to each other, with three large segments (S1–S3), three medium segments (S4–S6), and five small segments (S7–S11). The viral RNA species are mostly monocistronic, with the exception of small segment classes, including S7 or S11 segments that have two or more open reading frames (ORFs) encoding two or more proteins. Generally, the 11 genomic segments encode 12 primary polypeptides, including 7 identified structural (VP1–VP7) and 5 nonstructural (NS80/NS1, NS38/NS2, NS31/NS3, NS26/NS4, and NS16/NS5) proteins [3, 4]. An additional nonstructural protein, NS12, encoded by the grass carp reovirus (GCRV) S7 non-ATG ORF has also been reported [88]. The virion core consists of five structural proteins (VP1–VP4, VP6), including the inner core shell proteins that build the core framework, the highly conserved RNA-dependent RNA polymerase (RdRP) complex, and the RNA capping enzyme complex, which are associated with endogenous RNA transcription and replication. The outer shell is composed of two proteins, VP5 and VP7, which are mainly responsible for cellular entry and particle assembly. The remaining approved nonstructural proteins that are not contained within the viral particle play important roles in viral replication cycles.

Similar to other reoviruses, AqRVs have been confirmed to contain all the multifunctional enzymes responsible for the endogenous RNA synthesis activities in the core. The viral cores are transcriptionally self-sufficient and catalyze each genomic segment RNA strand synthesis using the minus strand as a template against the dsRNA-activated defense mechanisms of the host cell [35, 36, 83]. They can use viral-encoded enzymes for transcription initiation, elongation, 5′-capping, and final release of nascent mRNA into the host cytoplasm for protein synthesis. Structural biology studies indicate a high level of structural similarity between the genera *AqRV* and *Orthoreovirus* in their inner capsid shells. The conserved structures are largely related to the functional and enzymatic domains that are responsible for maintaining the inner core shell stability and endogenous transcriptional activity. Like other reoviruses, the mRNA transcripts of AqRVs are capped but not polyadenylated. The infectious cycle of AqRV is entirely cytoplasmic and occurs in particular structures of neoorganelles, termed as viral factories, viral inclusion bodies (VIBs), or viroplasms. The morphogenesis-related biological and molecular features will be further described in Chap. 2.

In addition, proteolytic cleavages also play an important role in AqRV infection during virus entry into cells. Protease treatment on AqRV in vitro or in vivo converts intact particles into morphologically distinct sub-viral particles, which is consistent with the uncoating mechanism of reovirus from the dormant to a metastable state during infection [6]. These intermediate sub-viral particles of AqRVs are significantly more infectious than intact virions [26, 51, 56], suggesting that the uncoating of outer shell proteins, VP5 and VP7, of AqRVs is indispensable for virus entry into the cell. Most AqRVs are fusogenic and can induce cell–cell fusion by lysis. Some

Table 1.1 General characteristics of aquareovirus

Particle	• ~75 nm icosahedral particles with 5:3:2 symmetry
	• Nonenveloped.
	• Two concentric capsids are composed of 7 proteins:VP1-VP7; inner shell proteins (VP1–VP4, VP6) in $T = 1$ symmetry, outer shell proteins (VP5 and VP7) in $T = 13$ lattice).
	• Turret protein VP1 extends from core surface to outer shell.
	• Penetration protein VP5 can be autocleavaged into VP5N and VP5C.
	• Subviral particle and core can be generated by protease treatment in vitro *and* in vivo.
Genome	• 11 segments of dsRNA (S1–S11)
	• Genome segments generally encode one protein, with exceptions of small class segments (S7 or S11) encoding 2 or 3 proteins.
	• Plus strands of genome segment have 5′ caps modification.
	• Conserved terminal regions at 3′ end with pentanucleotides (-UCAUC) and the extreme 5′ nucleotides conserved depending on species.
	• Nontranslated regions at 5′ end nucleotides are relatively shorter than that at 3′ end.
	• Total size of aquareovirus genome ~24,000 bp.
	• Small class genome segment encodes FAST protein.
Replication	• Fully cytoplasmic replication.
	• Typical inclusion body formation.
	• Broad replication temperatures ranging from 15 to 28 °C.
	• Transcription capping of viral mRNA occurs within particle and is mediated by particle-based endogenous enzymes.
	• Majority of aquareovirus are fusogenic, mature virions are efficiently released from infected cell induced by lysis.

recently isolated reovirus species from grass carp and marine fish have been recognized as non-fusogenic AqRVs. As more and more AqRV strains are discovered and characterized, it is likely that the evolutionary relationship complexity, in terms of genome sequences, will increase between AqRV and orthoreovirus or other reoviruses. The general properties of the fusogenic AqRV are listed in Table 1.1.

1.4 Taxonomy and Classification of the Genus *AqRV*

Early studies on the morphology and biochemical properties of AqRVs show that AqRV particles consist of 11 dsRNA genomic segments enclosed within the inner core, which is encapsulated by an outer shell, and the mature particle diameter is approximately 75 nm, as observed by electron microscopy. They possess physicochemical and physiological properties similar to those of reoviruses and can form plaque-like areas or syncytia as a typical cytopathic effect (CPE) when growing in permissive cell lines of piscine origin. Although AqRVs share common characteristics with the genera *Rotavirus* and *Orthoreovirus,* no antigenic relationships have been detected between them [42, 45, 68].

Based on host differences (AqRVs infect members of many poikilotherms, including marine and freshwater species, whereas orthoreoviruses primarily infect mammals, birds, and reptiles), genomic RNA electrophoretic mobility, RNA–RNA cross-hybridization assays, and serological tests, the reo-like viruses isolated from aquatic animals have been classified into a distinct genus in the family *Reoviridae*. The genus *AqRV* was initially classified in the family *Reoviridae* in 1991 [27]. Although the majority of the AqRVs reported to date have been isolated during routine examination of apparently healthy fish and shellfish with no clinical symptoms, pathogenesis studies indicate that AqRVs can cause subclinical infections, confer a carrier status, and cause significant clinical signs and even severe disease [22, 39, 45, 64]. Six different species (*AqRV A* to *F*) were identified among 42 AqRV isolates, and a subsequent seventh species (*AqRV G*) was defined, which suggests that GCRV probably represents a novel seventh group, as determined using reciprocal RNA-RNA blot hybridization [45, 64]. Later, GCRV was designated as the *AqRV C* (AqRV-C) species based on its complete genome sequence characterization, which is synonymous with that of GSRV [3, 4]. Subsequently, a complete genome sequence analysis of the American grass carp reovirus (AGCRV) showed that the AGCRV genome only shares 22–76% amino acid sequence identity for different viral proteins with GCRV (AqRV-C) and CSRV (AqRV-A). This suggests that AGCRV is a new *AqRV* species: the AqRV-G species, as classified by the International Committee on Taxonomy of Viruses (ICTV) [4, 55]. Thus far, more than hundreds of AqRVs have been isolated and identified, and most of the currently sequenced AqRV species have been isolated from cultured fish and shellfish displaying obvious disease symptoms.

1.5 Geographic and Seasonal Distribution

Mammalian reoviruses are ubiquitous under natural circumstances, and AqRVs are no exception. AqRVs have been found in any type of aquatic environment and aquatic animals. Studies indicate that AqRVs are widely distributed. They have been isolated from hosts in both freshwater and saline water environments worldwide [4, 45]. Indeed, all aquatic animal species living in warm or cold water can serve as hosts for AqRV infection. Unlike MRVs that infect only homoiothermous mammalian hosts, AqRVs possess a more extensive host range, for example, cold and warm aquatic animals, which constitute a wide range of hosts for AqRV replication. The reported representative and pathogenic AqRV distributions and related hosts are listed in Table 1.2. Based on varieties of host ranges and different growing temperatures as well as water environments, studies on the seasonal pattern of AqRV infection are very limited.

Many AqRV isolates are distributed across a wide range of geographical areas. Among the seven established AqRV species, isolates representing the species *AqRV A* and *B* (AqRV-A and -B) are known to infect a wide variety of salmonids, mainly located in the Pacific Northwest and Atlantic regions. Based on the currently

Table 1.2 Geographic distributions of representative and pathogenic AqRVs isolated from Fish and shellfish

Virus isolates	Host species	Geographic distribution	References
13p2 (American oyster)	*Crassostrea virginica*	New York, USA	[45, 52]
AFR or AFRV (Angelfish Reovirus)	*Pomacanthus semicirculatus*	Texas, USA	[45]
AHRV (Atlantic halibut reovirus)	*Hippoglossus hippoglossus*	Norway	[5, 76]
CCRV (Channel catfish)	*Ictaluras punctatus*	California, USA	[2, 45]
CoSRVs (Coho salmon CSR, ELC)	*Oncorhynchus kisutch*	Oregon, USA	[45, 47]
CSV or CSRV (Chum salmon reovirus)	*Oncorhynchus keta*	Hokkaido, Japan	[45, 84]
EFRV (*Etheostoma fonticola* reovirus)	*Etheostoma fonticola*	Texas, USA	[37]
AGCRV (American grass carp reovirus)	*Ctenopharyngodon idella*	California, USA.	[45, 55]
GCRVs (GCRV873,GCRV-HZ08/GD108/104/109 et al.)	*Ctenopharyngodon idella*	Southern China	[21, 39, 59, 79, 86]
GSV or GSRV (Golden shiner reovirus)	*Notemigonus crysoleucas*	Arkansas, USA	[45, 60]
MSRV (Masou salmon reovirus)	*Oncorhynchus masou*	Japan	[45]
MsReV (Micropterus salmoides reovirus)	*Micropterus salmoides*	China	[11]
SBRV (Striped bass reovirus)	*Morone saxatilis*	Maryland, USA	[45, 68]
TRV (Turbot reovirus)	*Scophthalmus maximus*	Galicia, Spain	[44, 45]
SMReV	*Scophthalmus maximus*	China	[38]
SRV (Smelt reovirus)	*Osmerus mordax*	New Brunswick, Canada	[45, 49]
TFV (Threadfin reovirus)	*Eleutheronema tetradactylus*	Singapore	[71]
TSRV (Tasmania strain of Atlantic salmon aquareovirus)	*Salmo salar*	Tasmania, Australia	[8, 45, 89]

available genomic sequence information, many AqRVs isolated from marine species belong to AqRV-A and -B or possibly AqRV-E, such as strains of SBRV [45, 68], CSRV [45, 84], Tasmanian Atlantic salmon AqRV (TSRV) [89], Atlantic halibut reovirus (AHRV) [5, 76], turbot *Scophthalmus maximus* reovirus (SMReV) [38], threadfin reovirus (TFV) [71], turbot reovirus (TRV, the proposed AqRV-E) [4, 44, 45], and fall chinook AqRV (FCRV, AqRV-B) [48]. All these AqRV strains have been isolated from American, European, and Asian countries. SBRV (AqRV-A), the type species of the genus *AqRV*, was isolated from a moribund striped bass (*Morone*

saxatilis) [68]. A new AqRV species (termed as AHRV), isolated from cultured Atlantic halibut (*Hippoglossus hippoglossus*) fry at a facility, can cause massive mortalities during the feeding-initiation phase. In particular, AHRV is the first AqRV strain isolated from a marine cold-water fish species and the second reovirus detected in farmed fish in Norway [5, 76]. A similar disease in halibut fry has also been reported in halibut production facilities in Canada and Scotland [5, 15]. TRV or SMReV has been isolated from Spain and China [38, 44, 45]. TSRV has been isolated from Tasmania, Australia [8, 89]. Some other unassigned AqRVs have been isolated globally, such as from cold- and warm-water areas, including TFV. TFV has been identified due to the massive death of threadfin fingerlings from an aquaculture farm in Singapore in 1998 [71]. Due to the extensive geographic distribution of saline water fish/shellfish, no specific seasonal case has been investigated from these isolations.

Grass carp is a general farmed freshwater fish in China. GCRV causes severe hemorrhage disease symptoms in infected fish mainly in southern China and other regions of Asia [1, 10, 30, 39, 45, 70, 81]. GCRV-873, an earlier isolate from Hunan, China, is classified as an AqRV-C species based on genomic sequence identity [3, 22, 23, 39]. GSRV, the type strain of AqRV-C, was originally isolated from a moribund golden shiner bait fish (*Notemigonus crysoleucas*) in North America at 30 °C [60, 85]. GSRV is a significant pathogen found in farmed grass carp and fathead minnows and detected in wild "creek chub" in the USA [28, 29]. Although GSRV has been isolated in Arkansas, USA, and is associated with minor losses of bait fish [60], the virion genomic segment sequence is nearly identical to that of a Chinese isolate of GCRV-873 (96–99% amino acid sequence identity) [3]. In addition, another AqRV, named AGCRV, has been isolated from several fish species in the USA in the 2004 winters, including healthy golden shiners and diseased grass carp fingerlings. However, complete genomic sequence comparisons with GCRV (AqRV-C) showed low amino acid sequence identity (approximately 22%) for different viral proteins. Accordingly, AGCRV is recognized as a distinct species, the AqRV-G species [55], thereby suggesting that grass carps can be infected by various AqRV species.

Many new AqRVs have been isolated from different regions of China from diseased grass carp in recent years. Genomic sequence information indicates that GCRV-ZH80/-GD108/-104/-109 belongs to a species group different from that of GCRV-873 [21, 59, 79, 86]. Despite the genome diversity of GCRV strains, the GCHD symptoms in young infected fish are almost similar. Epidemic investigations of GCHD indicate that an increased incidence or prevalence in fingerlings mainly occurs in the summer and early autumn (from June to September), which is associated with a relatively high temperature, i.e., above 25 or 30 °C. In addition, larger temperature shifts (19–33 °C) during the day and night are a major cause of GCHD [18, 80]. Further, studies of the GCRV prevalence in young carps have indicated no typical geographic distribution of GCRV in China; however, higher temperatures in summer and autumn have been found to be the key factors for the risk of epidemic disease in cultured grass carp populations.

A sequence analysis of AqRV strains with 11 genomic segments, isolated from a variety of fish or shellfish hosts, did not show any AqRVs that confer host range limits related to the gene segments. Furthermore, studies have shown that sequence divergence among AqRV isolates from different geographical locations may be related to freshwater or saline water environments [11, 38]. In addition, AqRV species have been isolated from not only farmed fish, but also some wild aquatic animals. These findings indicate the potential horizontal transmission of AqRVs from farmed to wild aquatic animals [66, 89]. In particular, the PRV, which has a 10-segmented genome, causes heart and skeletal muscle inflammation in farmed Atlantic salmon (*Salmo salar*), and is mainly found in Norway, has also been isolated from Canada and Japan [76]. Therefore, understanding the prevalence of AqRV infection in both cultured and wild populations and the respective geographic and seasonal distribution of each AqRV species is important for disease management.

1.6   Host Range and Viral Proliferation

AqRVs have been found in a wide variety of aquatic organisms worldwide, including cold- and warm-water areas. Evidence of AqRV infection, as documented for species of different genera, has been found in a wide variety of aquatic animals, including fish and shellfish. The clinical symptoms of AqRV infection in various aquatic animals include hemorrhagic disease, hepatitis, and pancreatitis [2, 54]. Moreover, the same aquatic animal host species can be infected by different AqRV species, such as grass carp. Conversely, a single AqRV species can be isolated from different aquatic animals. This complexity may relate to not only host factors, but also the highly mutated or re-assorted genome segments and replication mode of the AqRV dsRNA genome.

Studies indicate that isolates that are classified as AqRV-C and -G mainly infect cyprinid hosts, for example, GCRV can infect black carp and other cyprinids [28, 29, 55]. GCRV typically causes outbreaks of infectious hemorrhagic disease in grass carp and black carp (*Mylopharyngodon piceus*) and is fatal to rare minnow (*Gobiocypris rarus*) and topmouth gudgeon (*Pseudorasbora parva*) species. In addition, GCRV has been detected in silver carp (*Hypophthalmichthys molitrix*) and *Hemiculter bleekeri* showing no symptoms [19, 80]. The optimal replication temperature of GCRV or GCHV is between 24 and 30 °C. Therefore, the epidemic risk for GCHD decreases when the water temperature is below 20 and above 30 °C [19, 80].

AqRV species belonging to AqRV-A and -B are known to infect a wide variety of salmonid host species. Generally, they show a low prevalence in adult salmonids. However, AqRV-A can cause focal necrotizing hepatitis in several species of juvenile salmonids [5, 15]. Additionally, it has been shown that TFV can cross-infect sea bass, another marine fish [71].

Because of the extensive host range, AqRV can propagate in a variety of cultured cells and produce a typical CPE in permissive cell lines, such as the *Ctenopharyngodon idella* kidney (CIK), fathead minnow (FHM), chinook salmon embryo (CHSE)-214, bluegill fry (BF-2), and epithelioma papillosum cyprinid (EPC) cell lines. Most AqRVs isolated from cold-water fish replicate efficiently in fish cell lines at temperatures ranging from 15 to 20 °C. In contrast, AqRVs isolated from warm-water fish have optimal replication temperatures of 25–30 °C [22, 45], suggesting that the optimal replication temperature for AqRVs depends on the growing conditions of the host species. Furthermore, it has been shown that SBRV grows to similar titers in both CHSE and mammalian cells at 22 °C. Analysis of viral polypeptide and RNA syntheses suggests that the restriction of viral growth at higher temperatures occurs after adsorption but before transcription and translation of viral genes. However, at a temperature (35 °C or above) not permissive for SBRV replication in mammalian cells, no virus-specific RNA and proteins have been detected [69]. Studies have indicated that unlike orthoreovirus species (e.g., MRV or avian reovirus (ARV)), which only infect cells at relatively high temperatures (≥32 °C) [94], AqRV can establish active infection at or below 4 °C [67]. Another study showed that GCRV could replicate at 4 °C, along with NS80 protein expression [94]. The fact that AqRVs can replicate at low temperatures may depend on their genome-encoded protein properties that distinguish them from mammalian reoviruses. In addition, some AqRVs can replicate in mammalian origin cells and produce a characteristic CPE with large syncytia [69].

1.7 Antigenic and Serological Characterization of AqRV

Earlier studies indicate that some AqRVs, such as GSRV, 13p2, CSRV, GCRV, and SBRV, lack hemagglutination activity [45], similar to fusogenic ARV [16]. Their fusogenic nature and inability to agglutinate red blood cells differs from non-fusogenic MRVs. Indeed, no antigenic relationships have been detected between AqRVs and MRVs [68]. These antigenic differences between AqRV and mammalian *Orthoreovirus* may be attributed to their respective host-dependent outer capsid protein divergence and structural heterogeneity. It has been identified that AqRV particles, including the species AqRV-A (SBRV) and AqRV-C (GCRV), lack the cell attachment protein σ1 on their turret protein VP1 [12, 13, 25, 56, 75]. This suggests that the antigenic properties of these fusogenic AqRVs may correlate with the outer capsid proteins VP5 and VP7. A study on SBRV indicated that VP7 in AqRV-A is not the major neutralizing antigen; however, the outer shell protein VP7 shows neutralizing activity [45]. Immunoblotting analysis combined with plaque- and CPE-based median tissue culture infectious dose (TCID$_{50}$) assays of GCRV showed that both VP5 antibody (VP5Ab) and VP7Ab are capable of neutralizing viral infectivity, while VP7 may be a dominant epitope. Further combination of VP5Ab and VP7Ab appeared to show enhanced neutralizing capacity of GCRV [74]. This observation is supported by other similar studies [9, 33], indicating

that the GCRV outer capsid proteins VP5 and VP7 possess good neutralizing activity.

Serological investigations of some isolated AqRVs, such as GSRV, CCRV, 13p2, SBRV, Atlantic salmon reovirus HBR, Atlantic salmon reovirus ASV, smelt reovirus, and TRV, can only be found in early reports. Using cross-neutralization tests, Hedrick et al. [34] found that CCRV, GSRV, and CSRV are clearly serologically distinct in comparison with each other. These three viruses share some antigenic determinants as noted by partial neutralization assays with heterologous reactions; however, CCRV, GSRV, and CSRV can be considered as three different serotypes among AqRVs [45]. Other cross-neutralization studies of 13p2, GSRV, CCRV, and CSRV were conducted by Brady and Plumb [7]; they demonstrated that GSRV, 13p2, and CSRV are related to each other, and CCRV is related to GSRV but not to the other two viruses. Furthermore, using cross-neutralization assay, −immune dot-blot assay, and -ELISA, the antigenic relationships among SBRV, Atlantic salmon HBR, Atlantic salmon ASV, smelt reovirus, and TRV have been studied. The cross-neutralization assay shows a clear relationship between SBRV, Atlantic salmon HBR, Atlantic salmon ASV, and smelt reovirus, and these four viruses can be grouped into two different serotypes: SBRV-Atlantic salmon HBR and Atlantic salmon ASV-smelt reovirus. However, TRV is found to be unrelated to these four viruses and therefore represents a different serogroup. Similar results are obtained for cross-immune dot-blot assays but not cross-ELISA [20, 45]. In contrast with previous studies, Bandin and Dopazo did not find any serological relationship among SBRV (AqRV-A), coho salmon reovirus (CoSRV) (AqRV-B), GSRV (AqRV-C), CCRV (AqRV-D), TRV (AqRV-E), and gilthead seabream reovirus (genetically unclassified) via cross-neutralization and cross-immune dot-blot assays [45].

The antigenicity of GCRV-873 (AqRV-C) has only been compared with that of TFV (proposed to belong to the AqRV-A species group based on genomic sequence analyses) [71]. It is interesting to note that despite the differences between TFV and GCRV-873, antiserum against TFV could cross-react with some of the proteins found in the GCRV core with molecular weights of 136 kDa (VP1), 132 kDa (VP3), and 41 kDa (VP6), suggesting that TFV and GCRV share conserved core proteins. Unexpectedly, a TFV polyclonal Ab could recognize a structural protein with a molecular weight of 51 kDa. Although anti-TFV serum did not recognize all of the GCRV structural proteins, such as the outermost clamp VP7, the 51-kDa protein present in GCRV, which may be a cleaved fragment of VP5, as the sequence analysis indicated that VP5 is the analogue penetration protein in TFV, both TFV and GCRV shared genome segment-encoded functional domains [72, 73]. This suggests that the TFV and GCRV-873 might have some similar epitopes, although their RNA banding patterns differ significantly [71].

Therefore, due to extensive host ranges and cultivation temperatures, AqRV may possess type-specific and group-specific antigenic determinants. Members within a single *AqRV* species group may be antigenic correlative. Furthermore, members belonging to different species groups may show antigenic distinction; however, this requires further substantial experimental analyses. Minor antigenic cross-reactivity

has only been demonstrated between members of the AqRV-A and -B species groups. Distinct serotypes probably exist within each species. To understand the antigenic and serological relationships among identified AqRVs, extensive investigation in future studies is warranted. This will be beneficial for host-dependent AqRV antigenic classification and serologic assortment in taxonomy.

1.8 Representative and Pathogenic AqRV Strains

An increasing number of AqRVs have been identified since the genus *AqRV* was first recognized by the ICTV in 1991 [27]. Based on traditional RNA hybridization and former genome sequence information, seven AqRV species groups (*AqRV A–G*) have been identified from fish and shellfish isolates, with a particular 11-segmented dsRNA genome. The recent complete genome sequence of many AqRV isolates has provided additional information to assist with the classification of newly isolated AqRVs (Table 1.3). Although there is great divergence in AqRV species based on the released sequence information, the 11 segments of the AqRV genome encode at least 12 primary protein products, including 7 structural and 5 nonstructural proteins. Similar to MRV, most of the gene segments encode one protein, except for some small genes in the S class group, such as S7, S10, and S11, which are found to be bicistronic or tricistronic. This section describes some of the representative and pathogenic AqRV species.

CSRV CSRV, the first AqRV isolated from salmonids, was originally isolated from chum salmon (*Oncorhynchus keta*), which is routinely tested at a Japanese aquaculture facility prior to the exportation of eggs [84]. CSRV was originally isolated from CHSE-214 cells inoculated at 15 °C with homogenates of pooled samples of the kidney and liver and can induce plaque-like syncytia as the typical CPE 6 days after inoculation. After a few passages, syncytium formation begins at 2 days post-infection and grows larger over the next few days. Passaged CSRV can also cause CPE in CHH-1 and RTG-2 cell lines [17, 85]; however, the morphology and timing of the syncytia formed in RTG-2 cells differ from that in CHSE cells. The syncytia in CSRV-infected RTG-2 cells are smaller than that in CHSE cells. The CPEs of CSRV on salmonid epithelial (CHSE), fibroblast (RTG-2), and macrophage (RTS11) cell lines have been further investigated. CSRV can cause syncytia in cultures of CHSE-214 and RTG-2 cell lines, suggesting that the formation of syncytia triggers apoptosis, which enhances the release of CSRV. However, CSRV infection in cultures of RTS11 cells induces homotypic aggregation with no loss of cell viability. This suggests that CSRV infection may potentially modulate macrophage behavior in rainbow trout hosts. The different mechanisms underlying CSRV-induced syncytium formation in CHSE-214 and RTG-2 cells and homotypic aggregation in RTS11 cells may be related to viral infection-induced host macrophage response.

Morphological and biochemical studies indicate that CSRV possesses all the basic features of reoviruses. The virus is resistant to treatment with ether or

Table 1.3 Species and tentative species of aquareoviruses

Species	Virus name or abbreviations	Genome sequence status	References
AqRV-A	Angelfish reovirus AFRV Atlantic salmon reovirus HBR Atlantic salmon reovirus ASV Chinook salmon reovirus DRC Herring reovirus HRV/HRV Masou salmon reovirus MSV Smelt reovirus/SRV		[42, 45]
	Atlantic salmon reovirus TSV/TSRV	Partial	[89]
	Atlantic salmon reovirus / AtSRV	Partial	[63]
	Chum salmon reovirus CSV/CSRV	Partial	[3]
	Threadfin reovirus (TFV)	Partial	[72, 73]
	Striped bass reovirus (SBR, SBRV)	Partial	[3, 46]
	Atlantic halibut reovirus (AHRV)	Complete genome (S1–S11)	[76]
	Etheostoma fonticola reovirus (EFRV)	Complete genome (S1–S11)	[37]
AqRV-B	Chinook salmon reovirus B Chinook salmon reovirus LBS Chinook salmon reovirus YRC Chinook salmon reovirus ICR Coho salmon reovirus ELC Coho salmon reovirus SCS		[42, 45]
	Coho salmon reovirus CSR	Partial	[45, 47]
	Fall Chinook salmon (FCSV)	Complete genome (S1–S11)	[48]
AqRV-C	Golden shiner reovirus/GSRV Grass carp reovirus/GCRV-873	Complete genome (S1–S11)	
AqRV-D	Channel catfish reovirus		[2]
AqRV-E	Turbot reovirus		[42, 45]
AqRV-F	Chum salmon reovirus PSR Coho salmon reovirus SSR		[42, 45]
AqRV-G	American grass carp reovirus/AGCRV	S1–S11	[55]
Tentative species of AqRV	GCRV-ZH08 GCRV-GD-108 GCRV-104 GCReV/GCRV109	Complete genome (S1–S11)	[11, 59, 79, 86]
	Chub reovirus Landlocked salmon reovirus Tench reovirus		[42, 45]

chloroform and stable at 37 °C but not at 56 °C. In addition, it has been found that the intermediate sub-viral particles and core particles can be generated by treating the virus with α-chymotrypsin or exposing the virus to pH 3, and enhanced infectivity has been detected for sub-viral particles compared with intact particles. Serum testing assays indicate that CSRV does not agglutinate human erythrocytes [45, 84].

The CSRV genome contains 11 segments ranging from 781 nucleotides (S11) to 3947 nucleotides (S1) with a total size of approximately 2.14 kb (21,395 bp) without including genome segment S4. Ten of the eleven segments have been sequenced completely, with a partial sequence of the S4 segment. The functions of each gene segment-encoded protein are well predicted by multiple assignments of cognate genes to those characterized in MRV. Except for S11, which encodes two or three deduced proteins, the remaining genome segments have one predicted ORF [3]. CSRV belongs to the AqRV-A species group. The GenBank accession numbers for the CSRV genome segments S1–S3 and S5–S11 are AF418294–304.

SBRV SBRV is a well-characterized AqRV species belonging to the AqRV-A group. SBRV was isolated from diseased salt-water striped bass (*Morone saxatilis*) collected from Chesapeake Bay, Maryland, USA, in 1987 [68]. In addition, affected fish was co-infected with a bacterium of the genus *Moraxella*. SBRV infection can lead to a serious hemorrhagic syndrome with obvious pathological lesions of the skin and other viscous organs, such as the liver [45]. SBRV has been isolated from CHSE-214 cells incubated at 15 °C and found to produce plaque-like syncytia in cultured cells. The purified virions show icosahedral symmetry and a diameter of 70–75 nm; they were first termed as rotavirus-like agents based on preliminary molecular characterization [68]. SBRV is resistant to chloroform treatment and replicates in the presence of 5-IUdR. Moreover, enhanced infectivity of SBRV has been detected by treatment with protease [51]. Except for the common and molecular characteristics similar to those of MRV, SBRV does not share any relationship with reovirus (type 1 Lang, T1L) and rotavirus (SA11), as observed by RNA cross-hybridization and antigenicity assays. The polypeptides and the gene-coding assignments of the SBRV are the first to be determined among the identified AqRV species [77]. A total of 12 proteins, with apparent molecular weights of 130, 127, 126, 97, 73, 71, 46, 39, 35, 29, 28, and 15 kDa, have been detected in infected CHSE cells using [^{35}S]methionine-labeled lysates, and structural proteins are further identified by comparison with [^{35}S]methionine-labeled proteins from purified SBRV [68, 77]. It has been observed that each of the SBRV genome segments S1, S2, S3, S5, S6, S8, and S10 encodes a distinct structural protein, while the remaining genome segments S4, S7, S9, and S11 encode nonstructural proteins.

Generally, AqRVs replicate efficiently in cell cultures of fish origin. Interestingly, SBRV can grow under appropriate conditions in some mammalian cell lines and causes typical CPE at a low temperature of 22 °C [69]. Moreover, similar SBRV titers have been detected in both CHSE and mammalian cells. However, high-temperature incubation (at or above 35 °C) restricts SBRV proliferation because the viral polypeptide and RNA syntheses are suppressed at such high incubation temperatures, suggesting that AqRVs are unlikely to be human pathogens

[69]. Three-dimensional structural reconstruction of SBRV indicates that the AqRVs and orthoreoviruses exhibit extensive similarity, except for the absence of σ1 protein on the outside of the VP1 turret protein in AqRVs [56, 75]. Based on RNA hybridization assays and some genome sequence-based data, SBRV is a representative AqRV-A species. Partial sequences of SBRV genome segments have been released. Sequences of the SBRV genome segments S2, S3, S4, S8, and S10 have been characterized: S2 (AF450318), S3 (AF450319), S4 (AF450320), S8 (AF450321), and S10 (AF450322).

CoSRV CoSRV was first isolated during routine examination of sexually mature coho salmon (*Oncorhynchus kisutch*) returning to the Coquille River and Eel Lake in Oregon, USA [45]. The two collected CoSRV strains can induce syncytia in cultured CHSE-214 cells after several blind passages, with incubation at 15 °C. However, the isolate from the Eel Lake produces an identical CPE 6 days after the original inoculation, whereas the CoSRV isolate from the Coquille River produces syncytia 14 days after a blind passage, suggesting that there is little difference in the cell culture characteristics of the two CoSRV isolates. The morphology of CoSRV observed via electron microscopy of negatively stained preparations reveals the virus particles being 75 nm in diameter and having a double capsid shell. Sequence analysis of the genome segment S10 of the CoSRV strain of the AqRV-B species group showed that the segment is at least 936 nucleotides in length and has a major ORF encoding a protein of 293 amino acids with a calculated molecular mass of 31.7 kDa. Comparison of nucleotide and deduced amino acid sequences of the genome segment S10 of SBRV (AqRV-A) and AqRV-B strains indicates 55.7% and 36.5% identity at the nucleotide and amino acid levels, respectively. Baculovirus expression and serological identification of the genome segment S10 of the CoSRV strain indicated that this gene encodes the major outer capsid protein. From an evolutionary standpoint, it is possible that the VP7 proteins of AqRV-A and -B have evolved from a common ancestral precursor [46, 47]. Furthermore, it has been observed that the CoSRV VP7 protein does not contain any potential N-linked glycosylation site, as opposed to the three sites found in the VP7 protein of AqRV-A species by Lupiani et al. [45]. Nonetheless, the VP7 protein of CoSRV, similar to that of SBRV, has been found to be rich in cysteine residues 12 and 13, or contains a conserved CCHC motif near the N termini of VP7, homologous to the zinc-binding motif of the MRV σ3 [47], indicating that the structural features of VP7 in the two viruses are similar.

GSRV GSRV was the first AqRV to be reported and was isolated from diseased freshwater golden shiners (*Notemigonus crysoleucas*) in a freshwater-cultured farm in Arkansas, USA, in 1977 [60]. Infected fish showed macroscopic petechial hemorrhages in the cornea, dorsal muscle, ventral surface, internal fat, and intestinal mucosa, but the infection was associated with relatively low rates of mortality. GSRV has also been isolated from cultured FHM cells, and it produces typical CPE 3 days post-infection, with incubation at 30 °C. Five major structural proteins have been identified in GSRV and are compared with those in 13p2, CSRV, and CCRV [85]. Ultra-thin negatively stained sections of infected FHM cells observed

under electron microscopy have shown the presence of paracrystalline arrays as those found on icosahedral nonenveloped viruses, with an approximate diameter of 70 nm. GSRV is resistant to ether, heat (30 min at 50 °C), and either acid (pH 3) or alkaline (pH 10) condition. RNA hybridization and genome sequencing indicated that GSRV is a member of the AqRV-C species group. Although GSRV is isolated from a freshwater fishery farm in the USA, its genome sequence shares 96–99% amino acid identity with that of a Chinese isolate of GCRV [3]. It appears that they are variants of the same virus [50]. The total genome size of GSRV is 23,696 bp (with genome segments ranging from 820 to 3949 bp in size) [3, 23]. The GenBank accession numbers for the complete sequences of the 11 GSRV genome segments are AF403398–AF403408.

GCRV Similar to MRV, most AqRV isolates are nonpathogenic or have low virulence in their host species. However, GCRV is an exception and is recognized as the most pathogenic AqRV [64]. During the 1970s, an unusual epidemic GCHD, associated with significant losses of fingerling and yearling grass carp and high mortality (approximately 85%), was detected in the southern China freshwater fishery farm [70]. Affected fish showed exophthalmia and hemorrhages at the base of the fins, gills, muscle, and intestinal tract. The pathogen that caused severe GCHD was identified as a reovirus agent by two research groups in 1983 [10, 30].

More than 50 strains of GCRV, including GCRV-836 (fish reovirus 836 or FRV-836), GCRV-854 (or GCRV-IHB), GCRV-861, GCRV-873, GCRV-991, GCRV-H962, ZV-8802, GCRV-097, GCRV-JX-0901, GCRV-HZ08, GCRV-GD108, GCRV-104 (HGDRV), and GCReV-109 (GCRV-109), have been reported to date since the isolation of the initial reovirus species from diseased grass carp in China [24, 65, 80, 90, 91]. Some earlier and recently isolated stains of GCRV and their genomes have been well characterized. Transmission electron microscopy (TEM) analysis has revealed that GCRVs present spherical particles of approximately 75 nm in diameter with an obvious double capsid layer having 20 peripheral capsomers and no envelope. All isolated virus strains from grass carp have been shown to be resistant to treatment with ether and pH 3 conditions, with some showing a slight variation due to different isolation environments. For example, GCRV-HZ08 displays better stability at pH 2 and pH 11 than the other isolates, implying that GCRV-HZ08 may be more resistant to extreme conditions [80]. Further studies characterizing the GCRV growth in cells indicated that although the virus can replicate in cell lines originating from grass carp, such as CIK, grass carp fin (GCF), grass carp ovaries (COs or GCOs), GCK, ZC-7901, and grass carp snout fibroblasts, the production and phenotype of syncytia, and infectious virus titers appear largely different. GCRV infection induces the production of an interferon-like product in GCF and CO cells [45].

The GCRV genome consists of 11 linear dsRNA segments (S1–S11) with a total size of approximately 24 kb; however, the genome segment migration pattern (electropherotype) of different isolates shows variations, which is consistent with that observed for the complete genome sequences of GCRVs [3, 21, 59, 79, 86]. Based on the complete sequence of RdRP and the available VP6 core clamp

protein gene sequence, the established phylogenetic analysis revealed that at least three genotypes of GCRV occur in China, which are represented by genotype I (GCRV-I, GCRV-873), genotype II (GCRV-II, GCRV-HZ08), and genotype III (GCRV-III, GCRV-104 or HGDRV) [79]. In addition, three-dimensional images of a single GCRV particle have been obtained [12, 13, 25, 83], and some functional interactions between GCRV nonstructural proteins and host cells have been investigated [78, 87].

GCRV-873 GCRV or GCRV-873, the suggested prototype strain for GCRV belonging to the group AqRV-C, was sampled in 1987 from diseased fingerling and yearling grass carp in Shaoyang, Hunan, China [22, 39]. GCRV-873 was first isolated from infected CIK cell lines 4–5 days after inoculation at 28 °C, where it produced large syncytia as the unique CPE. After several passages, CPE was produced within 2–3 days. GCRV replicates efficiently in CIK and FHM cells but is not sensitive to BF2 and EPC fish cells and Vero and baby hamster kidney mammalian cells [24]. Morphological and biochemical investigations indicated that GCRV-873 is a new species of the family *Reoviridae* [39]. These showed that the virus is ether- and chloroform-resistant and stable at 56 °C for 30 min. The viral particles have no hemagglutination ability for human type 0 erythrocytes and no cross-antigenic relationships with rotavirus and reo-E10 strain. The original passaged culture fluid of infected CIK cells has been observed to cause hemorrhagic symptoms and lead to high mortality, via artificial injection of the GCRV into grass carp fingerlings. Notably, the GCRV-infected cell cultures with hundreds or thousands of generations in vitro appear nonpathogenic or exert low pathogenesis in farmed fish, suggesting some losses of antigenic activity against host cells.

Analyses of some of the molecular biology features of GCRV-873 have been conducted during the 1990s [39, 40]. The GCRV-873 genome is composed of 11 dsRNA segments, and the corresponding Mr. of the dsRNA segments ranges from 0.4 to 3.1×10^6. The total molecular weight is ~16×10^6 Da [39]. The 11 genomic segments (S1–S11) of GCRV-873 that migrate in both agarose and polyacrylamide gels appear to be classified into three size classes (large: S1–S3; medium: S4–S6; small: S7–S11). The GCRV reaction core exhibits RdRP activity, and the optimal temperature for RdRP activity is approximately 28 °C [36]. Nucleic acid release and reaction core images obtained via electron microscopy-based surface spreading and shadowing of RNA strands showed that the spike-like turret is supposed to be the site of nascent mRNA release into host cells [35, 40]. In addition, early studies of in vitro translation suggested that the 11 genomic segments of GCRV encode 12 proteins; however, these experiments failed to distinguish between structural and nonstructural proteins [82]. The full-length sequences of the genome segments S1, S2, and S3 of GCRV-873 were first obtained using random hexamer amplification method-cloned cDNA libraries [23]. The GCRV genome segments S1, S2, and S3 were found to be 3949, 3877, and 3702 nucleotides in length (accession numbers: AF260511–13), respectively. The highest amino acid sequence identities (26–41%) of the S1–S3 genome segment-encoded proteins (VP1–VP3) were first found with MRV proteins (λ1–λ3) by homologous sequence

comparisons. Generally, this degree of sequence identity is usually only found among members of the same genus. Indeed, unusual homology between several other genes has been noted upon characterizing the remaining genome segment sequences of GCRV-873 (S4–S11, accession numbers AF403390–AF403397) and other AqRV isolates, including GSRV, SBRV, and golden ide reovirus [3]. These sequence data undoubtedly indicate that AqRV shares a common evolutionary origin with MRV. This clear genetic relatedness between members of distinct genera is unique to the family *Reoviridae*. Based on the high sequence identities with GSRV, GCRV-873 has been reassigned to the AqRV-C group by ICTV [3, 4, 55]. Moreover, five major and two minor structural proteins in GCRV-873 and GCRV-991 have been identified and confirmed from purified particle preparations [24]. At almost the same time, the sequences of 10 genomic segments of GCRV-873 (GCHV-873), with the exception of S4, were released by another research group (accession numbers: S1: AF260511, S2: AF284502, S3: AF284503, S5: AF252162, S6: AF239175, S7: AF239174, S8: AF259053, S9: AF284504, S10: AF236688, and S11: AF234321) [61, 62]. Herein, the GCRV-873 genome sequence was the only double-sequenced species among all the sequenced AqRV isolates.

After characterizing the complete genome sequence of GCRV and obtaining highly purified viral particles, the viral structural and nonstructural proteins were identified and characterized. In addition, three-dimensional images of reconstructed singular particles ranging from 17 Å to atomic resolution have been obtained [12, 13, 25, 83, 94]. The three-dimensional structural reconstruction of single particle of GCRV-873 further confirmed that AqRVs and orthoreoviruses are closely related in their structural architecture, functional protein confirmation, and conserved protein domains, which are well matched at the genome sequence level. Furthermore, high-resolution three-dimensional image reconstruction clearly resolved the structures and localization of seven structural proteins in the particles. This indicates that the structural protein similarities between GCRV and MRV gradually diverge from the core to the outer shell, and no cell attachment σ1 protein (situated on λ2 turret protein at fivefold axes) is found at the corresponding position on the GCRV particle. The characteristic and related functions of some nonstructural proteins of GCRV (NS80, NS38, NS31, NS26, and NS16) have also been studied [31, 32, 87, 88, 92, 93] (see Chap. 2).

Tentative Reovirus Species Isolated from Grass Carp Many other reoviruses have been isolated from grass carp in recent years. Except for GCRV-873, the genome sequences of at least 12 GCRV strains have been completely characterized, and partial genome sequences of most of the strains have been released (NCBI database). The newly isolated GCRV strains show great diversity based on their cell culture characteristics, virulence, pathogenesis, and antigenicity, as well as genome sequence-based distinctions [80]. For example, the GCRV-097/JX-1 strain can induce significant CPEs in CIK cells and massive abdominal hemolysis and obvious hemorrhage in the muscle, skin, intestine, and gill of grass carp, resulting in a high mortality rate of grass carp [80], whereas GCRV-HZ08 and GCRV-GD108 cannot induce typical CPE in infected permissive fish cell lines [86]. The genomes of

GCRV-HZ08, GCRV-GD108, GCRV-104 (also named HGDRV), and GCReV-109 are well characterized [21, 59, 79, 86]. Based on the VP6 sequences, the known GCRV strains (isolated in China) are clustered into three groups, with the representative isolates GCRV-873 (GCRV I), GCRV-HZ08 (GCRV II), and HGDRV (GCRV III) [79]. However, Pei et al. classified GCRV-HZ08, GCRV-873, and HGDRV (GCRV-104) into groups GCRV I, II, and III, respectively [59]. Although different researchers have different views on clustering, one aspect remains common, i.e., GCRV-873, GCRV-HZ08, and HGDRV are classified into three different groups of reoviruses that are isolated from grass carp [59, 79]. Sequence analysis and predicted protein functions for GCRV-HZ08, GCRV-GD108, GCRV-104, and GCReV-109 revealed that the genome-encoded proteins differ largely from GCRV-873, and thus, these tentative species need to be further classified in the genus *AqRV*. The newly identified GCRV isolates sequence accession numbers are listed in Table 1.4.

AGCRV Some reoviruses were isolated from grass carps and golden shiners in the USA between 2001 and 2004 and thus referred to as AGCRV. AGCRV, which is atypical in syncytium formation in permissive cell cultures at neutral pH, has been implicated in the winter die-off of grass carp fingerlings on a commercial farm in Arkansas, USA. Furthermore, four AqRV isolates (PB02–24, PB04–123, PB04–151, and PB01–155) were isolated from grass carp and golden shiner, and among these, isolate PB04–151 was contributed by Ron Hedrick [55]. Tissue lysates from these fish were inoculated onto confluent monolayers of FHM cells by incubating at 22 °C. Isolate PB04–144 produced syncytia in inoculated FHM cells, while the three remaining isolates only caused the cells to round-up and detach from the plastic flask, thereby not inducing the typical syncytium formation in the cell culture as done by other AqRVs. Next, the four isolates were expanded by growing on FHM cells, with incubation at 30 °C. Isolate PB01–155 was selected to represent the group of the four isolates for further sequence analyses. Sequence analysis and assignment indicated that the complete genome sequence of AGCRV is not closely related to that of the members of species groups AqRV-A, AqRV-B, and AqRV-C. In contrast, the homologs of the two proteins encoded by the bicistronic S7 segment of AGCRV are found on two separate genome segments, upon comparing AGCRV and a non-turreted coltivirus, Colorado tick fever virus [55]. Complete nucleotide sequence analysis of the AGCRV genome and comparisons with other AqRVs showed that it is closely related to golden ide reovirus (>92% amino acid sequence identity for VP5 (NTPase) and VP2 (Pol)). Phylogenetic analyses indicated that golden ide reovirus represents the second isolate of the AqRV-G group. Comparisons of AGCRV with GCRV (AqRV-C) and CSRV (AqRV-A) showed only 22% to 76% amino acid sequence identity for different viral proteins. Interestingly, coltiviruses are members of the family *Reoviridae*, and it has been found that AGCRV is evolutionarily linked with coltiviruses [16, 55]. Coltiviruses are the non-turreted members of the family *Reoviridae*, and their prototypical member is the Colorado tick fever virus that has a genome comprising 12 dsRNA segments [42]; whereas the orthoreoviruses and AqRVs are the turreted members. The

Table 1.4 Complete and nearly complete genome sequence of representative aquareovirus species with 11 genome segments

No	Virus species	Host	Isolation region and time	Genome size(bp)	Access Nos.	References
1	AGCRV (PB01-155)	Grass carp	USA/2001	23,576	EF589098-108	[55]
2	AHRV-241013	Atlantic halibut	Norway/2015	24,171	MH108635-645	[76]
3	CSRV/CHSRV	Chum salmon	Japan/1981	23,015[a]	AF418294-304	[3, 84]
4	EFRV/EFAReV	Fountain Darter	USA/2003	23,958	KU194213-223	[37]
5	FCRV	Fall Chinook salmon	USA/2014	23,307	KX891216-226	[48]
6	GCRV-873	Grass carp	China/1987	23,695	AF260511-13, AF403390-397	[3, 23]
7	GCRV-HuNan794		China/2007	24,780	KC238676-686	[57, 65]
8	GCRV-HZ08		China/2008	24,707	GQ896334-37, GU350742-48	[79]
9	GCR-106		China/2009	24,788	KC201166-176	[57, 65]
10	GCRV-HeNan988		China/2009	24,780	KC847320-330	[57, 65]
11	GCRV 104		China/2009	23,706	JN967629-639	[21]
12	GCRV918		China/2010	24,780	KC201177-187	[57, 65]
13	GCRV-GD108		China/2010	24,703	HQ231198-208	[86]
14	GCRV-109		China/2014	24,625	KF712475-KF712485	[59]
15	GSRV	Golden shiner	USA/1979	23,696	AF403398-408	[3]
16	SMReV		China/2011	24,042	HM98993-940	[38]
17	MsReV	Largemouth bass	China/2010	24,024	KJ740724-734	[11]

[a]Mark indicates 10 genome segments sequence finished

accession numbers for the sequences of 11 genomic segments of AGCRV are EF585098–108.

TRV The first TRV, assigned to the AqRV-E group via RNA-RNA hybridization assay, was isolated from a cultured turbot (*Scophthalmus maximus*) population experiencing continuous but low levels of mortality in Northwest Spain and reported in 1989 by Lupiani et al. [45]. The affected fish was also infected with a bacterium of the genus *Vibrio*. TRV, isolated from the kidney, liver, and spleen tissue homomixtures, was inoculated into CHSE-214 cells at 15 °C and could induce syncytia on the infected monolayers 14 days after inoculation. Notably, TRV can

replicate at low temperatures, even at 2.5 °C [67]. TEM analysis of negatively stained virus concentrates from infected CHSE-214 cells showed 70 nm icosahedral particles with a double-layered capsid. TRV is resistant to treatment with ether and chloroform; pH 2, 3, and 9; and heating at 50 °C for 30 min. No sequence data have been reported.

SMReV and Largemouth Bass *Micropterus salmoides* Reovirus (MsReV)
SMReV, sampled from a fish farm in Shandong province of northern China, was isolated and identified from a diseased turbot, which is the first AqRV isolated from a marine fish in China [38]. SMReV was first inoculated in CHSE, flounder embryo, EPC, and GCF cell lines for the respective sensitivity assays. The optimal temperature for virus propagation was assayed by infecting monolayers of GCF cells at 15 °C, 20 °C, or 25 °C. SMReV could cause typical CPE in GCF and CHSE cell lines 4–5 days post-infection at 20 °C. Genome sequencing revealed that the full-length genome sequence of SMReV is 24,042 bp in length (the smallest S11: 784 bp; the largest S1: 3947 bp). In addition, a fusion-associated small transmembrane (FAST) protein NS22, which is translated from a non-AUG start site, has been identified in the S7 segment. Furthermore, the FAST protein with a non-AUG start site, which partially contributes to the CPE caused by SMReV infection, has been validated by a molecular biology analysis. Phylogenetic analysis based on the major outer capsid protein VP7 and RdRP protein sequence comparisons suggested that SMReV is a new AqRV and is proposed to belong to the AqRV-A species group. Interestingly, the aforementioned TRV, which was isolated from Spain, was classified in the AqRV-E species group by RNA–RNA hybridization and cross-immune dot-blot assays [4, 45].

More recently, a novel *Micropterus salmoides* reovirus (MsReV) was isolated from diseased largemouth bass in the Hubei province of China [11]. The filtered supernatant from the homogenized preparations of the diseased largemouth bass liver, spleen, and kidney tissues was inoculated on confluent monolayers of BF-2, CHSE, GCF, and GCO cell lines at temperatures of 15 °C, 20 °C, or 25 °C, and overt CPE was observed at 3–4 days post-infection. The genome segments S1–11 of MsReV were sequenced completely. The complete genome sequence of MsReV is 24,024 bp in length (S1: 3947 bp; S11: 783 bp) and encodes 12 putative proteins, including the VIB formation-related protein NS87 and FAST protein NS22. Furthermore, significant similarities (91.2%) have been found between the equivalent genome segments of SMReV and MSReV, along with a same-sized genome (24,042 bp). These studies revealed marked similarities in the genome and encoded proteins between MsReV and SMReV. Further phylogenetic analysis showed that AqRVs can be divided into freshwater and saline water environment subgroups, and MsReV is closely related to SMReV in the saline water environment subgroup. Consequently, these viruses from hosts in saline water environments were found to have more genomic structural similarities than that observed in viruses from hosts in freshwater environments. The accession numbers for the sequences of the 11 segments of the SMReV genome are HM989930–989940 and those of the MsReV genome are KJ740724–KJ740734.

AHRV A pathogenic reovirus infection causing mortality has been reported to occur in the commercial production of Atlantic halibut fry (*Hippoglossus hippoglossus*) in Canada, Scotland, and Norway at the beginning of the twenty-first century [5, 15]. AHRV, associated with necrosis of the liver and pancreas, has been isolated from cultured Atlantic halibut fry at a facility where massive mortalities occurred during the feeding-initiation phase. This constitutes a dominant/significant problem for Atlantic halibut production in Norway. Similar liver pathology has also been described in captive juvenile Atlantic halibut in the Atlantic and Canada [15, 76]. Typical syncytium formation in these tissues and distinct viroplasm areas in the diseased tissues of halibut fries have also been observed. In addition, AHRV has been detected in Atlantic halibut juveniles. AHRV has been isolated from both BF-2 and CHSE-214 cell lines. The virus replicates in BF-2 and CHSE-214 cell cultures and produces syncytia and plaque-like CPEs. The syncytium consists of large multinucleated cells, which appears at 6 days post-inoculation at 15 °C in BF-2 cells, and continues to grow until most of the monolayer is affected. Typical CPE in BF-2 or CHSE-214 cells can be induced by subsequent passage of the virus-infected supernatant by performing freeze/thaw cycles of the supernatant (−80 °C and 20 °C). No CPE has been observed in ASK and RT gill cells. TEM observation of ultra-thin sections revealed that the viroplasm contains virions that are nonenveloped icosahedral particles approximately 70 nm in diameter with a double capsid layer, amorphous material, and tubular structures, suggesting that VIB-like structures occur in the virus-infected cytoplasm. The complete AHRV genome sequence has been determined [76], which is the first complete genome sequence of an AqRV species isolated from a marine cold-water fish species in the North Atlantic. The 11 AHRV genome segments encode 13 putative proteins, which share the highest amino acid sequence identity with members of the species group AqRV-A and -B. Phylogenetic analysis of the most conserved proteins (VP1, VP2, VP3, and VP5) suggested that AHRV can be grouped in a major clade together with the AqRV-A and AqRV-B species. Further analysis of the RdRP sequence showed that AHRV is closely related to the AqRV-A group and SMReV [76]. However, the differences in the hosts and environments and the amino acid sequence identity of RdRP (~80%) with that of either AqRV-A or -B suggest that AHRV may represent a novel species within the genus *AqRV*. The complete genome sequence of AHRV provides insight into the molecular detection of AHRV RNA in the egg stage of asymptomatic Atlantic halibut brood fish to reduce outbreaks of disease caused by AHRV infection. The accession numbers for the sequences of the 11 AHRV genome segments are MH108635–MH108645.

Fall Chinook Reovirus (FCRV) Salmon is the primary fishery product in the Pacific Northwest area and paramount to its economy, ecology, history, and culture. Infectious diseases caused by viral pathogens are one of the major threats to salmon health and aquatic farming, with more than twenty known virus species isolated from infected salmon. A new member of the AqRV species, fall chinook reovirus (FCRV) has been detected during routine surveillance of salmonids [48]. The virus was first found in 2014 as part of a routine adult brood stock screening program, wherein the

kidney and spleen tissue samples from healthy-appearing adult fall chinook salmon (*Oncorhynchus tshawytscha*) returning to a hatchery in Washington State produced CPEs when inoculated into CHSE-214 cells. The FCRV genome contains 11 dsRNA segments totaling to 23.3 kb in size, with each segment flanked by the canonical sequence termini found in the AqRVs. Sequence comparisons and a phylogenetic analysis based on pairwise nucleotide and predicted protein sequence identity revealed sequence identities ranging from 63% (VP7) to 73% (VP3) between green river chinook AqRV and FCRV, thereby placing FCRV in the species group AqRV-B. The FCRV sequence data represent the first complete genome for the AqRV-B species group [48]. The accession numbers for the sequences of the 11 segments of the FCRV genome are KX891216–KX891226.

TFV Threadfin fish are a highly priced food fish in Asia. TFV was isolated from a threadfin (*Eleutheronema tetradactylus*) fingerling batch with massive death in an aquaculture farm in Singapore in February 1998 [71]. The diseased fish were lethargic and showed slight hemorrhage in the abdomen and below the pectoral fins with pale gills. Furthermore, using the liver, spleen, and kidney tissue sample homogenates, TFV was isolated from BF-2 cells at 25 °C, where it produced an unusual type of syncytia 3 days post-infection. Electron microscopy of negatively stained virions revealed icosahedral particles with a diameter of approximately 70–80 nm and two capsid layers. Thin-section electron microscopy of infected BF-2 cells indicated the presence of sub-viral particles approximately 30 nm in diameter and complete particles 70 nm in diameter scattered throughout the cytoplasm. Moreover, acridine orange staining revealed typical reovirus-like cytoplasmic inclusion bodies. TFV replication is not inhibited by 5-IUdR treatment. The virus is resistant to pH 3–11 and ether treatment. It is also stable when heated at 56 °C for 3 h. Indeed, the purified TFV particle is more stable than GCRV-873, as determined by SDS-PAGE analysis. Electrophoresis of the purified virus revealed 11 dsRNA segments and 5 major structural polypeptides of approximately 136, 132, 71, 41, and 33 kDa. The RNA and virion protein-banding pattern of TFV is different from that of another Asian AqRV isolate, GCRV. Artificial injection of TFV into threadfin fingerlings results in complete mortality, whereas sea bass (*Lates calcarifer*) fingerlings infected via bath exposure show severe mortality within a week of exposure, suggesting that TFV is another pathogenic AqRV isolate in Asia that can cross-infect another marine fish, the sea bass. The sequences of the genome segments S6 and S10 of TFV have been released, which shows that S6 and S10 encode the outer capsid proteins [72, 73]. Furthermore, sequence comparison revealed that the protein encoded by the TFV S10 gene is similar to the SBRV VP7 outer capsid protein. A conserved putative zinc-finger motif, CCHC, present in the MRV σ3 protein, has been identified on the VP7 protein of TFV and other AqRVs. Phylogenetic analysis of the TFV VP7 protein indicated that TFV is closely related to SBRV and CSRV and possibly belongs to the same species group as SBRV and CSRV (AqRV-A). Amino acid sequence analysis of the VP5 outer capsid protein revealed the presence of a putative conserved asparagine-proline (Asn-Pro) protease cleavage site, which has been found in all reported isolates of *AqRV* as well

as in the MRV µ1 protein. Moreover, N-terminal sequencing of the corresponding S6 native protein obtained from purified TFV particles has verified the presence of this cleavage site. Phylogenetic analysis of the TFV S6 protein revealed that TFV is closely related to CSRV in the AqRV-A group. The accession numbers for the sequences of the S6 and S10 segments of the TFV genome are AY 235428 and AY236219.

TSRV TSRV has been consistently isolated from Atlantic salmon in Tasmania and Australia, since it was first identified in 1990 under the Tasmanian Salmonid Health Surveillance Program. The distribution and prevalence of TSRV have been determined using the data from this program. The virus is present throughout Tasmania, with the highest reported prevalence of the virus in the southeast region of Tasmania [8]. As part of the surveillance program, TSRV has been regularly isolated from farmed Atlantic salmon in Tasmania for more than 20 years. Prior to the development of nucleic acid-based tests, immunocytochemistry served as a confirmatory diagnostic test for detecting TSRV in cell cultures exhibiting typical CPEs. These observations, together with other phenotypic differences observed among TSRV field samples, such as differences due to isolation from different cell lines (EPC and CHSE-214), raised questions regarding the existence of variants among TSRV isolates. Based on preliminary genotypic and phenotypic characterizations performed for more than 10 different isolates, typical and atypical TSRV variants have been identified. The differences between typical and atypical TSRV isolates have been observed in sequencing-based analyses as well as TEM, western blotting, and immunocytochemistry analyses. Segments S2 and S10 of the TSRV genome have been characterized (accession numbers EF434978 and EF434979, respectively). Sequence and phylogenetic analyses by Lupiani et al. have confirmed the assignment of TSRV to the species group AqRV-A [45]. The typical TSRV isolate also shows high sequence identity with the major outer capsid protein VP7 of the AtSRV [63] and SBRV. High homology between these isolates most likely reflects the homology present among viruses of the same species group, with TSRV, AtSRV, and SBRV belonging to the AqRV-A species group [89]. Phylogenetic analysis showed that the typical and atypical TSRV isolates originate from different lineages with major variations. However, as the sequence identities of the two different populations remain uncharacterized, it is difficult to determine the origin of the isolates. Collectively, sequence and phylogenetic studies of the two gene segments of TSRV (S2 and S10) and their deduced amino acid sequences allow definitive classification of the virus, some speculation on its origin, and the development of diagnostic tools [89].

1.9   Conclusions and Future Considerations

Numerous reoviruses have been isolated from fish and shellfish in freshwater and saline water environments since the initial report. The viruses isolated from aquatic animals with particular reovirus properties and 11 genomic segments are classified into the genus *AqRV* [27]. Seven *AqRV* species (AqRV-A to AqRV-G) have been classified by the ICTV [42], and many newly isolated AqRV genomes have been partially or completely sequenced. With an increase in the available sequence data for AqRVs, particularly for the non-fusogenic AqRVs, the fundamental aspects of diversity between the *Orthoreovirus* and *AqRV* or between distinct species within the genus *AqRV* should become even more evident. Thus, in terms of the evolutionary relationships between the genus *Orthoreovirus* (including fusogenic and non-fusogenic species) and *AqRV*, adding a non-fusogenic AqRV group within the genus needs to be considered for the taxonomic organization of the reoviruses.

Genome Segment-based Protein Conservation and Divergence Based on the complete and nearly complete genome sequences of AqRVs obtained, functionally equivalent genome segments among the AqRV species, such as AHRV, CSRV, GCRVs (GCRV-873, GCRV-ZH08/-GD108, GCRV-104, and GCRV-109), GSRV, AGCRV, MsReV, and SMReV, have been compared. It showed that almost all of the AqRV proteins encoded by the large and medium size genome segments (S1–S6) are highly conserved in their respective protein functions. It can be defined that the genome segments S1 through S6 encode proteins VP1 (core turret), VP2 (RdRP), VP3 (inner core shell), VP4 (core NTPase), NS80/NS1 (VIBs), and VP5 (outer shell or penetration protein), respectively. All six proteins from different AqRV isolates not only share high nucleic acid sequence identity but also contain similar conserved functional domains at the functional protein level (Fig. 1.2). It shows (Fig. 1.2a) that the VIB-like NS80 protein is generally encoded by genome segment S4 in most AqRVs, except the predicted VIB protein in FCRV and GCRV-104, which is encoded by the S6 genome segment [21, 48]. Indeed, three-dimensional image reconstruction of AqRVs has resolved the structural proteins and their localization (VP1–VP5) in the particle [12, 25, 83, 94], except for the S4-encoded VIB-related NS protein (NS80 in AqRV-C or NS1 in AqRV-A). The conservation is consistent with that observed in orthoreoviruses. Three large and three medium gene segments encode proteins catalogued in the λ and μ classes [58]. For example, it has been found that the genome segment S6-encoded outer shell protein VP5 of nearly all the AqRV species is strikingly similar in function to the genome segment M2-encoded membrane penetration protein μ1 in MRV (Fig. 1.3). Comparing the conserved and absent sequences and domains in the AqRV VP5 with μ1 in MRV may reflect the functional similarities and differences for the penetration protein VP5 in host cell entry and replication between the two genera. In addition, substantial genome sequence comparison and functional investigation of the related proteins indicated that these six proteins encoded by the genome segments S1–S6 inherit the main characteristics of reoviruses that are indispensable in virus entry, RNA transcription and replication, and particle assembly. Collectively, the proteins encoded by the
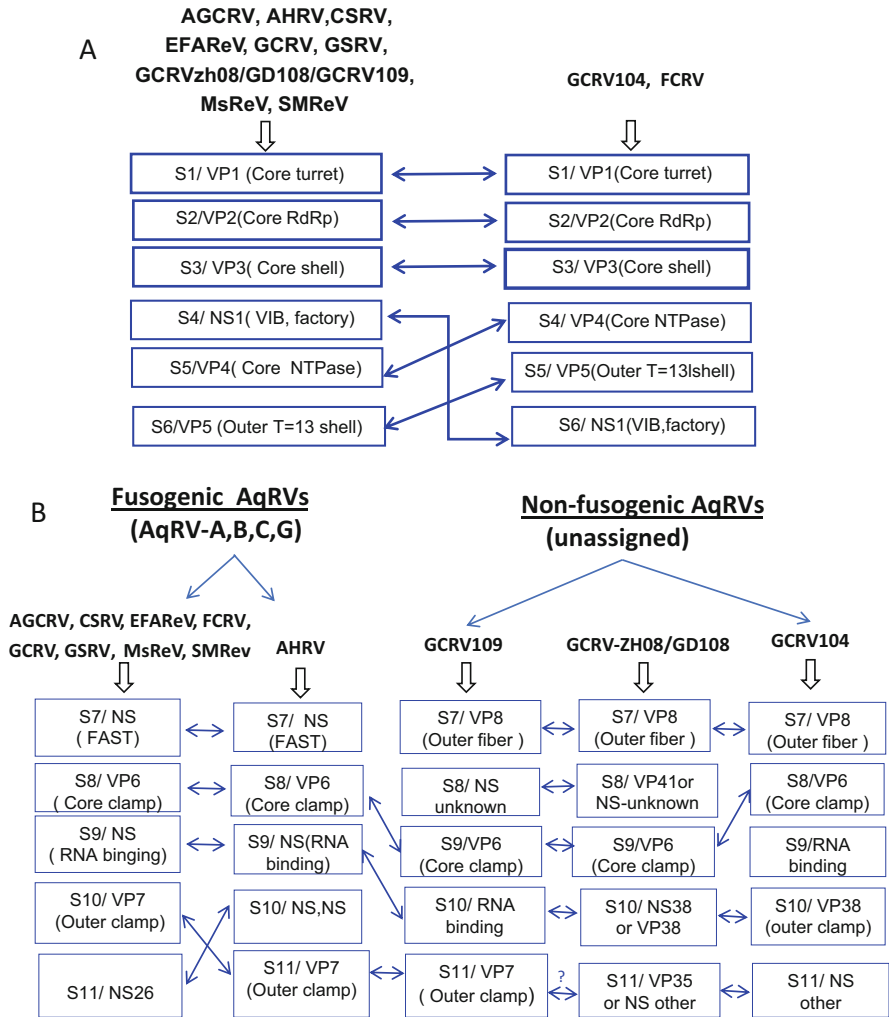
Fig. 1.2 Aquareovirus genome segments encoded putative structurally and functionally conserved and diverse proteins. (**a**) S1–S6 genome segments and conserved putative encoding protein of AqRVs. (**b**) S7–S11 genome segments and predicted diverse encoding protein of AqRVs. Representative strains in Aquareovirus-A (CSRV, EFAReV/EFRV, MsReV, SMReV), Aquareovirus-B (FCRV), Aquareovirus-C (GCRV873-, GSRV), Aquareovirus-G (AGCRV). Tentative Aquareovirus species are GCRV-HZ08/GD-108/109/104; All the sequence related papers are listed in references [3, 11, 21, 38, 48, 55, 59, 76, 79, 86, 90]

three large and medium genome segments are highly conserved between the AqRV and orthoreovirus species.

In contrast to the evolutionarily conserved S1–S6 genome segments, the proteins encoded by the AqRV small class genome segments (S7–S11) are largely divergent

Auto-cleavage site

N-terminal---

[Multiple sequence alignment of VP5 and μ1 proteins — N-terminal portion (top block) and C-terminal portion (bottom block). Strain labels at left: MRV-T1L, MRV-T3D, MRV-T2J, ARV-138, ARV-176, BRV, GCRV-104, GCRV-HZ08, GCRV-109, GCRV-GD108, AGCRV, GSRV, GCRV-873, GCHV-873, GCRV-GZ1208, GCRV-96, CSRV, SMReV, EFRV, TFV, MsReV, FCRV, GRCV, AHRV. Position numbers at right of top block: 120, 120, 120, 120, 120, 117, 94, 92, 92, 92, 91, 91, 91, 91, 91, 91, 83, 92, 92, 92, 92, 91, 66, 91. Position numbers at right of bottom block: 708, 708, 708, 676, 676, 676, 638, 650, 650, 650, 650, 648, 648, 648, 648, 648, 643, 653, 653, 653, 653, 652, 627, 652.]

C-terminal

Fig. 1.3 Multiple-sequence alignment of 18 aquareoviruses and 6 orthoreoviruses outer shell proteins VP5 and μ1. N-terminal (top) and C-terminal (bottom) portions of the alignments are shown. The alignment is generated using the program Clustal W2 as implemented at http://guidance.tau.ac.il. The number at the right end of each line indicates the position of the last amino acid in the sequence. Identities (*), strong similarities (:), and weaker similarities (.) in the aligned sequences are indicated at bottom. The autolytic cleavage site at the Asn42-Pro43 bond is indicated (arrow). The two green box markers indicate the absent sequences in VP5 of AqRVs in comparison with μ1 of orthoreoviruses. The virus strains and sequence accession numbers are MRV-T1L (AF490617), MRV-T3D(EF494439), MRV-T2J(M19355), ARV-138(AY750052), ARV-176 (AY750053), BRV(YP_004769551), GCRV-104(AFG73677), GCRV-ZH08(ADJ75338), GCRV-109(AHD25640), GCRV-GD108(ADT79743), AGCRV(ABV01044), GSRV (NP938065), GCRV-873(AF403392), GCHV-873(AAG17823), GCRV-GZ1208(ANE37527), GCRV-96(AFK88593), CSRV(YP398639), SMReV(ADZ31981), EFRV(YP009259501), TFV (AAP72182), MsReV(AJD09451), FCRV(KX891220), GRCV(AHJ14805), AHRV(MH108640)

(Fig.1.2b). Generally, except for the S7 and S11 segments, the remaining segments (S8, S9, and S10) in the S class encode functional proteins VP6 (core shell clamp), NS38/NS3 (RNA binding), and S10 (outer capsid shell clamp), which remain conserved with functional domains similar to those of σ2, σ3, and μNS of MRV, respectively [42, 58]. In most AqRVs, the S7 genome segments have two ORFs, which encode two proteins. One is the nonstructural FAST protein contained in AqRVs and most orthoreoviruses [14, 63], which induces syncytium formation by

promoting cell-to-cell fusion and then leads to complete release of progeny virions. The other is also an unknown nonstructural protein (NS31), which may play a role in regulating cellular proteins during infection [87]. This indicates that the proteins encoded by the small genome segments are more divergent than that encoded by the large and medium segments. In particular, it has been recently found that the gene segment S7 of GCRV-GD108/-ZH08, GCRV-104, and GCRV-109 encodes a σ1-like protein of MRV instead of the nonstructural FAST protein of AqRV [21, 59, 79, 86], which is also found in the PRV [41, 57]. In addition, a recent sequence analysis indicated that the S11 segment of AHRV and GCRV-109 (GCReV-109) encodes the outer shell clamp protein VP7 [59, 76], while most of the AqRV S11 segments encode nonstructural proteins (e.g., NS26), which may interact with host cell factors during viral replication [32].

Divergence of GCRV: Fusogenic and Non-fusogenic GCRV AqRVs are generally recognized to be fusogenic, except for PRVs (10 genomic segments) [41], and can produce large syncytia as a CPE in permissive cell cultures. Interestingly, some reovirus strains recently isolated from grass carp have been observed to be unable to produce syncytium in cultured fish cells, such that the nascent viral particles are incompletely released from infected cells. Studies have indicated that the ability of reoviruses to form a syncytium in infected cells is determined by the reovirus small class genome segments that encode the FAST protein [14]. Indeed, careful comparisons of cell culture characteristics between different GCRV isolates (such as GCRV-873 and GCRV-JX01; GCRV-ZH08/-GD108, GCRV-104, and GCRV-109) clearly showed that the GCRV-873 and GCRV-JX01 induced syncytium in permissive cells is dependent on their genome-encoded FAST proteins. No genome-encoded FAST protein assignment has been found in GCRV-ZH08/-GD108, GCRV-104, and GCRV-109 species, which do not exert any CPE in cultures of infected cells [59, 86]. The 11 genomic segments of GCRV-873 encode at least 12 proteins, and 7 structural proteins have been approved by cryo-EM and three-dimensional image reconstruction. The three predicted nonstructural proteins NS80, NS38, and NS16 and their functional domains, which are encoded by the S4, S7, and S9 segments, have been verified to be related to VIB formation, RNA binding, and syncytium formation, respectively [31, 92]. In addition, the remaining two nonstructural proteins NS26 and NS31 may regulate viral replication by interacting with cellular factors [32, 87]. NS12, encoded by the S7 segment of GCRV, has been identified as a novel membrane-associated protein [88].

More than 50 GCRV species have been isolated and identified to date; genome sequences of at least 12 GCRV strains have been characterized completely (Table 1.4), and most GCRV isolates have been partially sequenced [65, 91], which suggests that GCRVs are largely divergent in their genome sequence and virulence. Moreover, the GCRV core clamp protein VP6 gene sequence, determined for most GCRV isolates in China, is available for genetic comparison analyses. Three GCRV types have been catalogued based on genome sequence identity analysis. These are GCRV-I (GCRV-873, the original GCRV strain), GCRV-II (GCRV-ZH08/-GD108), and GCRV-III (GCRV-104) [79]. These recently reported

GCRV isolates are clearly divergent from isolates in the AqRV-C and -G groups, and thus should be classified as new species. The representative strain of GCRV I is the original GCRV-type strain (GCRV-873), which shares approximately 99% sequence identity with GSRV (the prototype strain of the AqRV-C group) [3]. In the GCRV I group, the identity among five GCRV isolates (GCRV-873, −096, −875, −876, and − 991) varies from 72.5% to 99.7%, whereas in the GCRV-II group, the identity among isolates GCRV-HZ08, -GD108, and -HA-2011 varies from 72.6% to 98.7% [79]. The representative strains of GCRV-II are GCRV-HZ08 and GCRV-GD108, and complete genome sequences from other newly identified isolates (including complete genome sequences of GCRV-106, GCRV-918, GCRV-HuNan794, and GCReV-109) and partial sequences of isolates (including GCRV-097, GCRV-JX02, GCRV-HA-2011, GCRV-ZS11, GCRV-QC11, GCRV-YX11, GCRV-QY12, GCRV-NC11, GCRV-JS12, GCRV-HS11, and GCRV-HN12) have been added to GenBank [57, 65]. A recent study showed that the GCReV-109 genome sequence is most closely related to that of GCRV-GD108 and shares 96.6–99.5% protein sequence identity, but shares only 16.7–46.1% and 15.1–45.4% identities with GCRV-873 and GCRV-104 (HGDRV), respectively [59]. These results indicate that GCRV-II is a dominant epidemic reovirus strain for grass carp [80, 90]. In addition, co-infection cases of GCRV-I and GCRV-II have been detected [59, 81]. GCRV-104 has no other closely related isolates found so far, based on sequence analysis and genome-based RNA detection [59, 90]. Thus, only one strain of GCRV-104 belongs to the GCRV III group, which shares 19.2% and 16.5% identities with GCRV-873 (GCRV-I) and GCRV-HZ08 (GCRV-II), respectively, indicating that several GCRV genotypes do exist simultaneously in grass carp hosts in China.

Genome Sequence-based Similarities and Differences Between Genera *AqRV* and *Orthoreovirus* Although AqRVs share basic common characteristics with orthoreoviruses, they are largely divergent based on complete and partial genome sequence information and phylogenetic analyses as well as the host ranges. The genome sequence-based evolution of conserved proteins and functional domains as well as the host adaptability and water environment-related divergent selection in AqRVs and orthoreoviruses may depend on the viral genome-encoded protein structure conformation and function in viral replication and assembly. In addition, although AqRVs and orthoreoviruses belong to different genera in the family *Reoviridae*, both viruses share a number of common structural characteristics, including particle-related protein architecture, replication-essential VIBs, and nonstructural proteins. However, the existence of great variability among the different AqRV isolates is based on not only the differences in virulence but also the increased complexity in phylogenetic relationships among the members of genera *AqRV* and *Orthoreovirus*. The divergence observed among coding sequences and proteins in the *AqRV* small class genome segments is often peculiar. It appears that the nucleotide sequences evolve to the point of apparent randomness, according to the obtained a mass of genome sequence information. Despite this divergence, the evolution of the AqRV cell penetration protein maintains a conserved functional

domain and conformation for cell entry (Fig. 1.3). In addition, the FAST proteins, even though a diverse group with little to no sequence homology between the identified NS16, NS22, or p22 in AqRVs, and the P10, P14, and P15 in ARV, retain similar structural motifs that are essential to their predicted membrane topology, and therefore their syncytium-producing abilities [14, 31, 38, 63].

In conclusion, over the last few decades, the isolation of AqRVs from healthy and diseased fish and shellfish has increased significantly, probably due to the increased surveillance of wild and cultured populations [76, 80, 89]. Although most AqRVs may not exhibit large mortalities among the cultured fish species, great attention needs to be paid to vertical and horizontal transmission via the carrier state of eggs, subclinical infection in cultivated aquatic animals, and shedding of the virus particles by carrier fish, all of which could infect susceptible fish species causing large epidemics and mortality. With our current understanding of the general biology, genetics, genome-encoded proteins, and protein structure-based functions of the AqRV, a more effective immune prevention and control strategy along with diagnostic testing tools to detect different AqRV species can be proposed. Despite the great diversity in AqRV species and the increased complexity of interactions between the individual virus and host cell response upon viral infection, the outer coat and viral replication-related proteins of particle and conserved functional protein domains should be the best targets for developing vaccines and safety drugs to prevent AqRV infection effectively. Further detailed studies on AqRV pathogenesis and host defense-related immune mechanisms will enrich our understanding of the mutual counterplots and common evolution among the virus and host cells during AqRV infection.

References

1. Ahne W (1994) Viral infectious of aquatic animals with special reference to Asia aquaculture. Annu Rev Fish Dis 4:375–388
2. Amend DF, McDowell T, Hedrick RP (1984) Characteristics of a previously unidentified virus from channel catfish (Ictalurus punctatus). Can J Fish Aquat Sci 41:807–811
3. Attoui H, Fang Q, Jaafar FM, Cantaloube JF, Biagini P, de Micco P, de Lamballerie X (2002) Common evolutionary origin of aquareoviruses and orthoreoviruses revealed by genome characterization of Golden shiner reovirus, grass carp reovirus, striped bass reovirus and Golden ide reovirus (genus Aquareovirus, family Reoviridae). J Gen Virol 83:1941–1951
4. Attoui H, Mertens PPC et al (2012) Reoviridae. In: King AMQ, Adams MJ, Carstens EB, Lefkowitz EJ (eds) Ninth report of the international committee on taxonomy of viruses. Elsevier Academic Press, San Diego, pp 541–637
5. Blindheim S, Nylund A, Watanabe K, Plarre H, Erstad B, Nylund S (2015) A new aquareovirus causing high mortality in farmed Atlantic halibut fry in Norway. Arch Virol 160:91–102
6. Borsa J, Copps TP, Sargent MD, Long DG, Chapman JD (1973) New intermediate subviral particles in the in vitro uncoating of reovirus virions by chymotrypsin. J Virol 11:552–564
7. Brady YJ, Plum JA (1988) Serological comparison of golden shiner, chum salmon virus, reovirus 13p2 and catfish reovirus. J Fish Dis 11:441–443

8. Carlile G, East IJ, McColl KA, Ellard K, Browning GF, Crane MSJ (2014) The spatial and temporal variation of the distribution and prevalence of Atlantic salmon reovirus (TSRV) infection in Tasmania, Australia. Prev Vet Med 116:214–219

9. Chen C, Sun X, Liao L, Luo S, Li Z, Zhang X (2013) Antigenic analysis of grass carp reovirus using single-chain variable fragment antibody against IgM from Ctenopharyngodon idella. Sci China Life Sci 56:59–65

10. Chen YX, Jiang Y (1983) Morphological and physico-chemical characterization of the hemorrhagic virus of grass carp. Kexue Tonboga 28:1138–1140

11. Chen ZY, Gao XC, Zhang QY (2015) Whole-genome analysis of a novel fish reovirus (MsReV) discloses aquareovirus genomic structure relationship with host in saline environments. Viruses 7:4282–4302

12. Cheng L, Fang Q, Shah S, Atanasov IC, Zhou ZH (2008) Subnanometer resolution structures of the grass carp reovirus core and virion. J Mol Biol 382:213–222

13. Cheng L, Zhu J, Hui WH, Zhang X, Honig B, Fang Q, Zhou ZH (2010) Backbone model of an aquareovirus virion by cryo-electron microscopy and bioinformatics. J Mol Biol 397:852–863

14. Ciechonska M, Duncan R (2014) Reovirus FAST proteins: virus-encoded cellular fusogens. Trends Microbiol 22:715–724

15. Cusack RR et al (2001) Pathology associated with an aquareovirus in captive juvenile Atlantic halibut Hippoglossus hippoglossus and an experimental treatment strategy for a concurrent bacterial infection. Dis Aquat Org 44(1):7–16

16. Day JM (2009) The diversity of the orthoreoviruses: molecular taxonomy and phylogentic divides. Infect Genet Evol 9:390–400

17. DeWitte-Orr SJ, Bols NC (2007) Cytopathic effects of chum salmon reovirus to salmonid epithelial, fibroblast and macrophage cell lines. Virus Res 126:159–171

18. Ding QQ, Yu LF, Ke LH (1990) Preliminary study of the influence of water temperature on the grass carp hemorrhage disease. Virol Sin 2:215–220

19. Ding QQ, Yu LF, Ke LH, Cai YQ (1991) Study of infecting other fishes with grass carp hemorrhage virus. Virol Sin 6:371–373

20. Dopazo CP, Toranzo AE, Samal SK, Roberson BS, Baya A, Hetrick FM (1992) Antigenic relationships among rotaviruses isolated from fish. J Fish Dis 15:27–36

21. Fan Y, Rao S, Zeng L, Ma J, Zhou Y, Xu J, Zhang H (2013) Identification and genomic characterization of a novel fish reovirus, Hubei grass carp disease reovirus, isolated in 2009 in China. J Gen Virol 94:2266–2277

22. Fang Q, Ke LH, Cai YQ (1989) Growth characteristics and high titer culture of grass carp hemorrhage virus (GCHV)-873 in vitro. Virol Sin (In Chinese with English Abstract)

23. Fang Q, Attoui H, Biagini JF, Zhu Z, de Micco P, de Lamballerie X (2000) Sequence of genome segments 1, 2, and 3 of the grass carp reovirus (genus aquareovirus, family reoviridae). Biochem Biophys Res Commun 274:762–766

24. Fang Q, Xiao TY, Ding QQ et al (2002) Virological properties of GCRV 991 strain. Virol Sin 17(2):183–187. (In Chinese with English Abstract)

25. Fang Q, Shah S, Liang Y, Zhou ZH (2005) 3D reconstruction and capsid protein characterization of grass carp reovirus. Sci China Ser C 48:593–600

26. Fang Q, Seng EK, Ding QQ, Zhang LL (2008) Characterization of infectious particles of grass carp reovirus by treatment with proteases. Arch Virol 153:675–682

27. Francki RIB, Fauquet CM, Knudson SL, Brown F (1991) Classification and nomenclature of viruses, 5th report of the international committee on taxonomy of viruses. Arch Virol 2 (Suppl):186–1991

28. Goodwin AE, Nayak DK (2006) Natural infections of wild creek chubs and cultured fathead minnow by Chinese grass carp reovirus (golden shiner virus). J Aquat Animal Health 18:35–38

29. Goodwin AE, Merry GE, Attoui H (2010) Detection and prevalence of the nonsyncytial American grass carp reovirus aquareovirus G by quantitative reverse transcriptase polymerase chain reaction. J Aquat Animal Health 22:8–13

30. Grass Carp Hemorrhagic Disease Research Group of Wuhan Institute Virology, Academia Sinica, and Yangtze River Fisheries Research Institute, Chinese Academy of Fishery Sciences (1983) Observation of grass carp hemorrhagic virus. Fresh Water Fishery of China 3:39–41

31. Guo H, Sun X, Yan L, Shao L, Fang Q (2013) The NS16 protein of aquareovirus-C is a fusion-associated small transmembrane (FAST) protein, and its activity can be enhanced by the nonstructural protein NS26. Virus Res 171:129–137

32. Guo H, Chen Q, Yan L, Zhang J, Yan S, Zhang F, Fang Q (2015) Identification of a functional motif in the AqRV NS26 protein required for enhancing the fusogenic activity of FAST protein NS16. J Gen Virol 96:1080–1085

33. He Y, Xu H, Yang Q, Xu D, Lu L (2011) The use of an in vitro microneutralization assay to evaluate the potential of recombinant VP5 protein as an antigen for vaccinating against grass carp reovirus. Virol J 8:132

34. Hedrick RP, Rosemark R, Aronstein D, Winton JR, McDowell T, Amend DF (1984) Characteristics of a new reovirus from channel catfish (Ictalurus *punctatus*). J Gen Virol 65:1527–1534

35. Huang J, Ke LH, Cai YQ (1992) Study on the reaction core of grass carp hemorrhage virus. Acta Biochem Biophys Sinica 24(2):132–139

36. Huang J, Ke LH, Cai YQ (1992) Ribonucleic acid transcriptase activity associated with purified grass carp hemorrhage disease. Chinese J Virol 8(1):50–56

37. Iwanowicz LR, Iwanowicz DD, Adams CR, Lewis TD, Brandt TM, Cornman RS, Sanders L (2016) Complete genome sequence of a novel Aquareovirus that infects the endangered fountain darter, Etheostoma fonticola. J Virol Genome Announc 4

38. Ke F, He LB, Pei C, Zhang QY (2011) Turbot reovirus (SMReV) genome encoding a FAST protein with a non-AUG start site. BMC Genomics 12:323

39. Ke L, Fang Q, Cai Y (1990) Characteristics of a new isolation of hemorrhagic virus of grass carp. Acta Hydrobiol Sin 14:153–159. (in Chinese with English Abstract)

40. Ke LH, Wang W, Fang Q, Cai YQ (1992) Studies on the in vitro translation of grass carp hemorrhage virus and its proteins. Chinese J Virol (8)2:169–193

41. Key T, Read J, Nibert ML, Duncan R (2013) Piscine reovirus encodes a cytotoxic, non-fusogenic, integral membrane protein and previously unrecognized virion outer-capsid proteins. J Gen Virol 94:1039–1050

42. King AMQ, Adams MJ, Carstens EB, Lefkowitz EJ (2012) Virus taxonomy, ninth report of the international committee on taxonomy of viruses. Elsevier, San Diego

43. Leland MM, Hubbard GB, Sentmore HT, Soike KF, Hilliard JK (2000) Outbreak of *Orthoreovirus*-induced meningoencephalomyelitis in baboons. Comp Med 50:199–205

44. Lupiani B, Dopazo CP, Ledo A, Fouz B, Barja JL, Hetrick EM, Toranzo AE (1989) New syndrome of bacterial and viral etiology in cultured turbot *Scophthalmus maximus*. J Aquat Animal Health 1:197–204

45. Lupiani B, Subramanian K, Samal SK (1995) Aquareovirus. Annu Rev Fish Dis 5:175–208

46. Lupiani B, Reddy SM, Subramanian K, Samal SK (1997) Cloning, sequence analysis and expression of the major outer capsid protein gene of an aquareovirus. J Gen Virol 78:1379–1383

47. Lupiani B, Reddy SM, Samal SK (1997) Sequence analysis of genome segment 10 encoding the major outer capsid protein (VP7) of genogroup B aquareovirus and its relationship with the VP7 protein of genogroup A aquareovirus. Arch Virol 142:2547–2552

48. Makhsous N, Jensen NL, Haman KH, Batts WN, Jerome KR, Winton JR, Greninger AL (2017) Isolation and characterization of the fall Chinook aquareovirus. Virol J 14:170. https://doi.org/10.1186/s12985-017-0839-9

49. Marshall SH, Samal SK, McPhillips TH, Moore AR, Hetrick FM (1990) Isolation of a rotavirus from smelt, Osmerus mordax (Mitchell). J Fish Dis 13:87–91

50. McEntire ME, Iwanowicz LR, Goodwin AE (2003) Molecular, physical, and clinical evidence that golden shiner virus and grass carp reovirus are variants of the same virus. J Aquat Animal Health 15:257–263

51. McPhillips TH, Dinan D, Subramanian K, Samal SK (1998) Enhancement of aquareovirus infectivity by treatment with proteases: mechanism of action. J Virol 72:3387–3389

52. Meyers TR (1979) A reo-like virus isolated from juvenile American oysters (Crassostrea virginica). J Gen Virol 43:203–212

53. Meyers TR (1980) Experimental pathogenicity of reovirus 13p2 for juvenile American oysters Crassostrea virginica (Gmelin) and bluegill fingerlings Lepomis macrochirus (Rafinesque). J Fish Dis 3:187–201

54. Meyers TR (1983) Serological and histopathological responses of rainbow trout, Salmo gairdneri Richardson, to experimental infection with the 13p2 reovirus. J Fish Dis 6:277–292

55. Mohd-Jaafar F, Goodwin AM, Merry G, Fang Q, Cantaloube J, Biagini P, De-Micco P, Mertens P, Attoui H (2008) Complete characterisation of the American grass carp reovirus genome (genus Aquareovirus: family Reoviridae) reveals an evolutionary link between aquareoviruses and coltiviruses. Virology 373:310

56. Nason EL, Samal SK, Venkataram Prasad BV (2000) Trypsin induced structural transformation in aquareovirus. J Virol 74:6546–6555

57. Nibert ML, Duncan R (2013) Bioinformatics of recent aqua- and orthoreovirus isolates from fish: evolutionary gain or loss of FAST and fiber proteins and taxonomic implications. PLoS One 8:e68607

58. Nibert ML, Schiff LA, Fields BN (2001) Reoviruses and their replication. In: Knipe DM, Howley PM (eds) Fields virology. Lippincott Williams and Wilkins, Philadelphia, pp 1679–1728

59. Pei C, Ke F, Chen ZY, Zhang QY (2014) Complete genome sequence and comparative analysis of grass carp reovirus strain 109 (GCReV-109) with other grass carp reovirus strains reveals no significant correlation with regional distribution. Arch Virol 159:2435–2440

60. Plumb J, Bowser PR, Grizzle JM, Mitchell AJ (1979) Fish viruses: double-stranded RNA icosahedral virus from a North American cyprinid. J Fish Res Board Can 36:1390–1394

61. Qiu T, Lu RH, Zhang J, Zhu ZY (2001a) Complete nucleotide sequence of the S10 genome segment of grass carp reovirus (GCRV). Dis Aquat Org 44:69–74

62. Qiu T, Lu RH, Zhang J, Zhu ZY (2001b) Molecular characterization and expression of the M6 gene of grass carp hemorrhage virus (GCHV), an aquareovirus. Arch Virol 146:1391–1397

63. Racine T, Hurst T, Barry C, Shou J, Kibenge F, Duncan R (2009) Aquareovirus effects syncytiogenesis by using a novel member of the FAST protein family translated from a noncanonical translation start site. J Virol 83(11):5951–5955

64. Rangel AAC, Rockemann DD, Hetrick FM, Samal SK (1999) Identification of grass carp haemorrhage virus as a new genogroup of aquareovirus. J Gen Virol 80:2399–2402

65. Rao Y, Su J (2015) Insights into the antiviral immunity against grass carp (Ctenopharyngodon idella) reovirus (GCRV) in grass carp. J Immunol Res 2015:670437

66. Raynard R, Wahli T, Vatsos I, Mortensen S (2007) Review of disease interactions and pathogen exchange between farmed and wild finfish and shellfish in Europe. VESO, Oslo

67. Rivas C, Noya M, Cepeda C, Bandin I, Barja JL, Dopazo CP (1998) Replication and morphogenesis of the turbot aquareovirus (TRV) in cell culture. Aquaculture 160:47–62

68. Samal SK, Dopazo CP, McPhillips TH, Baya A, Mohanty SB, Hetrick FM (1990) Molecular characterization of a rotavirus-like virus isolated from striped bass (Morone saxatilis). J Virol 64:5232–5240

69. Samal SK, McPhillips T H, Dinan D et al (1998) Lack of restriction of growth for aquareovirus in mammalian cells. Arch Virol 143(3):571–579

70. Section of Virus Study (Section of Virus Study, Third Laboratory, Institute of Hydrobiology, Academia Sinica) (1980) Studies on the causative agent of hemorrhage of the grass carp (Ctenopharyngodon idellus) II. Electron microscopic observation. Acta Hydrobiol Sin 7:75–79. (In Chinese)

71. Seng EK, Fang Q, Chang SF, Ngoh GH, Qin QW, Lam TJ, Sin YM (2002) Characterisation of a pathogenic virus isolated from marine threadfin fish (Eleutheronema tetradactylus) during a disease outbreak. Aquaculture 214:1–18

72. Seng EK, Fang Q, Sin YM, Lam TJ (2005) Molecular characterization of a major outer capsid protein encoded by the threadfin aquareovirus (TFV) gene segment 10 (S10). Arch Virol 150:2021–2036

73. Seng EK, Fang Q, Sin YM, Lam TJ (2005) Molecular cloning, DNA sequence analysis, and expression of cDNA sequence of RNA genomic segment 6 (S6) that encodes a viral outer capsid protein of threadfin aquareovirus (TFV). Virus Genes 30:209–221

74. Shao L, Sun X, Fang Q (2011) Antibodies against outer-capsid proteins of grass carp reovirus expressed in E. coli are capable of neutralizing viral infectivity. Virol J 8:347

75. Shaw AL, Samal S, Subramanian K, Prasad BVV (1996) The structure of aquareovirus shows how different geometries of the two layers of the capsid are reconciled to provide symmetrical interactions and stabilization. Structure 15:957–968

76. Skoge RH, Nylund A, Solheim K, Heidrun Plarre H (2019) Complete genome of Atlantic halibut reovirus (AHRV) associated with mortality in production of Atlantic halibut (Hippoglossus hippoglossus) fry. Aquaculture 509:23–31

77. Subramanian K, McPhillips TH, Samal SK (1994) Characterization of the polypeptides and determination of genome coding assignments of an aquareovirus. Virology 205(1):75–81

78. Wang H, Yu F, Li J, Lu L (2016) Laminin receptor is an interacting partner for viral outer capsid protein VP5 in grass carp reovirus infection. Virology 490:59–68

79. Wang Q, Zeng W, Liu C, Zhang C, Wang Y, Shi C, Wu S (2012) Complete genome sequence of a reovirus isolated from grass carp, indicating different genotypes of GCRV in China. J Virol 86:12466

80. Wang Q, Zeng WW, Yin L (2016) Comparative study on physical-chemical and biological characteristics of grass carp reovirus from different genotypes, J. World Aquac Soc 47:862–872

81. Wang T, Li J, Lu L (2013) Quantitative in vivo and in vitro characterization of co-infection by two genetically distant grass carp reoviruses. J Gen Virol 94:1301–1309

82. Wang W, Cai YQ, FangQ LY, Kel (1994) Gene-protein-coding assignments of grass carp hemorrhage virus genome RNA species. Virol Sin 9(4):356–361

83. Wang X, Zhang F, Su R, Li X, Chen W, Chen Q, Yang T, Wang J, Liu H, Fang Q, Cheng L (2018) Structure of RNA polymerase complex and genome within a dsRNA virus provides insights into the mechanisms of transcription and assembly. Proc Natl Acad Sci 115:7344–7349

84. Winton JR, Lannan CN, Fryer JL, Kimura T (1981) Isolation of a new reovirus from chum salmon in Japan. Fish Pathol 15:155–162

85. Winton JR, Lannan CN, Fryer JL, Hedrick RP, Meyers TR, Plumb JA, Yamamoto T (1987) Morphological and biochemical properties of four members of a novel group of reoviruses isolated from aquatic animals. J Gen Virol 68:353–364

86. Ye X, Tian YY, Deng GC, Chi YY, Jiang XY (2012) Complete genomic sequence of a reovirus isolated from grass carp in China. Virus Res 163(1):275–283

87. Yu F, Wang LL, Li WJ, Wang H , Que SJ, Lu LQ (2019) Aquareovirus NS31 protein serves as a specific inducer for host heat shock 70-kDa protein. J Gen Virol. https://doi.org/10.1099/jgv.0.001363

88. Yu F, Wang LL, Wanjuan Li WJ, Lu L (2019) Identification of a novel membrane-associated protein from the S7 segment of grass carp reovirus. J Gen Virol 100(3):369–379

89. Zainathan SC, Carson J, Nowak BF (2017) Preliminary characterization of Tasmanian aquareovirus (TSRV). Arch Virol 162:625–634

90. Zeng WW, Yao W, Wang Q et al (2017) Molecular detection of genotype II grass carp reovirus based on nucleic acid sequence-based amplification combined with enzyme-linked immunosorbent assay (NASBA-ELISA). J Virol Methods 243:92–97

91. Zeng WW, Wang YY, Guo YM, Bergmann SM, Yin JY, Li YY, Ren Y, Shi CB, Wang Q (2018) Development of a VP 38 recombinant protein-based indirect ELISA for detection of antibodies against grass carp reovirus genotype II (iELISA for detection of antibodies against GCRV II). J Fish Dis 41(12):1811–1819

92. Zhang J, Guo H, Chen Q, Zhang F, Fang Q (2016) The N-terminal of aquareovirus NS80 is required for interacting with viral proteins and viral replication. PLoS One 11:e0148550

93. Zhang J, Guo H, Zhang FX, Chen QX, Chang MX, Fang Q (2019) NS38 is required for aquareovirus replication via interaction with viral core proteins and host eIF3A. Virology 2019 (529):216–225

94. Zhang X, Jin L, Fang Q, Hui WH, Zhou ZH (2010) 3.3 Å cryo-EM structure of a nonenveloped virus reveals a priming mechanism for cell entry. Cell 141:472–482

Chapter 2
Molecular Biology of Aquareoviruses

Qin Fang, Jie Zhang, and Fuxian Zhang

Abstract Aquareoviruses are nonenveloped multiple-shelled particles composed of a genome of 11 double-stranded RNA segments, which encode at least 12 proteins. Among the seven approved *Aquareovirus* species (*Aquareovirus A-G*), the striped bass reovirus in the *Aquareovirus A* (AqRV-A) group and grass carp reovirus (GCRV) in the *Aquareovirus-C* (AqRV-C) group have been well studied. Intact virions are composed of five inner shell proteins (ISPs; VP1–VP4 and VP6) and two outer capsid proteins (OCPs; VP5 and VP7). The inner core proteins contain all endogenous enzymes responsible for viral transcription and replication. During cellular entry, intermediate sub-viral particles or core particles can be generated by the uncoating of the OCPs VP5 and VP7. In addition to the seven structural proteins of the viral particle, the remaining five proteins have been approved as nonstructural (NS) proteins (NS80/NS1, NS38/NS2, NS31/NS3, NS26/NS4, and NS16/NS5), except the newly identified NS12. Three genotypes of GCRVs (GCRV-I, -II, and -III) have been classified from infected grass carp in China. Studies indicate that NS80 and NS38 of GCRV-I are related to viral inclusion body formation during replication and morphogenesis. Furthermore, NS16 and NS12, encoded by the S7 segment, have been found to play critical roles as fusion-associated small transmembrane proteins to induce syncytium formation via cell–cell fusion. However, no such protein, instead of a fiber protein on the particle surface, which is a counterpart of the orthoreovirus σ1-cell attachment protein, has been found in GCRV-II. Moreover, other NS proteins may be involved in viral replication and pathogenesis via interaction with host cells. This chapter outlines the molecular biology of aquareoviruses.

Q. Fang (✉)
State Key Laboratory of Virology, Wuhan Institute of Virology, Chinese Academy of Sciences, Wuhan, China
e-mail: qfang@wh.iov.cn

J. Zhang
State Key Laboratory of Freshwater Ecology and Biotechnology, Institute of Hydrobiology, Chinese Academy of Sciences, Wuhan, China

F. Zhang
College of Animal Science, Yangtze University, Jingzhou, Hubei, China

Abbreviations

AHRV	Atlantic halibut reovirus
AqRV	Aquareovirus
ARV	Avian reovirus
BF-2	Bluegill fry
CCRV	Channel catfish reovirus
CHSE	Chinook salmon embryo
CIK	*Ctenopharyngodon idella* kidney
CoSRV	Coho salmon reovirus
CPE	Cytopathic effect
CSRV	Chum salmon reovirus
FAST	Fusion-associated small transmembrane
FHM	Fathead minnow
GCHV	Grass carp hemorrhage virus
GCRV	Grass carp reovirus
GSRV	Golden shiner reovirus
ISPs	Inner shell proteins
MRV	Mammalian orthoreovirus
MSReV	*Micropterus salmoides* reovirus
NCR	Non-coding region
NS	Nonstructural
OCPs	Outer capsid proteins
ORF	Open reading frame
p.i.	Post-infection
PB	Polybasic
PRV	Piscine orthoreovirus
RdRP	RNA-dependent RNA polymerase
SBRV	Striped bass reovirus
SMReV	Turbot *Scophthalmus maximus* reovirus
SVP	Sub-viral particle
TEM	Transmission electron microscopy
TFV	Threadfin reovirus
TM	Transmembrane
TRV	Turbot reovirus
VIBs	Virus inclusion bodies

2.1   Introduction

Genus *Aquareovirus* is one of the approved members of the family *Reoviridae* and grouped in the *Spinareovirinae* or "turreted" sub-family [30]. The viruses have been isolated from freshwater and seawater aquatic organisms in a wide range of global water areas. Generally, aquareoviruses (AqRVs) are of low pathogenicity in breeding aquatic animals and often detected by routine examination of seemingly healthy fish and shellfish [32]. However, some members of this genus are important fish pathogens that are capable of causing severe hemorrhagic disease, hepatitis, and pancreatitis, leading to a high mortality rate in some cases [12, 32, 33, 37, 52, 54, 60]. Therefore, these viruses pose a significant threat to global aquaculture.

Similar to other members of the *Reoviridae* family, AqRVs contain 11 double-stranded RNA (dsRNA) genome segments that are packaged into two well-organized concentric protein shells, called the inner or core shell and outer capsid. The viral particles are nonenveloped icosahedral particles with a diameter of approximately 75 nm, which has been determined by negative staining in transmission electron microscopy (TEM) analysis [27, 32, 46, 67]. AqRVs, belonging to the *Spinareovirinae* group, have relatively large spikes or turret structures situated at the 12 icosahedral vertices of either the intact virion or the core particle [2, 17]. Morphologically, these viruses resemble mammalian orthoreoviruses (MRVs), while the 11 genomic segments are similar in composition to those in the members of the "non-turreted" genus *Rotavirus* [30]. Based on the morphological and genomic properties of AqRVs isolated from aquatic animals, these were initially referred to as reovirus-like or rotavirus-like agents [36, 46, 54]. However, no cross-reactions are detected between turreted MRVs and non-turreted rotaviruses according to the antigenicity and reciprocal RNA–RNA dot-blot hybridization analyses in earlier studies [9, 32, 38, 52]. Recent nucleotide sequence analysis and comparisons between *Aquareovirus* and other genera in the family *Reoviridae* have suggested that there is a close evolutionary relationship between members of the genera *Aquareovirus* and *Orthoreovirus* [1, 2, 13], which has been further supported by three-dimensional structural reconstruction studies (in Chap. 3). Seven *Aquareovirus* species (*Aquareovirus A-G*) have been approved by the International Committee on Taxonomy of Viruses [30, 39].

Since the first AqRV, golden shiner reovirus (GSRV), reported in the 1970s [46], a large number of AqRVs have been discovered [11, 27, 32, 36, 39, 45, 54, 60, 64, 71], and some pathogenic isolates have complete genome sequences characterized. However, their pathogenic roles in aquaculture remain to be fully elucidated. This chapter summarizes the molecular characteristics of several well-characterized AqRVs, especially grass carp reovirus (GCRV) and striped bass reovirus (SBRV), thus providing a general understanding of the natural biology and molecular properties of AqRVs. For GCRV, the strain GCRV-873 (GCRV-I), originally named as grass carp hemorrhage virus (GCHV), has been suggested as the prototype strain of GCRV species, and hence, it will be referred to as GCRV throughout this chapter.

2.2 Particle-Based Properties

2.2.1 Virus Proliferation and Sample Preparation

Unlike non-fusogenic orthoreoviruses, most AqRV isolates, such as GSRV, American oyster reovirus (strain 13p2), chum salmon reovirus (CSRV), channel catfish reovirus (CCRV), SBRV, GCRV, threadfin reovirus (TFV), and Atlantic halibut reovirus (AHRV), can efficiently replicate in permissive cell lines and induce syncytia as a typical cytopathic effect (CPE). The mature virions can be efficiently released from infected cells by cell lysis; hence, they are fusogenic. Cell lines such as chinook salmon embryo (CHSE), fathead minnow (FHM), bluegill fry (BF-2), *Ctenopharyngodon idella* kidney (CIK), and others are the most commonly used cell lines for plaque assays and proliferation of AqRVs for viral purification [11, 27, 32, 36, 39, 45, 54, 60, 64, 67, 71]. In addition, SBRV has been reported to replicate well in permissive mammalian cell lines (such as CV-1, HeLa, and Vero) and form typical syncytia [53]. In general, AqRV-infected cell cultures are harvested 3–6 days post-infection (p.i.) or when the CPE is extensive enough for virus purification and identification.

There are many different methods used for AqRV particle isolation and purification from infected cells or diseased fish tissues [16, 52, 67]. Despite their respective advantages in virion isolation, the traditional centrifugation method is commonly used. For general purification, some chemical and physical methods have been used on infected cells in the early stages. Sonication has been used to break virus-infected cells; thus, nascent virus particles can be efficiently released from infected cells. Next, using deoxycholate and Freon extraction, the virus particles are disassociated from the infected cell culture mixtures [52, 67]. In addition, owing to its fusogenic nature, AqRV can be disassociated from cell lysates using physical methods with several freeze-thaw cycles [14–16, 54]. After obtaining the virus-cell suspension, centrifugation at several different speeds generally needs to be performed to remove cell debris extensively. The first low-speed centrifugation is used to remove cell debris from the infected culture supernatant, followed by ultracentrifugation to precipitate viral particles. The virus pellet is suspended in $1\times$ SSC (0.15 M NaCl, 0.015 M sodium citrate, pH 7.4) or $1\times$ phosphate-buffered saline (PBS, 137 mM NaCl, 2.7 mM KCl, 8.1 mM Na_2HPO_4, 1.5 mM KH_2PO_4, pH 7.5). To obtain viral components for viral protein analyses or reconstruct three-dimensional images of viral particles, a CsCl equilibrium density or sucrose gradient purification is required for isolating various virus particle components from pelleted virus-cell preparations [15, 16, 67]. After obtaining a uniform viral layer in the centrifugation tube, harvested virions are either extensively dialyzed against TM buffer (50 mM Tris-HCl, pH 7.6, 10 mM $MgCl_2$) or further centrifuged to remove sucrose or salts. The concentrations of the purified viral particles can be determined from optical density measurements at 260 nm, as previously described [15, 16]. For freshly purified virions, short-term storage at 4 °C is the best for further TEM analysis. For long-term

storage or maintenance of the structural integrity of purified AqRV virions, storage temperatures of $-30\,^{\circ}\text{C}$ or $-80\,^{\circ}\text{C}$ are recommended.

2.2.2 Different Particle Components Extracted from Purified Virus Preparations

Intact virions are the predominant form of mature particles released from infected cell cultures or extracted from aquatic animal tissue homogenates. Intact virions of AqRV can readily undergo particle uncoating to yield intermediate or infectious sub-viral particles (SVPs) and core particles. This phenomenon is consistent with the orthoreoviruses or MRVs, wherein the SVP or the core also appears naturally in the course of infection and plays specific roles in the early and late replication stages [16, 43]. In addition, SVPs or cores can be generated in vitro by protease treatment of purified virions. Chymotrypsin or trypsin is commonly used to convert reovirus virions into infectious SVPs or cores in vitro [16, 35, 40].

MRV virions are relatively stable in natural environments and maintain infectivity for years when stored below 4 °C [43]. Similarly, AqRVs retain relatively high infectivity when stored at or below 4 °C [16, 51]. However, unlike the relatively stable MRV particles, the AqRV SVPs can easily be generated after few days of storage at 22–26 °C or 4 °C in laboratory conditions without undergoing any external treatment with proteases [16, 40]. In most cases, various viral components (including empty and core particles) can be observed from purified sample preparations by TEM.

2.2.2.1 Intact Virions and Empty Particles

During AqRV purification, two viral component layers with a clear opalescent appearance are often obtained after CsCl density gradient centrifugation, which correspond to approximately 1.31 and 1.37 g/cm^3 in buoyant density from the top of the tube to the bottom. The upper layer (top component) largely comprises double-shelled empty particles, while the lower layer contains intact virions or native virions (Fig. 2.1, upper panel). Electron micrograph of negatively stained purified virus preparations shows that an AqRV appears as a nonenveloped icosahedral particle with a double-layered capsid and is approximately 75 nm in diameter with 5:3:2 symmetry. The particles viewed along the fivefold axis of symmetry exhibit 20 capsomeres on the periphery of the outer capsid shell. Consistent with MRVs, purification of AqRV particles from infected cells often yields a substantial proportion of particles that lack genomic dsRNA [16, 67]. These empty particles have a lower buoyant density in the CsCl gradient and their respective layer is closer to the top of the gradient in comparison with intact particles (containing dsRNA genome), and hence, the empty particle is termed as the "top component." Both intact and
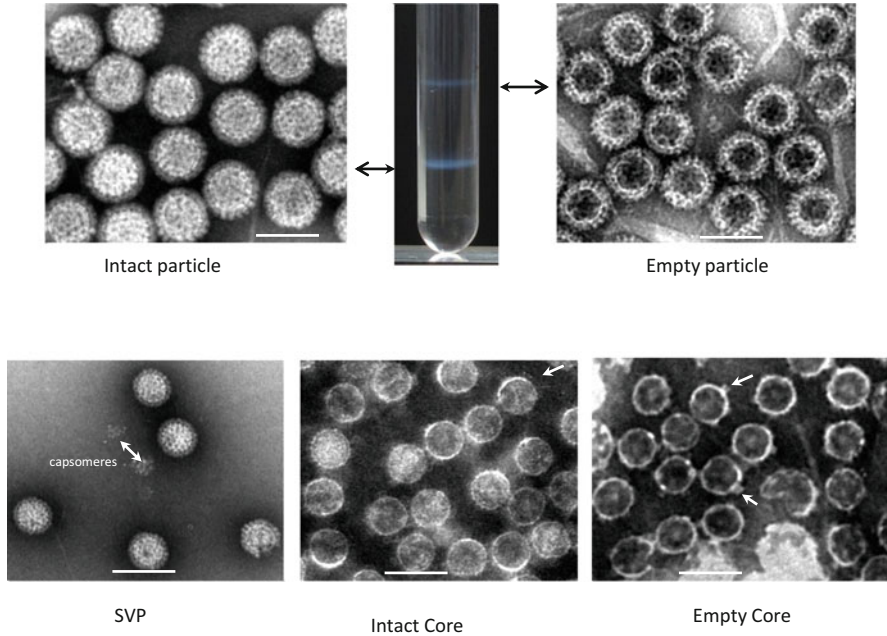
Fig. 2.1 Electron micrographs of negatively stained GCRV particles showing various particle components. Intact (left in upper panel) and empty particles (right in upper panel) are isolated from CsCl gradient centrifugation tube (medium in upper panel). Intermediate SVP, intact and empty cores are shown in lower panel. The SVP, intact and empty cores are generated by treatment with 100 mg/ml trypsin at 28 °C for 30 and 120 min, respectively. Double arrowhead in SVP image (left in lower panel) indicates some outer viral capsomeres removed from GCRV particle. Arrowheads indicate pentonal turrets situated at fivefold vertices in intact and empty core images (lower panel). The scale bars represent 100 nm

incomplete (empty) particles are observed in most purified AqRV preparations [11, 14–16, 45, 54, 71]. Moreover, the morphology of AqRV particles is strikingly the same as that of MRVs [15, 67]. The top component particles appear similar to intact virions in their morphology, but the central region of these particles can be penetrated by the stain, reflecting the absence of genomic dsRNA in the interior region of the top component particles [16].

2.2.2.2 SVP and Virus Core

For a detailed understanding of the particle components of AqRV, different forms of GCRV particles have been isolated from mock-treated and protease-treated virion preparations using an established CsCl gradient centrifugation procedure and then examined under an electron microscope. A visual inspection of the gradient centrifugation showed that the different particles form homogeneous layers with an opalescent appearance [16]. The four distinct layers, including two top component

layers, one medium, and one bottom layer, correspond to approximately 1.30, 1.31, 1.38, and 1.44 g/cm^3, respectively, in buoyant density from the top of the tube to the bottom. TEM observations revealed that after CsCl gradient centrifugation, the viral top components, including the empty double-layered capsids and empty single core shells, are located in the two top layers, and the intact virions and intact cores stand in the medium and bottom layers, respectively. Here, it should be noted that the intact virion with 1.38 g/cm^3 buoyant density might contain a few intermediate SVPs [16], which is very similar to naturally degraded particles of SBRV [40]. This result suggests that parts or some residues of the outermost protein VP7 may fall off from native particles in the virus preparations.

Treatment of AqRVs with proteases (chymotrypsin and trypsin) can generate intermediate SVPs and cores, similar to those reported in other AqRV isolates, such as SBRV [35, 40]. It has been reported that the digestion of the outermost capsid protein (OCP) VP7 of SBRV is associated with increased infectivity [35]. Examination of purified viruses treated with chymotrypsin showed that intact core particles are about 50–60 nm in diameter, which appeared to lack outer capsid capsomeres/proteins in comparison with intact virions of approximately 75 nm. Similarly, infectious SVPs of GCRV can be obtained by treating intact particles with protease (chymotrypsin or trypsin) for a short time. Long protease treatment removes all of the OCPs and exposes prominent turrets, while the core particle structure remains intact (Fig. 2.1, lower panel). Negatively stained TEM images reveal that the core particles exhibit projections at each fivefold vertex and some indistinct projections can be visualized on the empty core shell.

Of note, a few empty single outer capsid shells, empty double outer capsid shells, or single core particles are often found in preparations of natural viral particles without protease treatment, during the purification process or during long-term storage of viral stock at 4 °C. This indicates that the AqRV (or GCRV-873) particle structures are not stable during purification or long-term storage at 4 °C. The related structural architecture of GCRV-873 has been elucidated by three-dimensional image reconstruction [7, 15, 66], and it is described in Chap. 3.

In fact, similar to MRVs, different components of AqRVs (such as SVPs, empty particles, and cores) are also commonly observed in infected cells or tissue sample preparations, except for purified virus preparations that have been treated with chymotrypsin or trypsin under controlled conditions in vitro or virion disassembly during infection of cells [11, 16, 45, 50, 67]. The characteristics and properties of the various AqRV particle components are shown in Table 2.1.

2.2.3 The Virus-Antibody Immunocompound of GCRV

The immunocompound particle of GCRV, which includes its antibody, has been obtained by directly inoculating virions in infected cell culture supernatants with prepared anti-GCRV polyclonal antibodies [14]. In particular, an excellent aggregation of GCRV–antibody immune complexes has been visualized clearly by direct

Table 2.1 Characteristics of various aquareovirus particles and components

Particle forms	Buoyant density (g/cm^3 in CsCl)	Proteins	Genome	Size (TEM/cryo-EM)
Intact virions	1.37–1.38	VP1–VP7	+	75~85
Intact Core	1.44	VP1–VP4, V6	+	55~65
SVP[a]	1.38–1.39	VP1–VP6/ and Partial VP7	+	70~75
Empty particle	1.30	VP1–VP7	–	~75
Empty core	1.31	VP1–VP4, V6	–	50~60

[a]Mark indicates that partial VP7 fragment may remain in SVP [40, and unpublished data]

GCRV in infected CIK culture supernatants

GCRV after incubation with anti-GCRV-Ab

GCRV after incubation with anti-VP5Ab

GCRV after incubation with anti-VP7Ab

GCRV after incubation with anti-OCPs(VP7+VP5)pAbs
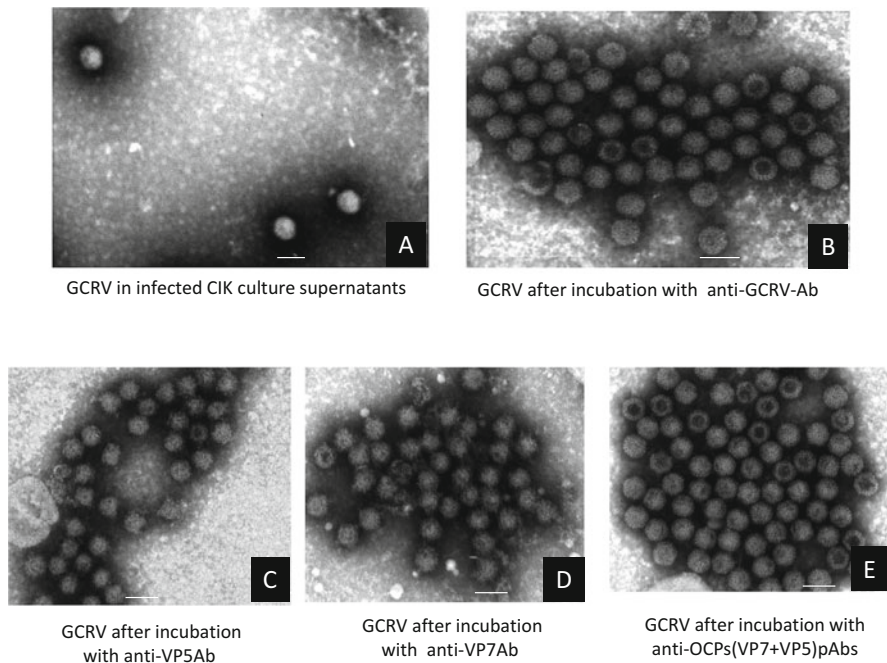
Fig. 2.2 TEM analysis of the immunocompound complex of GCRV. (**a**) TEM image of mock-treated GCRV-CIK culture supernatants. (**b, c, d, e**) TEM image of GCRV after incubation with anti-GCRV-Ab, VP5Ab, VP7Ab, and OCPs (VP5 + VP7)Abs. The scale bars represent 100 nm

immune electron microscopy after inoculating virus-infected cell supernatants with either anti-VP5 and/or VP7 polyclonal antibody (VP5Ab and VP7Ab) or intact GCRV antibody without performing purification (Fig. 2.2). These results clearly indicate that individually prepared antibodies of outer shell proteins (either VP5Ab or VP7Ab) effectively bind with GCRV particles in cultured cell suspensions, and the binding effect is mostly similar to that of the antibody generated using intact GCRV particles as an antigen. In the case of the control, only a few dispersed

particles can be found in GCRV-infected cell supernatants. In fact, the GCRV immunocompound derived from anti-VP7Ab is observed more easily by TEM than that derived from anti-VP5Ab (statistical data for each field not shown here). Furthermore, this is consistent with a previous study showing that enhanced GCRV-neutralizing capacity can be obtained by incubation of GCRV-infected CIK cell culture supernatants with the combination of anti-OCPs (VP5andVP7) Abs [20, 57]. The excellent neutralizing ability of anti-VP5Ab and VP7Ab may be related to the structure and confirmation of the AqRV VP5-VP7 heterodimer complex [7, 15]. It has been reported that the σ1 cell attachment protein of MRV is a major antigen that is able to neutralize reovirus [43]. Despite the lack of σ1 cell attachment protein in GCRV, GCRV VP5 and VP7 proteins represent excellent antigenic epitopes, suggesting that the AqRV VP5 and VP7 proteins have the potential to be used as antigens for vaccines.

2.2.4 Recombinant GCRV Particles

Reoviruses, such as MRV, rotavirus, and bluetongue virus, can automatically assemble into virions by expression of major structural proteins in vitro. As it is known that the AqRV particle is composed of the inner core capsid and the outer shell, an in vitro viral assembly model could be established for AqRVs. Using the baculovirus-based Bac-to-Bac expression system for dual expression of the OCPs VP5 and VP7 or mutant $VP5^{N42A}$ and VP7, which are then combined with purified cores, an in vitro assembly of the recovered native and mutant GCRV intact particles (R-GCRV, $R-VP5^{N42A}$) has been obtained [70]. Recoated GCRV (R-GCRV, $VP5^{N42A}$/VP7 R-GCRV) particles closely resemble native GCRV (N-GCRV) in terms of particle morphology and protein composition.

Furthermore, infectivity assays indicate that the recoated particles display infectious properties similar to those of native virions; R-GCRVs with a $VP5^{N42A}$ mutation have been shown to be defective in infectivity and progeny protein expression in infected cells, indicating that a $VP5N^{42A}$ substitution almost completely blocks the autocleavage of the VP5 N-terminus. This observation is consistent with a previous study on MRVs, wherein cores recoated with σ3 and μ1 bearing the N42A mutation have been shown as defective in infectivity [4, 42, 44]. These data indicate that the autocleavage of GCRV VP5 is required for efficient AqRV infection [70].

2.2.5 Surface Labeling of AqRV Particles

Methods of fluorescent labeling of virus particles and cellular structures have been developed to monitor virus trafficking in live infected cells. For enveloped viruses, fluorescent labeling has been successfully applied to trace virus entry and

interactions with host cell factors. For nonenveloped viruses, surface coat proteins modified with fluorescent materials can also be realized. Studies have shown that some reoviruses, such as fluorescent-labeled MRV and tetracysteine-tagged blue-tongue virus, can retain their biological properties after modification in vitro [76]. To elucidate the AqRV entry into live cells and its interactions with host cell organelles, GCRV virions have been modified in vitro via modification of the surface proteins with biotinylation, followed by conjugation with streptavidin-quantum dots. The GCRV particles modified by quantum dots retain their native biological functions and infectivity. In addition, the quantum dot-labeled GCRV particles show intact, and hence, quantum dots are suitable for use as fluorescent markers to study the molecular mechanisms of viral entry. Moreover, using quantum dot-labeled GCRV, the caveolae/raft-mediated endocytosis viral entry pathway has been identified for efficient AqRV infection [76].

2.2.6 Infectivity Assays of Purified or Modified Virions and SVPs

AqRV infectivity is less affected by particle purification and modification. Studies indicate that the intermediate SVPs of SBRV and GCRV are more infectious than the intact virion and core particle [16, 35]. Several experiments indicated that treatment with 200μg/mL of trypsin or chymotrypsin for approximately 5, 15, or 30 min at 37 °C increases infectivity by more than 2–3 logs in viral titer compared with that of the mock-treated viral particles. However, longer treatments of AqRVs with pro-teases consistently decrease viral titers because the AqRV core is less infectious, similar to that of the MRV or rotavirus [35], suggesting that AqRVs share common infectivity characteristics with other reoviruses. Plaque assays determining the infectivity of purified and quantum dot-labeled AqRVs have shown that these retain excellent infectivity similar to that of native GCRV [76].

2.3 AqRV Structural Protein Profile

2.3.1 Identification of AqRV Particle Proteins

Following established purification methods, highly purified virions of AqRV have been obtained. The structural protein profiles of AqRVs purified through sucrose gradient show protein components and gel-mobility types similar to those obtained by separating proteins from the purified virion preparation via CsCl gradient centri-fugation and analyzed using vertical slab polyacrylamide gels (SDS-PAGE) of 10–15% concentration [15, 16, 52, 54, 67].

CSRV structural proteins were first characterized in 1983 [38]. Five major structural proteins with molecular weights of 137, 126, 72, 44, and 34 kDa have been identified by SDS-PAGE analysis. The two proteins with molecular weights of approximately 72 and 34 kDa have been shown to be present at higher concentrations compared with the other identified proteins. Moreover, SDS-PAGE analysis of purified CSRV has shown five major (132, 130, 68, 43, and 32 kDa) and two minor (110 and 56 kDa) structural proteins [32]. In addition, few minor polypeptides with molecular weights of 110, 94, 80, 62, and 31 kDa have also been detected [32, 67]. In 1984, similar findings were reported for CCRV by Hedrick et al. [21].

In 1987, the first comparative analysis of structural proteins between four AqRV isolates (GSRV, 13p2, CCRV, and CSRV) was performed [67]. Five major structural proteins were compared using SDS-PAGE. Two large polypeptides (approximately 135 and 125 kDa), one medium-sized polypeptide of approximately 70 kDa, and two small polypeptides of 45 and 34 kDa were separated. Of the major structural proteins identified, two proteins with molecular weights of approximately 70 and 34 kDa were consistently present in the highest amount among the four isolates [67]. Minor virion proteins were detected but not characterized. Indeed, due to the limited copy numbers of minor virion proteins in particles, weak bands can be observed sometimes on the stained gel with the naked eye, but are hardly imaged at most times. In addition, SDS-PAGE analysis of isolated landlocked salmon aquareovirus polypeptides revealed the presence of five structural polypeptides with molecular weights ranging from 139 to 32 kDa. The polypeptide separation pattern is similar, but unique when compared with that of GSRV, CSRV, CCRV, and 13p2 [32].

In 1990, five polypeptides with molecular weights ranging from 130 to 35 kDa were identified from purified SBRV [52]. Further, the viral proteins of SBRV have been compared with those of the Atlantic salmon reovirus HBR, Smelt reovirus, Atlantic salmon reovirus (ASV), and turbot reovirus (TRV) by SDS-PAGE [32]. Similar to the identified structural proteins in AqRVs, all five viruses have been shown to contain five major structural proteins (two large, one medium, and two small), with molecular weights ranging from 137 to 34 kDa. The SBRV protein separation pattern is very different from that of SA11 and reovirus type 1 (T1L) [52].

In 1992, the polypeptides of GCRV with molecular weights ranging from 120 to 27 kDa were reported, which were analyzed by SDS-PAGE of purified particles, with separation of 11 polypeptide segments on the gel [28]. In 2002, a comparative analysis of structural proteins between TFV and GCRV revealed that structural proteins with similar molecular weights were present in both the AqRV species [14, 54]. SDS-PAGE of the virion proteins revealed five major structural proteins, approximately 136, 132, 70, 41, and 33 kDa in size. Similarities in the 136-, 132-, and 41-kDa protein bands are observed. The only major difference in the separation pattern between the two species is that with respect to the approximately 70-kDa band in TFV and the approximately 65-kDa band present in GCRV (Fig. 2.3). However, the smallest major protein band was not observed in GCRV in this study [54], which might be because of protein degradation due to the purified GCRV specimen being shipped to Singapore.

Fig. 2.3 Structural protein
analysis of GCRV and TFV.
The two aquareoviruses
were purified, and their
virion polypeptides are
analyzed on a 12%
SDS-PAGE gel. The gel was
stained with 0.25%
Coomassie Brilliant Blue
R-250
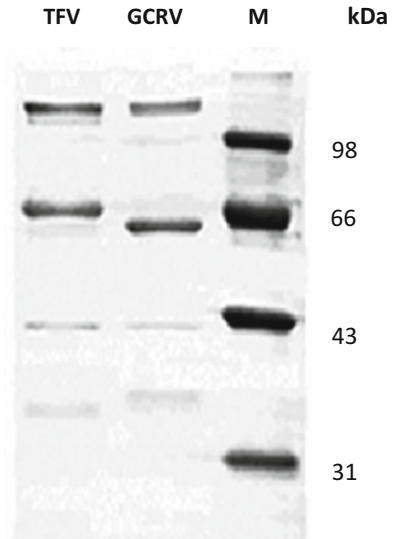
In addition, patterns of seven structural proteins have been determined for
GCRV-991 with five major and two minor structural proteins [14]. The seven
identified structural protein components (VP1–VP7) are approximately 138, 137,
136, 79, 67, 43, and 34 kDa in size, respectively. Three of the seven proteins, VP1,
VP2, and VP3, have similar large molecular masses. VP6 and VP7 have relatively
small molecular masses. Furthermore, VP5 is the most abundant protein, while VP4
is the least abundant. Similar to the structural protein profiles of GSRV, 13p2,
CCRV, and CSRV, minor virion proteins can often be detected but hardly imaged
based on the purified virion concentration. The GCRV protein components identified
by SDS-PAGE analysis match perfectly with the GCRV structural proteins and their
localization in the particle as resolved by three-dimensional image reconstruction of
a single particle [7, 15, 16]. Moreover, these results are also consistent with the
protein properties of AqRVs and MRVs [34, 67] and predictions deduced from
amino acid sequences of GCRV [1, 13].

2.3.2 Various Particle Forms and Related Protein Profiles

It is known as difficult to obtain highly pure virus particles and exactly distinguish
the viral particle components from infected cell lysate components upon careful
virus purification, unless the virus is labeled with radioactive material during
proliferation in infected cells or using western blot analysis with antibodies specific
to each viral protein. In addition, avoiding degradation of intact virions during the
whole purification process is also a preexisting condition for obtaining highly
purified virus particles and their complete particle components. Indeed, the viral

particles need to be purified very cautiously because the outermost protein VP7 of the AqRV is readily uncoated in native surroundings or purification processes. Although each step in virion purification is performed carefully at 4 °C, it is very common to observe various particle forms by TEM. Intact AqRV protein components and other viral-type particle components (including the top component, SVP, and inner core) have been identified in GCRV, SBRV, or other AqRV species [16, 32, 35, 40, 67]. For the protein components of GCRV cores (both intact and empty), two major bands are visualized by SDS-PAGE [16]. One large band represents VP1–VP3, while the other represents the VP6 protein. Furthermore, the VP6 band appears very weak in the top empty core sample, suggesting that some of the VP6 molecules in the empty core shell may have been lost during the uncoating of VP5 and VP7 by protease treatment or automatically detached during virus purification. For intact virions and double-shell empty particles, the separated one or two large, one or two medium, and two small protein bands with molecular sizes of 139–132, 70, 43–34, respectively, can be visualized in gel by staining with Coomassie brilliant blue. Of note, in most cases, two bands of the VP5 protein (68 kDa, full-length VP5) and its cleavage segment VP5C (64 kDa) can be detected by SDS-PAGE, which is consistent with the observations for µ1 and cleaved µ1C of MRV [42, 44]. The other cleavage segment VP5N is hardly detectable because it weighs 4 kDa. Consistently, µ1 protein is also mostly found in virions as fragments, µ1N/VP5N (4 kDa) and µ1C/VP5C (72 kDa), which are generated by autocleavage at the site N42-P43, as confirmed by biochemical analysis and three-dimensional imaging at atomic resolution [44, 66]. This suggests that the VP5 protein in the GCRV particle can exist either in two conformations or mainly in the VP5C conformation, as observed in most cases [16, 70]. In addition, since the molecular weights of the identified structural proteins of GCRV are between 34 kDa (VP7) and 136–138 kDa (VP1–VP3), it is not possible to resolve the higher-molecular-weight proteins VP1–VP3 and lower-molecular-weight protein VP7 using the same electrophoretic conditions. Because of the instability of AqRV particles and particle related nature of autocleavage or protease induced cleavage as well as the remaining minor protein components or purification issues with experimental condition limitations, it is not surprising that more than seven structural proteins have been identified in earlier studies [28, 65].

2.4 In Vitro Endogenous Transcription Assays of GCRV Particles

Similar to other reoviruses, the dsRNA genome segments of AqRVs are enclosed by the inner capsid shell. Enzymes that catalyze RNA transcription, capping, and replication are contained within the inner capsid, which serves as the site for the self-RNA synthetic activities. The RNA-dependent RNA polymerase

(RdRP)-related endogenous transcription activities of GCRV have been confirmed in earlier studies.

2.4.1 GCRV Nucleic Acid Release

To directly observe the genome of GCRV, the viral RNA component is released using the nucleic acid shadowing method with viral cores being prepared by digesting purified virus with a-chymotrypsin as described previously [28]. The released RNA strand of GCRV is attached to the core turrets (Fig. 2.4a), indicating that the hollow-like spike at the fivefold axes is the channel for RNA release from the inner core into the cytoplasm, which is the same as that in MRVs [3].
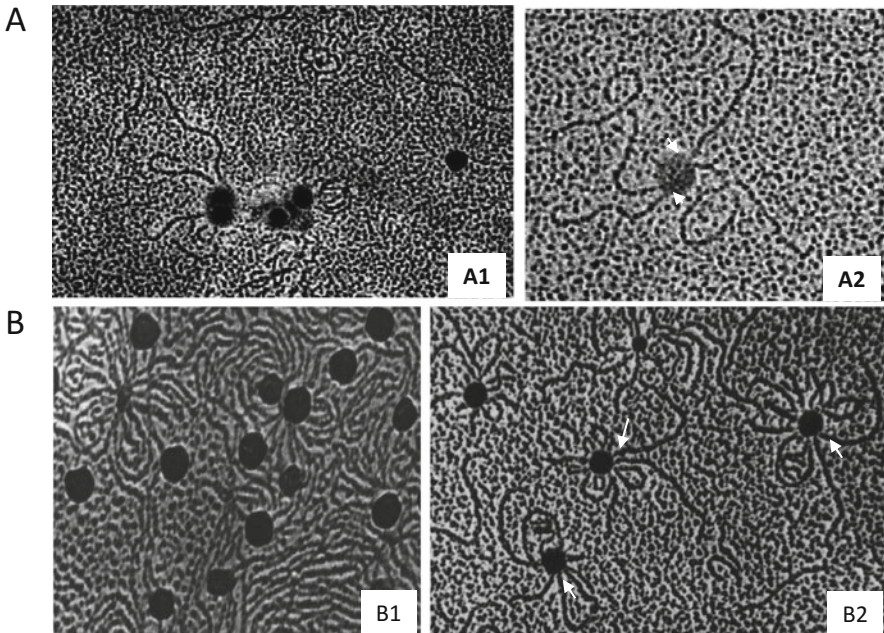
Fig. 2.4 Electron micrographs of stained and shadowed preparations of GCRV core and reaction cores. (**a**, **b**) GCRV nucleic acid release image of non-transcribing (**a**) and transcribing GCRV reaction core (**b**). Few GCRV genome RNA strands released and attached to cores from non-transcribing GCRV core in A2 as arrow indicated, and the non-transcribing core looks loosen after nucleic acid released. Many nascent nucleic acid released from transcribing cores in B. Arrowheads in B2 indicate where strands appear to emerge from spikes, and the transcribing core looks solid after some nascent nucleic acid released. The GCRV nucleic acid release from non-transcribing and transcribing GCRV reaction core preparations is followed as references [22, 28]

2.4.2 GCRV Reaction Core

RNA transcript products in GCRV reaction cores synthesized in vitro have been observed using a combined staining and shadowing method [22]. Up to 12 strands of nascent mRNA have been exhibited in reaction cores by TEM. The reaction cores that are intact and contain attached single-stranded RNA strands have a buoyant density of 1.48 g/cm^3 and an A260 to A280 ratio of 1.52. The transcribed genome products of the GCRV reaction cores with [α-^{32}P]-ATP labeling have been detected by analyzing in SDS-PAGE, which are consistent with the full-length copies of their dsRNA templates. An obvious feature of the reaction cores is that the sites of extrusion are probably the 12 hollow projections located on the surface of the core, and many strands are extruded in the form of loops (Fig. 2.4b). This evidence clearly indicates the endogenous transcription activity of GCRV [22].

2.4.3 In Vitro *Transcription Assays*

The endogenous RdRP activity of various GCRV particles (intact virion, top component, and core) has been assayed by in vitro transcription using [α-^{32}P]-ATP as a marker in earlier studies [23]. Transcriptase activation can be affected by different salt concentrations, temperatures, and reaction times. It has been shown that the cores can be activated for transcription, but the intact GCRV virions are incompetent for producing mRNA. Moreover, the intact GCRV virion can only possess transcriptase activity when the virus sample is resolved in a low-salt buffer, thereby showing effective transcriptase activity. Transcriptase activity assays performed for intermediate SVPs showed SVPs with activity higher than that of the purified viral core particles, suggesting that transcriptase can be activated by uncoating intact GCRV outer capsid shell because the outer capsid shell of intact GCRV can be loosened in a low-salt reaction buffer. Indeed, purified cores possess RNA transcriptase activity, but under the presence of the protective outermost shell, the enzyme activity can be affected. In addition, RdRP is more effective at 28 °C than at a temperature lower or higher than 28 °C, indicating that the optimum temperature for AqRV transcription is 28 °C, as determined by in vitro transcription assays. This is consistent with the optimal replication temperature for GCRV, as demonstrated by in vivo infection and in vitro expression studies of RNA polymerase (VP2) activities [12, 68]. The GCRV RdRP-related transcriptase complex has been verified by recent three-dimensional structural imaging analyses [66].

2.5 The AqRV Genome

The AqRV genome, which is encased by a double-layered protein capsid shell (designated as the inner core and outer capsid), has been shown to be a dsRNA genome due to its resistance to treatment with RNase I and green orthochromatic appearance with acridine orange staining [27, 32, 54, 67]. The genome of AqRVs is composed of 11 dsRNA segments that are packaged in equimolar ratios within a concentrated core. Seven distinct species (*Aquareovirus A* to *Aquareovirus G*) have been proposed by the International Committee on Taxonomy of Viruses based on reciprocal RNA–RNA hybridization and nucleotide sequence analyses.

2.5.1 Nomenclature and Electrophoresis Profile of the AqRV dsRNA Genome

The electrophoretic patterns of almost all isolated AqRVs are very similar to each other with three large (segments 1–3), three medium (segments 4–6), and five small segments (segments 7–11). Therefore, the dsRNA genome of AqRVs is generally grouped into three size classes, commonly referred to as the large (S1–S3, about 3.9–3.8 kb), medium (S4–S6, approximately 2.3–2.0 kb), and small (S7–S11, about 1.6–0.9 or 1.6–0.7 kb) classes.

Viral dsRNA of AqRVs has been analyzed by SDS-PAGE using vertical slab gels (10% polyacrylamide gel) immersed in Laemmli's buffer or 1% agarose gel electrophoresis [2]. Almost all AqRV species show unique electropherotypes in SDS-PAGE. Despite the differences in gel mobility, some similar electrophoretic patterns have been observed among AqRV isolates, e.g., dsRNA genome electrophoretic patterns of GCRV and TFV (Fig. 2.5). However, the RNA profiles of some AqRVs (e.g., SBRV, Atlantic salmon reovirus HBR, Smelt reovirus, and Atlantic

Fig. 2.5 The segmented genome profiles of GCRVs and TFV. (**a**) The genomes of GCRV-873 and GCRV-991 were resolved by 7% polyacrylamide gel; M: λ-DNA/EcoRI+HindIII. (**b**) The genomes of GCRV-873 and TFV were resolved by 1% agarose gel electrophoresis; M: 1 kb DNA ladder. Viral dsRNA genome segments in **a** and **b** were visualized following ethidium bromide staining
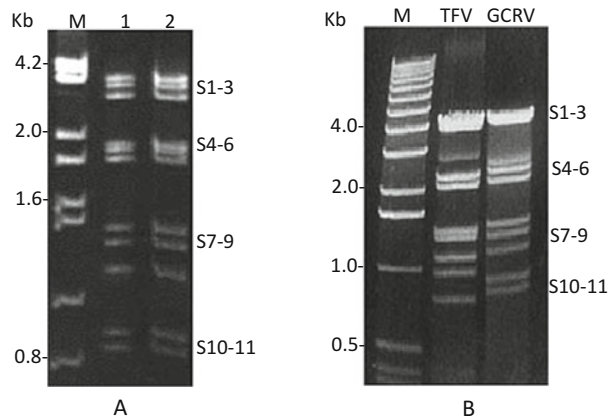
salmon reovirus (ASV)) in agarose gels have been observed to be very similar [32]. The differences in the mobility of dsRNA segments in SDS-PAGE or agarose gel electrophoresis depend on the gel properties. In addition, the mobility of dsRNA segments in SDS-PAGE gels depends on both their size and secondary structure, while in agarose gels it depends mostly on their size. In fact, the dsRNA genome of AqRVs is more expediently detected on agarose gels than on SDS-PAGE gels when adequate amounts of dsRNA from virus samples are extracted. In contrast, SDS-PAGE is recommended in cases of lower amounts of AqRV dsRNA genomic material, by staining with silver. Of note, despite the fact that most reoviruses isolated from aquatic animals have 11 dsRNA genomic segments, the genomes of some AqRVs contain 10 and/or 12 segments, as noted for piscine orthoreovirus (PRV) and reoviruses having crab hosts [29, 30], respectively, suggesting a complex and diverse molecular evolutionary course of the AqRV genome.

2.5.2 Genome Sequence-Based Features of AqRVs

The complete genomic sequences of the prototype AqRV strains GSRV and GCRV-873 classified in the species group *Aquareovirus-C* (AqRV-C) and other AqRV species isolates, such as CSRV and AHRV, have been characterized using the single-primer amplification method-cloned cDNA libraries or an optimized strategy for full-length amplification of cDNA [1, 11, 39, 45, 64, 71]. According to the GenBank data, at least 17 full-length AqRV genome sequences and many partial genome sequences have been deposited thus far. The total length of the AqRV genome sequence is in the range of approximately 23,500–24,500 bp. The lengths of individual gene segments vary from 728 bp (the shortest; S11 gene segment) to 3949 bp (the longest; S1 gene segment), according to the National Center for Biotechnology Information (NCBI). Generally, the GC content of the AqRV genome ranges from 52% to 60%; however, the recently reported AHRV genome consists of 11 segments (with a total size of 24,171 bp) and has a relatively low GC content (ranging from 47.8% to 52.7%) [60]. Most homologous gene segments of different isolates display little or no variation in segment length, such as those of GSRV or GCRV, CSRV, Turbot *Scophthalmus maximus* reovirus(SMReV), *Micropterus salmoides* reovirus (MSReV), and SBRV. However, gene segments in the small class vary greatly in length and are more divergent at nucleic acid and protein levels, compared with the large and medium class segments. Generally, each segment encodes one protein, but the S7 segment in the different species groups appears to be bicistronic or tricistronic [2, 30, 73]. Notably, AqRVs are recognized to be fusogenic with syncytia formation as a typical CPE in their permissive cell cultures, which is consistent with the predicted protein functional features of the S7 segment homologous to that of fusogenic avian reovirus (ARV) [8, 24]. However, few AqRV species, such as GCRV-ZH08, GCRV-GD108, and GCRV-104/109, and PRV, show non-fusogenic characteristics [11, 29, 45, 64, 71], which is consistent

with that observed for MRVs [43]. The fusogenic and non-fusogenic properties of AqRVs are related to the nature of the S7 segment-encoded proteins.

2.5.3   Terminal Non-coding Regions

The partial and complete genomic sequences of a number of AqRV strains have been determined [1, 2, 11, 39, 45, 47, 48, 55, 56, 64, 71]. In AqRVs, genomic dsRNA segments contain six and five conserved nucleotides at the 5′ terminus and 3′ terminal basic group, respectively (Table 2.2). Particularly, the conserved nucleotide terminal region, with five nucleotides "-UCAUC," at the 3′ end in AqRVs is same as that in MRV [43], and the extreme 5′ end with six-nucleotides is conserved within a particular virus species. For example, the conserved 5′-and 3′-terminal sequences of isolates in AqRV-C are 5′-GUUAUU……UCAUC-3′, compared to 5′-GUUUUA……UCAUC -3′ in AqRV-A,-B, and –G, and 5′-GUAAUU……UCAUC -3′ or 5′-GUAACU……UCAUC -3′ in unclassified GCRV-ZG08/108 and GCRV-109 species [1, 25, 45, 55, 56, 64, 71]. Similar to other reoviruses, each AqRV gene segment also contains terminal non-coding regions (NCRs) of a particular length. The lengths of the NCRs of genome segments vary across different AqRV species. Generally, the NCRs at the 5′ ends are shorter than that at the 3′ ends in AqRVs. The length ranges from 12 to 35 bp at the 5′ ends, while the 3′ ends contain NCRs of length ranging from 20 to more than 50 or 100 bp depending on the isolated virus

Table 2.2 Conserved terminal sequences (positive strand) of aquareovirus genome segments

AqRV species	Terminal sequence 5′NCR……3′NCR
AqRV-A (AHRV, CSRV, EFRV, SBRV, TFV, TSRV, AtSRV, SMReV, MsReV)	5′-GUUUUA… …UCAUC-3′
AqRV-B (FCRV, CoSRV)	5′-GUUUUA… …UCAUC-3′
AqRV-C (GSRV, GCRV873)	5′-GUUAUU… …UCAUC-3′
AqRV-D,E,F	–
AqRV-G (AGCRV)	5′-GUUUUA… …UCAUC-3′
Unassigned strains	
GCRV-ZH08	5′-GUAAUU… …UCAUC-3′
GCRV-GD108	5′-GUAAUU… …UCAUC-3′
GCRV-104	5′-GAAUU …… …UCAUC-3′
GCRV-109	5′-GUAACU… …UCAUC-3′

strains [25, 45]. Moreover, the first and last nucleotides in the NCRs of all segments are complementary (G-C) and are known to be highly conserved within all AqRV species. Similar to other reoviruses, the NCRs of AqRVs are likely to include sequences important for RNA packaging, recognition by their RdRP for initiating positive- and negative-sense RNA strand synthesis, and translational efficiency [43].

2.5.4 Protein-Coding Assignments and Nomenclature

The coding assignments and properties of the AqRV proteins encoded by each of the 11 genomic segments are now fairly well characterized. The final assignments were determined by in vitro translation using mRNA or genome sequencing using denatured dsRNA combined with three-dimensional structural reconstruction-based methods. It has been confirmed that the 11 genomic segments of AqRVs encode seven structural and five nonstructural (NS) proteins. According to the nomenclature of the viral structural proteins (that are contained in the virion), structural proteins are designated as VP followed by a number, with VP1 being the largest and VP7 being the smallest structural protein. Moreover, the genome segments encode proteins that are not contained in the viral particle, termed as NS proteins. For the NS proteins, two sets of nomenclature are currently used based on either the molecular weight or a number, for example, GSRV NS80 or NS1. The initial assignment of individual proteins to specific gene segments of AqRVs has been performed by in vitro translation of viral mRNAs in early studies on SBRV and GCRV [28, 52, 62, 65]. GCRV polypeptides encoded by each of the gene segments are designated by the molecular weights corresponding to the respective genome segments S1–S11 (Fig. 2.6).

2.5.4.1 SBRV Gene-Protein-Coding Assignment

The gene-protein-coding assignments of SBRV have been well characterized by in vitro translation of individual genome segments [52, 62]. [^{35}S]methionine-labeled SBRV-infected cell lysates were used to analyze the polypeptides and gene-protein-coding assignments of SBRV. Twelve proteins with apparent molecular weights of 130, 127, 126, 97, 73, 71, 46, 39, 35, 29, 28, and 15 kDa were detected in the infected cell lysate, but not in the uninfected cells [32, 52], suggesting that these proteins are encoded by the SBRV genome. Analyzing radiolabeled cell lysates and radiolabeled purified virus proteins using SDS-PAGE and autoradiography for self-exposed X-ray film, seven structural (VP1–VP7) and five NS proteins (NS97, NS39, NS29, NS28, and NS15) have been further classified. There are two major structural proteins, whereas the other five structural proteins are present in smaller amounts. In addition, segments 1–10 of the SBRV genome encode one protein each, while segment 11 encodes two proteins.

Fig. 2.6 Gene-protein-coding assignment of GCRV. A SDS-PAGE gel shows the 11 segments of dsRNA that comprise GCRV genome and the proteins encoded by each of these genes (**a**). The genome segments encode nonstructural (NS) and structural (virion) proteins marked at left and right, respectively. The virion proteins are analyzed on a 12% SDS-PAGE gel (**b**). The viral genome and structural proteins of GCRV are obtained from purified particle
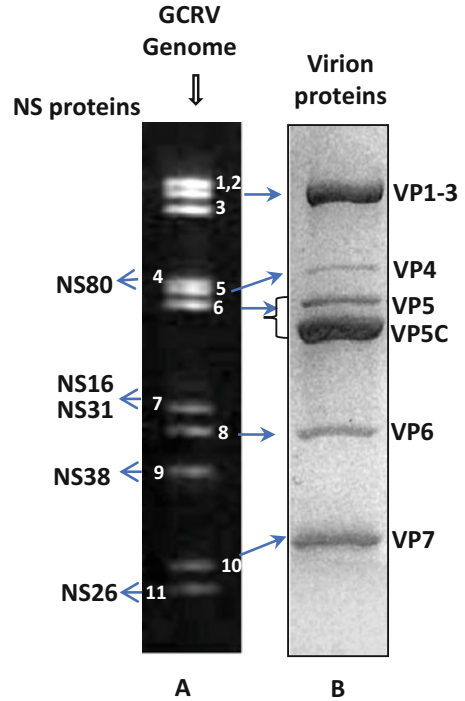
To confirm the above data, further translational analysis of the individual genome segments using a nuclease-treated rabbit reticulocyte lysate in vitro was conducted by Subramanian et al. in 1994 [62]. The synthesis of viral proteins by in vitro translation was quantitatively and qualitatively very similar to that observed in SBRV-infected CHSE-214 cells. Of the 12 proteins, the genome segment 11 codes for two proteins, NS29 and NS15. According to the understanding of the proteins encoded by the 11 genome segments of SBRV and their three-dimensional image reconstruction, the proteins VP5 (S5; 71 kDa) and VP7 (S10; 34 kDa) comprise the outer shell [40]. VP1–VP3 and VP6 are the core proteins. Additionally, VP1 is the most likely candidate protein responsible for the turret structure, while the role of VP4 is unknown [40].

2.5.4.2 GCRV Gene-Protein-Coding Assignment

The gene-protein-coding assignment of GCRV was reported by Ke et al. in 1992 [28]. The 11 polypeptides isolated from purified virus particles with molecular weights ranging from 130 kDa to 27 kDa were observed by SDS-PAGE analysis. Furthermore, the denatured viral genome segments were translated using a cell-free rabbit reticulocyte translation system labeled with L-[^{35}S]methionine, which showed 11 protein bands in the exposed X-ray film with autoradiography. Further

gene-protein-coding assignment of GCHV was conducted with the wheat germ translation system labeled with L-[^{35}S]methionine using each separated GCRV genome segment [65]. The translation products displayed on the X-ray film showed 12 protein bands with probable molecular weights in the range of 130–19.5 kDa. However, the study failed to distinguish the structural and NS proteins of GCRV. This might be due to poor experimental conditions and some technology-related problems in the 1990s. Indeed, the gene-protein-coding assignments of GCRV were obscure until 2002 [1]. Complete sequence determination and identification of GCRV structural proteins from purified natural virus particles indicated that the GCRV 11 dsRNA genome segments encode 12 proteins. Segments 1, 2, 3, 4, 6, 8, and 10 encode seven structural proteins that form the virus particle [1, 7, 15, 76], and the remaining segments encode five NS proteins that are involved in viral replication and transcription [18, 19, 77, 78].

Further full-length sequence analysis indicated that each dsRNA genome segment of GCRV generally contains a single gene encoding a single protein, except the S7 segment. Twelve proteins have been translated from the 11 gene segments of GCRV, such that 10 of these gene segments encode a single protein, and only the S7 gene encodes two proteins. Genome sequence-based homologous protein analysis indicated that 7 of the 12 proteins are structural components of the virion (VP1–VP7) and five are NS (NS80, NS38, NS31, NS26, and NS16) proteins involved in viral replication [1]. The GCRV particle structural protein compositions were further confirmed by SDS-PAGE, cryo-electron microscopy, and three-dimensional image reconstruction analyses [7, 15, 66]. The 11 segments of dsRNA that comprise GCRV genome and the proteins encoded by each of these genes are shown in Fig. 2.6. Recently, a putative NS12 protein has been identified to be encoded by the S7 genomic segment [73].

2.5.5   In Vitro *and* In Vivo *Protein Expression Analyses*

Based on the obtained genome sequence of AqRVs, almost all proteins (including 7 structural and 5 NS proteins) encoded by GCRV genome have been expressed in vitro using different expression vectors (including prokaryotic and yeast expression plasmids, recombinant baculovirus Bac-to-Bac insect expression system, and mammalian expression plasmids) [63, 69, 72]. All the expressed proteins in vitro have been shown to correspond to the predicted protein products from the corresponding GCRV genome, which validates the deduced protein sequences from the corresponding dsRNA genome segment open reading frame (ORF). In addition, the structural and NS protein expressions in virus-infected cells were detected and confirmed with prepared multi-clonal antibodies generated from individual genome segments [69, 76–78]. It is important to note that some additional or truncated isoforms of the GCRV proteins, such as VP5/VP5C, NS80/NS80C, which are homologous to MRV protein μ1 and μNSC, respectively, have been detected in both transfected and infected cells [5, 26, 69, 70]. Moreover, NS80 and NS38

expressions are detected prior to that of the structural proteins, indicating that the NS proteins are important for viral replication [69, 78]. As a fusogenic reovirus, the fusion-associated small transmembrane (FAST) protein NS16/NS12, which is similar in function to the ARV p10, p14, and p15 [49], has also been detected in infected and transfected cells. These findings indicate that the AqRV genome may perform translation in infected cells beyond the ATG in-frame rules [25, 49]. The structural proteins and their functions are described in Chap. 3, while the AqRV replication-related NS proteins are described further in this chapter.

2.6 AqRV Morphogenesis

The most characteristic feature of reovirus replication in infected cells is the formation of cytoplasmic factories, named viral inclusion bodies (VIBs), viral factories, or viroplasms, which consist of progeny viruses, usually appearing as paracrystalline arrays of full and empty virions. VIBs are specific intracellular compartments for reovirus replication and assembly [43]. AqRV morphogenesis in host cells has been studied extensively using the ultrastructure and molecular biology methods, which are related to evaluating the mechanism of VIB formation in infected cells [5, 45, 58, 69, 77, 78]. It has been found that the NS proteins NS80 and NS38 of the AqRV as well as the viral core structural proteins play critical roles in AqRV morphogenesis.

2.6.1 TEM Analysis of VIB Formation in Infected Cells

The thin-section ultrastructural TEM images revealed that the AqRV replication and assembly occur within VIBs in infected fish or cultivated cells [32, 51]. Paracrystalline arrays have been observed in cell lines infected by various AqRVs, such as GSRV, 13p2, TRV, GCRV, TFV, TSRV, and AHRV [10, 32, 54, 74]. It has been found that the AqRV particles bind to the plasma membrane of permissive cells at 0 or 10 min post-infection (p.i.) and are subsequently internalized. The SVPs are found in the cytoplasm at 40 and 60 min p.i [51, 76]. It has been shown that the core particles of AqRV are observed within the dense viroplasms in the early stages of infection, and the size and number of viroplasmic inclusions increase as the infection progresses; mature virions are formed with an overall size of about 70–80 nm in the late stage of replication [10, 51]. In addition, a number of viroplasms can be detected at one time in the cytoplasm of a cell, suggesting that there is no limitation on the number of virions penetrating and replicating in a single cell [10, 51].

Once an AqRV species enters the cell, electron-dense particles condense in the periphery of the viroplasms, and the cellular ultrastructural changes can be observed in ultra-thin section images during early infection [10, 32]. The AqRV infection forms neoorganelles in infected cells. The dense globular inclusion bodies/
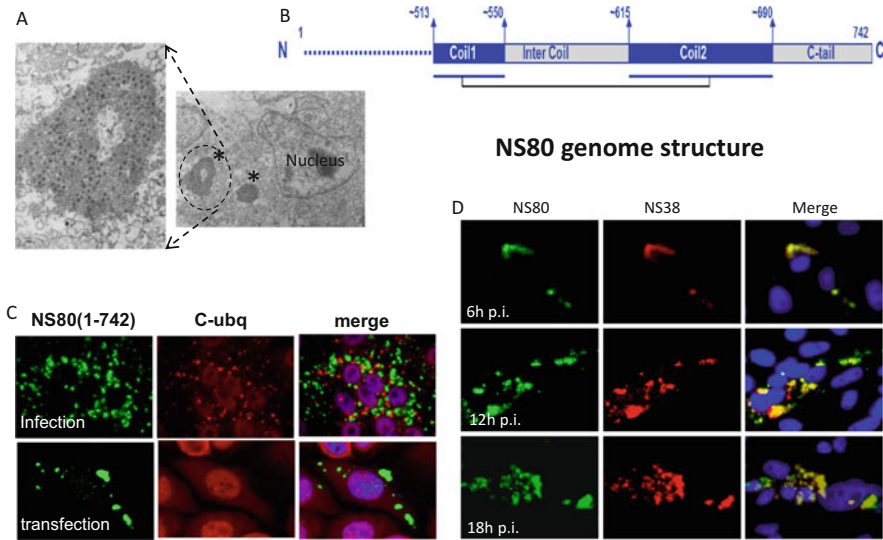
Fig. 2.7 NS80 and NS38 are involved in viral inclusion formation. (**a**, right) VIBs in cytoplasm of infected cells (left is the zoomed-in view of the VIB shown in right). (**b**) Schematic representation of aquareovirus NS80 C-terminal regions with four potential inclusion formation related domains. (**c**) NS80 induced VIBs were detected in infected and transfected cells. (**d**) The subcellular localizations of NS80 and NS38 were detected in GCRV-infected CIK cells by IF. The subcellular localizations of NS80 and NS38 immunostained with rabbit anti-NS80 or/and mouse anti-NS38 polyclonal antibodies followed by FITC-conjugated goat anti-rabbit IgG (green) and Texas Red-conjugated goat anti-mouse IgG (red), respectively. Nuclei were counterstained with DAPI (blue). Images in **c** and **d** are modified from reference [58]

viroplasms appear to be the site for initiating assembly of the viral progeny in the AqRV replication cycle (Fig. 2.7a). The presence of viral polypeptides inside the viroplasms at the medium and late replication stages has been observed by immune electron microscopy and immunofluorescence assays [51, 69, 77, 78]. During replication and assembly of AqRVs, these VIB-like structures have a peculiarly dense consistency that distinguishes them from the adjacent cytoplasm and causes them to appear highly refractile when viewed by phase-contrast microscopy, and they contain fully or partially assembled viral particles, viral proteins, dsRNA, and microtubules [58, 77]. VIBs are formed throughout the cytoplasm of infected cells as the infection progresses. Studies clearly indicate that the AqRV replication is typical to the cytoplasm of infected cells, which is consistent with the reovirus replication features in general.

2.6.2 NS80: A Scaffold of VIBs

The AqRV NS protein NS80, also termed NS1, has been identified as the major constituent for forming globular VIBs [58]. GCRV NS80 consists of 742 amino

acids and is encoded by a gene on S4 (2320 nt), with a molecular weight of approximately 80 kDa. Phylogenetic analyses indicated that the NS protein NS80 of GCRV or the homologous protein in other AqRV isolates is related to the formation of VIBs. BLAST analysis comparing the GCRV NS80 analogue with that of CSRV in the genus *Aquareovirus* and MRV and ARV in the genus *Orthoreovirus* showed identities mostly within the C-terminal region of the protein. In particular, the NS80 homologous proteins across different AqRV species share two typical coiled-coil regions (513–548 and 615–700 amino acids) in their carboxyl-proximal region (Fig. 2.7b), which have been shown to be important in VIB formation in MRVs [10, 26, 58]. Immunofluorescence assay showed that NS80 can form VIBs when expressed alone in transfected cells or during viral infection (Fig. 2.7c). It has been also identified that the C-terminus of NS80 is responsible for VIB formation, and the N-terminal NS80 interacts with viral proteins [58, 77]. In addition, a shorter specific fragment of NS80, an approximately 58-kDa product of NS80, has been detected in infected and transfected cells [5]. As NS80 is a multi-functional protein, the different isoforms of NS80 proteins present in infected cells may be functional at various replication stages, suggesting that the isoforms may play different functions during viral replication.

2.6.3   Interaction of NS80 with Viral Proteins

It has been observed that NS80 retains five ISPs (VP1–VP4 and VP6) and NS38 within VIBs in co-transfected or infected cells (Fig. 2.7d). NS80 interacts with each core protein and newly synthesized viral RNAs colocalized with VIBs [26, 69, 77]. Furthermore, time-course analysis of the viral structural protein expression showed that the expression of NS80 is first detected, followed by that of the ISP VP3 and other ISPs, suggesting that VIBs are essential for the formation of progeny virions. Further experiments indicated that knockdown of NS80 by shRNA not only inhibits the expression of the AqRV structural proteins, but also reduces viral infection. These results indicate that NS80-based VIBs are formed at an earlier stage of viral infection, and the protein NS80 is able to coordinate the expression of viral structural proteins and viral replication [69, 77].

2.6.4   Role of NS38 in GCRV Morphogenesis

AqRV NS38, encoded by GCRV S9 (1130 nt), contains 352 amino acids with a molecular mass of approximately 38 kDa. BLAST analyses suggested that there is approximately 23% similarity between the AqRV NS38 and MRV σNS at the protein level. It has been found that protein σNS of MRVs, together with another NS protein μNS, and protein σ3 can associate with mRNA molecules to form single-stranded RNA-containing complexes [43, 78]. Some studies have implicated σNS as

a minimally essential viral component for forming VIBs together with µNS, which then recruits other reovirus proteins and RNA to initiate viral genome replication. Studies have indicated that the AqRV NS38, a virus genome-encoded putative single-stranded RNA-binding protein, interacts with not only NS80 in VIBs, but also ISPs (VP1–VP4 and VP6). Interactions between NS38 and NS80-RNA complexes in both transfected and infected cells have also been detected. Knockdown of NS38 by siRNAs-115/219 clearly reduces viral infection, with decreased mRNA and protein yields. Moreover, NS38 can interact with the host cellular eukaryotic translation initiation factor 3 subunit A (eIF3A) in transfected cells. Furthermore, it has been identified that NS38 directly interacts with outer shell protein VP5 and VP7 (unpublished data). These findings indicate that NS38 may function as a mediator by interacting with the viral and host cellular components in VIBs during viral replication and particle assembly [78].

2.7 GCRV S7 Genome Segment-Encoded FAST Protein and Associated Syncytium Formation

Similar to fusogenic orthoreoviruses that can promote the formation of multinucleated syncytia in infected cells [8, 49], AqRVs are able to induce typical CPEs and finally lead to multinucleated syncytium formation in permissive cell lines during cultivation. AqRVs and fusogenic orthoreoviruses are the only known examples of nonenveloped viruses that lead to cell–cell fusion and syncytium formation in virus-infected cells [24, 49]. Studies have indicated that the FAST protein encoded by the AqRV S7 genome segment is responsible for cell–cell fusion during the viral replication cycle.

2.7.1 Detection of FAST Protein

Early investigations have revealed that ARVs can induce multinucleated syncytia formation in infected cell cultures, which distinguishes them from non-fusogenic MRVs [49]. It has also been found that the fusogenic nature of ARVs is such that the formation of cellular syncytia is not related to viral cellular entry or exit, as is the case for enveloped viruses, such as the human immunodeficiency virus (HIV) gp41 (HIV-1), which mediates fusion between target cells through a complex interaction of viral glycoproteins with cell receptors [24]. FAST proteins are small (95–198 amino acids) and expressed as NS proteins during the viral replication cycle [49]. Studies on the reovirus fusion mechanism suggest that the reovirus FAST proteins may function as virus genome-encoded fusogens and utilize many accessory host factors to drive cell–cell fusion, and therefore, may benefit the rapid spread of infection after being expressed in infected cells [8, 49]. A recent study on ARVs

demonstrated that cell–cell fusion induced by the reovirus FAST proteins enhances replication and pathogenicity of nonenveloped dsRNA viruses [24].

2.7.2   Sequence-Based Features of FAST Protein

Fusogenic reovirus-induced cell–cell fusion and syncytium formation are dependent on a distinct family of FAST proteins encoded by polycistronic genomic segments. Some FAST proteins of the ARV, such as p10, p14, and p15, have been well characterized in the genus *Orthoreovirus* [8, 24]. A few FAST proteins, such as the p22 protein from AtSRV, SMReV, and MSReV (AqRV-A) and NS16 from GCRV and GSRV (AqRV-C), have been predicted in the genus *Aquareovirus* based on bioinformatics analyses [18, 25, 49]. Subsequently, the proteins NS16, NS22, or p22 encoded by the polycistronic genome segment S7 of AtSRV, MSReV, SMReV, and GCRV have been identified as FAST proteins in the genus *Aquareovirus* [6, 18, 25]. Generally, the basic structure of the FAST protein (Fig. 2.8a), including the transmembrane (TM) domain, polybasic (PB) region, hydrophobic region, and polyproline and proline-rich motif, has been determined in the AtSRV p22, GCRV NS16, and MSReV/SMReV NS22 [6, 18, 25, 49]. In particular, sequence analysis has also suggested an additional dileucine motif in the cytoplasmic region at amino acid positions 113–114, which may regulate protein sorting and other cellular processes.

Bioinformatics analysis has shown that NS16 and NS22 of the AqRV share basic structural motifs with the ARV FAST proteins p10, p14, and p15. NS16 and NS22 in AqRV-C and AqRV-A species, respectively, have been predicted to be single-pass membrane proteins comprising 146 and 198 amino acids, respectively, which display essential features similar to those of the identified FAST protein motifs and are assumed to possess an N-terminus-outside/C-terminus-inside asymmetric topology on the plasma membrane. In the N-terminal region, there is a strong TM domain (covering 37–60 amino acids for NS16 and 35–57 amino acids for NS22). Following the TM domain, there is a PB region that contains a stretch of basic residues (covering 63–78 amino acids for NS16 and amino acid positions 61–68 and 82–95 for NS22). The PB region is thought to support the translocation of the N-terminal domain (34 amino acids for NS22 and 36 amino acids for NS16) into the extracellular environment [18], and it has been implicated as essential for FAST protein activity. In addition to the TM domain, a hydrophobic region called the hydrophobic patch has been predicted to exist in the C-terminal fragment of both proteins (amino acid positions 113–121 for NS16 and 140–150 for NS22). Moreover, two regions rich in arginine, proline, and histidine have been found in NS22 [25]. In contrast, there are three regions rich in arginine, proline, and histidine in the S7 encoded FAST protein of the AtSRV [49], despite its high sequence similarity with the SMReV NS22. Furthermore, some differences have been found in the motifs in NS22 and NS16. A myristoylation consensus sequence (MGXXXS) has been identified at the N-terminus of NS22 [25], but no such myristoylation site exists
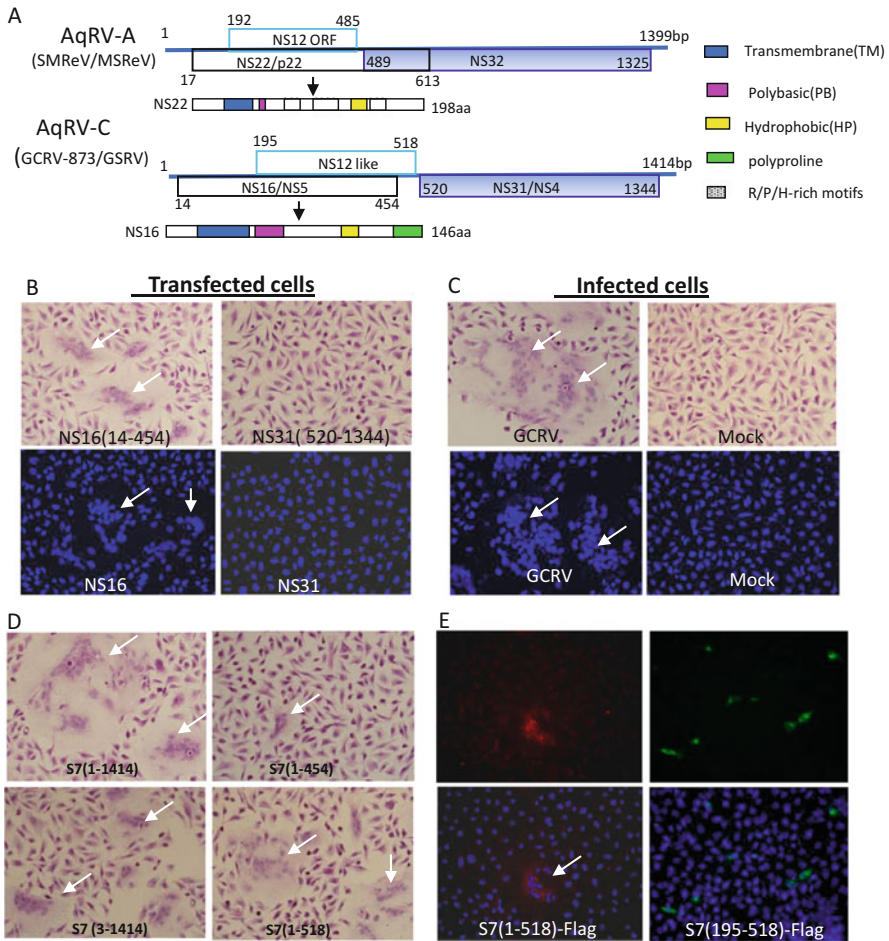
Fig. 2.8 Identification of GCRV genome S7 encoded FAST protein. (**a**) Diagram of AqRVs genome segment S7 encoded proteins NS16/NS22, NS12, and NS31/NS32. Virus strains and accession numbers for segment 7 of the genomes are as follows: AqRV-A: MsReV (KJ740731.1), SMReV (HM989936.1); AqRV-C: GCRV-873 (AF403393.1), GSRV (AF403404.1). (**b**) Expression of GCRV S7 encoded NS16 and NS31 protein. NS16 induced cell–cell fusion and multinucleated syncytium formation in transfected CIK cells (left), no syncytium formation is observed with NS31 expression (right). Cells were fixed at 48 hpt and stained with HE or Hoechst. (**c**) Cytopathic effects are observed in GCRV-infected CIK cells at 12 hpi. Mock-infected cells served as a negative control. (**d**) Syncytia formation in transfected CIK cells with recombinant plasmids (pCI-Neo) containing different truncation regions of GCRV S7 sequence. (**e**) Immunofluorescence assays of truncated S7 fragment expressions in transfected cells. The expressed proteins were detected by IF assay at 24 hpt with an anti-FLAG MAb followed by Alexa 488 (green) or 568 (red) labeled secondary antibody, respectively. Arrows indicate the syncytia and nucleus aggregation

in NS16 of GCRV or GSRV. It has been reported that N-terminal myristoylation is necessary for the fusion activity of the reptilian reovirus protein p14 [8, 41]. Notably, the viruses utilize a noncanonical CUG codon for initiating translation to produce the fusion protein p22 responsible for syncytiogenesis [25, 49, 73].

Interestingly, GCRV-104 initially appeared to lack an NS FAST protein. However, further careful analysis indicated that the potential N-terminal region of NS15 (ORF2) in the S11 segment may contain a TM domain with its size consistent with that of the FAST protein ectodomains; additionally, a cluster of basic residues contained at the C-terminus that is enriched in arginine and proline residues, and several cysteine residues that may be palmitoylated [41]. Similarly, a bioinformatics assay predicted that the GCRV-HZ08 NS41 and/or GCRV-GD108 NS11/9 (ORF2) potentially encode membrane-interacting NS proteins having one or more TM domains [41]. These may be additional examples of non-fusogenic integral membrane proteins encoded by AqRVs that are similar to the PRV protein p13 [29]. However, these predicted transmembrane proteins with relative biological functions are not clearly defined in AqRVs and orthoreoviruses.

2.7.3   NS16 and NS22: The AqRV FAST Proteins

Bioinformatics analysis has shown that NS16 and NS22 (p22 for the AtSRV) of the AqRV share basic structural motifs with the reovirus FAST proteins, suggesting that the AqRV NS proteins NS16/NS22 may be a fusion protein responsible for AqRV-C and AqRV-A syncytiogenesis. As expected, the expression of NS16 (ORF14-454 nt) in transfected cells could induce cell–cell fusion and multinucleated syncytium formation (left panel in Fig. 2.8b), consistent with typical CPE formed in CIK cells infected with GCRV (Fig. 2.8c). However, the expression of S7 cDNA with another ORF (GCRV NS31: 520–1344 nt; SMReV NS32: 489–1325 nt) does not cause cell–cell fusion (right panel in Fig. 2.8b). Especially, many large syncytia formed when full-length cDNA of the S7 segment expressed in transfected CIK cells at 24 hpt, hinting that one more membrane fusion relevant ORF contained in the 5′ end sequence of S7 segment. In fact, detailed analyses have shown that cell–cell fusion and nucleus aggregation could be formed when truncated constructions of S7 fragment, such as S7(1-454), S7(1-518), expressed in transfected cells (Fig. 2.8d,e), indicating that the initial 5′ end ORFs of the GCRV and SMReV/MSReV S7 segment encode proteins critical for cell–cell fusion [6, 25]. It may need to note that the NS16 alone is capable of inducing cell–cell fusion and syncytium formation in transfected cells; nevertheless, the fusion activity is less efficient in comparison with the viral infection [18]. Unlike NS16, which has an AUG ORF, NS22 of SMReV has been found to be translated from a non-AUG translation start site. In addition, the NS16 FAST protein has been observed to display an N-terminus-outside/C-terminus-inside orientation, with the N-terminal ectodomain critical for effective fusion [18]. Moreover, immunofluorescence assays of GCRV have revealed that NS16 co-localizes with the NS protein NS26 in co-transfected cells.

The enhanced fusion efficiency can be detected when NS16 is co-expressed with NS26, implying that NS26 may participate in cell–cell fusion through cooperation with NS16 in AqRV infection [18, 19].

2.7.4 NS12: A Novel Membrane-Associated Protein

It is known that the GCRV S7 segment encodes two proteins NS16 and NS31. A neglected ORF, tentatively named NS12, residing between NS16 and NS31 in the S7 segment, has been found to have atypical fusogenic activity [73]. With an additional ORF(195-518), the nucleotide sequence of NS12 partially overlaps with the 3′ expressible nucleotide sequence of NS16 (Fig. 2.8a). Furthermore, bioinformatics analysis has indicated that NS12 is a transmembrane protein, which has been confirmed by its exclusive presence in the membrane-associated fraction of the cell lysate. In particular, the NS12 product can be detected in infected cells, indicating that NS12 is expressed in cells with GCRV infection. However, the expression of NS12 alone cannot induce visible syncytium formation in transfected CIK cells (Fig. 2.8e), which distinguishes it from the approved FAST protein NS16. Subsequent bioinformatics analysis showed that NS12-like ORFs (with an AUG or non-AUG initiation codon) are also present in the S7 segment of other AqRVs [73], suggesting that NS12 homologs may be widely distributed in the genus *Aquareovirus*. Collectively, the novel membrane-associated protein NS12 is functionally distinct from the known AqRV FAST protein NS16. The identification of bicistron/tricistron mRNAs in AqRVs and their genetic variety provides a basis for further understanding the mechanism of molecular evolution of fusogenic AqRVs.

2.7.5 Role of NS31 in Virus Replication

Compared with the aforementioned AqRV NS proteins, very little is known about the role of NS31 or NS32, which is encoded by the GCRV or SMReV/MsReV genomic segment S7 downstream of NS16 or NS22 (Fig. 2.8a). When NS31 or NS32 solely expressed in transfected cell, no syncytium formation can be observed [25] (right panel in Fig. 2.8b). Immunofluorescence assays showed that NS31 colocalized with NS16 in transfected cells (unpublished data), hinting that NS31 might associate with NS16 during cell–cell fusion. However, no biological relationship has been determined between the GCRV S7 segment-encoded FAST proteins NS16 and NS31. Bioinformatics analysis has predicted that the NS31 protein contains a helix-turn-helix-like domain and a C-terminal acidic α-helix motif. Using a GAL4-based yeast reporter system and a grass carp cDNA library, it has been found that a fusion protein composed of the Gal4-BD domain and NS31 (BD-NS31) is able to activate the expression of reporter genes (*Gal1/MEL1* promoter) without the Gal4-AD domain. In addition, NS31 homologues from other AqRVs have been shown to

possess a similar transcriptional activation in yeast, suggesting that the AqRV/GCRV NS31 protein may be a potent transcription regulator. Further analyses are found that GCRV NS31 and other NS31-like proteins in Aquareovirus genus could efficiently induce host heat-shock 70-kda protein (HSP70) expression, and GCRV protein synthesis or progeny virus yields was restrained by an inhibitor of host HSP70 in infected cells. All these results indicated NS31 cognate proteins in the Aquareovirus genus should play a regulating role during aquareovirus replication [72].

2.7.6 Possible Function of GCRV NS26 in Syncytia Formation

GCRV NS26 is encoded by the S11 genomic segment, which shares no sequence homology with the known proteins in MRVs. NS26 has been found to interact with NS80 and co-localize with NS16 in co-transfected cells. Co-expression of NS16 with NS26 has been observed to enhance cell–cell fusion efficiency [18]. These results suggest that NS26 may participate in the fusion process of viral infection. Further functional analysis of NS26 has suggested that the TLPK motif is important for NS26 to enhance the fusogenic activity of NS16, and NS26 may utilize lysosomes to benefit the fusion activity [19].

2.8 MRV σ1-like Cell Attachment Protein of GCRV-II Species

In contrast to the majority of AqRVs, the newly identified GCRV-ZH08, GCRV-GD108, and GCRV-104/-109 have been found to have the MRV σ1-like cell attachment protein (VP55 or VP56) on the particle surface [11, 41, 45, 64, 71]. The recombinant MRV σ1 protein of GCRV-GD108 can bind to grass carp snout fibroblast cells, as observed by cell attachment assays. Neutralization tests have shown that the polyclonal antibody generated from the expressed fiber protein VP55 is able to prevent viral infection in both fish and grass carp snout fibroblast cells. A more recent study indicated that fiber-like protein VP55 can repress interferon production by degrading the phosphorylated cellular transcription factor interferon regulatory factor 7 (IRF7) [75]. As σ1 protein is a major epitope and possesses hemagglutination activity, further studies on the GCRV-ZH08/-GD108/-104/-109 (GCRV-II) S7 segment-encoded cell attachment protein will provide a basis for understanding the mechanism of VP55 in cell entry and pathogenesis.

2.9   Conclusions and Future Considerations

According to classic gene-protein-coding assignment and genome sequence-based protein prediction, the 11 dsRNA genome segments of GCRV (AqRV-C) encode at least 12 proteins. Of the 12 approved proteins, seven structural proteins VP1–VP7 have currently been confirmed by high-resolution single-particle three-dimensional image reconstruction, as well as SDS-PAGE analysis of the structural proteins of the viral particle. The basic biological and molecular characteristics of the remaining proposed NS proteins NS80, NS38, NS31, NS26, and NS16 have also been investigated [5, 10, 18, 25, 26, 58, 69, 72, 78]. In addition, a novel protein NS12, encoded by the S7 genomic segment of GCRV, has recently been identified to play a partial role in syncytium formation [73]. This evidence suggests that another unknown NS protein may be expressed in virus-infected host cells and facilitate AqRV replication. Much progress has been made in the elucidation of the AqRV molecular biology in the past 30 years. However, for more in-depth knowledge, some issues need to be addressed in future studies.

Particle Instability of AqRVs A number of morphological studies have shown that various particle components (intact virions, SVPs, empty particles, and inner cores) can be observed in highly purified or partially purified AqRV preparations by TEM. Indeed, based on the fusogenic properties of most AqRVs inoculated in permissive host cells, mature virions can be released from infected cells by lysis. For general purification of the GCRVs, the collected virus-cell suspension can be purified directly without undergoing any physical methods, such as sonication, or chemical treatment, such as treatment with deoxycholate and extraction with freon, which are frequently used in the purification of the non-fusogenic *Orthoreovirus* [16, 43, 61]. A combination of freeze-thaw cycles before conducting differential centrifugation or ultracentrifugation might be a routine preparatory procedure used in the AqRV purification to obtain a high yield of virus from infected cell lysates. Despite the lack of protease treatment in the general purification of GCRV from lysed cellular components, some degraded viral particles can be observed in untreated viral sample preparations, suggesting that the GCRV particle is capable of degrading spontaneously without the action of exogenous proteases. The fact that there are some SVPs present in the purified viral stock leads us to speculate that the AqRV particle capsid structures are not stable or outer shell protection protein VP7 can easily become detached from penetration protein VP5 under natural conditions or during storage. Based on this phenomenon, stringent and careful handling of viral preparations is needed during AqRV purification. The unstable nature of the AqRV particles might be related to the host-dependent conditions beneficial for establishing efficient infection.

Gene-Protein-Coding Assignment and Protein Nomenclature Generally, each protein of AqRVs encoded by a genome segment is named by its corresponding size. The coding assignments of the SBRV genome segments were the first to be well

determined among the identified AqRVs by in vitro translation in 1994 [32, 62]. Comparison of [^{35}S]methionine-radiolabeled proteins from infected cell lysates and purified virions has led to the distinction of the structural and NS proteins [52, 62]. In this way, 12 proteins (with molecular weights of 130, 127, 126, 97, 73, 71, 46, 39, 35, 29, 28, and 15 kDa) that are encoded by the 11 genomic segments have been identified. Each SBRV segment is monocistronic, with the exception of segment 11, which encodes two NS proteins. Furthermore, of the 12 proteins, seven are structural proteins: VP1 (~130 kDa), VP2 (~127 kDa), VP3 (~126 kDa), VP4 (~73 kDa), VP5 (~71 kDa), VP6 (~46 kDa), and VP7 (~35 kDa) [32, 59, 62], and the remaining five are NS proteins. Further studies on SBRV with SVP-enhanced infectivity assays and single-particle three-dimensional images have shown that segments S5 and S6 encode proteins VP4 and/or VP5, respectively, which resemble the protein product µ1 in MRV encoded by the M2 genome segment [40]. VP4 and VP5 may be isoforms of protein VP5, as reported by McPhillips et al. [35]. The VP5 protein appears to be generated from the products of "VP4," which correspond to the homologous MRV proteins µ1 and µ1C [44]. In fact, comparing the native virion and 5 minut trypsinized [5MT] structures of SBRV shows a noticeable structural change in the trimeric subunits [40]. This observation is highly correlated with the biochemical data of SBRV infectivity assays performed by treatment with protease and visualized by SDS-PAGE [35, 62]. It has been shown that the putative VP5 protein is cleaved after 5 min of trypsin treatment, resulting in a 52-kDa fragment that stays associated with the particle [35]. Further, three-dimensional image reconstruction has been used to determine the VP5 density in an SBRV particle [40]. Therefore, in this regard, the protein VP4 encoded by the S6 segment of the SBRV [35, 62] should be termed as VP5, although no further studies have been conducted on SBRV. Similarly, the copy number of the VP4 protein encoded by the GCRV S5 segment is low, and it is very difficult to detect the protein from purified viral preparations via SDS-PAGE. Early studies have failed to define GCRV gene-protein-coding assignments accurately [28, 64]. Nonetheless, the appropriate gene-protein-coding assignment of GCRV has been obtained and confirmed from purified GCRV proteins by combining full-length genome sequence analysis and three-dimensional image reconstruction [1, 13, 15]. In fact, in another study on MRV [31] and the GCRV S6 sequence [48], the S6 segment-encoded protein has also been defined as VP5. Therefore, based on the current understanding of the molecular virology and high-resolution structural biology of GCRV or AqRVs, it is time to modify the nomenclature of the GCRV-873 (GCRV-I) S6 genome segment-encoded VP4 protein to VP5 to avoid further confusion between VP4 and VP5, which are encoded by genome segments S5 and S6, respectively, in AqRVs.

Proteins Involved in AqRV Morphogenesis The GCRV NS80, a protein homologous to the µNS protein of MRV, has been well characterized [5, 10, 26, 58, 69, 77, 78]. Studies have shown that the NS protein NS80 of GCRV can form VIBs in singly expressed or infected cells and recruit all the ISPs (VP1–VP4 and VP6) in addition to NS38 within its VIBs [69, 78]. It has been confirmed that the coiled-coil motifs in the C-terminal regions of NS80 are crucial for forming VIBs in infected cells, whereas

the N-terminal regions of NS80 play important roles in interacting with viral proteins and supporting viral replication [58, 77]. Similar to σNS in MRV, NS38 is considered to have single-stranded RNA-binding ability and is thought to be involved in viral protein synthesis. In addition to NS80, the GCRV NS38 has also been found to interact with five viral core structural proteins, RNA, and host eIF3A during viral replication for efficient viral protein synthesis. Furthermore, recent evidence showed that NS38 interacts with the OCPs VP5 and VP7 in transfected and infected cells, suggesting that NS38 plays a significant role in progeny particle assembly via interactions with viral proteins and host cell factors. The detailed roles of the viral structural and NS proteins in AqRV morphogenesis remain obscure; therefore, it is further necessary to elucidate the function of each AqRV genome-encoded protein and the interaction among all the proteins during AqRV morphogenesis.

Fusogenic Characteristics of AqRVs Based on the currently characterized genome sequences and deduced protein functions related to the presence or absence of cell fusion-related NS FAST or surface structural σ1-like cell attachment protein, the genus *Aquareovirus* should be subdivided into two distinct subgroups relative to the fusogenic and non-fusogenic orthoreoviruses. The evidence for their phylogenetic classification based on this distinct feature is dependent on the diversity of the S7 genomic segment of the AqRVs. In the genus *Orthoreovirus*, this differentiation is determined by the S class gene, especially the S1 gene in most cases. In fact, most orthoreoviruses, except MRV, are found to encode FAST proteins responsible for inducing cell–cell fusion and syncytium formation [8, 49]. Along with the proteins encoded by fusogenic orthoreoviruses, which are well-characterized examples of transmembrane fusion proteins encoded by nonenveloped viruses, the AqRV FAST proteins are the other known examples. In contrast, the newly identified PRV with 10 genomic segments and the GCRV-II or -III (GCRV-ZH08, GCRV-GD108, and GCRV-104/-109) species have been found to possess a fiber-like cell attachment protein that is similar to σ1, the cell adsorption protein of MRV [41]. Interestingly, it appears that GCRV-104 can induce a typical CPE in infected permissive cells 5 days p.i [11]. This phenomenon may be related to the potential membrane-associated protein NS15 (ORF2), which contains a FAST protein-specific TM domain in the N-terminal region that is found to be encoded by the GCRV-104 genome S11 segment. If this is the case, then GCRV-104 might not only possess σ1-fiber protein in the particle, but also bear fusogenic activity in cell cultures. In addition, a novel membrane-associated protein NS12 has been found to be encoded by the GCRV-I S7 gene segment residing between the gene segments encoding NS16 and NS31. Therefore, this indicates that the fusogenic nature is too complex in AqRVs. To understand the molecular mechanism underlying the pathogenesis of GCRV and other AqRVs, it is important to conduct further extensive and in-depth investigations of the NS FAST-related proteins and their roles in AqRV replication.

To summarize, the molecular characteristics of AqRVs have been extensively studied in recent years. Our current knowledge of the AqRV particle, genome, and encoded protein functions provides a strong basis for further understanding the detailed molecular mechanism of action of AqRV pathogenesis in host cells during

infection. Studies on the interactions between NS80 and NS38 and the OCPs VP5 and VP7 as well as the five core proteins during morphogenesis and particle assembly and those on different fusogenic mechanisms used by AqRVs to enhance viral replication efficiency are warranted. In addition, understanding the role of other unknown NS proteins, such as NS26 and NS31, in regulating viral replication in cooperation with host cellular factors is also critical to reveal the detailed events involved in AqRV replication and pathogenesis.

References

1. Attoui H, Fang Q, Jaafar FM, Cantaloube JF, Biagini P, de Micco P, de Lamballerie X (2002) Common evolutionary origin of aquareoviruses and orthoreoviruses revealed by genome characterization of Golden shiner reovirus, grass carp reovirus, striped bass reovirus and golden ide reovirus (genus Aquareovirus, family Reoviridae). J Gen Virol 83:1941–1951

2. Attoui H, Mertens PPC et al (2012) Reoviridae. In: King AMQ, Adams MJ, Carstens EB, Lefkowitz EJ (eds) Ninth report of the international committee on taxonomy of viruses. Elsevier Academic Press, San Diego, pp 541–637

3. Bartlett NM, Gillies SC, Bullivant S, Bellamy AR (1974) Electron microscopy study of reovirus reaction cores. J Virol 14:315–326

4. Chandran K, Walker SB, Chen Y, Nibert ML (1999) In vitro recoating of reovirus cores with baculovirus-expressed outercapsid proteins μ1 and σ3. J Virol 73(5):3941–3950

5. Chen Q, Zhang J, Zhang F, Guo H, Fang Q (2016) Identification and characterization of two cleavage fragments from the Aquareovirus nonstructural protein NS80. Virol Sin 31:314–323

6. Chen ZY, Gao XC, Zhang QY (2015) Whole-genome analysis of a novel fish reovirus (MsReV) discloses aquareovirus genomic structure relationship with host in saline environments. Viruses 7:4282–4302

7. Cheng L, Fang Q, Shah S, Atanasov IC, Zhou ZH (2008) Subnanometer resolution structures of the grass carp reovirus core and virion. J Mol Biol 382:213–222

8. Ciechonska M, Duncan R (2014) Reovirus FAST proteins: virus-encoded cellular fusogens. Trends Microbiol 22:715–724

9. Dopazo CP, Toranzo AE, Samal SK, Roberson BS, Baya A, Hetrick FM (1992) Antigenic relationships among rotaviruses isolated from fish. J Fish Dis 15:27–36

10. Fan C, Shao L, Fang Q (2010) Characterization of the nonstructural protein NS80 of grass carp reovirus. Arch Virol 155:1755–1763

11. Fan Y, Rao S, Zeng L, Ma J, Zhou Y, Xu J, Zhang H (2013) Identification and genomic characterization of a novel fish reovirus, Hubei grass carp disease reovirus, isolated in 2009 in China. J Gen Virol 94:2266–2277

12. Fang Q, Ke LH,Cai YQ (1989) Growth characteristics and high titer culture of grass carp hemorrhage virus (GCHV)-873 in vitro. Virol Sin (In Chinese with English Abstract)

13. Fang Q, Attoui H, Biagini JF, Zhu Z, de Micco P, de Lamballerie X (2000) Sequence of genome segments 1, 2, and 3 of the grass carp reovirus (genus aquareovirus, family reoviridae). Biochem Biophys Res Commun 274:762–766

14. Fang Q, Xiao TY, Ding QQ (2002) Virological properties of GCRV 991 strain. Virol Sinica 17 (2):183–187. (In Chinese with English Abstract)

15. Fang Q, Shah S, Liang Y, Zhou ZH (2005) 3D reconstruction and capsid protein characterization of grass carp reovirus. Sci China Ser C 48:593–600

16. Fang Q, Seng EK, Ding QQ, Zhang LL (2008) Characterization of infectious particles of grass carp reovirus by treatment with proteases. Arch Virol 153:675–682

17. Francki RIB, Fauquet CM, Knudson SL, Brown F (1991) Classification and nomenclature of viruses, 5th report of the international committee on taxonomy of viruses. Arch Virol 2 (Suppl):186–1991
18. Guo H, Sun X, Yan L, Shao L, Fang Q (2013) The NS16 protein of aquareovirus-C is a fusion-associated small transmembrane (FAST) protein, and its activity can be enhanced by the nonstructural protein NS26. Virus Res 171:129–137
19. Guo H, Chen Q, Yan L, Zhang J, Yan S, Zhang F, Fang Q (2015) Identification of a functional motif in the AqRV NS26 protein required for enhancing the fusogenic activity of FAST protein NS16. J Gen Virol 96:1080–1085
20. He Y, Xu H, Yang Q, Xu D, Lu L (2011) The use of an in vitro microneutralization assay to evaluate the potential of recombinant VP5 protein as an antigen for vaccinating against grass carp reovirus. Virol J 8:132
21. Hedrick PR, Rosemark R, Atonstein D, Winton JR (1984) Characteristics of a new reovirus from channel catfish (Ictalurus punctatus). J Gen Viral 65:1527–1534
22. Huang J, Ke LH, Cai YQ (1992) Study on the reaction core of grass carp hemorrhage virus. Acta Biochem Biophys Sinica 24(2):132–139
23. Huang J, Ke LH, Cai YQ (1992) Ribonucleic acid transcriptase activity associated with purified grass carp hemorrhage disease. Chinese J Virol 8(1):50–56
24. Kanai Y, Kawagishi T, Sakai Y, Nouda R, Kobayashi T (2019) Cell–cell fusion induced by reovirus FAST proteins enhances replication and pathogenicity of non-enveloped dsRNA viruses. PLoS Pathog 15(4):e1007675
25. Ke F, He LB, Pei C, Zhang QY (2011) Turbot reovirus (SMReV) genome encoding a FAST protein with a non-AUG start site. BMC Genomics 12:323
26. Ke F, He LB, Zhang QY (2013) Nonstructural protein NS80 is crucial in recruiting viral components to form aquareoviral factories. PLoS One 8:e63737. https://doi.org/10.1371/journal.pone.0063737 PMID: 23671697
27. Ke L, Fang Q, Cai Y (1990) Characteristics of a new isolation of hemorrhagic virus of grass carp. Acta Hydrobiol Sin 14:153–159. (in Chinese with English Abstract)
28. Ke LH, Wang W, Fang Q, Cai YQ (1992) Studies on the in vitro translation of grass carp hemorrhage virus and its proteins. Chinese J Virol (8)2:169–193
29. Key T, Read J, Nibert ML, Duncan R (2013) Piscine reovirus encodes a cytotoxic, non-fusogenic, integral membrane protein and previously unrecognized virion outer-capsid proteins. J Gen Virol 94:1039–1050
30. King AMQ, Adams MJ, Carstens EB, Lefkowitz EJ (2012) Virus taxonomy, ninth report of the international committee on taxonomy of viruses. Elsevier, San Diego
31. Liemann SK, Chandran K, Nibert ML (2002) Structure of the reovirus membrane-penetration protein, mu1, in a complex with is protector protein, sigma3. Cell 108(2):283–295
32. Lupiani B, Subramanian K, Samal SK (1995) Aquareovirus. Annu Rev Fish Dis 5:175–208
33. Marshall SH, Samal SK, McPhillips TH, Moore AR, Hetrick FM (1990) Isolation of a rotavirus from smelt, Osmerus mordax (Mitchell). J Fish Dis 13:87–91
34. McCrae MA, Joklik WK (1978) The nature of the polypeptides encoded by each of the 10 double-stranded RNA segments of reovirus type 3. Virology 89:578–593
35. McPhillips TH, Dinan D, Subramanian K, Samal SK (1998) Enhancement of aquareovirus infectivity by treatment with proteases: mechanism of action. J Virol 72:3387–3389
36. Meyers TR (1979) A reo-like virus isolated from juvenile American oysters (Crassostrea virginica). J Gen Virol 43:203–212
37. Meyers TR (1980) Experimental pathogenicity of reovirus 13p2 for juvenile American oysters Crassostrea virginica (Gmelin) and bluegill fingerlings Lepomis macrochirus (Rafinesque). J Fish Dis 3:187–201
38. Meyers TR (1983) Serological and histopathological responses of rainbow trout, Salmo gairdneri Richardson, to experimental infection with the 13p2 reovirus. J Fish Dis 6:277–292
39. Mohd-Jaafar F, Goodwin AM, Merry G, Fang Q, Cantaloube J, Biagini P, De-Micco P, Mertens P, Attoui H (2008) Complete characterisation of the American grass carp reovirus

genome (genus Aquareovirus: family Reoviridae) reveals an evolutionary link between aquareoviruses and coltiviruses. Virology 373:310

40. Nason EL, Samal SK, Venkataram Prasad BV (2000) Trypsin induced structural transformation in aquareovirus. J Virol 74:6546–6555

41. Nibert ML, Duncan R (2013) Bioinformatics of recent aqua- and orthoreovirus isolates from fish: evolutionary gain or loss of FAST and fiber proteins and taxonomic implications. PLoS One 8:e68607

42. Nibert ML, Fields BN (1992) A carboxy-terminal fragment of protein u1/u1C is present in infectious subvirion particles of mammalian reoviruses and is proposed to have a role in penetration. J Virol 66:6408–6418

43. Nibert ML, Schiff LA, Fields BN (2001) Reoviruses and their replication. In: Knipe DM, Howley PM (eds) Fields virology. Lippincott Williams and Wilkins, Philadelphia, pp 1679–1728

44. Odegard AL, Chandran K, Zhang X, Nibert ML (2004) Putative autocleavage of outer capsid protein u1, allowing release of myristoylated peptide u1N during particle uncoating, is critical for cell entry by reovirus. J Virol 78(16):8732–8745

45. Pei C, Ke F, Chen ZY, Zhang QY (2014) Complete genome sequence and comparative analysis of grass carp reovirus strain 109 (GCReV-109) with other grass carp reovirus strains reveals no significant correlation with regional distribution. Arch Virol 159:2435–2440

46. Plumb J, Bowser PR, Grizzle JM, Mitchell AJ (1979) Fish viruses: double-stranded RNA icosahedral virus from a North American cyprinid. J Fish Res Board Can 36:1390–1394

47. Qiu T, Lu RH, Zhang J, Zhu ZY (2001a) Complete nucleotide sequence of the S10 genome segment of grass carp reovirus (GCRV). Dis Aquat Org 44:69–74

48. Qiu T, Lu RH, Zhang J, Zhu ZY (2001b) Molecular characterization and expression of the M6 gene of grass carp hemorrhage virus (GCHV), an aquareovirus. Arch Virol 146:1391–1397

49. Racine T, Hurst T, Barry C, Shou J, Kibenge F, Duncan R (2009) Aquareovirus effects syncytiogenesis by using a novel member of the FAST protein family translated from a noncanonical translation start site. J Virol 83(11):5951–5955

50. Rangel AAC, Rockemann DD, Hetrick FM, Samal SK (1999) Identification of grass carp haemorrhage virus as a new genogroup of aquareovirus. J Gen Virol 80:2399–2402

51. Rivas C, Noya M, Cepeda C, Bandin I, Barja JL, Dopazo CP (1998) Replication and morphogenesis of the turbot aquareovirus (TRV) in cell culture. Aquaculture 160:47–62

52. Samal SK, Dopazo CP, McPhillips TH, Baya A, Mohanty SB, Hetrick FM (1990) Molecular characterization of a rotavirus-like virus isolated from striped bass (Morone saxatilis). J Virol 64:5232–5240

53. Samal SK, McPhillips T H, Dinan D (1998) Lack of restriction of growth for aquareovirus in mammalian cells[J]. Arch Virol 143(3):571–579

54. Seng EK, Fang Q, Chang SF, Ngoh GH, Qin QW, Lam TJ, Sin YM (2002) Characterisation of a pathogenic virus isolated from marine threadfin fish (Eleutheronema tetradactylus) during a disease outbreak. Aquaculture 214:1–18

55. Seng EK, Fang Q, Sin YM, Lam TJ (2005a) Molecular characterization of a major outer capsid protein encoded by the threadfin aquareovirus (TFV) gene segment 10 (S10). Arch Virol 150:2021–2036

56. Seng EK, Fang Q, Sin YM, Lam TJ (2005b) Molecular cloning, DNA sequence analysis, and expression of cDNA sequence of RNA genomic segment 6 (S6) that encodes a viral outer capsid protein of threadfin aquareovirus (TFV). Virus Genes 30:209–221

57. Shao L, Sun X, Fang Q (2011) Antibodies against outer-capsid proteins of grass carp reovirus expressed in E. coli are capable of neutralizing viral infectivity. Virol J 8:347

58. Shao L, Guo H, Yan LM, Liu H, Fang Q (2013) Aquareovirus NS80 recruits viral proteins to its inclusions, and its C-terminal domain is the primary driving force for viral inclusion formation. PLoS One 8:e55334. https://doi.org/10.1371/journal.pone.0055334

59. Shaw AL, Samal S, Subramanian K, Prasad BVV (1996) The structure of aquareovirus shows how different geometries of the two layers of the capsid are reconciled to provide symmetrical interactions and stabilization. Structure 15:957–968
60. Skoge RH, Nylund A, Solheim K, Heidrun Plarre H (2019) Complete genome of Atlantic halibut reovirus (AHRV) associated with mortality in production of Atlantic halibut (Hippoglossus hippoglossus) fry. Aquaculture 509:23–31
61. Smith RE, Zweerink HJ, Joklik WK (1969) Polypeptide components of virions, top component, and cores of reovirus type 3. Virology 39:791–810
62. Subramanian K, McPhillips TH, Samal SK (1994) Characterization of the polypeptides and determination of genome coding assignments of an aquareovirus. Virology 205(1):75–81
63. Wang H, Yu F, Li J, Lu L (2016) Laminin receptor is an interacting partner for viral outer capsid protein VP5 in grass carp reovirus infection. Virology 490:59–68
64. Wang Q, Zeng W, Liu C, Zhang C, Wang Y, Shi C, Wu S (2012) Complete genome sequence of a reovirus isolated from grass carp, indicating different genotypes of GCRV in China. J Virol 86:12466
65. Wang W, Cai YQ, Fang Q, Liu Y, Ke L (1994) Gene-protein-coding assignments of grass carp hemorrhage virus genome RNA species. Virol Sin 9(4):356–361
66. Wang X, Zhang F, Su R, Li X, Chen W, Chen Q, Yang T, Wang J, Liu H, Fang Q, Cheng L (2018) Structure of RNA polymerase complex and genome within a dsRNA virus provides insights into the mechanisms of transcription and assembly. Proc Natl Acad Sci 115:7344–7349
67. Winton JR, Lannan CN, Fryer JL, Hedrick RP, Meyers TR, Plumb JA, Yamamoto T (1987) Morphological and biochemical properties of four members of a novel group of reoviruses isolated from aquatic animals. J Gen Virol 68:353–364
68. Yan L, Liu H, Li X, Fang Q (2014) The VP2 protein of grass carp reovirus (GCRV) expressed in a baculovirus exhibits RNA polymerase activity. Virol Sin 29:86–93
69. Yan L, Zhang J, Guo H, Yan S, Chen Q, Zhang F, Fang Q (2015) Aquareovirus NS80 initiates efficient viral replication by retaining core proteins within replication-associated viral inclusion bodies. PLoS One 10:e0126127
70. Yan S, Zhang J, Guo H, Yan L, Chen Q, Zhang F, Fang Q (2015) VP5 autocleavage is required for efficient infection by in vitro recoated aquareovirus particles. J Gen Virol 96:1795–1800
71. Ye X, Tian YY, Deng GC, Chi YY, Jiang XY (2012) Complete genomic sequence of a reovirus isolated from grass carp in China. Virus Res 163(1):275–283
72. Yu F, Wang LL, Li WJ, Wang H , Que SJ, Lu LQ (2019) Aquareovirus NS31 protein serves as a specific inducer for host heat shock 70-kDa protein. J Gen Virol. https://doi.org/10.1099/jgv.0.001363
73. Yu F, Wang LL, Li WJ, Lu L (2019) Identification of a novel membrane-associated protein from the S7 segment of grass carp reovirus. J Gen Virol. https://doi.org/10.1099/jgv.0.001223
74. Zainathan SC, Carson J, Nowak BF (2017) Preliminary characterization of Tasmanian aquareovirus (TSRV). Arch Virol 162:625–634
75. Zhang C, Lu LF, Li ZC, Xiao-Yu Zhou XY, Zhou Y, Chen DD, Li S, Zhang YA (2020) Grass carp reovirus VP56 represses interferon production by degrading phosphorylated IRF7. Fish Shellfish Immunol 99:99–106
76. Zhang F, Guo H, Zhang J, Chen Q, Fang Q (2018) Identification of the caveolae/raft-mediated endocytosis as the primary entry pathway for aquareovirus. Virology 513:195–207
77. Zhang J, Guo H, Chen Q, Zhang F, Fang Q (2016) The N-terminal of aquareovirus NS80 is required for interacting with viral proteins and viral replication. PLoS One 11:e0148550
78. Zhang J, Guo H, Zhang FX, Chen QX, Chang MX, Fang Q (2019) NS38 is required for aquareovirus replication via interaction with viral core proteins and host eIF3A. Virology 2019 (529):216–225

Chapter 3
The Aquareovirus Particle Structure and Protein Functions

Qin Fang, Fuxian Zhang, and Jie Zhang

Abstract Aquareoviruses and orthoreoviruses belong to two different genera in the *Spinareovirinae* group of the family *Reoviridae*, but they share many common features in genome evolution, replication, and particle assembly. Using three-dimensional image reconstruction and cryo-electron microscopy, a mass of structural information of the aquareovirus particles has been revealed. Each aquareovirus particle contains 11 double-stranded RNA (dsRNA) genomic segments enclosed by multilayered proteinaceous shells: the inner and outer shells comprising seven structural proteins (VP1–VP7). The inner core particle is composed of five proteins: VP1, VP2, VP3, VP4, and VP6. The inner core shell is formed by two conformers of VP3 (VP3A and VP3B), which are clamped by equivalent molecules of VP6 (VP6A and VP6B, respectively). A distinct pentameric turret structure formed by five copies of the protein VP1 sits around the 12 fivefold axes crossing over the inner and outer shell. The RNA polymerase protein VP2 and co-factor protein VP4 are anchored to the inner surface near the fivefold axis and found to directly interact with the genomic dsRNA and VP3. The outer shell of the viral particle comprises 200 trimers of VP5–VP7 heterodimers. These seven structural proteins of the aquareovirus are closely related to the proteins λ1, λ2, λ3, μ1, μ2, μ3, and σ3 of the mammalian orthoreovirus (MRV) in the overall protein structure and functional domains. An obvious difference is that the aquareovirus lacks σ1 protein situated on each fivefold vertex, which functions as the cell attachment protein in the MRV. This chapter describes the aquareovirus particle structure and protein functions.

Q. Fang (✉)
State Key Laboratory of Virology, Wuhan Institute of Virology, Chinese Academy of Sciences, Wuhan, China
e-mail: qfang@wh.iov.cn

F. Zhang
College of Animal Science, Yangtze University, Jingzhou, Hubei, China

J. Zhang
State Key Laboratory of Freshwater Ecology and Biotechnology, Institute of Hydrobiology, Chinese Academy of Sciences, Wuhan, China

Keywords *Aquareovirus* · *Orthoreovirus* · Cryo-electron microscopy · Three-dimensional image · Structural protein function

Abbreviations

AqRV   Aquareovirus
ARV   Avian reovirus
BRV   Baboon reovirus
BTV   Bluetongue virus
CPV   Cytoplasmic polyhedrosis virus
Cryo-EM   Cryo-electron microscopy
FAST   Fusion-associated small transmembrane
GCRV   Grass carp reovirus
GTase   RNA guanylyltransferase
ISPs   Inner shell proteins
MRV   Mammalian orthoreovirus
NTPase   Nucleoside-triphosphatase
OCPs   Outer capsid proteins
RdRP   RNA-dependent RNA polymerase
SBRV   Striped bass reovirus

3.1   Introduction

Genome sequence analysis has revealed a highly close evolutionary relationship between the two different genera in the *Reoviridae* family *Aquareovirus* and *Orthoreovirus* [2]. Seven aquareovirus species *Aquareovirus A-G* (AqRV A-G) and some unclassified members have been recognized by the International Committee for the Taxonomy of Viruses mainly based on their host ranges, particular 11 genomic segments, and related sequence characteristics [3]. Interestingly, a piscine reovirus with 10 genomic segments has been recently identified and proposed to represent the prototype strain of a new orthoreovirus, the *Piscine orthoreovirus* genus, and it is not grouped with the *Aquareovirus* genus [26]. In general, aquareoviruses share the syncytium-inducing capacity of fusogenic orthoreoviruses, an uncommon property for nonenveloped viruses. However, few recently reported grass carp reovirus (GCRV) strains (GCRV-HZ08/-GD108/-104/-109) with 11 double-stranded RNA (dsRNA) genome segments isolated from *Ctenopharyngodon idella* show features with no syncytium formation in cultured cells, which distinguishes them from most fusogenic aquareoviruses [18, 39, 50, 55]. Furthermore, instead of the nonstructural fusion-associated small transmembrane (FAST) protein that induces cell–cell fusion in most aquareoviruses, the GCRV-HZ08/-GD108 and GCRV-104/-109 isolates appear to produce a protein

close to the S7 segment-encoded σ1 cell-attachment-like protein found in the non-fusogenic mammalian reovirus (MRV) by genome sequence and bioinformatics analyses [34]. Therefore, it is clear that a meaningful multiple sequence alignment can only be performed for closely related pathogenic agents, and the present means of bioinformatics analyses are truly unable to recognize the structural and functional similarities in viruses within the same genus or between different genera based only on their sequence alignments.

Although increasing numbers of the aquareovirus species have been sequenced in recent years, only the striped bass reovirus (SBRV) (AqRV-A) and GCRV (AqRV-C) have been characterized by three-dimensional image reconstruction using cryo-electron microscopy (Cryo-EM). Traditional negatively stained images can simply show the overall viral particle morphology; the purified structural protein components contained in the aquareovirus particles need to be identified using SDS-PAGE. However, it is not always possible to separate unique viral proteins from the remaining minor host cell components accurately by classic biological analysis methods. Notably, current progress in the structural biology of individual proteins and virus particles from different genera of the family *Reoviridae* or other types of viruses can precisely identify the localization of each structural protein in the particle and has revealed an architectural principle common to some seemingly unrelated enveloped or nonenveloped viruses. Furthermore, it has also been recognized that the structural organization of a number of dsRNA viruses placed in different genera exhibits similar biological functions in virus infection and replication, even though they have widely divergent genome sequences. Three-dimensional image reconstruction by Cryo-EM of the aquareovirus has demonstrated that the capsid proteins of the SBRV and GCRV share marked similarities with those of the members of the genus *Orthoreovirus*, including the MRVs, avian reoviruses (ARV), and baboon reovirus (BRV) [20, 47, 54]. Studies involving single-particle Cryo-EM and three-dimensional image reconstruction of the reovirus particles, as well as X-ray diffraction of crystalline structure have shown that the virus particle organization and structures of different virus types correspond to their functions in viral infection and replication cycles [13, 31, 45, 56, 60]. The diversity of viruses from these different genera suggests that additional comparative studies on the viral protein structure are likely to provide important new insights into not only their molecular evolutionary cues, but also the structural and functional basis of their viral particle construction.

Analyses of reconstructed particle images have revealed a common evolutionary architecture for structurally different reoviruses, such as the turreted MRV and non-turreted reoviruses, including the rotavirus and bluetongue virus (BTV) [26]. In addition, the progress in Cryo-EM techniques has fostered the use of structural data to understand the functions of the complex molecular architectures. Some near-atomic or atomic-resolution reconstructions using Cryo-EM have allowed integration of structural and functional information into a coherent mechanism for understanding the reovirus replication and assembly. In recent years, the three-dimensional structures of the aquareovirus particles have been well studied by

Cryo-EM. Therefore, in this chapter, we summarize the current progress on the structural basis of the aquareovirus and related functions.

3.2 The Aquareovirus Particle and Its Structural Protein Localization

3.2.1 Similarities and Differences between the Aquareovirus, Orthoreovirus, and Other Viruses in the Family Reoviridae

The family Reoviridae is a diverse group of viruses with 9–12 segmented dsRNA genomes contained within one-, or double-, or triple-layered protein capsids. The genus demarcation criteria in the family have been originally based on mainly the virus host ranges and number of genome segments. Analyses of the reconstructed particle images obtained by three-dimensional image reconstruction have revealed a common evolutionary architectural principle for structurally different reoviruses. According to the particle surface structure with or without a spike situated at the 12 icosahedral vertices of either the virus or the core particle, the proposed 15 genera have been assigned to either of the two subfamilies *Spinareovirinae* and *Sedoreovirinae* in the family *Reoviridae* [26]. The subfamily *Spinareovirinae* comprising nine genera includes viruses such as the MRV (a reovirus prototype with typical turreted morphology). The subfamily *Sedoreovirinae* comprising six genera includes viruses such as the rotaviruses, and BTVs, which are well-characterized non-turreted reoviruses. Based on the structural differences in the outer shell surface between the turreted and non-turreted reoviruses, it is clear that the outer capsid proteins (OCPs) are directly involved in the virus and host cell interactions and exhibit a great level of divergence.

Virus members in the genus *Aquareovirus* of the subfamily *Spinareovirinae* can infect a variety of aquatic animals, including finfish and crustaceans. Their genome contains 11 linear dsRNA segments (termed as S1–S11), which is similar in composition to that of the members of the genus *Rotavirus* in the subfamily *Sedoreovirinae* of the family *Reoviridae* [26]. The aquareovirus genome segments can be categorized into three classes (S1–S3, S4–S6, and S7–S11) based on the size of each segment in gel electrophoretic analysis. These 11 segments encode at least 12 proteins, with seven of them building the viral particle [11, 12, 20, 51]. The structural proteins are VP1 to VP7; however, the outer capsid penetration protein VP5 is often detected by biochemical analysis in two isoforms: full-length VP5 (68 kDa) and cleaved VP5C* (64 kDa) [21, 53]. With the same number of genomic segments as the rotaviruses, which cause animal and human diarrhea, the virus particle has a "smooth" appearance. In a virus with a typical triple-layered protein capsid shell encompassing a genome of 11 linear dsRNA segments (S1–S11) that encodes 13 primary proteins, six structural proteins VP1–VP6 of rotavirus have been

identified. Similar to the aquareovirus VP5, the spike protein VP4 (87 kDa) can produce two isoforms: VP5* (60 kDa) and VP8* (28 kDa) by in vitro treatment with trypsin [10, 16, 17, 45].

Orthoreoviruses infect reptiles, birds, and mammals (including humans). All members of the orthoreoviruses have 10 linear dsRNA segments that encode 11 proteins. These segments are grouped into three size classes, commonly referred to as the large (L1–L3), medium (M1–M3), and small (S1–S4) classes, based on their electrophoretic mobility in gels. The MRVs are well-characterized members of the orthoreoviruses. The eight identified structural proteins have been designated in terms of their relative sizes and size classes using the Greek symbols: λ (λ1, λ2, and λ3), μ (μ1 and μ2), and σ (σ1, σ2, and σ3) [37]. In general, penetration protein μ1 can be cleaved into μ1N and μ1C, and isoforms μ1 and μ1C are often detected in particles [7–9, 38]. As a homologue protein μ1 in MRV, VP5 and its cleavage fragment VP5N and VP5C atomic model in GCRV particles have been resolved [51, 61].

The innermost protein layer of the reovirus particles in the two subfamilies (*Spinareovirinae* and *Sedoreovirinae*) has an internal diameter of approximately 50–60 nm and surrounds the dsRNA genome segments. Despite the structural differences in the core particles, all the reovirus cores consist of multi-enzyme machinery that is responsible for self-RNA synthesis. The enzymatic proteins in the cores of different groups of reoviruses are greatly conserved not only in the sequence of functional domains at the genomic level but also in the structural conformation at the protein level.

Interestingly, both aquareoviruses and rotaviruses have 11 genomic segments, but no cross-serological reaction has been detected between the two viruses. In contrast, despite the differences in the number of segments and host range between the aquareoviruses and orthoreoviruses, they show not only high genome sequence homology, but also structural similarity in the particle protein shell. In fact, the aquareoviruses and orthoreoviruses species share a set of seven homologous structural proteins in addition to two nonstructural proteins, with each protein encoded by a single long open reading frame in each of the seven cognate genome segments [34]. Apparently, this clear genetic relationship between members of distinct genera is unique within the family *Reoviridae*. Based on sequence identities and structural similarities, there is no doubt that the aquareoviruses and orthoreoviruses originate from a common evolutionary ancestor. Apart from the homologous proteins in the two genera, two proteins with distinct biological functions are not consistently homologous between the two genera. One is the outer fiber protein present in most orthoreoviruses and few aquareoviruses, which anchors atop the turret protein at the icosahedral fivefold axes of virions and mediates attachment to cell-surface receptors [34, 43]. The other is the nonstructural FAST protein of the aquareoviruses and some fusogenic orthoreoviruses, which promotes cell–cell fusion fostering formation of syncytium and release of progeny virions via syncytium-induced cytopathic effects [34]. As described in the previous chapter, the two functionally distinct proteins are encoded by the small (S) class genes (by S7 segment in some aquareoviruses or by S1 segment in some orthoreoviruses) in both genera. The S class gene segments are
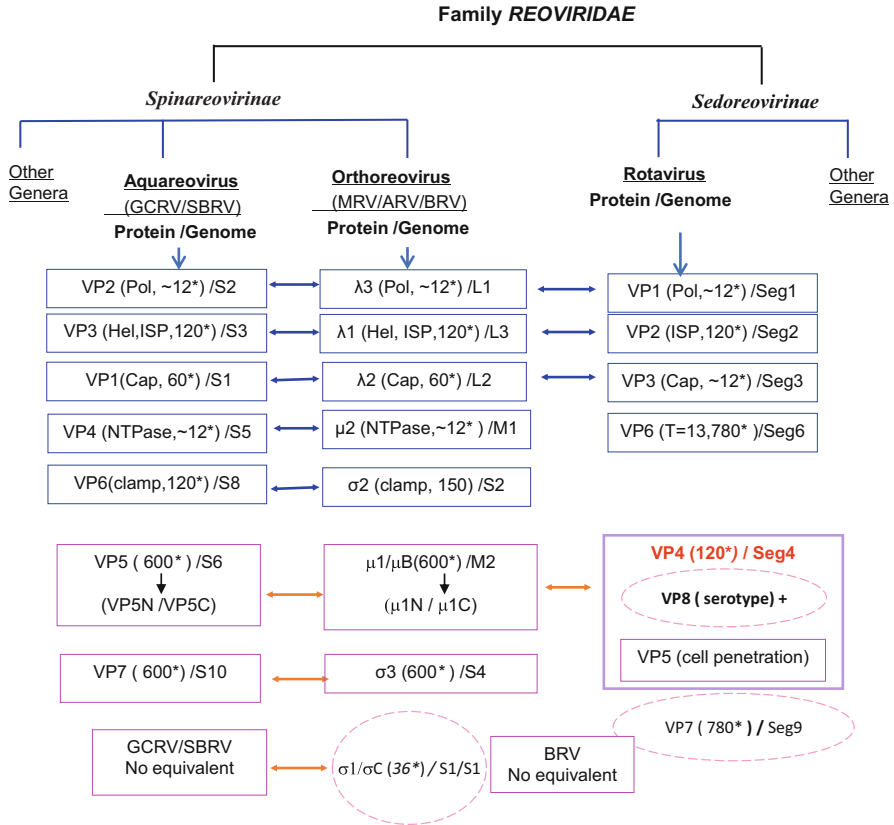
Fig. 3.1 Properties of proteins in aquareovirus, orthoreovirus, and rotavirus particles. The reovirus particle is composed of a core and an outer shell. Core proteins are shown in blue boxes and outer shell proteins in pink boxes, the proteins in dashed pink ellipses are serotype-specific antigens. * indicates molecular copies of proteins in one particle

often bicistronic or multicistronic. The evolution of these bicistronic or tricistronic genome segments is important for not only the virus-induced cell toxicity, but also the antigenicity-related particle structure. Structural biology determined using single-particle three-dimensional image reconstruction has confirmed that the proteins encoded by the large genome segments of the reoviruses, which perform endogenous enzymatic functions, remain conserved, whereas the proteins encoded by the small genome segments, which initiate viral infection and cell entry, are divergent. The properties of the structural proteins of the virus in the genera *Aquareovirus* and *Orthoreovirus* in the subfamily *Spinareovirinae* and *Rotavirus* in the subfamily *Sedoreovirinae* are schematically depicted in Fig. 3.1.

3.2.2   Comparison of Structural Proteins in the Aquareoviruses and Orthoreoviruses

Recent sequencing efforts and three-dimensional image reconstruction of the aquareovirus and orthoreovirus particles have contributed a great deal of new molecular and structural biology information, suggesting origination from a common evolutionary ancestor. Thus, aquareoviruses and orthoreoviruses are likely to share a common viral ancestor from which the genome segment-encoded proteins have been inherited [2, 19]. The mature aquareovirus particles are composed of seven structural proteins (VP1–VP7). Moreover, the inner core of the aquareovirus is formed by five proteins; these are VP1 (core turret), VP2 (RNA-dependent RNA polymerase, RdRP), VP3 (core shell), VP4 (nucleoside RdRP co-factor protein), and VP6 (core clamp). These five core proteins strongly correspond to the MRV/ARVλ2/λC, λ3/λB, λ1/λA, μ2/μA, and σ2/σA. The remaining two proteins, VP5 and VP7, and their homologous proteins, μ1/μB and σ3/σB, in the MRV/ARV comprise the viral outer coat. The inner core proteins are involved in initiating the endogenous transcriptional activity, which is responsible for viral transcription and replication, while the outer capsid layers are important for facilitating cell entry. The only aspect of their particle structural composition that is different across the two genera is the absence of σ1 protein in aquareoviruses, which mediates attachment to cell-surface receptors in the MRV [37]. In most orthoreoviruses, including MRV and ARV, the cell attachment protein σ1/σC is situated atop the turret protein at the 12 icosahedral fivefold axes [43, 54, 59]. However, the aquareovirus lacks σ1-like cell attachment protein at the corresponding position on the particle surface. It is clear that σ1 protein plays a significant biological role in the non-fusogenic orthoreoviruses and some fusogenic ARVs, but it is not found in the mature aquareovirus particles and few fusogenic orthoreoviruses, such as the BRVs (Fig. 3.1). BRV is the prototype strain of the distinct fusogenic MRV species. Cryo-EM studies indicate that BRV lacks the outer fiber protein that binds to cell-surface receptors [54], which is consistent with the genome sequence data of BRV. It has been revealed that the BRV S4 segment is bicistronic, and the second encoded protein is the nonstructural FAST protein p16, which shows no sequence similarity with the outer fiber protein. The surface structural features of the BRV particles are more similar to those of the aquareovirus virions rather than the MRV and ARV [54]. The three-dimensional image reconstruction of the aquareovirus enhances our understanding that the virus species evolution may be in accordance with their particle structural protein function.

3.3   Cryo-EM Analysis of the Aquareovirus/GCRV Virions

3.3.1   Electron Cryomicrograph Records of the Purified GCRV Cores and Virions

The purification of the aquareovirus virions, including the GCRV and SBRV, from infected permissive cells by differential and density gradient centrifugation has been described [20, 21, 33, 47]. Transmission electron cryomicrographs have been recorded from unstained frozen hydrated virion and core specimen suspensions. The intact virion is ~850 Å in diameter. The minor size differences depend on the micrographs of unstained frozen hydrated specimen preparations of the virus. The morphology of the GCRV protein capsid shows the typical double-layered nature. An obvious electron-lucent boundary divides the virion capsid into the inner and outer layers. The individual particles appear largely round, and no evident projections of structures farther from the particle surfaces are observed. Striated features in some areas on the surface, viewed in the morphological profile, are reminiscent of regularly spaced subunits. The boundary separating the outer shells and inner cores is demarcated by a prominent white ring (~610 Å in diameter). The overall size of the core particles is ~810 Å in diameter, including the turret projections at its fivefold axes (Fig. 3.2 a, b). These projections are analogous to the turret-like structures located at the pentameric vertices in the reovirus core structure [42]. Overall, the structural images are very similar to those constructed for orthoreoviruses.

Fig. 3.2 Electron cryomicrograph of purified aquareovirus particles. (**a** and **b**) Transmission electron cryomicrograph of unstained GCRV intact virion (**a**) and core (**b**). (**c**) SDS-PAGE of GCRV genomic dsRNA from GCRV virion and core. (**d**) Protein gel lane of purified GCRV virion and core. The arrow in **a** points to an electron-lucent boundary between the inner and outer layers; and the arrowhead in **b** indicates a turret. M is standard molecular marker in **c** and **d**
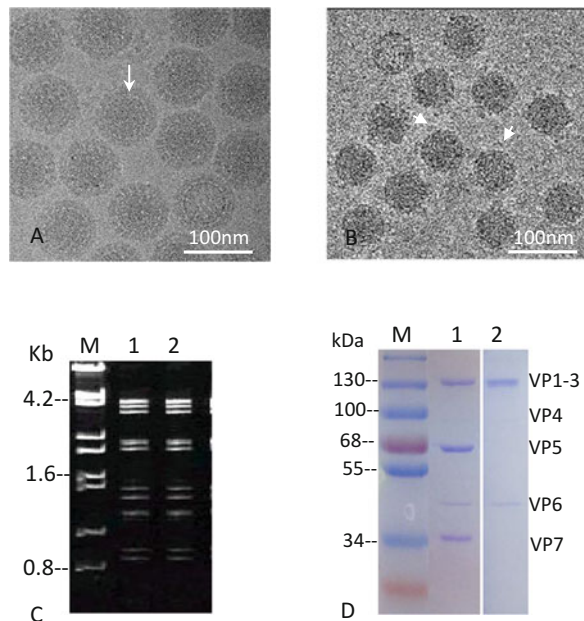
The viral particle components have been confirmed by analyzing the viral dsRNA and protein profiles of purified virion specimens. The 11 genomic segments in both intact particles and viral cores have been detected using classic SDS-PAGE. In addition, seven structural proteins, VP1 (138 kDa), VP2 (137 kDa), VP3 (136 kDa), VP4 (79 kDa), VP5 (67 kDa), VP6 (43 kDa), and VP7 (34 kDa) have been detected by SDS-PAGE (Fig. 3.2 c, d), indicating that the purified virions are intact.

3.3.2 Overall Three-dimensional Structures of the Aquareovirus Virion

The surface view of the three-dimensional reconstructed image shows the aquareovirus to be a nonenveloped icosahedral particle. Each GCRV particle has a diameter of 850 Å and is composed of multiple density layers. The particle architecture is composed of the inner core, including genome dsRNA segments and inner shell protein and the outer capsid shells (Fig. 3.3 a, b, c). Seven viral proteins have been verified in the mature aquareovirus particles [11, 12, 20, 51]. The inner core structure, which is composed of five proteins (VP1, VP2, VP3, VP4, and VP6) shows a $T = 1$ symmetry capsid shell of approximately 610 Å diameter, excluding the turret projections at the fivefold vertices. In particular, the main core shell frame is formed by 60 VP3 dimers, which are clamped tightly by 60 dimers of VP6 molecules. A notable feature is that the pentameric spikes, residing on the surface of the core at the fivefold axes of the 12 typical icosahedral vertices, are built with five copies of VP1 molecules, thereby constituting 60 copies of the turret protein VP1 in total. In addition, a strong density beneath each turret has been observed, which is attributed to the GCRV transcriptase complex that is likely a heterologous complex of RdRP (VP2) and its putative co-factor VP4. The VP2–VP4 complex is closely related to VP3 protein and viral dsRNA genome [51]. The GCRV outer shell has an incomplete $T = 13$ icosahedral symmetry, which comprises VP5 and VP7, of approximately 40 Å thickness. Each aquareovirus virion contains 200 trimers of VP5–VP7 heterodimers, which associate with each other and interact with the inner clamp protein VP6 and turret protein VP1.

3.3.3 Features of the Aquareovirus Outer Capsid

Radially color-coded surface views of the three-dimensional reconstructed image show the detailed overall architecture of the aquareovirus virions. On the surface of the aquareovirus virion, there are 200 trimers of VP5–VP7 heterodimers arranged on an incomplete $T = 13$ icosahedral lattice in regions between the turret structures (Fig. 3.3a). Three characteristic density rings surround the threefold symmetry axis
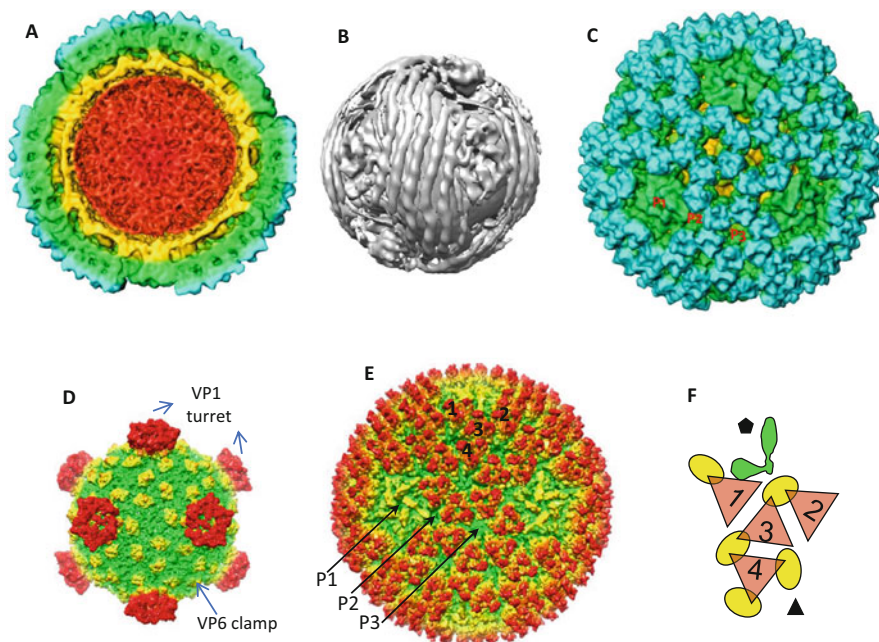
Fig. 3.3 3D reconstruction image of GCRV core and intact particle. Central cross-sections of the 3D image (17 Å) of GCRV virion, which is color coded according to particle radius. RNA core is red, inner layer is orange, middle layer and outer layer are green and aquamarine, respectively (**a**). The 3D image of GCRV genomic dsRNA (**b**). Surface views of GCRV 3D image at 17 Å resolution (**c**). Radially colored shaded surface representation of GCRV core (**d**) and virion (**e**) at 9 Å resolution. A cartoon illustrating organization of capsid proteins VP5–VP7 trimers (red) interactions with the clamp protein VP6 (yellow) (**f**). The triangles represent the VP5–VP7 heterodimers on the virion. Four kinds of quasi-equivalent trimers are marked by 1, 2, 3, and 4. Three types of conduits P1, P2, and P3 are indicated. The images in **a** and **c** are modified from reference [20]

at each icosahedral vertex comprising six shared trimmers. These intra- and inter-trimeric interactions between VP5 and VP7 heterodimers lead to the formation of a network of densities on the outer shell, and thus, further stabilize the outer layer. These trimers associate with the adjacent pentameric proteins VP1 to form three types of conduits (open) perforating the outer capsid layer: P1, P2, and P3 (Fig. 3.3 c, e). Consequently, this leads to the formation of 132 solvent-filled channels (including 12 P1-, 60 P2-, and 60 P3-bearing positions of the lattice) on the whole outer capsid of the aquareovirus particles, which is the same as that found on the turreted orthoreoviruses, including the MRVs, ARVs, and BRVs [14, 54, 59]. In contrast, the non-turreted rotavirus, which also contains a genome of 11 dsRNA segments, comprises 260 subunits of trimers on the outer layer [16, 45], thus having a different outer shell structure. Notably, similar to the ARV and BRV, and unlike that in MRV, the inner capsid protein density is visible through all the conduits on the aquareoviruses. This feature indicates that VP5 in the GCRV/SBRV lacks the counterpart densities corresponding to the C-terminal of µ1 protein, which have

been observed to form the hub-and-spoke structures in the interior of P2 and P3 conduits of the MRVs [14, 28]. A distinguishing feature on the outer layer is the fivefold proximal depressions resulting from missing peripentonal trimers. The absence of these trimers exposes the protein subunit arrangement of the inner layer.

3.3.4 Specialized Regions Around the Five-Fold Axes

The viruses containing cores with turret structures are classified in the *Spinareovirinae* subfamily because these virus members have pentameric spikes residing on the surface of the core at the fivefold axes on the 12 typical icosahedral vertices, which distinguish these viruses from the smooth reoviruses that belong to the *Sedoreovirinae* subfamily. The features of the aquareovirus surface structure at the icosahedral fivefold axes are different from the adjacent icosahedral threefold and twofold vertices, indicating that the particle organization appears in an ordered arrangement around the icosahedral fivefold vertices. In particular, the aquareovirus turret protein VP1 pentamer is a hollow cylinder-like structure located at the icosahedral fivefold symmetry axis passing through the outer shell to the inner core, thereby functioning as a tunnel that caps newly synthesized RNAs and transports the transcribed products from the core to the cytoplasm for protein synthesis. In the MRV/ARV, the outward projecting σ1 protein is on top of the protein λ2 (protein homologous to VP1) at the icosahedral fivefold axis. As the intact GCRV particle lacks the MRV σ1 cell attachment protein, a depressed structure appears around the fivefold axis (Fig. 3.3d). In addition, unlike the closed turret in the MRV, the GCRV VP1 turret is open in both the core particle and the virion. The open turret structure has also been observed in the BRV, which is the only known fusogenic MRV [54]. The open turrets observed in fusogenic aquareoviruses and the BRV may be attributed to the lack of σ1 cell attachment protein, as found in the MRV/ARV [54, 59].

3.3.5 Differences in the Features of the Aquareovirus and MRV Core Structures

The overall three-dimensional image reconstruction of the aquareovirus core has shown that it is composed of five proteins (VP1, VP2, VP3, VP4, and VP6), which are strikingly identical to the core proteins λ2, λ3, λ1, μ2, and σ2 of the MRV, respectively [42]. The core protein structure similarities and sequence identities between the GCRV and MRV exhibit a decreasing trend. The sequences of the viral proteins (VP1–VP4) related to replication and transcription are more conserved at the genome level than that of the VP6 clamp protein, which is located at the intermediate layer and exhibits some obvious divergence across the species of the

turreted virus genera of the family *Reoviridae*. Furthermore, three-dimensional image reconstruction shows that aquareoviruses, including the GCRV and SBRV, contain 120 copies of VP6 (VP6A and VP6B) as compared to 150 copies of σ2 found in orthoreoviruses (including the MRV, ARV, and BRV) with three con- formers [54, 59]. The clamping protein on the GCRV core is more similar to that found in the cytoplasmic polyhedrosis virus (CPV) of the genus *Cypovirus* in the *Reoviridae* family, which consists of only a single protein shell [12, 29].

3.3.6 Centrally Condensed dsRNA Genome

The GCRV genome has recently been resolved using Cryo-EM and three- dimensional image reconstruction. It shows that the aquareovirus genome is enclosed in a central spherical core of approximately 60 nm in diameter (Fig. 3.3 b). The dsRNA genome is well ordered, runs in parallel, and exhibits discontinuous dsRNA fragments, which are the same as that observed in the CPV [56, 62]. The distances between two adjacent parallel dsRNA fragments within the same layer have been noted as being ~28 Å. It has been observed that two adjacent layers are also ~28 Å apart, and the helix pitch is ~30 Å. The double helices of the dsRNA fragments are located close to the inner capsid protein VP3 and interact with the RdRP complexes (VP2 and VP4) [51].

3.4 Protein Localization and Functional Analysis

3.4.1 The Inner Shell Proteins (ISPs)

3.4.1.1 Core Frame Protein VP3

Protein VP3 of the GCRV is 1214 amino acids long (~132 kDa) and encoded by the S3 genomic segment (3702 nt). There are 120 VP3 molecules in the GCRV and SBRV, which form a continuous spherical inner core shell. VP3 has a plate-like, helix-rich structure that resembles the ISP structures of other dsRNA viruses [42]. Two slightly different conformers of VP3 (VP3A and VP3B) form the $T = 1$ symmetry core shell through self-associations of 60 asymmetric VP3 homodimers [11, 12]. Similar to the corresponding proteins of other members in the *Reoviridae* family, such as λ1 protein in the MRV, both conformers of VP3 have a plate-shaped structure with three domains: apical, carapace, and dimerization domains [42]. VP3 not only connects with clamp protein VP6 and core spike protein VP1 on its outer surface in viral particles, but also binds the RdRP complex (VP2 and VP4) and dsRNA genome on its inner surface to form viral transcriptase complexes. It is supposed that VP3 plays a role in both transcription and particle assembly.

The two structural conformers of the ISP VP3 occupy different positions in the viral particle with icosahedral symmetry. VP3A is near the fivefold axis, and VP3B is near the threefold axis. The main differences between the two conformers VP3A and VP3B are presented by their amino terminal domain and peripheral regions. Similar to mammalian reovirus λ1A, VP3A has a plate-like structure with two subdomains: subdomain I (amino acid residues 410–858) and subdomain II (amino acid residues 188–409 and 859–1214). VP3B has an additional subdomain III (i.e., amino acid residues 19–187). Excluding the flexible N-terminal residues 1–18 of VP3B and residues 1–149 of VP3A (1–149 or 1–177), all remaining aquareovirus VP3 residues have been resolved [12, 51].

Comparing the homologous aquareovirus VP3 and MRV λ1, the VP3 inner shell shows a high degree of structural similarity to λ1, which is consistent with the close evolutionary relationship of about 31% overall sequence identity [2, 19]. Furthermore, a direct comparison of the aquareovirus VP3 and MRV λ1 density map indicates that most of the secondary structure elements overlap and are thus highly structurally conserved. In addition, equivalent framework and general domains of VP3 have also been identified in other dsRNA viruses, such as the CPV [56]. The density map of the aquareovirus VP3 fits well with almost all the α-helices of the MRV λ1, except the N-terminal α-helix region [12]. This N-terminal α-helix is located on the inner surface facing the viral RNA genome, suggesting that distinct RNA organizational and transcriptional functions may be exhibited by the ISPs because of varying dsRNA genome segments and some transcriptase-related protein domains across the two genera.

It should be noted that the N-terminal region (subdomain III) of the aquareovirus VP3B has the least similarity to its counterpart λ1B in the MRV, despite the overall identity and similarity for VP3 and λ1B, which suggests that the N-terminal region of VP3 is the most divergent among VP3 homologs in other members of the *Reoviridae* family. Moreover, it has been determined that the N-terminal region of VP3B is connected to a highly conserved zinc-finger motif (residues 119–140) via a long loop with an obviously visible knot near amino acid residue Pro103. This typical zinc-finger motif belongs to the "Cys-Cys-His-His" class, which is a well-characterized class of zinc fingers and known to bind RNA. Such a zinc-finger motif near amino acid residue 200 (residues 183–203) has also been observed to bind zinc in the core crystal structure of the MRV [4, 22, 42]. In addition, the extended subdomain III of VP3B may play a structural role in core stability by strengthening the molecular contacts surrounding the threefold and twofold axes. Indeed, the two conformers of VP3 (VP3A and VP3B) form the ISP architecture, and interaction between VP3A and VP3B and the outward clamp protein VP6 greatly strengthens the inner shell and provides flexibility. Therefore, the aquareovirus VP3 protein is involved in the viral core assembly. Biochemical data on recombinant cores in vitro have shown that the N-terminal region of λ1B is indispensable for the MRV core assembly [42].

It is known that the reovirus cores are endogenous transcriptional machines, wherein nascent viral mRNA is produced. In the MRV, λ1 has been proposed to play a role in transcription, and its capacity to bind RNA may be significant

[24, 25]. Another study has shown that recombinant λ1 can mediate nucleoside-triphosphatase (NTPase), RNA helicase, and RNA capping activities [5], suggesting multiple roles of λ1 in viral RNA synthesis. Previous biological data obtained by recoating particles have indicated that the MRV cores and sub-viral particles lacking OCPs μ1, σ3, or σ1 can synthesize mRNA, but the dormant intact virions that contain complete outer capsids cannot synthesize mRNA. Similarly, the GCRV cores can be activated for transcription, but the dormant intact GCRV virions that contain OCP complexes of VP5 and VP7 are unable to produce mRNA [12]. This evidence indicates that the transcription activity of the GCRV core may be activated upon the uncoating of the outer shell containing VP5–VP7 complexes. Indeed, VP3B–RNA interactions and conformational changes of VP3B between the virion and the transcription-competent core have been observed by fitting the core protein structures from the virion into the 9-Å resolution reconstructed image of the transcription-competent core. It has been shown that two α-helices in the N-terminal region of VP3B of the virion disappeared in the transcription-competent core, while the remaining portions of the VP3A and VP3B in the virion fit well with that in the core [12], suggesting that the N-terminal segment of VP3B is structurally flexible and can generate the transcription-competent core. Furthermore, interaction between the N-terminal segment (residues 19–29) of subdomain III of one VP3B molecule and the C-terminal loop (residues 175–186) of subdomain III of its neighboring VP3B has been observed for all VP3B molecules. It is possible that the core protein interacts with the RNA inside through this portion of the inner capsid. Similarly, it has been proven that the hydrophilic N-terminal segment of λ1 of the MRV has dsRNA-binding properties [12]. The observed conformational change in the VP3B N-terminal segment from the GCRV virion to the transcription-competent GCRV core, significant sequence divergence, and the RNA-binding ability of this VP3B N-terminal region suggest possible roles of subdomain III of VP3B in recognizing specific RNA, mediating RNA packaging during capsid assembly, and regulating genomic RNA transcription. An additional atomic image of the GCRV has further revealed that the VP3A N-termini are critical in recruiting VP2 and VP4 during virus assembly. Collectively, VP3 has been shown to have RNA-binding activity and play a role in viral particle assembly.

3.4.1.2   Core Clamping Protein VP6

VP6 of the GCRV is encoded by the S8 genomic segment (1287 nt) and has a molecular weight of approximately 44 kDa (412 amino acids). VP6 has a total of 120 copies or 60 dimers; it is located close to the outer ISP VP3 to secure the VP3-formed inner shell and acts as a bridge connecting the outer shell with the inner core. Corresponding to the ISP VP3, there are two conformers of VP6: VP6A and VP6B, which are located at two different positions in an asymmetric unit surrounding each fivefold and threefold axis, respectively. VP6A and VP6B have different modes of interaction with the underlying VP3 molecules despite being identical in structure. Furthermore, analyses of three-dimensionally reconstructed images

obtained by Cryo-EM have revealed two conformations of the GCRV VP6 (VP6A and VP6B) located at two different positions in a $T = 1$ asymmetric core. The GCRV VP6A surrounds each fivefold axis, while VP6B surrounds each threefold axis, which is similar to that observed for LPP clamp protein in the CPV from the turreted subfamily of the family *Reoviridae* but different from that observed in the MRV or ARV core with 150 protein clamps. The globular monomer σ2 in the MRV binds at three distinct locations within each icosahedral asymmetric unit. There are 60 copies of σ2 at the fivefold axes and another 60 at the threefold axes, which correspond to the localizations of the GCRV VP6A and VP6B subunits. In addition, σ2 in the MRV has been found to have another 30 copies at the twofold axes, which are absent in the aquareovirus core, such as in the CPV [11, 56]. Moreover, the GCRV VP6 shares approximately 33% sequence similarity with its homolog protein σ2 in the MRV. Each VP6A molecule interacts with one copy each of VP3A and VP3B, whereas each VP6B molecule is in contact with one copy of VP3A and two copies of VP3B, which is similar to the interactions observed for LPP in the CPV. In addition, VP6 has an additional role of bridging the inner core with the outer shell. These interactions involve the OCP VP5 and the ISPs VP6 and VP1. Correspondingly, VP6A has been observed to have a weak interaction with turret protein VP1. The clamping protein VP6 has different interaction modes with the four types of trimers of VP5–VP7 complex (Fig. 3.3 f). However, since VP6 in the aquareovirus has 120 copies as opposed to 150 copies of σ2 in the orthoreovirus, the interactions between the mediator VP6 and VP5–VP7 trimers are not as stable as that of σ2 with μ1 and σ3 complex [14]. In fact, the outer shell of the aquareovirus can be readily removed without conducting any physical or chemical treatment. Therefore, the aquareovirus VP5–VP7 layer detachment prior to endogenous RNA transcription in the cytoplasm may be related to such unstable/loose interactions between VP6 and VP5–VP7 trimers during the early stage of viral infection [12].

The biological function of the GCRV VP6 or its homolog is poorly understood, except for its stabilizing role in viral particles. It has been found that no icosahedral particles can be formed when the λ1 MRV is singly expressed in mouse L cell fibroblasts or insect cells, unless σ2 (the homologous VP6 protein) is also co-expressed [42]. The recombinant particle structure obtained in vitro has confirmed that σ2 functions as a stabilizing clamp protein. However, in non-turreted reoviruses, previous studies have shown that the inner layers of the rotavirus and BTV do not have any decorated element on their core shell. In addition, viruses lacking clamp proteins, such as the rotaviruses lacking VP2 and orbiviruses lacking VP3, can self-assemble into icosahedral particles [23, 27, 42]. This suggests that σ2 of the MRV or its analog VP6 of the aquareovirus in the *Spinareovirinae* subfamily is indispensable for core shell assembly. These results also indicate that structural relationships directly affect the biological function of VP6.

3.4.1.3 Turret Protein VP1

The GCRV protein VP1 is encoded by the S1 genomic segment (S1, 3949 nt) and has a molecular weight of approximately 141 kDa (1299 amino acids). Five copies of the VP1 protein form a turret, which is a cylindrical pentameric complex that sits around each of the fivefold axes of the 12 vertices. As such, each viral particle consists of 60 copies of VP1 subunits in total. The aquareovirus turret protein VP1 has enzymatic activities, including guanylyltransferase (GTase) and methyltransferase activities in mRNA capping, highly conserved with its homologous protein λ1 in the orthoreovirus [11, 12, 19], which is consistent with the approximately 45% similarity and 23–26% sequence identity obtained by pairwise sequence alignments with core turret protein λ2 of the MRV and ARV and λA of the BRV [54]. The three-dimensional structural images of the aquareovirus VP1 and orthoreovirus λ2 have revealed that these proteins comprise multiple domains. The turret protein is an mRNA-capping complex and functions in catalyzing the mRNA 5′ cap synthesis, and the GTase activity of VP1 has been demonstrated [41]. Owing to the distinct localization, wherein the protein passes through the inner and outer shell surfaces, VP1 has direct and indirect interactions with adjacent structural proteins: ISPs VP3, clamp protein VP6, and RdRP complex VP2–VP4, and OCP VP5.

The structures of individual domains of VP1 closely resemble those of the domains of λ2 protein of the orthoreovirus core. VP1 can be divided into seven domains: the GTase domain (amino acid residues 1–389), the bridge domain (amino acid residues 390–437 and 695–805), the first methyltransferase domain (methylase-1, amino acid residues 438–694), the second methyltransferase domain (methylase-2, amino acid residues 806–1029), and three immunoglobulin domains that form a flap (amino acid residues 1030–1299). It has been revealed that the overall topological structure and conserved domains involved in RNA capping and RNA release through the turret is similar between the aquareovirus VP1 and the MRV λ2 [11, 47].

It has been found that the turret protein VP1 in the aquareovirus (the GCRV and SBRV) core and virion reconstructions is in an open conformation. However, in both the GCRV and MRV, turrets can adopt two conformational states: an open and a closed state [12], suggesting the existence of a transition between the open and closed states in both the viruses. The structural conformational changes are mainly related to four regions of VP1: the immunoglobulin (i.e., the flap), methylase-2, bridge, and GTase domains. The tilt of the flap can be considered as a pivot-type of movement characterized by the rotation of the flap around a pivot at residue Gly1123 of VP1. In the GTase domain, the β-hairpin (Leu47–Thr57) forming the constriction inside the channel is tilted farther away from the fivefold axis. These two major conformational changes may occur in regions where VP1 and VP5 interact, suggesting a possible association of the coat protein trimers with regulation of the open/closed states. In fact, it is reasonable that minor conformational changes in the particle proteins can be observed in a batch of purified viral specimens by Cryo-EM and three-dimensional image reconstruction because of the biological nature of the

viral particles. As a bioactive macromolecular material, the virion cannot be kept intact or in a dormant or stable state when it undergoes physical or chemical processing (such as during purification or undergoing protease treatment in vitro or in vivo).

3.4.1.4 RdRP Protein VP2

The aquareovirus protein VP2 is encoded by the S2 genomic segment (3877 nt) and has a calculated molecular weight of ~142 kDa (1274 amino acids). VP2 is a minor structural protein, which functions as an RdRP and plays a critical role in catalyzing the synthesis of the positive-sense RNA strands using the negative-sense strands in each genomic dsRNA segment as the template for packaging into progeny particles. This function is similar to that exhibited by its homologues in the turreted group of viruses in the family *Reoviridae*, including the MRV and CPV. It has been deemed that the VP2 homologous protein RdRP is present in approximately 12 copies per particle and located underneath VP3A near each fivefold axis. Moreover, a recent study has found that the total number of RdRP complexes (VP2 and co-factor protein VP4) within the capsid is 11, which corresponds to the number of genomic segments [48, 51]. The atomic model of the aquareovirus has revealed that the structure of VP2 is almost identical to the crystal structure of the recombinant orthoreovirus λ3 [48]. The structural similarity of the GCRV VP2 and MRV λ3 is consistent with their highly conserved sequence identities (approximately 43%) [2, 19].

According to the nomenclature of the domains of λ3 of the MRV, the aquareovirus VP2 protein can be divided into three domains: an N-terminal domain (amino acid residues 1–386), a central polymerase domain (amino acid residues 387–897), and a C-terminal "bracelet" domain (amino acid residues 898–1273). These domains have been resolved by Cryo-EM and three-dimensional image reconstruction at a resolution of 3.8 Å [51]. In addition, as previously identified in the crystal structure of the MRV λ3, four channels that facilitate RNA synthesis have been observed in the VP2 structure; they are responsible for the RNA template entry, NTP entry, RNA template exit, and RNA transcript exit. The interactions among VP2, VP4, VP3, and dsRNA genome have been observed in the GCRV three-dimensional image reconstruction at a resolution of 3.8 Å [51].

Among the five structural proteins of the GCRV core, RdRP shares the highest similarity and identity with one of the proteins of the MRV, i.e., λ3. Interestingly, both RdRP VP2 and λ3 of the GCRV and MRV, respectively, share almost the same molecular weight, 142 kDa (1267 amino acids in the MRV and 1273 amino acids in the GCRV), which is the highest identity among all the proteins that are homologous between them. Furthermore, the high RdRP identity is uncommon between the two different genera *Aquareovirus* and *Orthoreovirus*, suggesting a similar RdRP construction and transcription mechanism for the two virus genera. Bioinformatics analysis has indicated the presence of several conserved domains within the VP2 protein, such as the motifs SG (688–700 amino acids) and GDD (738–740 amino acids) in the central domain, which are necessary for RdRP activity [19, 52]. A

central domain/region (450–750 amino acids) in the sequence alignment of VP2 with λ3 indicates consistently higher identity scores than that for the N- and C-terminal regions and encompasses the enzymatically important palm and finger domains. In fact, the two sequences can be aligned without gaps from residues 291 to 851 in λ3 [19]. Furthermore, comparing the cryo-EM density structure of VP2 to λ3 crystal structure has revealed that the central domain arrangement in the GCRV RdRP highly corresponds to that in the MRV λ3 [48].

Two major interactions between the VP2 protein and the dsRNA genome have been observed. One interaction site is closely located to the RdRP bracelet domain and adjacent region of the polymerase domain, while the other dsRNA-binding site approaches the template entry channel. Although the structures of VP2 and λ3 are almost identical, the RNA cap binding site in VP2 differs from that identified in the crystal structure of the orthoreovirus RdRP λ3 [48], suggesting that the observed differences in the dsRNA-binding sites between the aquareovirus VP2 and MRV λ3 may reflect different stages of viral transcription. Comparing the structures of the VP2 and λ3 elongation complexes has revealed that some elements in the central region and part of the C-terminal region (from 488 to 1132 amino acids) are absent in the observed VP2 structure. These absent elements may be involved in the dynamic process of RNA transcription. In addition, a loop (1121–1132 amino acids), which is thought to separate the RNA template and transcript, has been found to localize in the template exit channel and connect the flexible α-helix region (1112–1120 amino acids) and interact with the apical domain of the capsid shell protein, suggestive of a mechanism for regulating RdRP replication and transcription. The amino acid residues 1127–1132, which form part of the VP2 switch loop (amino acid residues 1121 to 1132), have been found to be fully conserved with that in λ3. An interaction between the switch loop and a loop (amino acid residues 521–524) in the apical domain of a copy of the innermost ISP VP3A has been observed [51]. These findings suggest that the structure of the innermost ISP and conformational changes is critical to RdRP activities of the reoviruses.

3.4.1.5   RdRP Co-factor Protein VP4

Similar to RdRP VP2, the aquareovirus VP4 is also a low-copy core protein of the particle. It is encoded by the S5 segment (2239 nt) and approximately 80 kDa (728 amino acids) in molecular weight. It shares about 22% amino acid sequence identity with the orthoreovirus μ2 protein [2, 25]. In the GCRV atomic model, VP4 has been found to interact closely with and occupy almost the same localization as VP2 RdRP. The structure of VP4 can be divided into three domains: an N-terminal nodule domain (amino acid residues 1–265), a plate domain (amino acid residues 266–599), and a C-terminal domain (amino acid residues 600–715). Except the flexible region of the nodule domain (amino acid residues 83–190), the structure of VP4 and its interaction with VP2 and VP3A has been resolved in the atomic model of the GCRV [51].

It has been observed that the VP4 plate domain contains fully conserved motifs (KxxxK and SDxxG) for NTP binding with the homologous µ2 protein of the turreted MRV. In fact, few residues important to the putative enzymatic activities of µ2 have been identified by comparison with the conserved sequences in VP4, such as Pro414 in µ2 is conserved in the GCRV VP4 (Pro409) and embedded in one of the most highly conserved regions: 413-LPKGSFKSTI-422 in µ2 and 408-LPKGSYKSTI-417 in VP4. In the atomic model of VP4, an additional density feature has been observed to be surrounded by three of the five fully conserved residues (Lys410, Lys414, and Ser439) in the plate domain of the aquareovirus VP4. Therefore, the plate domain is related to NTP binding in both the GCRV VP4 and MRV µ2. In addition, structural comparison between the GCRV VP4 and homologous cypovirus VP4 has revealed that the VP4 N-terminal nodule domain exhibits almost no similarity to its counterpart in the cypovirus VP4. However, their central plate domains have a markedly similar structural topology, suggesting that the central plate domains must serve an identical critical function in NTP binding among the homologous proteins of the turreted viruses in the family Reoviridae. The C-terminal domain is located at the entrance of the RdRP template entry channel and interacts with the dsRNA fragment approaching the channel. The interactions noted between the aquareovirus VP4 and dsRNA genome are consistent with the RNA-binding activity of its homology protein µ2 [6]. Furthermore, the aquareovirus atomic model has revealed that VP4 has the NTPase and helicase activities during transcription, similar to that observed for the MRV µ2 protein.

3.4.1.6 Interactions of the VP2–VP4 Complex with the N-termini of VP3A and VP3B

The aforementioned description indicates that the GCRV VP2 and VP4 form a complex in each viral particle, and the complex is anchored at the inner surface of the capsid shell. It has been found that the RdRP complex (VP2 and VP4) interacts with genomic dsRNA and four of the five asymmetrically arranged N-termini of the VP3 ISPs beneath the fivefold axis. The interactions between the VP2–VP4 complex and N-terminal structures of five copies of VP3A around the fivefold axis have been elucidated. The observed interaction between the VP2–VP4 complex and different VP3A conformations suggests that the unresolved part of the N-terminal nodule is flexible [51]. In addition, it has been found that the individual VP3A N-termini bind to the VP2–VP4 complex first, followed by the complexes anchoring to the innermost capsid shell. The interactions between VP2–VP4 and VP3 may be indispensable for the GCRV transcription.

3.4.2   The Outer Capsid Proteins

3.4.2.1   The Membrane Penetration Protein VP5

OCP VP5 of the GCRV is encoded by the S6 segment (2039 nt) and has a molecular weight of 68 kDa (648 amino acids) [2, 20]. VP5 is a major structural protein present in the form of 200 trimers (total 600 copies) in each particle. In mature aquareovirus virions, including the GCRV and SBRV, VP5 tightly binds with the outermost protection protein VP7. As such, the two proteins combine to form the bulk of the outer shell of the virion. A series of different resolution three-dimensional images has shown that the outer shell of the aquareovirus is composed of 200 trimers of VP5 and VP7, forming a heterohexameric complex organized into an incomplete $T = 13$ lattice in intact virions. In addition to its close interaction with complex VP7, VP5 also interacts with inner core clamp VP6 and turret protein VP1 to maintain particle strength and stability [11, 12].

The structure of VP5 has been well resolved. Based on the atomic model of the aquareovirus, the VP5 monomer appears in a "Z" shape and can be divided into three domains: a jelly roll domain (head), a linker domain (middle), and a base domain (bottom). The jelly roll domain (at the tip of the Z shape, amino acid residues 287–484) at the outer surface mainly consists of a β-hairpin on the top, a five-stranded β-sheet in the middle, and a four-stranded β-sheet at the bottom. Four α-helices and several long loops (amino acid residues 2–242) form the base domain (at the bottom of the Z shape). The linker domain (linking the jelly roll and base domains, amino acid residues 243–286 and 485–648) is composed of six α-helices and several short loops. Based on the crystal structure of the MRV μ1 and σ3, the penetration protein μ1 can be divided into four distinct domains: domain I (amino acid residues 30–186), domain II (amino acid residues 2–29, 187–278, and 641–657), domain III (amino acid residues 279–305 and 515-640), and domain IV (amino acid residues 306–514). Domains I, II, and III form the lower part of the μ1 trimer and appear predominantly μ1 α-helical domains, while the domain IV is a jelly roll-like domain that corresponds to the GCRV head domain and is present as β-barrels. Comparing the VP5 protein of GCRV to the μ1 protein in complex with the protection protein σ3 of the orthoreovirus, it appears that a conformational difference exists between the two proteins in some of the loops in the helix-rich region and the β hairpin and the middle five-stranded β-sheet in the jelly roll domain [28, 51, 61].

The aquareovirus OCP VP5 is a homolog of the orthoreovirus MRV/ARV and BRV proteins μ1 and μB, respectively. The GCRV VP5 protein shares about 22–24% sequence identity and 38–46% similarity with the μ1 and μB protein of the MRV or ARV and BRV, respectively, and their protein structures have also been found to be very similar [11, 54, 59]. In multiple sequence alignments, the VP5 protein has been shown to align well with the homologous proteins of the orthoreoviruses. The sequences near the N-terminus of VP5 of the aquareoviruses and μ1 of the orthoreoviruses are highly conserved, such as the autocleavage site

(42N–43P). However, there are approximately 30 more C-terminal extensions present in the MRVs that are missing in the aquareoviruses, as well as other fusogenic orthoreoviruses (including the BRV, Broome reovirus, and ARV) [54, 59]. Furthermore, the C-terminal extension of µ1 in the MRV particle is known to form the hub-and-spoke complexes within the P2 and P3 channels of the MRV outer capsid, as observed by Cryo-EM [14, 28, 59], while these structures are missing in the aquareovirus, ARV and BRV virions [54, 59]. The structural diversity of the C-terminal of the aquareovirus VP5 and the MRV µ1 may reflect different biological functions between the two species.

Consistent with sequence alignment and previously determined structural data, the atomic structure of the aquareovirus VP5 does not show two major structural segments, a helix (amino acid residues 72–96) and hub structure (amino acid residues 675–708), as found in the orthoreovirus penetration protein. These segments in orthoreoviruses interact with neighboring penetration protein trimers to stabilize the lattice of the penetration proteins further [59]. The absence of these stabilization segments in the GCRV is supposed to be related to its ability to infect cold-blooded aquatic animals at low temperatures [59]. In fact, the aquareovirus can establish active infection at a broad temperature range of 15–30 °C and at even lower temperatures of 4 and 2.5 °C [44, 61], which is different from the homo MRV that can only infect homoiothermous animal hosts at relatively high temperatures (e.g., ≥ 32 °C) [8]. The missing C-terminal extensions in the ARV and BRV that infect mammalians, just as the MRV, suggest that the difference in the structure and conformation of the VP5/µ1 analogous proteins is more closely related to their respective viral particle host nature.

Similar to the MRV µ1 protein, two conformations of VP5 (72 and 68 Da) have often been detected by analyzing the purified native GCRV particles and VP5 protein expressed in vitro. This evidence indicates that most of the VP5 proteins in cultured cells undergo assembly-related cleavage (scissors) into small amino terminal and large carboxyl terminal fragments (VP5N and VP5C, respectively), which is consistent with the MRV µ1N and µ1C [8, 9, 35, 38, 49]. Furthermore, in the GCRV atomic model, autocleavage at the Asn42-Pro43 bond of VP5 has been observed (Fig. 3.4a). In fact, two conformations of VP5: VP5 (68 kDa) and VP5C (64 kDa), and not VP5N (4 kDa), are often detected in native and recombinant particles by regular SDS-PAGE [21, 32, 33], indicating that VP5 does exist in two confirmations in infected cell cultures or mature intact particles.

Early biochemical data have shown that a myristol group is linked to the N-terminal amino acid in the reovirus µ1 protein [35, 36]. Importantly, in the GCRV high-resolution three-dimensional image reconstruction (Fig. 3.4), the myristoylated group covalently linked to the N-terminus and embedded in the hydrophobic pockets of the protein VP5 has been directly observed (Fig. 3.4b). However, the myristoyl group has not been observed in the crystal structure of the orthoreovirus $\mu 1_3 \sigma 3_3$ heterohexamer, since the myristoyl group, along with nine residues in the N-terminal region is disordered in the crystal structure [28]. It has been revealed that autocleavage at the Asn42-Pro43 bond of VP5 and the myristoyl group modification at its N-terminus are required for viral entry into host cells during
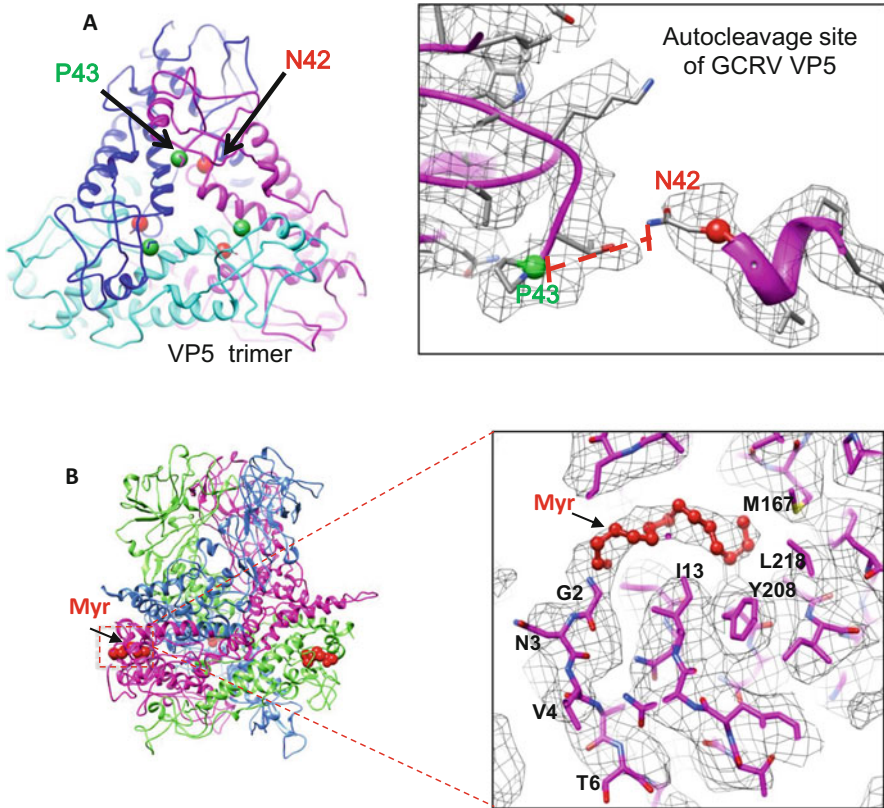
Fig. 3.4 GCRV VP5 autocleavage site and Myristol group observed in atomic model. GCRV VP5 trimer structure, each monomer of the trimer contains an autocleavage site at Asn42-Pro43 (**a**). Myristol group linked to the N-terminus of VP5 structure (**b**). The picture is modified from references [51, 61]

infection [53]. The structure and biological function of the VP5 autocleavage site and myristoyl group in viral entry have further been confirmed by in vitro studies with the recombinant native and mutant GCRV. The experimental evidence indicates that autocleavage of the penetration protein VP5/µ1 is a critical step in cell entry of the aquareovirus and MRV [21, 53, 57].

3.4.2.2 Interaction of VP5 with Other Proteins

The GCRV three-dimensional structural image indicates that VP5 has a close-grained interaction with few proteins in the particle coat. VP5 interacts with ISPs VP6 and VP1, as well as forms a complex with VP7 in the outer shell. Four types of contact modes among these proteins are shown in Fig. 3.3f, i.e., four different interaction modes exist between the VP5–VP7 complex and clamping protein

VP6. Trimer 4 has three copies of VP5 interacting with three copies of VP6B, and trimer 3 has two copies of VP5 interacting with VP6A and VP6B, respectively; Trimer 2 has one copy of VP5 interacting with only VP6A, while trimer 1 has one copy of VP5 interacting with both VP6A and VP1 [11]. These interactions between the core clamping protein VP6 and OCP VP5–VP7 trimers are tenuous, as judged from the small contact areas and agree well with the experimental observation that the GCRV outer shell can readily be removed from the inner core, as indicated in the previous chapter (Chap. 2).

3.4.2.3   Surface Protection Protein VP7

The outermost shell protein VP7 in the GCRV is encoded by the S10 genomic segment (909 nt) and has a molecular weight of approximately 29.7 kDa (276 amino acids). Similar to its homologous protein σ3 in the MRV, which is in complex with μ1, VP7 is also present as 600 molecules per viral particle. Three copies of the finger-like VP7 stack upon three copies of VP5 forming a VP5–VP7 complex (Fig. 3.5). This interaction mode is similar to that of the clamp protein VP6 with VP3, in order to reinforce VP3; thus, VP7 plays a role of protecting VP5 [11, 12]. Comparing with other fully resolved structural proteins of the GCRV, only a partial amino acid sequence (3–88 amino acids) of VP7 has been resolved so far, and the complete sequence of VP7 has not been fully characterized probably due to the instability or flexibility of the outermost or surface protein VP7 [32, 51].

 Among all the 7 homologous structural proteins between the aquareovirus and orthoreovirus (MRV/ARV), VP7 shares the lowest sequence identity (13%) with its counterpart σ3 of the MRV. The structural divergence of aquareovirus OCPs may be
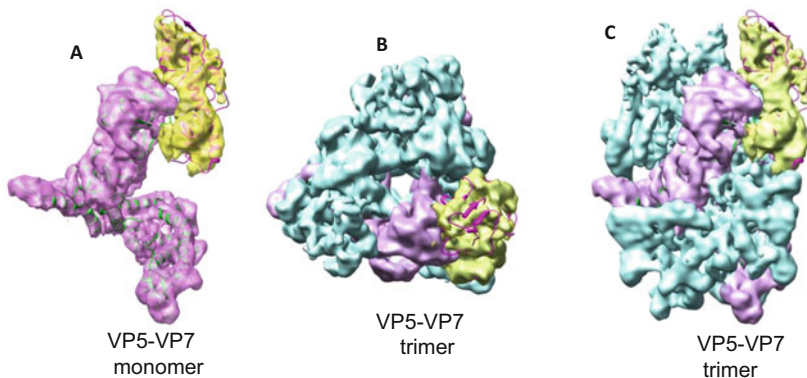
Fig. 3.5 Image of outer capsid proteins VP5 and VP7 Complex. VP5–VP7 monomer (**a**). Top view of VP5–VP7 trimer (**b**) and side view of GCRV VP5–VP7 trimer (**c**). The VP7 molecule is located on top and shown in yellow. The molecules of VP5 are at the bottom and are shown in purple in **a**, **b**, and **c**, and the rest two VP5–VP7 complex molecules in **b** and **c** are shown in bright blue

consistent with specific cell tropisms observed across the different reoviruses [58]. However, a zinc-finger motif (Cys-Cys-His-Cys (CCHC) zinc-binding motif) has been found in the N-terminal portion of VP7 across the aquareovirus species [25, 30, 40]. A significantly homologous zinc-finger motif has also been found in σ3 and σB of the orthoreovirus, indicating that the zinc-finger motifs of the aquareovirus VP7 and the MRV σ3 share structural functions. For the MRV, there is evidence that mutations in the coordinating zinc-finger motif (CCHC) residues decrease the capacity of σ3 to bind μ1 and its stability in cells in vitro [37]. Despite the least sequence identity between the GCRV VP7 and MRV σ3, VP7 appears to have an overall structural conformation similar to that of σ3, suggesting that VP7 may also play a role similar to the MRV σ3 in the regulation of viral transcription and particle assembly, as well as cell attachment.

3.4.2.4 Biological Functions of VP5 and VP7

The autocleavage site and a myristoyl group linked to the N-terminal amino acid residue of VP5 have been directly observed by atomic-resolution three-dimensional image reconstruction of the GCRV [51, 61], and it has been suggested that the release of the myristoyl group from autocleaved VP5 is essential for cell entry during membrane penetration. The biological function of the autocleavage of the Asn42-Pro43 bond in VP5 and myristoyl group modification at VP5 N-terminus (myr-VP5N) has further been elucidated by establishing native and mutant recombinant particles carrying an Asn-to-Ala substitution at residue 42 of VP5. Using the baculovirus expression system, high expression of recombinant VP5 and VP7 proteins and in vitro particle assembly, by recoating the purified GCRV cores with the expressed proteins, has been achieved. Infectious wild type R-GCRV can only be produced by recoating core particles with both VP5 and VP7 proteins, and not VP5 or VP7 alone, indicating that VP7 is required for particle assembly and cell entry, which is consistent with that observed for the recoated particles generated using baculovirus-expressed OCPs μ1 and σ3 in vitro [7]. Furthermore, the GCRV particles carrying an Asn-to-Ala substitution at residue 42 of VP5 (VP5^{N42A}/VP7) are not infectious in vitro, indicating that the VP5 autocleavage site is required for efficient infection [53]. In addition, the role of myr-VP5N in cell entry and infection has also been investigated using fluorescently labeled VP5N for direct visualization of the cell permeation. It has been found that myr-VP5N quickly permeates live cell membranes. Moreover, in permissive or non-permissive cells with the GCRV infection, it has been observed that the myristoylated peptide required for cell membrane permeation is not cell-specific. Further infectivity assays have suggested that cleavage of myristoylated VP5N is critical for promoting virus activity, while the non-cleaving mutant VP5^{N42A}/VP7 particles have been found to be defective in infectivity, despite synthetic myr-VP5N being able to associate with the cells. This indicates that the myristoylated VP5N peptide is required for cell entry but is not sufficient to initiate productive reovirus infection. The experiment demonstrated that

myr-VP5N not only causes cell membrane permeation, but also promotes virion activity for more effective infection.

Due to lack of the MRV σ1 cell attachment protein homologue, the fusogenic aquareovirus may use a different mechanism to bind cell receptor. As the MRV σ1 surface fiber protein is recognized to be a neutralization protein [37, 43], r-cores and virions can use similar routes of entry into L cells despite lacking the σ1 protein in recoated particles, thereby indicating a complex entry mechanism used by the reovirus [7, 37]. Incubating prepared polyclonal VP5 or VP7 antibodies with the infectious GCRV cell suspension has revealed that both VP5 and VP7 can effectively neutralize viral infectivity. Moreover, VP7 antiserum shows better neutralization ability than that of VP5 antiserum, indicating that VP7 possesses a dominant epitope [46]. As for the VP5 antibody, it shows excellent binding activity with surface protein, and this may be related to the VP5–VP7 heterodimer conformations. Given that VP7 is the outermost protein, it binds with equal number of copies of VP5, thereby forming the outer capsid hexon. Furthermore, three trimers of the VP5–VP7 heterodimer complex are similar to the $\mu1_3\sigma3_3$ counterpart of the MRV, and it is possible that both VP5 and VP7 have respective epitopes on the surface to bind to the cell receptor domain. Recent Cryo-EM studies of antigen–antibody complexes are beginning to clarify the mechanisms of epitope–paratope recognition at atomic resolution [1, 15]. Therefore, identifying the epitope sites and resolving the VP5 and VP7 antigen–antibody complexes will provide basis for further understanding of the viral epitope structures using virus-based platforms, thereby providing a fundamental road map for future vaccine development for aquareoviruses. A major role of VP7 is to function as a protection protein of VP5; however, other functions of VP7 in the GCRV infection, such as critical roles in cell attachment and involvement in signal transduction to help host recognition and attachment, remain to be elucidated.

3.5 Conclusions and Future Considerations

More than hundreds of aquareovirus isolates have been reported, with some of them having been sequenced, and three-dimensional images of only two aquareovirus species (the SBRV and GCRV) have been reconstructed. From the first reconstruction of the three-dimensional image of the SBRV by Cryo-EM at a resolution of 20 Å to the construction of an atomic model of the GCRV [47, 51, 61], the knowledge of crucial particle-based features obtained, including particle organization, structural protein conformation, and related functional domains, enhances our understanding of the virion structure. Among viruses in the current nine genera of the subfamily *Spinareovirinae* of the family *Reoviridae*, it has been revealed that the structural proteins involved in particle construction and overall conformation of functional domains are strikingly similar between the genus *Aquareovirus* and *Orthoreovirus*. It is clear that the highly conserved inner core protein architectural organization and divergent outer shell among the aquareoviruses and orthoreoviruses or other

members of the family *Reoviridae* reflect not only in their common genome evolutionary principle for inheriting their particular endogenous reovirus replication mechanism, but also in their respective adaptability to host cells.

Conserved Endogenous Transcription Core Across Aquareoviruses and Orthoreoviruses Different from other viruses, members of the family *Reoviridae* have particular endogenous transcription apparatuses, also called viral molecular machines, which provide excellent replication and transcription systems within the inner cores of the dsRNA viruses. All the reoviruses can carry out their genomic RNA transcription within intact viruses to synthesize capped positive-sense RNA strands prior to their release into the host cytoplasm. For turreted core structures, three of the genera, *Aquareovirus*, *Orthoreovirus*, and *Cypovirus*, have been well studied by Cryo-EM and three-dimensional image reconstruction [11, 12, 42, 51, 61]. The resolved three-dimensional images have indicated that the transcriptionally competent core of all the turreted reovirus members shares a common icosahedral plate-like scaffold structure formed by 120 subunits of an ISP (λ1/VP3). In orthoreoviruses and aquareoviruses, each virus has an additional µ2/VP6 protein decorating the inner frame of the core particles to strengthen the core shell frame. The endogenous transcription apparatus in the GCRV and MRV contains the RdRP (VP2/λ3) in complex with its co-factor (VP4/µ2), which is anchored beneath the inner surface of the VP3 capsid shell around the fivefold axes and interacts with the dsRNA genome [12, 42, 61]. The endogenous transcription apparatus transcribes mRNA conservatively from dsRNA genomic segments. They also copy the negative-sense strands of the segments in situ from the positive-sense strands packaged during assembly of the capsid shell. The extrusive cylindrical pentameric capping complexes VP1/λ2 are ordered structures displayed on the outside of the core shell at the fivefold axes, which play a role in nascent mRNA capping before release of the transcript into host cytoplasm. The exceptional 11-copy RdRP complex (VP2 and co-factor VP4) has been identified in each aquareovirus particle, and the 10-copy RdRP complex in CPV has been resolved [29, 62]. Although the in situ RdRP complex of the orthoreovirus has not been resolved, these findings suggest that the number of RdRP complexes may be consistent with the number of dsRNA genome segments.

Despite the striking similarities in the core components related to endogenous enzyme activities of the aquareovirus and orthoreovirus, some differences have also been found. An obvious difference in the orientation of the flap domains between the aquareovirus turret protein VP1 and the MRV λ2 has been noted [33]; however, the orientation of these domains has been observed to vary among cores from different orthoreovirus isolates as well [14, 42]. Therefore, it is speculated that any difference in the orientation of the VP1/λ2 flap domains that indeed exists between the aquareovirus and orthoreovirus cores does not have a significant effect on the functions of the core in mRNA synthesis. Another difference between the aquareovirus and orthoreovirus cores is the absence of a monomer of the σ2 homolog VP6 atop each icosahedral twofold axis of the core shell in the aquareovirus [11, 12, 33, 47]. As a result, only 120 copies of VP6 are present in

the SBRV and GCRV cores, as opposed to 150 copies of σ2 in orthoreovirus cores (including the ARV and BRV) [54, 59]. Indeed, the 30 additional σ2 subunits in the orthoreovirus contribute more to stabilize the inner shell frame, which suggests that the MRV core shell is more stable than that of the aquareoviruses.

OCP Diversity As mentioned above, the conserved structures of the aquareoviruses and orthoreoviruses are mainly that of the functional and enzymatic domains responsible for maintaining the inner core shell stability and endogenous transcription activity. In contrast to the conserved core framework and related endogenous proteins, the surface structures of the dsRNA viruses appear relatively divergent, reflecting different mechanisms in the course of evolving distinct patterns of virus–cell interactions for viral maturation and entry. Among all the homologous structural proteins between the GCRV and MRV, the OCPs VP5/μ1 and VP7/σ3 share a relatively lower sequence identity than that noted for their transcription-responsible inner core proteins; however, the overall conformation of functional domains in VP5/μ1 remains conserved. Notably, the overall structure of the aquareovirus VP5 appears to be very similar to that of μ1 in the MRV because the VP5 density map obtained by Cryo-EM fits well with the crystal structure of μ1. In fact, the N-terminal region around the autolytic cleavage site (Asn42-Pro43) of VP5 is highly conserved with that of the MRV μ1, suggesting that VP5 and μ1 share a similar myristoyl switch mechanism for membrane penetration during virus entry into host cells [11, 12]. Furthermore, the overall protein structural similarities found in the outermost protein σ3 of the MRV and VP7 of the aquareovirus contradict to the lowest sequence identity (12%) obtained between them, and the two proteins have similar overall structural conformation. In addition, all the VP7 proteins in the aquareovirus and the corresponding homologues in the orthoreovirus species maintain the CCHC motif at the N-terminal, suggesting that both proteins have similar functions in cell entry [25]. Similar to σ3 functioning as a protector of μ1 in the MRV, VP7 also plays critical roles in regulating the conformational status in order to expose VP5 for facilitating membrane penetration [37]. Due to excellent epitope characteristics of VP7, it is supposed that VP7 may likely play roles in cell attachment and be involved in signal transduction to help host cell recognition and attachment. Apart from the homologous structural proteins between the *Aquareovirus* and *Orthoreovirus*, the only distinctive difference in the outer capsid organization between the two genera is that the MRV contains a hemagglutinin protein σ1 for cell attachment located at the distal end of the fivefold axis; however, no such protein has been found in majority of the aquareoviruses [11, 12, 20, 51]. In this regard, the fusogenic aquareovirus appears to be closer to the ARV or BRV in their molecular evolution. Given that σ1 in the MRV has been identified as a host cell acceptor, an analogous protein has also been found in the newly isolated GCRV-ZH08/-GD108/-104/-109 strains (unassigned *Aquareovirus* species), which are supposed to be non-fusogenic aquareoviruses [18, 34, 40, 50, 55]. To understand the evolutionary cues of an enormous number of aquareovirus species at the particle-based protein level, it would be interesting to resolve the structure of the GCRV-II

group members and investigate the role of the σ1 analog and other proteins in the non-fusogenic GCRV particles.

The overall conservation and divergence of the structural protein conformations and functional domains between the aquareoviruses and orthoreoviruses has been disclosed by the current Cryo-EM-based three-dimensional image reconstruction and bioinformatics analyses. However, many molecular details about the core structure-related transcriptase activity and cleavage activity in the OCP-related cell entry events remain to be explored. It will be beneficial to investigate the assembly of the aquareovirus and orthoreovirus cores, which remain largely unknown, in infected cells; particularly, the mechanism underlying the packaging of the different aquareovirus (11 segments) or orthoreovirus (10 segments) dsRNA genomic segments during particle assembly. Our current knowledge suggests that these two genera may assume a similar packaging mechanism; thus, comparative studies with both groups and with fusogenic and non-fusogenic aquareoviruses may expedite our understanding of this mechanism. In addition, owing to the lack of the MRV σ1 fiber-like cell attachment protein in the aquareoviruses, the mechanisms of action of the fusogenic aquareovirus interaction with host cell receptor need to be elucidated. Moreover, many aspects of the fundamental immunology of the aquareovirus infection remain obscure. For example, the exact nature of the specific peptide epitopes recognized by the GCRV-specific antibodies and host immune cells and the roles played by cytokines in host defense against the aquareovirus infection need to be evaluated. Structural biology-related immunology may be powerful in providing insights into this aspect. It is believed that further high-resolution structures combined with the molecular biology tools will provide insights into not only the aquareovirus structure-based replication mechanism, but also the mode of interaction with host cell receptors during the aquareovirus infection.

References

1. Aoki ST, Settembre EC, Trask SD, Greenberg HB, Harrison SC, Dormitzer PR (2009) Structure of rotavirus outer-layer protein VP7 bound with a neutralizing Fab. Science 324:1444–1447
2. Attoui H, Fang Q, Jaafar FM, Cantaloube JF, Biagini P, de Micco P, de Lamballerie X (2002) Common evolutionary origin of aquareoviruses and orthoreoviruses revealed by genome characterization of Golden shiner reovirus, Grass carp reovirus, Striped bass reovirus and Golden ide reovirus (genus Aquareovirus, family Reoviridae). J Gen Virol 83:1941–1951
3. Attoui H, Mertens PPC et al (2012) Reoviridae. In: King AMQ, Adams MJ, Carstens EB, Lefkowitz EJ (eds) Ninth report of the international committee on taxonomy of viruses. Elsevier Academic Press, San Diego, pp 541–637
4. Bartlett JA, Joklik WK (1988) The sequence of the reovirus serotype 3 L3 genome segment which encodes the major core protein λ1. Virology 167:31–37
5. Bisaillon M, Bergeron J, Lemay G (1997) Characterization of the nucleoside triphosphate phosphohydrolase and helicase activities of the reovirus λ1 protein. J Biol Chem 272:18298–18303
6. Brentano L, Noah DL, Brown EG, Sherry B (1998) The reovirus protein μ2, encoded by the M1 gene, is an RNA-binding protein. J Virol 72:8354–8357

7. Chandran K, Walker SB, Chen Y, Nibert ML (1999) In vitro recoating of reovirus cores with baculovirus-expressed outer capsid proteins μ1 and σ3. J Virol 73(5):3941–3950

8. Chandran K, Farsetta DL, Nibert ML (2002) Strategy for nonenveloped virus entry: a hydrophobic conformer of the reovirus membrane penetration protein μ1 mediates membrane disruption. J Virol 76:9920–9933

9. Chandran K, Parker JS, Ehrlich M, Kirchhausen T, Nibert ML (2003) The delta region of outer-capsid protein micro 1 undergoes conformational change and release from reovirus particles during cell entry. J Virol 77:13361–13375

10. Chen JZ, Settembre EC, Aoki ST, Zhang X, Bellamy AR, Dormitzer PR, Harrison SC, Grigorieff N (2009) Molecular interactions in rotavirus assembly and uncoating seen by high-resolution cryo-EM. Proc Natl Acad Sci USA 106:10644–10648

11. Cheng L, Fang Q, Shah S, Atanasov IC, Zhou ZH (2008) Subnanometer resolution structures of the grass carp reovirus core and virion. J Mol Biol 382:213–222

12. Cheng L, Zhu J, Hui WH, Zhang X, Honig B, Fang Q, Zhou ZH (2010) Backbone model of an aquareovirus virion by cryo-electron microscopy and bioinformatics. J Mol Biol 397:852–863

13. Dormitzer PR, Nason EB, Prasad BV, Harrison SC (2004) Structural rearrangements in the membrane penetration protein of a nonenveloped virus. Nature 430:1053–1058

14. Dryden KA, Wang G, Yeager M, Nibert ML, Coombs KM, Furlong DB, Fields BN, Baker TS (1993) Early steps in reovirus infection are associated with dramatic changes in supramolecular structure and protein conformation: analysis of virions and subviral particles by cryoelectron microscopy and image reconstruction. J Cell Biol 122:1023–1041

15. Earl LA, Subramaniam S (2016) Cryo-EM of viruses and vaccine design. Proc Natl Acad Sci USA 113:8903–8905

16. Estes MK, Kapikian AZ (2007) Rotaviruses. In: Knipe DM, Howley PM (eds) Fields virology, 5th edn. Lippincott, Williams & Wilkins, Philadelphia, pp 1918–1974

17. Estes MK, Graham DY, Mason BB (1981) Proteolytic enhancement of rotavirus infectivity: molecular mechanisms. J Virol 39:879–888

18. Fan Y, Rao S, Zeng L, Ma J, Zhou Y, Xu J, Zhang H (2013) Identification and genomic characterization of a novel fish reovirus, Hubei grass carp disease reovirus, isolated in 2009 in China. J Gen Virol 94:2266–2277

19. Fang Q, Attoui H, Biagini JF, Zhu Z, de Micco P, de Lamballerie X (2000) Sequence of genome segments 1, 2, and 3 of the grass carp reovirus (Genus aquareovirus, family reoviridae). Biochem Biophys Res Commun 274:762–766

20. Fang Q, Shah S, Liang Y, Zhou ZH (2005) 3D reconstruction and capsid protein characterization of grass carp reovirus. Sci China Ser C 48:593–600

21. Fang Q, Seng EK, Ding QQ, Zhang LL (2008) Characterization of infectious particles of grass carp reovirus by treatment with proteases. Arch Virol 153:675–682

22. Harrison SJ, Farsetta DL, Kim J, Noble S, Broering TJ, Nibert ML (1999) Mammalian reovirus L3 gene sequences and evidence for a distinct amino-terminal region of the λ1 protein. Virology 258:54–64

23. Hewat EA, Booth TF, Loudon PT, Roy P (1992) Three-dimensional reconstruction of baculovirus expressed bluetongue virus core-like particles by cryo-electron microscopy. Virology 189:10–20

24. Kim J, Zhang X, Centonze VE, Bowman VD, Noble S, Baker TS, Nibert ML (2002) The hydrophilic amino-terminal arm of reovirus core-shell protein λ1 is dispensable for particle assembly. J Virol 76:12211–12222

25. Kim J, Tao Y, Reinisch KM, Harrison SC, Nibert ML (2004) Orthoreovirus and Aquareovirus core proteins: conserved enzymatic surfaces, but not protein-protein interfaces. Virus Res. 101:15–28

26. King AMQ, Adams MJ, Carstens EB, Lefkowitz EJ (2012) Virus taxonomy, ninth report of the international committee on taxonomy of viruses. Elsevier, San Diego

27. Labbé M, Charpilienne A, Crawford SE, Estes MK, Cohen J (1991) Expression of rotavirus VP2 produces empty corelike particles. J Virol 65:2946–2952

28. Liemann S, Chandran K, Baker TS, Nibert ML, Harrison SC (2002) Structure of the reovirus membrane-penetration protein, μ1, in a complex with is protector protein, σ3. Cell 108:283–295
29. Liu HR, Cheng LP (2015) Cryo-EM shows the polymerase structures and a nonspooled genome within a dsRNA virus. Science 349:1347–1350
30. Lupiani B, Reddy SM, Samal SK (1997) Sequence analysis of genome segment 10 encoding the major outer capsid protein (VP7) of genogroup B aquareovirus and its relationship with the VP7 protein of genogroup A aquareovirus. Arch Virol 142:2547–2552
31. McClain B, Settembre E, Temple BR, Bellamy AR, Harrison SC (2010) X-ray crystal structure of the rotavirus inner capsid particle at 3.8 Å resolution. J Mol Biol 397:587–599
32. McPhillips TH, Dinan D, Subramanian K, Samal SK (1998) Enhancement of aquareovirus infectivity by treatment with proteases: mechanism of action. J Virol 72:3387–3389
33. Nason EL, Samal SK, Venkataram Prasad BV (2000) Trypsin induced structural transformation in aquareovirus. J Virol 74:6546–6555
34. Nibert ML, Duncan R (2013) Bioinformatics of recent aqua- and orthoreovirus isolates from fish: evolutionary gain or loss of FAST and fiber proteins and taxonomic implications. PLoS One 8:e68607
35. Nibert ML, Fields BN (1992) A carboxy-terminal fragment of protein μ1/μ1C is present in infectious subvirion particles of mammalian reoviruses and is proposed to have a role in penetration. J Virol 66:6408–6418
36. Nibert ML, Schiff LA, Fields BN (1991) Mammalian reoviruses contain a myristoylated structural protein. J Virol 65:1960–1967
37. Nibert ML, Schiff LA, Fields BN (2001) Reoviruses and their replication. In: Knipe DM, Howley PM (eds) Fields virology. Lippincott Williams and Wilkins, Philadelphia, pp 1679–1728
38. Odegard AL, Chandran K, Zhang X, Nibert ML (2004) Putative autocleavage of outer capsid protein u1, allowing release of myristoylated peptide u1N during particle uncoating, is critical for cell entry by reovirus. J Virol 78(16):8732–8745
39. Pei C, Ke F, Chen ZY, Zhang QY (2014) Complete genome sequence and comparative analysis of grass carp reovirus strain 109 (GCReV-109) with other grass carp reovirus strains reveals no significant correlation with regional distribution. Arch Virol 159:2435–2440
40. Qiu T, Lu RH, Zhang J, Zhu ZY (2001) Complete nucleotide sequence of the S10 genome segment of grass carp reovirus (GCRV). Dis Aquat Organ 44:69–74
41. Qiu T, Luongo CL (2003) Identification of two histidines necessary for reovirus mRNA guanylyltransferase activity. Virology 316:313–324
42. Reinisch KM, Nibert ML, Harrison SC (2000) Structure of the reovirus core at 3.6 angstrom resolution. Nature 404(6781):960–967
43. Reiter DM, Frierson JM, Halvorson EE, Kobayashi T, Dermody TS, Stehle T (2011) Crystal structure of reovirus attachment protein sigma1 in complex with sialylated oligosaccharides. PLoS Pathog 7:e1002166
44. Rivas C, Noya M, Cepeda C, Bandin I, Barja JL, Dopazo CP (1998) Replication and morphogenesis of the turbot aquareovirus (TRV) in cell culture. Aquaculture 160:47–62
45. Settembre EC, Chen JZ, Dormitzer PR, Grigorieff N, Harrison SC (2011) Atomic model of an infectious rotavirus particle. EMBO J 30:408–416
46. Shao L, Sun X, Fang Q (2011) Antibodies against outer-capsid proteins of grass carp reovirus expressed in E. coli are capable of neutralizing viral infectivity. Virol J 8:347
47. Shaw AL, Samal S, Subramanian K, Prasad BVV (1996) The structure of aquareovirus shows how different geometries of the two layers of the capsid are reconciled to provide symmetrical interactions and stabilization. Structure 15:957–968
48. Tao Y, Farsetta DL, Nibert ML, Harrison SC (2002) RNA synthesis in a cage—structural studies of reovirus polymerase λ3. Cell 111:733–745
49. Tillotson L, Shatkin AJ (1992) Reovirus polypeptide σ3 and N-terminal myristoylation of polypeptide μ1 are required for site specific cleavage to μ1C in transfected cells. J Virol 66:2180–2186

50. Wang Q, Zeng W, Liu C, Zhang C, Wang Y, Shi C, Wu S (2012) Complete genome sequence of a reovirus isolated from grass carp, indicating different genotypes of GCRV in China. J Virol 86:12466
51. Wang X, Zhang F, Su R, Li X, Chen W, Chen Q, Yang T, Wang J, Liu H, Fang Q, Cheng L (2018) Structure of RNA polymerase complex and genome within a dsRNA virus provides insights into the mechanisms of transcription and assembly. Proc Natl Acad Sci USA 115:7344–7349
52. Yan L, Liu H, Li X, Fang Q (2014) The VP2 protein of grass carp reovirus (GCRV) expressed in a baculovirus exhibits RNA polymerase activity. Virol Sin 29:86–93
53. Yan S, Zhang J, Guo H, Yan L, Chen Q, Zhang F, Fang Q (2015) VP5 autocleavage is required for efficient infection by in vitro recoated aquareovirus particles. J Gen Virol 96:1795–1800
54. Yan XD, Parent KN, Goodman RP, Tang JH, Jingyun Shou JY, Nibert ML, Duncan R, Baker TS (2011) Virion structure of Baboon reovirus, a fusogenic orthoreovirus that lacks an adhesion fiber. J Virol 85(15):7483–7495
55. Ye X, Tian YY, Deng GC, Chi YY, Jiang XY (2012) Complete genomic sequence of a reovirus isolated from grass carp in China. Virus Res 163(1):275–283
56. Yu X, Jin L, Zhou ZH (2008) 3.88 Å structure of cytoplasmic polyhedrosis virus by cryo-electron microscopy. Nature 453:415–419
57. Zhang L, Chandran K, Nibert ML, Harrison SC (2006) Reovirus m1 structural rearrangements that mediate membrane penetration. J Virol 80:12367–12376
58. Zhang L, Agosto MA, Ivanovic T, King DS, Nibert ML, Harrison SC (2009) Requirements for the formation of membrane pores by the reovirus myristoylated m1N peptide. J Virol 83:7004–7014
59. Zhang X, Tang JG, Walker SB, O'Hara D, Nibert ML, Duncan R, Baker TS (2005) Structure of avian orthoreovirus virion by electron cryomicroscopy and image reconstruction. Virology 343:25–35
60. Zhang X, Settembre E, Xu C, Dormitzer PR, Bellamy R, Harrison SC, Grigorieff N (2008) Near-atomic resolution using electron cryomicroscopy and single-particle reconstruction. Proc Natl Acad Sci USA 105:1867–1872
61. Zhang X, Jin L, Fang Q, Hui WH, Zhou ZH (2010) 3.3 Å cryo-EM structure of a nonenveloped virus reveals a priming mechanism for cell entry. Cell 141:472–482
62. Zhang X, Ding K, Yu XK, Chang W, Sun JC, Zhou ZH (2015) In situ structures of the segmented genome and RNA polymerase complex inside a dsRNA virus. Nature 527:531–534

Chapter 4
The Aquareovirus Infection and Replication

Liqun Lu

Abstract Knowledge of the aquareovirus replication in the host has been limited to several representative fish reovirus strains. Among them, infection of the grass carp reovirus (GCRV) in grass carp (*Ctenopharyngodon idella*) cells has been extensively investigated, and therefore, the GCRV is considered as the aquareovirus type stain for elucidating viral replication. In addition, functional characterization of viral replication events through biochemical analysis, transcriptome sequencing, and proteomatic identification have provided systematic insights into understanding the mechanism of the GCRV infection. Current knowledge indicates that the GCRV infection, coupled with cell necrosis and/or apoptosis, is a gradual and integrated process involving virion adsorption, virion entrance, synthesis of viral proteins and genome, virion assembly in inclusion bodies, and nascent virus release. Specifically, mechanisms underlying tissue tropism and the GCRV cell tropism have been clarified in detail to demonstrate the host factors involved in viral attachment and entrance. Furthermore, key viral replication events have been characterized via extensive progress in research on viral proteins involved in viral replication factory formation in the cell cytoplasm. Additionally, non-lytic excretion or intracellular spread of progeny virus dominates the early phase and lytic excretion of virions occurs in the late phase during the GCRV replication in permissive cells.

Keywords GCRV · Absorption · Entrance · Synthesis · Release · Inclusion body

Abbreviations

CIK	*Ctenopharyngodon idella* kidney
CPE	Cytopathic effect
FAST	Fusion-associated small transmembrane

L. Lu (✉)
Department of Aquatic Medicine, College of Life and Fishery Science, Shanghai Ocean University, Shanghai, China
e-mail: lqlv@shou.edu.cn

GCO	Grass carp ovary
GCRV	Grass carp reovirus
Hsp70	Heat shock protein 70
ITGB1	Integrin β-1
JAM-A	Junctional adhesion molecule-A
LamR	Laminin receptor
MRV	Mammalian orthoreovirus
NTPase	Nucleoside triphosphatase
QD	Quantum dot
RdRP	RNA-dependent RNA polymerase
SMReV	Turbot *Scophthalmus maximus* reovirus
TRAP1	Tumor necrosis factor receptor-associated protein 1
VFLS	Viral factory-like structure
VIB	Virus inclusion body

4.1 Introduction

Accumulating information regarding host–pathogen interactions during the aquareovirus infection provides a comprehensive understanding of its replication and infection course. Replication and morphogenesis of aquareoviruses resemble those of orthoreoviruses and rotaviruses, and the similarities have contributed to the progress in research on aquareovirus. However, aquareoviruses differentiate from other viruses of the family *Reoviridae* in genome segment number, specific econiches, and genomic sequence similarities [6,39]. Among all the recognized *Aquareovirus* species, this chapter will focus on the GCRV (grass carp reovirus). Similar to other *Reoviridae* members, the GCRV enters host cells via receptor-mediated endocytosis. After adsorption, it penetrates the cell membrane using virus-encoded membrane penetration proteins. The inner capsid of the GCRV remains intact in the cytoplasm during the infection course after stripping of the outer capsid shell in the endosome, where the endogenous transcription occurs. The nascent mRNA is released from the inner capsid and serves as a template for protein synthesis or recruits new structural proteins from the progeny capsid in the virus inclusion bodies. After assembly, the virions rapidly disseminate through the syncytium induced by it, release from the apoptotic cells in the early phase, and burst out via cell lysis in the late phase of infection (Fig. 4.1).

Taking advantage of the computer-based protein–protein interaction prediction system, the GCRV-host protein–protein interactions on the genome scale have been systematically predicted to understand the GCRV infection comprehensively. The functional annotation and pathway enrichment analyses have revealed that the GCRV proteins specifically interact with host proteins for efficient replication, involving the interferon-gamma, VEGF, EGF receptor signaling pathways, and B cell and T cell activation [63]. Transcriptome analysis of grass carp cells infected
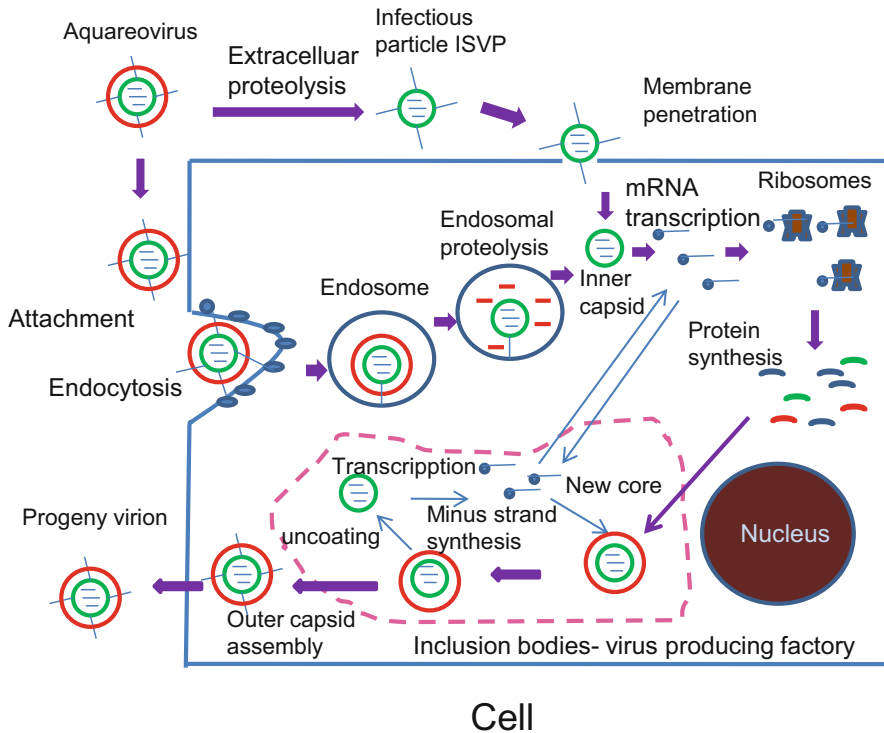
Fig. 4.1 Schematic illustration of the aquareovirus life cycle. Aquareovirus generally enters host cells by attachment to a cellular receptor and utilization of multiple endocytic pathways, and some viruses may penetrate cell membrane by membrane penetration protein. Aquareovirus uncoating only occurs for its outer capsid shell, and viral genome remains in inner capsid after entrance for mRNA synthesis. Once released from the inner capsid, virion mRNA serves as a template for translation of viral proteins, and assembles with some of the synthesized viral proteins to form new inner capsid shell in inclusion bodies. After genomic synthesis and outer capsid assembly, the virions can be released by cell lysis (this is just for fusogenic aquareovirus) or non-lytic egress mechanisms.

with the GCRV has indicated that three cellular components/processes are most seriously affected by viruses, including ribosomes, proteasomes, and oxidative phosphorylation. Additionally, immune-related pathways have been implied to be regulated by the GCRV, such as the leukocyte transendothelial migration, antigen processing and presentation, chemokine signaling pathway, and T cell receptor signaling pathway [8]. Two-dimensional electrophoresis and matrix-assisted laser desorption/ionization tandem mass spectroscopy have revealed 22 significantly altered proteins in *Ctenopharyngodon idella* kidney (CIK) cells infected with the GCRV, including cytoskeleton proteins, macromolecular biosynthesis-associated proteins, stress response proteins, signal transduction proteins, energy metabolism-associated proteins, and ubiquitin proteasome pathway-associated proteins [54]. These studies indicate that the GCRV infection results in global changes in

the host gene expression, and the complex interactions between the virus and host form the basis for efficient infection and replication of aquareoviruses in vitro and in vivo.

4.2 Tissue Tropism

The GCRV strains isolated in the past decades can be classified into three major groups based on their genome homology, which are represented by the strains GCRV-873 [17], GCRV-HZ08 [50], and GCRV-104 [16]. The three groups (designated as groups GCRV I, II, and III) share less than 20% similarity in nucleotide sequence and display significant differences in other characteristics, such as in vitro cytopathic effect (CPE), in vivo virulence, and presence of spiking outer shell protein antigenicity [39]. Epidemiological surveys and RT-PCR assays of clinical samples collected from different regions have suggested that GCRV I and GCRV II (represented by GCRV-873 and GCRV-HZ08, respectively) serve as the two dominant GCRV genotypes in southern China and show similar tissue tropism [59]. Sequence analysis has shown the co-existence of two genetically distant GCRVs, such as GCRV-JX01 and GCRV-JX02, in the same diseased grass carp tissues collected in 2011. Furthermore, GCRV-JX01 and GCRV-JX02 shared high homology with GCRV-873 and GCRV-GD08, respectively. In contrast to GCRV-JX01, GCRV-JX02 induces no CPE in infected grass carp cells. Although GCRV-JX02 reduces the cellular replication level of GCRV-JX01 by up to 10 folds during co-infection, no significant impact on the productive virus progeny level in the supernatant has been observed in comparison to that in cells infected with GCRV-JX01 alone. Analysis of clinical samples from two different fish farms in 2012 has shown that 55% of the collected fish samples are co-infected with GCRV-JX01 and GCRV-JX02, with a single virus infection rate of 10% for GCRV-JX01 and 20% for GCRV-JX02. For both viruses, the in vivo viral loads under co-infection and individual infection have been found to be similar [52]. However, no genome recombination has been reported until now between the three GCRV genotypes, although the genetic distances among strains within one group are small and potential high homologous recombination rates are therefore expected to be unavoidable [58].

As the pathogen for grass carp hemorrhagic disease, GCRV may cause hemorrhage in some characteristic tissues during acute infection with observable and clinical bleeding symptoms, especially in the muscle, gill, and intestine [60]. A comprehensive pathological analysis has indicated that the hematopoietic organs shall serve as the major target organs for the GCRV infection in vivo, including the kidney, liver, and spleen. The fact that disseminated intravascular coagulation in small blood vessels destroys the endothelium cells suggests that blood circulatory systems may play a significant role during viral transmission and propagation [28]. Due to decreased circulating blood volume and obstruction of small blood

vessels, most tissues and organs are denatured and necrotic because of the lack of oxygen, which accelerates the death of diseased fish during acute infection [70].

Similar to other nonenveloped viruses, tissue tropism of the GCRV is determined by the interaction of the viral outer shell proteins with host extracellular or cellular cytoplasmic membrane proteins. The first evidence supporting the involvement of fibulin-4 in tissue tropism of GCRV has shown that fibulin-4 interacts with the outermost capsid protein of all three GCRV groups. In a yeast-two hybrid screening for host proteins that interact with the GCRV outer capsid proteins, grass carp fibulin-4 has been suggested to potentially bind the outermost capsid protein VP7 of GCRV I, σ1-like protein VP56 of GCRV II, and σ1-like protein VP55 of GCRV III in yeast (*Saccharomyces cerevisiae*) [60, 61]. Subsequently, molecular and cellular data have confirmed the interaction between fibulin-4 and outermost capsid proteins of all three groups of GCRV both in vitro and in vivo. VP7, VP56, and VP55 individually co-localize with fibulin-4 in grass carp cells during co-transfection experiments. In both His-pull-down and dot-blot overlay assays, bacterially expressed grass carp fibulin-4 has been shown to associate individually with His-VP7, His-VP55, or His-VP56 purified from SF9 cells using Bac-to-Bac baculovirus expression system [49, 68].

As an essential component of the extracellular matrix, fibulin-4 is associated with elastic fiber formation and connective tissue development, and tissue distribution of fibulin-4 in mice has been shown to have considerable heterogeneity across different tissues or within the same tissue [20]. The putative amino acid sequence of grass carp fibulin-4 [KT899334] is 92%, 85%, 72%, and 72% identical to the fibulin-4 homologues in *Danio rerio*, *Salmo salar*, *Homo sapiens*, and *Mus musculus*, respectively. Interestingly, analysis of tissue expression patterns has demonstrated that grass carp fibulin-4 mRNA is highly expressed in the muscle, expressed at moderate levels in the intestine, gill, and brain, and expressed at significantly low levels in other tissues evaluated [60]. Similar to other members of the fibulin family, grass carp fibulin-4 is a significant cellular exocrine protein component of the extracellular matrix. Furthermore, the relatively abundant expression of fibulin-4 in specific tissues correlates with the tissue-specific clinical symptoms during the GCRV pathogenesis; thereby supports the idea that fibulin-4 plays important roles in tissue tropism of all the GCRV types. It is reasonable to speculate that fibulin-4 can confer the free GCRV virions with enough efficiency to target specific fish tissues by interacting with viral outer capsid proteins. The hemorrhage pattern in infected grass carp may be related to fibulin-4 expression patterns in different tissues.

In addition, the expression pattern of fibulin-4 at both translational and transcriptional levels during the course of the GCRV infection has indicated that fibulin-4 is significantly suppressed upon viral challenge in grass carp ovary (GCO) cells. Overexpression of fibulin-4, achieved by transduction of pEGFP-fibulin-4 plasmids into GCO cells, has been found to promote viral protein synthesis and progeny virus production significantly [43]. These findings indicate that fibulin-4 is a pro-viral protein in vitro. Thus, repression of endogenous fibulin-4 expression after the GCRV infection represents an anti-viral response by grass carp.
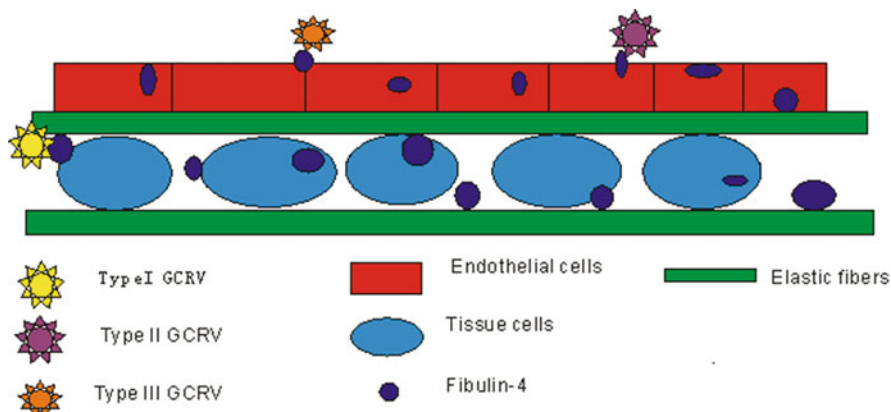
Fig. 4.2 Fibulin-4 mediates tissue tropism of three types of GCRVs. Both elastic fibers and fibulin-4 are involved in connective tissue development and fibulin-4 is necessary for elastic fiber formation that serves as the extracellular matrix. Fibulin-4 can bind cell surface-located heparan sulfate of both tissue cells and endothellial cells. The outmost capsid protein of three genotypes of GCRV physically associates with fibulin-4, enabling the proximity of GCRV to its target cells

Fibulin-4 can bind cell surface-located heparan sulfate, as demonstrated by solid phase binding assays [12]. Thus, the pro-viral function of fibulin-4 at least lies in the fact that fibulin-4 could enhance viral attachment to the cell surface-located heparan sulfate and subsequently initiate viral entrance. To test this hypothesis, the effect of heparan and heparan analogues in inhibiting the GCRV infection has been monitored in vitro. It has been observed that post-treatment with 20 mg/mL heparan or heparan analogue, the viral replication and viral protein synthesis are both inhibited significantly for either GCRV I or GCRV III species [44]. The ability of soluble heparan sulfate to inhibit the GCRV infection competitively also supports fibulin-4 mediating viral tissue tropism as necessary for the efficient GCRV infection.

In summary, extracellular fibulin-4 is an important pro-viral factor involved in tissue tropism of the GCRV through interaction with membrane-associated heparan sulfate, as well as the outer shell proteins of the GCRV (Fig. 4.2).

4.3 Cell Attachment

The availability of specific receptor proteins or other macromolecules on the host cell membrane determines the ability of a virus to attach to host cells. Similar to other viruses, the GCRV infection is initiated by binding of the GCRV particle to a specific cellular receptor that mediates viral attachment and membrane penetration. Investigations on the interactions of viral proteins with molecules on the surface of susceptible grass carp cells are important for understanding the host specificity of the GCRV. Although physically resembling the double-layered icosahedral capsid of

GCRV II and III, GCRV I capsid differs in one aspect by lacking the hemagglutinin spike (σ1 protein). Therefore, it is generally believed that the receptor for GCRV I may be different from that for GCRV II and III. For GCRV I, subnanometer-resolution structures of GCRV-873 have revealed that the outer capsid comprises 200 trimers of VP5-VP7 heterodimers, with VP7 stacking upon VP5 [10]. Keeping in mind that VP5 and VP7 are the only viral structural proteins displayed on the outer shell of GCRV I species, it is natural to believe that either one of them or both may be involved in viral attachment. Complete removal of VP7 protein alone from the outer shell by limited protease-treatment has displayed significant enhancement of viral infectivity [18], suggesting that VP5 of GCRV I species, and not VP7, may serve as the candidate viral outer capsid protein for receptor binding. The σ1 outer capsid protein of the mammalian orthoreoviruses (MRVs) mediates virus entry by binding junctional adhesion molecule-A (JAM-A), a homodimeric member of the immunoglobulin superfamily located in tight junctions, with high affinity [2]. Next, μ1-mediated membrane penetration occurs to facilitate the entry of MRVs [5, 29]. Therefore, the lack of a counterpart for the σ1 protein on the outer shell of GCRV I species suggests that an alternate receptor may be involved in virus adherence. However, VP5 of GCRV I species contains the homologous domain of μ1 involved in membrane penetration and may therefore, enter the cell via the same mechanism as that of MRVs after binding to an alternate receptor [57]. As expected, the laminin receptor (LamR) has been identified as the cellular attachment molecule mediating GCRV I infection through association with the outer capsid protein VP5, which has been demonstrated by both in vivo and in vitro protein–protein interaction assays [47].

With an overall identity of over 90%, LamR has been observed to be highly conserved among vertebrates, and the 308-amino acid sequence of grass carp LamR (accession no. KC825346.1) shares a maximum identity of 98% with that of zebrafish LamR. Similar to the identification of fibulin-4 interacting with VP7, LamR has been identified as a potential factor interacting with VP5 of GCRV I species by yeast two-hybrid screening of a grass carp cDNA library in *Saccharomyces cerevisiae*. Moreover, confocal microscopy has indicated the cell surface localization of grass carp LamR and the attachment of GCRV I virions to membrane LamR at the beginning of infection. In addition, a co-immunoprecipitation test has shown that GCRV I virions efficiently bind to soluble LamR extracted from the cellular membrane, pull-down assay has demonstrated that *Escherichia coli*-expressed LamR efficiently pulls down *Escherichia coli*-expressed VP5, and solid phase binding analysis has confirmed the binding of GCRV I virion to VP5 [47]. Therefore, these analyses validate the LamR–VP5 interaction. Furthermore, reduction of LamR expression in grass carp cells using RNA interference has demonstrated significantly reduced infection efficiency of GCRV I particles. CIK cells pretreated with a polyclonal antibody against LamR have been shown to be resistant to GCRV I infection; blockage of LamR with either EGCG or laminin has been found to significantly impair GCRV I attachment and infection [47]. These observations collectively support that grass carp LamR serves as a receptor for
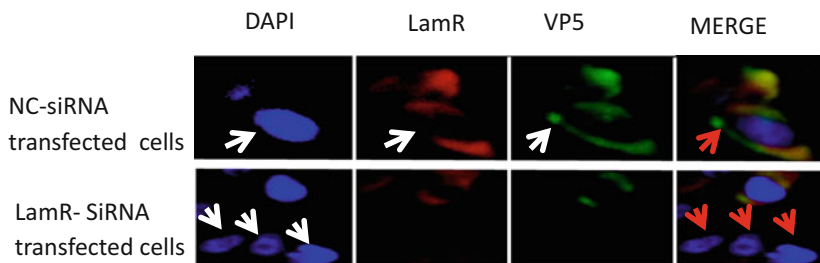
Fig. 4.3 Knocked out of LamR resulted in the failure of cellular attachment of type I GCRV. LamR-siRNA efficiently silence the gene expression of LamR, in contrast to the control NC-siRNA. The CIK cells transfected with siRNAs were infected with GCRV at an MOI of 1. The infected CIK cells were then fixed for IFA at 24 h p.i. before incubation with anti-LamR monoclonal antibody and anti-VP5 polyclonal antibody. The nuclei of CIK cells are stained with DAPI. The fixed cells were incubated with rabbit anti-VP5 or mouse anti-LamR monoclonal antibody for 1 h, and subsequently stained with FITC-labeled anti-rabbit antiserum, Rhodamine-labeled anti-mouse antiserum to get GCRV-FITC(green) and LamR-Rhodamine (red) in confocal microscopy analysis, respectively

GCRV I particle attachment through interaction with the viral outer capsid protein VP5 (Fig. 4.3).

VP56 is a protein encoded by the S7 gene segment of GCRV II species, while VP55 is that encoded by the S7 gene segment of GCRV III species. Both these proteins have been predicted to share homology with the fiber protein of the MRV, which is responsible for binding to JAM-A. Thus, it is reasonable to speculate that either VP55 or VP56 mediates the GCRV infection through interaction with the grass carp JAM-A. The fiber protein VP56 of GCRV II particles contains 512 amino acids, and neutralization assays have shown that polyclonal antibodies against VP56 efficiently block viral infection in fish cells. The ability of soluble recombinant fiber protein to bind to fish cells in attachment assays suggests that the fiber protein VP56 functions as a cell attachment protein of GCRV II virions [45]. Furthermore, bioinformatics analysis has also predicted the interaction between VP56 and JAM-A, although no biological data are available to support it. For example, a strategy identifying motif-domain interaction pairs has been used to predict the GCRV-host protein interaction, and JAM-A protein has been successfully predicted to interact with motifs of σ1-like protein VP56 of GCRV II virions [63]. JAM-A seems to be essential for efficient infection of different types of the GCRV, as suggested by infection experiments in cells with JAM-A knockout. Suppressed CPE and reduced progeny virus production have been observed in infected cells with specific knock-out of the grass carp JAM-A using CRISPR/Cas9 gene editing. Ectopic expression of gcJAM-A in non-permissive cells derived from the Chinese giant salamander (*Andrias davidianus*) muscle has been shown to confer the fish with susceptibility to the infection of the three types of the GCRV [32].

However, no direct molecular or cellular evidence is available to support the interaction between VP56 or VP55 and JAM-A. Yeast-two hybrid screening has failed to confirm the interaction between VP56 and JAM-A [61]. Therefore, the

possibility of JAM-A functioning as a receptor for either GCRV II or GCRV III virions remains to be characterized at the protein–protein interaction level. In a study screening host factors on the CIK cell membrane that may interact with GCRV III virions, a virus overlay protein binding assay and liquid chromatography with tandem mass spectrometry analysis have identified twelve proteins with potential virus-binding ability. Interestingly, JAM-A does not belong to this group of twelve proteins, and, instead, heat shock protein 70 (Hsp70) localized on the cell membrane has been determined to serve as a potential binding partner for GCRV III virion. The fact that inhibition of Hsp70 by Hsp70 inhibitors reduces GCRV III virion attachment further suggests that a fully functional Hsp70 on the cell membrane is required for the efficient GCRV III infection [42]. Although this study has suggested that membrane-associated Hsp70 plays a role in viral attachment, the existing knowledge is not sufficient to support its function as a receptor for GCRV III virions. Evidence on the interaction between VP55 and Hsp70 is lacking, which merits further clarification. However, recent studies have indicated that grass carp Hsp70 can be induced by GCRV I and III virions in different grass carp cell lines, while the heat shock cognate 71 kDa protein expression is at a relatively constant level throughout the viral infection cycle. Furthermore, inhibitor assays have indicated that Hsp70 is required for the efficient GCRV replication, but not heat shock cognate 71 kDa protein [26, 62]. Although this study supports the pro-viral property of Hsp70, its findings indicate that Hsp70 is not present in normal grass carp cells and only induced in response to a GCRV challenge. Thus, Hsp70 does not seem to act as a receptor for the GCRV due to its absence in normal grass carp cells. Hence, the receptor proteins of GCRV II or III virions remain unresolved.

4.4 Membrane Penetration

Enveloped viruses generally enter host cells through a membrane fusion reaction driven by conformational changes of specific viral envelope proteins that act as membrane fusion proteins. However, receptor-mediated endocytic pathways such as the dynamin-dependent clathrin and caveolar pathways are well characterized as viral entry portals for most nonenveloped viruses, in which viral capsid proteins interact with cellular membranes and ensure their efficient permeabilization. Both enveloped and nonenveloped viruses might enter host cells through fluid phase uptake, a cellular process that aids viral infection by its ability to intersect with the endocytic pathway. Involvement of different host endocytic pathways during the GCRV infection, including the clathrin-mediated pathway, caveolar-mediated pathway, macropinocytosis, and the so-called clathrin and caveolae-independent endocytic pathways, has been tested by several research groups [25, 33]. Current investigations have indicated that the GCRV can employ different pathways for cellular entry similar to the MRV, which uses multiple pathways to enter host cells [40].
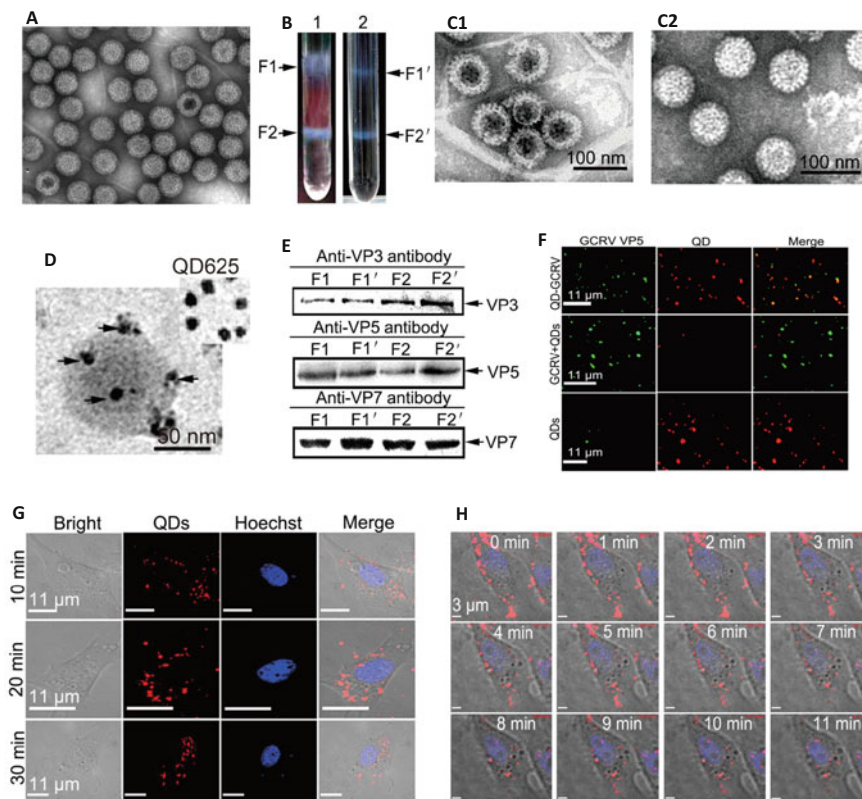
Fig. 4.4 Characteristics of the QD-labeled GCRVs. (**a**) GCRV particles. (**b**) Ultra-centrifugation images of QD-labeled and unmodified GCRV preparations. (C1, C2) Negatively stained GCRV image from F1' and F2' in tube 2. Empty particle (C1), intact virion (C2). (**e**) Unstained QD-GCRV image from F2 in tube 1. Arrowheads in D indicate QD-conjugated GCRV particles. (**e**) Western blot analysis of major structural protein composition from the bands of purified QD-GCRVs and native particles using polyclonal antibodies against VP3, VP5, and VP7. (**f**) Fluorescence colocalization assay of the purified QD-GCRV conjugates. (**g**) Time-lapse images of QD-GCRVs in CIK cells at different time points post-infection. (**h**) In situ real-time images of QD-GCRVs in live cells after performing synchronized infection. This figure is modified from reference [64]

Quantum dot (QD) labeling (Fig. 4.4) has been employed to study the cell entrance of nonenveloped aquareoviruses, wherein inorganic nanoparticle QDs are used to label GCRV I virions, and QD-GCRVs have been found to maintain their native particle properties with excellent infectivity in host cells [64]. QD labeling provides a promising strategy for revealing the ability of GCRV I virions to use caveolae/raft-mediated endocytosis as the primary entry pathway to initiate productive infection. This conclusion is supported by the fact that cellular membrane cholesterol and caveolin-1 are required for efficient internalization of the GCRV virions. The QD-labeled GCRV particles have been found to be co-localized with

caveolin-1, and transfection of cells with dominant-negative mutant of caveolin-1 (caveolin-1 Y14F) has been shown to significantly reduce GCRV I infection [65].

Both GCRV-JX01 (GCRV I) and GCRV-104 (GCRV III) strains have been shown to propagate in grass carp CIK cells with a typical CPE; however, GCRV-104 has been found to replicate slower than GCRV-JX01 in CIK cells, and the titer of GCRV-104 has been observed to be thousand times lower than that of GCRV-JX01 at 24 h post-infection. Based on these in vitro infection systems, GCRV I and III virions have been shown to enter CIK cells through clathrin-mediated endocytosis in a pH-dependent manner [46, 48]. These conclusions are mostly bolstered by inhibitor analysis, especially by specific inhibitors for clathrin, including pitstop 2 and chlorpromazine. GCRV-JX01 or GCRV-104 virions have been treated with a range of twofold concentrations of pitstop2 (0–25μM) or chlorpromazine (0–10μM) in the inhibitor analysis, and a significant decrease in viral entry of both GCRV types has been observed in cells treated with concentrations ≥5μM chlorpromazine or ≥20μM pistop2. Furthermore, GCRV-104 and GCRV-JX01 infection of CIK cells depends on dynamin and acidification of the endosome, which is evident by the significant inhibition of viral infection following prophylactic treatment with the lysosomotropic drug ammonium chloride or dynasore [46, 48]. Considering that the most commonly utilized endocytic pathway by viruses is the clathrin-mediated endocytosis [34], it is not surprising to find clathrin-mediated endocytosis also being involved in cellular entry of different types of GCRV strains. Many viruses have been reported to utilize multiple endocytic pathways to enter cells. For example, the MRVs can use both dynamin-dependent and dynamin-independent endocytic pathways to enter host cells [40]. African swine fever virus infects macrophages through clathrin- and cholesterol-dependent endocytosis [19]. Ebola virus enters host cells via macropinocytosis and clathrin-mediated endocytosis [1].

To achieve cell entry, many nonenveloped viruses must transform from a dormant to a primed state. The GCRV particle uptake depends on the structural transformation of the viral outer shell proteins. Much of the knowledge comes from the molecular biology of GCRV I virions, especially the outer capsid protein VP5, which is responsible for membrane penetration using a membrane-insertion finger structure [69]. Combining information from a 3.3 Å resolution structure of the primed penetration protein VP5 and an atomic structure of the primed aquareovirus inner sub-viral particle, the structural transformation of VP5 has been determined to be accompanied by an autocleavage at the Asn-42-Pro bond. In addition, the release of a myristoyl group from the N-terminal pocket of VP5 is required during membrane penetration [69]. The study of GCRV I particles has suggested a well-orchestrated process of nonenveloped virus entry involving autocleavage of the penetration protein VP5, which has been found to primarily exist as cleaved fragments within virions. Supporting this theory, VP5 autocleavage has been determined to be essential for efficient infection by in vitro-recovered aquareovirus particles. In insect SF9 cells overexpressing VP5 and VP7, in vitro assembly of the GCRV has been achieved. These virus-like particles closely resemble the native GCRV in morphology and infectivity, and the recovered particles carrying an Asn→Ala substitution at residue 42 of VP5 have been found to be no longer infectious

[57]. The GCRV I VP5 has been shown to interact with VP7 in yeast-two hybrid screening and dot-blot overlay assay in vitro [30]. Particularly, the enhancement of GCRV I infectivity has been shown to correlate with the complete digestion of the outer capsid protein VP7 and partial cleavage of VP5 by either trypsin- or chymotrypsin-treatment [18]. Thus, current data provide strong evidence that the proteins VP5 and VP7 of GCRV I particles play an indispensable role in membrane penetration.

Moreover, there is evidence for the possible involvement of host proteins in the GCRV membrane penetration. Integrin β-1 (ITGB1), a transmembrane protein belonging to the integrin family, is known to play an important role in promoting the GCRV entry. The relative copy number of GCRV, as well as the levels of clathrin-mediated endocytosis-associated and apoptosis-related gene expression, has been shown to be significantly lower in the ITGB1b$^{-/-}$ rare minnows generated with the CRISPR/Cas9 system than in the wild type minnows following the GCRV infection. Thus, ITGB1 may mediate the entry of GCRV particles into cells via clathrin [7]. To understand the molecular mechanism by which the aquareovirus initiates productive infection, the roles of endosomes and microtubules in cell entry of GCRV I virions have been investigated, and it has been observed that viral particles are transported along microtubules during cell entry by using the QD-labeled GCRV. Furthermore, the GCRV infection and viral protein synthesis are found to be significantly inhibited by pretreating host cells with endosome acidification inhibitors NH_4Cl, chloroquine, and bafilomycin A1 [66].

Confocal images have indicated that GCRV particles can co-localize with Rab5, Rab7, and lysosomes in host cells; disruption of microtubules with nocodazole has been shown to block the GCRV entry, suggesting that intracellular transportation via endocytic uptake of the GCRV in infected cells is through microtubules [66]. Thus, initiating productive infection by the GCRV requires assistance of endosomes and microtubules for its cell entry.

4.5   Endogenous Transcription

Reoviruses are transcriptionally self-sufficient and characterized by endogenous transcription, such that they transcribe their genetic material inside sealed inner capsids using viral transcription enzymes with minimal host protein involvement [14]. To avoid the double-stranded RNA (dsRNA)-activated host defense mechanisms against the dsRNA genome of the reovirus, the aquareovirus core also remains intact in the cytoplasm after membrane penetration and functions as a multi-enzyme machine for RNA synthesis. The RNA-dependent RNA polymerase (RdRP) protein VP2 and nucleoside triphosphatase (NTPase) VP4 catalyze the synthesis of the positive-sense RNA strands using negative-sense strands of each dsRNA genomic segment as the template in the core. The nascent positive-sense RNA strands are released into the cytoplasm after synthesis through the endogenous transcription and known to serve as mRNA for viral protein translation, as well as positive-sense RNA
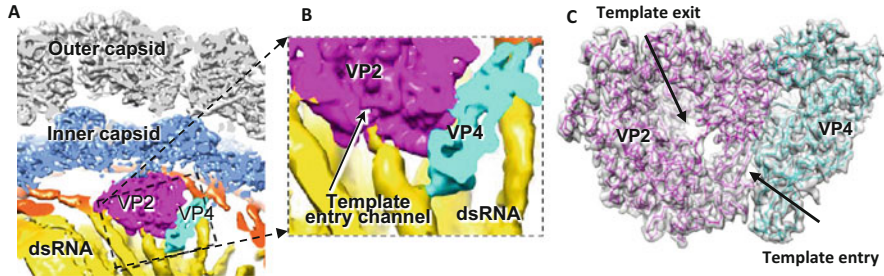
Fig. 4.5 The resolved structures of the GCRV RdRP complex (VP2 and cofactor VP4) and its genome within particle. (**a**) The localization and interactions between the RdRP complex (VP2 and VP4) and dsRNA showed by cut open views. (**b**) Zoomed-in view of the area marked by the black box in A. (**c**) the density map of VP2 and VP4 superimposed with their atomic model (only the backbone is shown). This figure is modified from reference [53]

strands for packaging of the core inside inclusion bodies. During virion assembly or in the newly assembled core, the protein VP2 can switch from being an RdRP to catalyzing the synthesis of negative-sense RNA strands, which produce genomic dsRNA segments using the positive-sense RNA strands as template in the enclosed reovirus core [35]. Research on the endogenous transcription of the GCRV focuses on VP2 and VP4 of GCRV I virions, which are associated with RdRP and NTPase activities, respectively.

To characterize the GCRV RdRP, a recombinant full-length VP2 (rVP2) has been expressed as a fusion protein with an attached His-tag using a baculovirus expression system. The purified rVP2 exhibits poly(C)-dependent poly(G) polymerase activity in vitro in the GCRV particles, and this polymerase activity requires the divalent cation Mg^{2+} [55]. Protein VP4 (μ2 in the MRV) can function as NTPase, RNA 5-triphosphatase, and dsRNA helicase [38]. VP4 of GCRV I virions, a low-copy core component protein, has been suggested to play a similar role in viral genome transcription and replication. VP4 in the GCRV-infected cells has been found to appear as a granule structure concentrated mainly in the cytoplasm, while in transfected cells overexpressing VP4 alone, a diffuse distribution in the cytoplasm and nucleus has been observed. In addition, VP4 protein has been predicted to play a role in regulating the cell cycle [56].

Although the GCRV endogenously synthesizes nascent RNA within its viral inner capsid, the mechanism underlying the assembly of dsRNA genome segments, an NTPase (VP4), a polymerase (VP2), and capsid proteins into a double-layered virion has only recently been resolved. It has been understood with the help of near-atomic resolution structures of the VP2-VP4 complex and genomic dsRNA within an aquareovirus capsid constructed using 200 kV cryo-electron microscopy (Fig. 4.5). The RdRP protein VP2 of GCRV I virion contains three domains: an N-terminal domain (amino acid residues 1–386), a central polymerase domain (amino acid residues 387–897), and a C-terminal "bracelet" domain (amino acid residues 898–1273). Three domains contained in VP4 include an N-terminal nodule domain (amino acid residues 1–265), a plate domain (amino acid residues 266–599),

and a C-terminal domain (amino acid residues 600–715). The C-terminal domain of VP4 is located at the entrance of the template entry channel for the RdRP complex and is involved in the interaction with the dsRNA fragment. VP4 interacts closely with VP2 through its plate domain by binding to the surface region of the VP2 polymerase domain [53]. Furthermore, detailed structural analysis has indicated that the VP2-VP4 complex is anchored at the inner surface of the capsid shell and found to interact with genomic dsRNA and four of the five asymmetrically arranged N-termini of the capsid shell proteins. A loop in the VP2 protein, which separates the RNA template and transcript, interacts with an apical domain of the capsid shell protein and may be involved in regulating RdRP replication and transcription. A conserved NTPase binding site localized in VP4 has been determined for the interactions between VP4 and the genomic dsRNA [53].

4.6 Virus-Producing Cytoplasmic Factories

Replication of orthoreoviruses is characterized by the development of cytoplasmic factories, named as virus inclusion bodies (VIBs), in infected cells, which consist of crystalline arrays of progeny viruses [36]. Paracrystalline arrays have also been described in cells infected by certain aquareoviruses, including the golden shiner reovirus and GCRV. The pioneering work on the VIBs in the aquareovirus has focused on the role of nonstructural protein NS80 of GCRV I virions, which is recognized to be similar to the turbot *Scophthalmus maximus* reovirus (SMReV) NS88 and orthoreovirus μNS, which play common roles in VIB formation (Fig. 4.6). Bioinformatics analyses have predicted that NS80 is related to the formation of viral factory-like structures (VFLSs) according to its homologous protein sequences from avian reoviruses and MRVs. Transmission electron microscopy has indicated that infection of the GCRV occurs within VIB-like structures in the perinuclear region of the cell cytoplasm. VIB-like structures have also been observed in Vero cells transfected with plasmids overexpressing GFP-tagged NS80; however, the N-terminal sequence of NS80 overexpressed in Vero cells alone failed to form the VIB structure, suggesting that the NS80 C-terminal conserved region is responsible for the formation of VIBs. Two coiled-coil regions (amino acid residues ~513–550 and ~615–690) in the carboxyl-proximal terminus of NS80 have further been determined to be essential for forming VFLSs by transfection experiments [4, 15]. Current knowledge about NS80 of GCRV I virions supports its key function in forming virus-producing cytoplasmic factories, similar to that observed for its homologous protein μNS in the genus *Orthoreovirus*. NS88, a nonstructural protein of SMReV, has been found to share high homology with NS80 of GCRV I virions and predicted to be involved in the formation of VIBs along with NS38, another nonstructural protein of SMReV [23].

   NS80 is also responsible for recruiting other viral proteins into formation of VFLSs, including NS38, VP4, VP1, VP3, and VP6, as indicated by both yeast-two hybrid assay and co-immunoprecipitation analysis in co-transfection
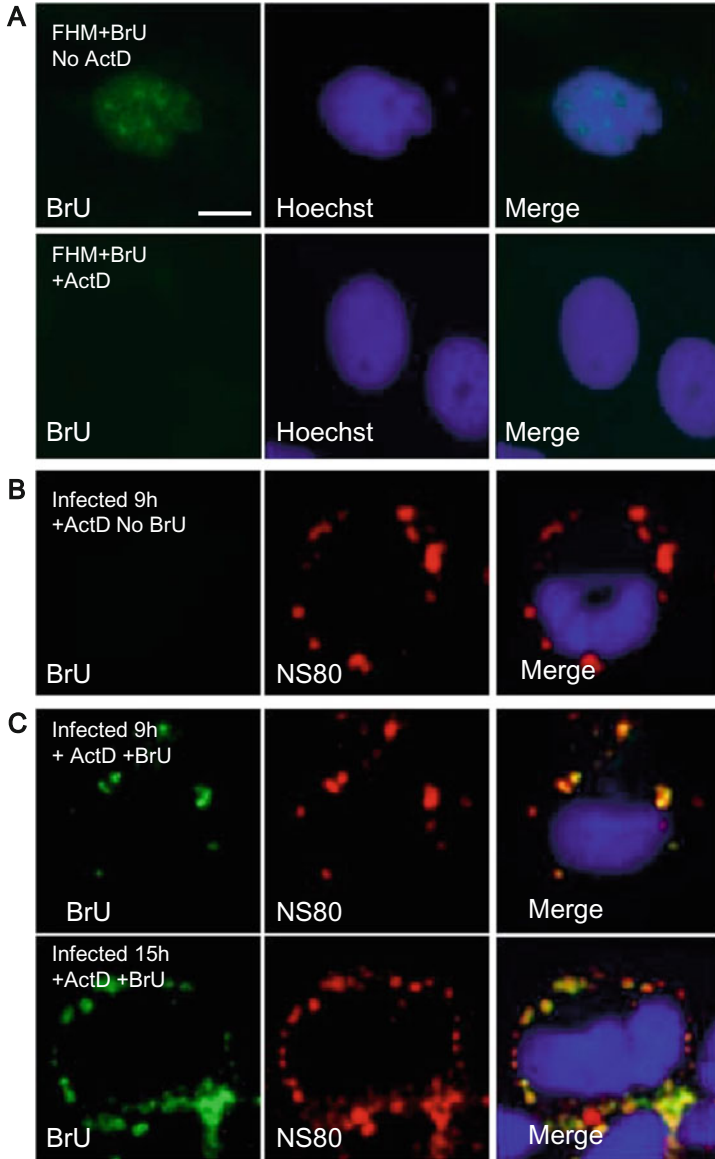
Fig. 4.6 Localization of newly synthesized RNAs to VIBs. (**a**) FHM cells were transfected with BrU in treatment with or without ActD and stained with mouse monoclonal antibody against BrU. (**b**) FHM cells infected with GCRV at MOI of 1 were transfected without BrU (No BrU) in the presence of ActD for 1 h at 9 h post-infection. (**c**) FHM cells infected with GCRV at MOI of 1 were transfected with BrU (+BrU) in the presence of ActD for 1 h at 9 h or 15 h post-infection. Infected cells were stained with mouse monoclonal antibody against BrU and rabbit polyclonal antibody against NS80. Cell nuclei were counterstained with Hoechst. Scale bars, 10μm. (This Figure is modified from reference [56]

experiments. Moreover, immunofluorescence images have indicated that viral proteins VP1, VP4, VP6, and NS38 may associate with different N-terminal regions of NS80 (amino acid residues 1–471), which has been further confirmed by co-immunoprecipitation analysis [4, 24, 67]. When NS80 is inhibited by shRNA, no VIB is present in infected cells and viral replication is abolished. Therefore, NS80 is necessary for viral replication [24, 67]. A detailed study of the truncated forms of NS80 has shown that the a minimum of 193 amino acids at the C-terminal of NS80 and amino acids 1–55 and 55–85 of its N-terminal region are required for recruiting the viral nonstructural protein NS38 and structural protein VP3, respectively, in VFLS formation; the amino acid residues 550–742 (Δ549) are sufficient for recruiting viral structural proteins VP1, VP2, and VP4, and the amino acid residues 506–742 (Δ505) are required for NS80 self-aggregation in the cytoplasm [24]. However, these assertions are not fully consistent with the findings reported by another group [67]. NS80 consists of 742 amino acids with a molecular weight of approximately 80 kDa. Interestingly, a 58-kDa larger fragment and 22-kDa smaller fragment have been confirmed in various infected and transfected cells by immunoblotting analyses using specific antibodies. Additionally, these two fragments have been found to result from cleavage near the N-terminus of NS80, and different subcellular localization patterns have been observed for these two fragments with their individual functions remaining unknown [9].

The scaffolding properties of microtubules have been determined to be critical determinants of efficient reovirus genome packaging by analysis of the ultrastructural organization of the reovirus factories combined with fluorescence microscopy, electron microscopy, and tomography of high-pressure frozen and freeze-substituted cells [41]. Interference with microtubule filaments in cells infected with the microtubule-dependent reovirus strains has been shown to result in a significant increase in the number of genome-lacking virus particles, which can be reversed by rebuilding viral factories in the actin cytoskeleton [41]. For aquareoviruses, GCRV I particles have been observed to be transported along microtubules by using QD-labeled GCRV, and endosomes and microtubules are employed by the GCRV to initiate productive infection [66]. Thus, microtubules may participate in VIB formation in aquareoviruses, which merits further investigation.

4.7 Nascent Virus Release

Generally, the mechanisms involved in the later stages of the aquareovirus infection, i.e., those underlying viral particle maturation and cellular exit, are less characterized. Nonenveloped viruses, such as members of the families *Picornaviridae* and *Reoviridae*, are assembled in the cytoplasm and are generally released by cell lysis. However, recent evidence suggests that some nonenveloped viruses exit from the infected cells without lysis, indicating that these viruses may utilize non-lytic means for egress without losing the cellular integrity. Nonenveloped viruses such as the bluetongue virus and rotavirus have been reported to interact with lipid rafts during

the trafficking of newly synthesized progeny viruses [3]. Current knowledge of the production of the GCRV progeny virus from infected cells suggests that both lytic and non-lytic pathways are involved in the release of nascent virus.

Lytic release has been observed for both GCRV I and III particles, but not for GCRV II particles. For GCRV I particles, virion release starts at 8 h post-viral infection in both CIK and GCO cells, attaining peak levels at 36 h post-viral infection. In contrast, GCRV III virion release occurs at 36 h post-infection, reaching the peak level at 120 h post-viral infection [26, 62]. Compared with the cell lysis observed in GCRV-JX01 infection at 24 h post-infection, GCRV-104 replication is slower and the observable CPE of cell lysis is detectable at five days post-infection [62]. The type strain GCRV-873 of GCRV I species can propagate in many fish cell lines and produce CPEs, observable under a microscope, during infection [17]. The GCRV II particles, however, have been found to propagate in grass carp cell lines without any detectable CPE [59]. In recent years, GCRV II virions have been determined to be the dominant virus type that causes obvious severe clinical signs in fish but produce no CPE in presently available cell cultures [51]. Generally, GCRV II virions replicate with lower efficiency in susceptible cell lines with a reduction of 1–2 log steps in the number of viruses determined by qPCR in comparison with GCRV I or III virions. Analysis of RNA synthesis level using real-time RT-PCR has indicated that genome replication in productive infection of GCRV II follows a pattern similar to that of GCRV I particles [52].

A limited apoptotic response has been detected in grass carp cells when infected with the GCRV, and the apoptotic release of the GCRV virion is believed to be involved in the early release of the GCRV when no cell lysis occurs in infected cells (Fig. 4.7). For cells infected with the GCRV for 8, 24, and 72 h, only 74.66%, 56.88%, and 36.95% cell viability, respectively, has been observed using the Cell Counting Kit-8 Assay [7]. Typical characteristics of apoptosis have been observed in CIK cells infected with GCRV I virions by DAPI staining, DNA ladder electrophoresis, TUNEL assay, and Annexin V labeling [27]. Recombinant TNF-α has been shown to trigger significant apoptosis in CIK cells, which is characterized by increased mRNA levels of TNF-α, TRADD, or caspase-8 and enhanced caspase-8 activity in CIK cells. Treatment with an anti-TNF-α polyclonal antibody has been shown to significantly decrease the degree of apoptosis in infected CIK cells, which confirms that TNF-α is a key mediator involved in the GCRV-induced cell apoptosis [31]. In an in vivo study, iNOS-induced cell apoptosis with hematoxylin and eosin staining has shown that the vascular wall breaks after the GCRV infection, and inhibition of iNOS has been observed to correlate with decreased levels of NO content, apoptosis rate, caspase activity, and hemorrhage. Therefore, iNOS seems to play a key role in the apoptosis of vascular endothelial cells during the GCRV-induced hemorrhage [28]. GCRV induces activation of caspase proteases as early as 12 h post-infection and maximum activity is recorded at 24 h or 48 h post-infection in CIK cells, which suggests that apoptosis is triggered early (12–24 h) in the viral infection cycle and may be independent of virus replication [22].

It is worth noting that the host anti-apoptotic genes may be activated to reduce apoptosis in the late phase of viral infection. For example, tumor necrosis factor

MOI=30 6h p.i   MOI=30 12h p.i

MOI=30 12h p.i   MOI=30 24h p.i
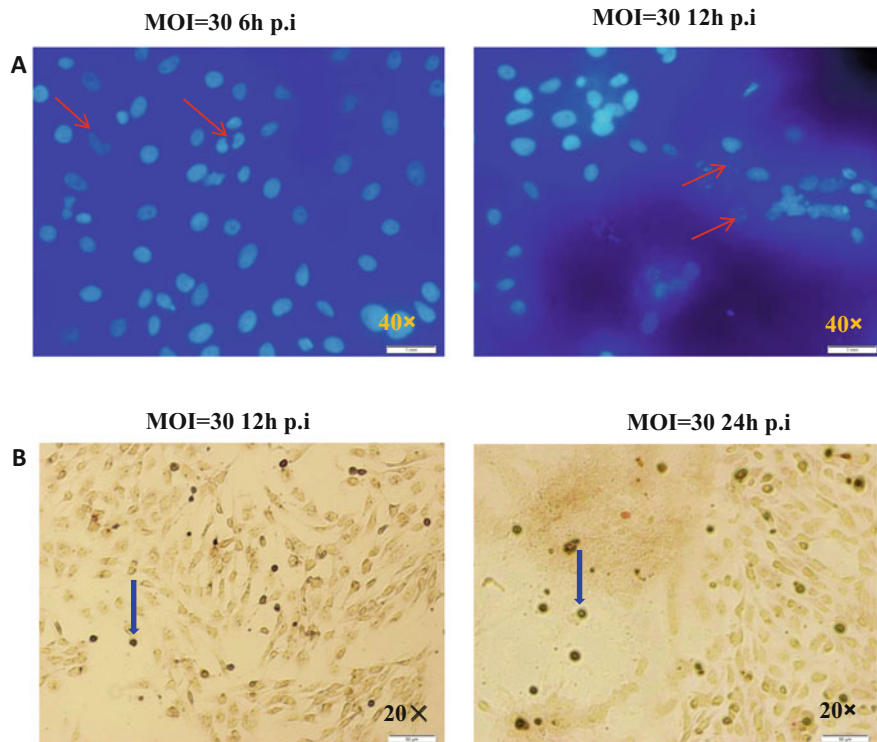
Fig. 4.7 Limited apoptosis induced by GCRV infection. (**a**) Apoptotic cells with nuclear morphological changes after infection with GCRV at 6 h and 12 h p.i. under the fluorescence microscope. Cells were stained with DAPI. Arrows indicate nuclei with morphological change. (**b**) Apoptotic cells detected by TUNEL reactions in CIK cells infected with GCRV at 12 h and 24 h p.i. The cells were assayed with TUNEL Apoptosis Assay Kit (Roche Applied Science), and viewed under an inverted light microscope. Arrows indicate TUNEL positive DNA fragments due to apoptosis

receptor-associated protein 1 (TRAP1), which plays an important role in protecting cells from oxidative stress and apoptosis, has been found to be upregulated after virus infection, as well as after poly(I:C) stimulation. The fact that RNAi-mediated silencing of CiTRAP1 in CIK cells results in an enhanced rate of virus-induced cell apoptosis further supports that CiTRAP1 is involved in the host's innate immune response to viral infection, possibly by protecting infected cells from apoptosis [27]. One outcome of the activation of the anti-apoptotic pathway is that apoptosis is only significant in a part of the infected cells or in the early phase of infection, and cell necrosis dominates especially in the late phase of infection.

The mechanism underlying cell lysis following the aquareovirus infection relates to the fusion-associated small transmembrane (FAST) proteins, which are a unique family of cell–cell membrane fusion proteins encoded by the fusogenic reoviruses [11]. A burst of infectious progeny viruses generally results from apoptosis-induced disruption of the syncytia formed via cell–cell fusion by FAST proteins [13]. Similar

to fusogenic orthoreoviruses, aquareoviruses can induce cell–cell fusion and multinucleated syncytium formation [47]. Bioinformatics analysis has indicated that NS16 of GCRV I virions shares basic structural motifs with the reovirus FAST proteins, which has further been confirmed by transfection assays, wherein NS16 alone is able to induce cell–cell fusion with its N-terminal ectodomain considered as critical for effective fusion. Furthermore, immunofluorescence assays have revealed that NS16 co-localizes with nonstructural protein NS26 of GCRV I particles in co-transfected cells, and NS26 can enhance the fusion efficiency of NS16, suggesting that NS26 may participate in cell–cell fusion by cooperating with NS16 in GCRV I infection [21]. A FAST protein NS22, which is translated from a non-AUG start site, has been identified in the S7 segment of the SMReV [23]. However, FAST proteins are not present in all aquareoviruses. For instance, the piscine reovirus does not encode a FAST protein, and no FAST protein is present among the group of encoded nonstructural proteins in GCRV II and III virions [37]. Therefore, current data have indicated that not all aquareovirus infections result in syncytium formation and only the FAST-encoding aquareovirus benefits from viral fusogens for viral dissemination and pathogenicity.

4.8 Conclusions and Future Considerations

Although many aquareoviruses have been isolated from various fish and shellfish species, few have been investigated for their replication in host cells. As grass carp is important to the aquaculture industry in China, the GCRV has been investigated continuously for over sixty years by Chinese researchers, and the accumulation of knowledge on the GCRV-encoded proteins and their interaction with host proteins forms the basis for obtaining a picture of the aquareovirus infection and replication. Methodological advances in molecular biology will help solve the present limitations in characterizing the replication cycle of aquareoviruses. Further studies are warranted in order to understand the complete function of all virus-encoded and nonstructural proteins. Moreover, the receptor proteins of more aquareovirus species remain to be determined for better knowledge of host ranges. In addition, little is known about the shellfish reoviruses due to the lack of cell lines supporting their viral replication, thereby suggesting the development of novel research models.

References

1. Aleksandrowicz P, Marzi A, Biedenkopf N, Beimforde N, Becker S, Hoenen T, Feldmann H, Schnittler HJ (2011) Ebola virus enters host cells by macropinocytosis and clathrin-mediated endocytosis. J Infect Dis 204(Suppl 3):S957–S967
2. Barton ES, Chappell JD, Connolly JL, Forrest JC, Dermody TS (2001) Reovirus receptors and apoptosis. Virology 290(2):173–180

3. Bhattacharya B, Roy P (2010) Role of lipids on entry and exit of bluetongue virus, a complex non-enveloped virus. Viruses 2(5):1218–1235

4. Cai L, Sun X, Shao L, Fang Q (2011) Functional investigation of grass carp reovirus nonstructural protein NS80. Virol J 8:168

5. Campbell JA, Schelling P, Wetzel JD, Johnson EM, Forrest JC, Wilson GA, Aurrand-Lions M, Imhof BA, Stehle T, Dermody TS (2005) Junctional adhesion molecule a serves as a receptor for prototype and field-isolate strains of mammalian reovirus. J Virol 79(13):7967–7978

6. Carmen R, Manuel N, Catalina C, Isabel B, Juan LB, Carlos PD (1998) Replication and morphogenesis of the turbot aquareovirus (TRV) in cell culture. Aquaculture 160(1):47–62

7. Chen G, Xiong L, Wang Y, He L, Huang R, Liao L, Zhu Z, Wang Y (2018) ITGB1b-deficient rare minnows delay grass carp reovirus (GCRV) entry and attenuate GCRV-triggered apoptosis. Int J Mol Sci 19(10):3175

8. Chen J, Li C, Huang R, Du F, Liao L, Zhu Z, Wang Y (2012) Transcriptome analysis of head kidney in grass carp and discovery of immune-related genes. BMC Vet Res 8:108

9. Chen Q, Zhang J, Zhang F, Guo H, Fang Q (2016) Identification and characterization of two cleavage fragments from the Aquareovirus nonstructural protein NS80. Virol Sin 31(4):314–323

10. Cheng L, Fang Q, Shah S, Atanasov IC, Zhou ZH (2008) Subnanometer-resolution structures of the grass carp reovirus core and virion. J Mol Biol 382(1):213–222

11. Clancy EK, Duncan R (2009) Reovirus FAST protein transmembrane domains function in a modular, primary sequence-independent manner to mediate cell-cell membrane fusion. J Virol 83(7):2941–2950

12. Djokic J, Fagotto-Kaufmann C, Bartels R, Nelea V, Reinhardt DP (2013) Fibulin-3, -4, and -5 are highly susceptible to proteolysis, interact with cells and heparin, and form multimers. J Biol Chem 288(31):22821–22835

13. Duncan R, Chen Z, Walsh S, Wu S (1996) Avian reovirus-induced syncytium formation is independent of infectious progeny virus production and enhances the rate, but is not essential, for virus-induced cytopathology and virus egress. Virology 224(2):453–464

14. Estes MK (1990) Rotaviruses and their replication. Virology 141:1353–1404

15. Fan C, Shao L, Fang Q (2010) Characterization of the nonstructural protein NS80 of grass carp reovirus. Arch Virol 155(11):1755–1763

16. Fan Y, Rao S, Zeng L, Ma J, Zhou Y, Xu J, Zhang H (2013) Identification and genomic characterization of a novel fish reovirus, Hubei grass carp disease reovirus, isolated in 2009 in China. J Gen Virol 94(Pt 10):2266–2277

17. Fang Q, Ke LH, Cai YQ (1989) Growth characteristics and high titer culture of grass carp hemorrhage virus (GCHV)-873 in vitro. Virol Sin 03:315–319

18. Fang Q, Seng EK, Ding QQ, Zhang LL (2008) Characterization of infectious particles of grass carp reovirus by treatment with proteases. Arch Virol 153(4):675–682

19. Galindo I, Cuesta-Geijo MA, Hlavova K, Muñoz-Moreno R, Barrado-Gil L, Dominguez J, Alonso C (2015) African swine fever virus infects macrophages, the natural host cells, via clathrin- and cholesterol-dependent endocytosis. Virus Res 200:45–55

20. Giltay R, Timpl R, Kostka G (1999) Sequence, recombinant expression and tissue localization of two novel extracellular matrix proteins, fibulin-3 and fibulin-4. Matrix Biol 18(5):469–480

21. Guo H, Sun X, Yan L, Shao L, Fang Q (2013) The NS16 protein of aquareovirus-C is a fusion-associated small transmembrane (FAST) protein, and its activity can be enhanced by the nonstructural protein NS26. Virus Res 171(1):129–137

22. Jia R, Cao LP, Du JL, Liu YJ, Wang JH, Jeney G, Yin GJ (2014) Grass carp reovirus induces apoptosis and oxidative stress in grass carp (Ctenopharyngodon idellus) kidney cell line. Virus Res 185:77–81

23. Ke F, He LB, Pei C, Zhang QY (2011) Turbot reovirus (SMReV) genome encoding a FAST protein with a non-AUG start site. BMC Genomics 12:323

24. Ke F, He LB, Zhang QY (2013) Nonstructural protein NS80 is crucial in recruiting viral components to form aquareoviral factories. PLoS One 8(5):e63737

25. Kumari S, Swetha M, Mayor S (2010) Endocytosis unplugged: multiple ways to enter the cell. Cell Res 20:256–275
26. Li W, Yu F, Wang H, Hong X, Lu L (2020) Induction of pro-viral grass carp Ctenopharyngodon idella Hsp70 instead of Hsc70 during infection of grass carp reovirus. Fish Shellfish Immunol 98:1024–1029
27. Li Y, Zhang Y, Wang T, Podok P, Xu D, Lu L (2015) Proteomic identification and characterization of Ctenopharyngodon idella tumor necrosis factor receptor-associated protein 1 (CiTrap1): an anti-apoptosis factor upregulated by grass carp reovirus infection. Fish Shellfish Immunol 43(2):449–459
28. Liang HR, Li YG, Zeng WW, Wang YY, Wang Q, Wu SQ (2014) Pathogenicity and tissue distribution of grass carp reovirus after intraperitoneal administration. Virol J 11:178
29. Liemann S, Chandran K, Baker TS, Nibert ML, Harrison SC (2002) Structure of the reovirus membrane-penetration protein, Mu1, in a complex with is protector protein, Sigma3. Cell 108 (2):283–295
30. Liu W, Wang H, Yu F, Lu L (2017) Grass carp reovirus outer capsid proteins VP5 and VP7 interact in vitro. Arch Virol 162(8):2375–2380
31. Lu J, Li Y, Shen Z, Lu C, Lu L (2016) TNF-α is involved in apoptosis triggered by grass carp reovirus infection in vitro. Fish Shellfish Immunol 55:559–567
32. Ma J, Fan Y, Zhou Y, Liu W, Jiang N, Zhang J, Zeng L (2018) Efficient resistance to grass carp reovirus infection in JAM-A knockout cells using CRISPR/Cas9. Fish Shellfish Immunol 76:206–215
33. Mayor S, Pagano RE (2007) Pathways of clathrin-independent endocytosis. Nat Rev Mol Cell Biol 8:603–612
34. Mercer J, Schelhaas M, Helenius A (2010) Virus entry by endocytosis. Annu Rev Biochem 79:803–833
35. Mertens P (2004) The dsRNA viruses. Virus Res 101:3–13
36. Miller CL, Arnold MM, Broering TJ, Hastings CE, Nibert ML (2010) Localization of mammalian orthoreovirus proteins to cytoplasmic factory-like structures via nonoverlapping regions of microNS. J Virol 84(2):867–882
37. Nibert ML, Duncan R (2013) Bioinformatics of recent aqua- and orthoreovirus isolates from fish: evolutionary gain or loss of FAST and fiber proteins and taxonomic implications. PLoS One 8(7):e68607
38. Nibert ML, Kim J (2004) Conserved sequence motifs for nucleoside triphosphate binding unique to turreted reoviridae members and coltiviruses. J Virol 78:5528–5530
39. Pei C, Ke F, Chen ZY, Zhang QY (2014) Complete genome sequence and comparative analysis of grass carp reovirus strain 109 (GCReV-109) with other grass carp reovirus strains reveals no significant correlation with regional distribution. Arch Virol 159(9):2435–2440
40. Schulz WL, Haj AK, Schiff LA (2012) Reovirus uses multiple endocytic pathways for cell entry. J Virol 86(23):12665–12675
41. Shah PNM, Stanifer ML, Höhn K, Engel U, Haselmann U, Bartenschlager R, Kräusslich HG, Krijnse-Locker J, Boulant S (2017) Genome packaging of reovirus is mediated by the scaffolding property of the microtubule network. Cell Microbiol 19(12):https://doi.org/10.1111/cmi.12765
42. Shan LP, Chen XH, Ling F, Zhu B, Wang GX (2018) Targeting Heat Shock Protein 70 as an antiviral strategy against grass carp reovirus infection. Virus Res 247:1–9
43. Sheng J, Yu F, Chen D, Wang H, Lu L (2018) Infection of grass carp reovirus induced the expressional suppression of pro-viral Fibulin-4 in host cells. Fish Shellfish Immunol 77:294–297
44. Sun H, Wan S, Wang H, Lyu L (2019) Inhibitory effect of heparin and chondroitin sulfate on the proliferation of grass carp reovirus Type I and Type III in vitro. Chinese J Virol 4:612–621
45. Tian Y, Jiao Z, Dong J, Sun C, Jiang X, Ye X (2017) Grass carp reovirus-GD108 fiber protein is involved in cell attachment. Virus Genes 53(4):613–622

46. Wang H, Liu W, Yu F, Lu L (2016) Disruption of clathrin-dependent trafficking results in the failure of grass carp reovirus cellular entry. Virol J 13:25
47. Wang H, Yu F, Li J, Lu L (2016) Laminin receptor is an interacting partner for viral outer capsid protein VP5 in grass carp reovirus infection. Virology 490:59–68
48. Wang H, Liu W, Sun M, Chen D, Zeng L, Lu L, Xie J (2018) Inhibitor analysis revealed that clathrin-mediated endocytosis is involed in cellular entry of type III grass carp reovirus. Virol J 15(1):92
49. Wang L, Yu F, Sun H, Lu L (2019) Characterization of the interaction between outer-fiber protein VP55 of genotype III grass carp reovirus and Fibulin-4 of grass carp. Fish Shellfish Immunol 86:355–360
50. Wang Q, Zeng W, Liu C, Zhang C, Wang Y, Shi C, Wu S (2012) Complete genome sequence of a reovirus isolated from grass carp, indicating different genotypes of GCRV in China. J Virol 86 (22):12466
51. Wang Q, Xie H, Zeng W, Wang L, Liu C, Wu J, Wang Y, Li Y, Bergmann SM (2018) Development of indirect immunofluorescence assay for TCID50 measurement of grass carp reovirus genotype II without cytopathic effect onto cells. Microb Pathog 114:68–74
52. Wang T, Li J, Lu L (2013) Quantitative in vivo and in vitro characterization of co-infection by two genetically distant grass carp reoviruses. J Gen Virol 94(Pt 6):1301–1309
53. Wang X, Zhang F, Su R, Li X, Chen W, Chen Q, Yang T, Wang J, Liu H, Fang Q, Cheng L (2018) Structure of RNA polymerase complex and genome within a dsRNA virus provides insights into the mechanisms of transcription and assembly. Proc Natl Acad Sci USA 115 (28):7344–7349
54. Xu D, Song L, Wang H, Xu X, Wang T, Lu L (2015) Proteomic analysis of cellular protein expression profiles in response to grass carp reovirus infection. Fish Shellfish Immunol 44 (2):515–524
55. Yan L, Liu H, Li X, Fang Q (2014) The VP2 protein of grass carp reovirus (GCRV) expressed in a baculovirus exhibits RNA polymerase activity. Virol Sin 29(2):86–93
56. Yan L, Zhang J, Guo H, Yan S, Chen Q, Zhang F, Fang Q (2015) Aquareovirus NS80 initiates efficient viral replication by retaining core proteins within replication-associated viral inclusion bodies. PLoS One 10:e0126127
57. Yan S, Zhang J, Guo H, Yan L, Chen Q, Zhang F, Fang Q (2015) VP5 autocleavage is required for efficient infection by in vitro-recoated aquareovirus particles. J Gen Virol 96 (Pt 7):1795–1800
58. Yan XY, Wang Y, Xiong LF, Jian JC, Wu ZH (2014) Phylogenetic analysis of newly isolated grass carp reovirus. Springerplus 3:190
59. Ye X, Tian YY, Deng GC, Chi YY, Jiang XY (2012) Complete genomic sequence of a reovirus isolated from grass carp in China. Virus Res 163(1):275–283
60. Yu F, Wang H, Liu W, Lu L (2016) Grass carp Ctenopharyngodon idella Fibulin-4 as a potential interacting partner for grass carp reovirus outer capsid proteins. Fish Shellfish Immunol 48:169–174
61. Yu F, Wang H, Zong Q, Zhang Y, Liu H, Chen B, Lü L (2016) Screening of potential host proteins interacting with VP56 of type II grass carp reovirus by yeast two-hybrid system. J Fisheries China 3:371–378
62. Yu F, Wang L, Li W, Wang H, Que S, Lu L (2020) Aquareovirus NS31 protein serves as a specific inducer for host heat shock 70-kDa protein. J Gen Virol 101(2):145–155
63. Zhang A, He L, Wang Y (2017) Prediction of GCRV virus-host protein interactome based on structural motif-domain interactions. BMC Bioinformatics 18(1):145
64. Zhang F, Yan S, Guo H, Chen Q, Fang Q (2017) Characterization of viral entry and infection of quantum dot-labeled grass carp reovirus. Virol Sin 32(2):163–166
65. Zhang F, Guo H, Zhang J, Chen Q, Fang Q (2018) Identification of the caveolae/raft-mediated endocytosis as the primary entry pathway for aquareovirus. Virology 513:195–207
66. Zhang F, Guo H, Chen Q, Ruan Z, Fang Q (2020) Endosomes and microtubles are required for productive infection in aquareovirus. Virol Sin 35(2):200–211

67. Zhang J, Guo H, Chen Q, Zhang F, Fang Q (2016) The N-Terminal of Aquareovirus NS80 is required for interacting with viral proteins and viral replication. PLoS One 11(2):e0148550
68. Zhang M, Sheng J, Yu F, Wang H, Lv L (2018) Studies on the interaction of grass carp Fibulin-4 protein with grass carp reovious outer capsid proteins. Chinese J Virol 4:557–564
69. Zhang X, Jin L, Fang Q, Hui WH, Zhou ZH (2010) 3.3 A cryo-EM structure of a nonenveloped virus reveals a priming mechanism for cell entry. Cell 141(3):472–482
70. Zheng D, Huang Q, Zhao L, Zhou X (1991) Electron microscopic observation on the hemorrhage disease of grass carp. J Fisheries China 4:317–321

Chapter 5
Epidemiology of the Grass Carp Reovirus

Ke Zhang, Jie Ma, and Yuding Fan

Abstract Grass carp (*Ctenopharyngodon idella*) aquaculture accounts for a large share of the freshwater fishery industry in China. However, frequent outbreaks of grass carp hemorrhagic disease (GCHD) caused by the grass carp reovirus (GCRV) infection poses a great threat and causes a tremendous loss to grass carp aquaculture farming almost every year. Epidemiological studies have shown that the GCRV can infect many kinds of fish, and different genotypes of the GCRV have been isolated from diseased grass carps with typical hemorrhagic symptoms. According to the genome sequence analyses, a mass of the GCRV isolates in China is mainly divided into three genotypic groups, namely GCRV I (representative strain GCRV-873; *Aquareovirus C*), GCRV II (representative strain GCRV-HZ08), and GCRV III (representative strain HGDRV, formerly named as GCRV-104). GCHD outbreak appears to be seasonal, occurring mainly in the summers at temperatures ranging from 25 °C to 30 °C. However, no obvious characteristic pattern pertaining to the GCRV genotypic diversity in the geographical distribution has been found. In addition, various GCRV isolates have different virulence factors towards their host and permissive cell lines. Recent epidemiological data analysis has indicated that the GCRV species grouped in GCRV II are prevalent in China, and the phenomenon of combined infection of different genotypes exists in the general population of grass carp. Therefore, timely and accurate epidemiological investigation of GCHD is necessary for better prevention and control of the GCHD outbreak.

K. Zhang
Yangtze River Fisheries Research Institute, Chinese Academy of Fishery Sciences, Wuhan, China

National Demonstration Center for Experimental Fisheries Science Education, Shanghai Ocean University, Shanghai, China

J. Ma
Department of Fish and Wildlife Sciences, University of Idaho, Moscow, ID, USA

Y. Fan (✉)
Yangtze River Fisheries Research Institute, Chinese Academy of Fishery Sciences, Wuhan, China
e-mail: fanyd@yfi.ac.cn

Abbreviations

AHRV   Atlantic halibut reovirus
CIK   *Ctenopharyngodon idella* kidney
CPE   Cytopathic effect
ELISA   Enzyme-linked immunosorbent assay
GCHD   Grass carp hemorrhagic disease
GCHV   Grass carp hemorrhage virus
GCRV   Grass carp reovirus

5.1   Introduction

Aquareoviruses are a group of viruses in the family *Reoviridae*. A large number of aquareoviruses have been isolated from various aquatic animals, such as fish and shellfish species. To our knowledge, the aquareovirus has not yet been established as a standard serotype; seven distinct species (*Aquareovirus A* to *Aquareovirus G*) and some unassigned viruses have been classified based on RNA–RNA hybridization [1]. Aquareoviruses have been first isolated from North American cyprinids and initially known as "reovirus-like" or "rotavirus-like" aquatic viruses [2, 3]. Grass carp reovirus (GCRV) is the first viral pathogen identified from aquatic animals in China in 1983 [4–6] and shown to be a member of the species group *Aquareovirus C* [7, 8]. Grass carp is an important freshwater aquaculture fish widely cultured in the Asian countries. In China, the annual production has been estimated to exceed five million tons. The GCRV causes serious disease in this fish, which is characterized by severe hemorrhage and up to 80% mortality in fingerling and yearling populations [5]. According to previously established statistics, outbreaks of grass carp hemorrhagic disease (GCHD) can reduce the annual yield by 30% and lead to significant economic losses in grass carp aquaculture in China. Therefore, the epidemiological analysis of the GCRV can provide a theoretical basis for controlling GCHD.

5.2   Geographical Distribution

GCHD is widely prevalent in central, southern, and eastern China, especially along the Yangtze River, and includes Hubei, Guangdong, Jiangxi, Jiangsu, Hunan, Zhejiang, Fujian, and Henan [9–25]. At present, more than 25 strains of GCRV have been isolated (Table 5.1). It has been determined that the GCRV strains isolated

Table 5.1 The strains, localities, and genotype of GCRV isolated in China from 1978–2014

Virus strains	Localities	Year	Genotype
GCRV 854	Hubei	1978	II
GCRV 875	Hubei	1983	I
GCRV 861	Hubei	1986	II
GCRV 873	Hunan	1989	I
GCRV 991	Hunan	2002	I
GCRV-Hunan 794	Hunan	2007	II
GCRV-Henan 988	Henan	2009	II
GCRV 097	Hubei	2009	II
GCRV 876	Hubei	UN	I
JX2007	Jiangxi	2007	II
JX2008	Jiangxi	2008	II
GCRV HZ08	Zhejiang	2008	II
GCRV-HN	Hunan	2012	II
GCRV-HS	Guangdong	2011	II
GCRV-JS	Jiangsu	2012	II
GCRV-NC	Jiangxi	2012	II
GCRV-QC	Hubei	2011	II
GCRV-QY	Guangdong	2011	II
GCRV-YX	Hubei	2011	II
GCRV-ZS	Guangdong	2011	II
GCRV-106	UN	2009	II
GCRV-918	UN	2010	II
GCRV-104	Hubei	2009	III
GCRV-0901	Jiangxi	2010	I
GCRV-0902	Jiangxi	2009	II
GCRV-030	UN	UN	I
GCRV-HA2011	UN	2011	II
GCRV-GD108	Guangdong	2012	II
GZ1208	Guangzhou	2012	I
GCRV-Huan1307	Hunan	2013	II
GCReV-109	Hubei	2013	II
GCRV 096	Hubei	2014	I

UN: unknown

in China can be divided into three genotypic groups (Table 5.1), and GCRV-873, GCRV-HZ08, and HGDRV are the representative strains of the three different groups.

Ni et al., in as early as 1953, have noticed that diseased grass carp exhibit bleeding symptoms [26]. In the summer of 1970, GCHD had been discovered in an aquaculture farm in Huangpi County, Hubei. Chen et al. have studied the physicochemical characteristics of the grass carp hemorrhage virus (GCHV),

which is the first fish virus isolated and identified in China [27]. The pathogen that causes severe GCHD had been identified as a reovirus agent until 1983 by two research groups [28]. Analysis of the physicochemical characteristics, SDS-PAGE analysis of the genome, and nucleic acid identification of the GCHV-854 strain have been performed [29–31]. A few years later, Fang et al. isolated a strain of the GCHV-873 from Shaoyang, Hunan province, and provided detailed reports [5]. Since 1990, the disease has been under control, mainly because of extensive vaccination, and has not occurred on an epidemic scale in southern China, although it is sporadic in some fish farms. However, around the year 2000, the incidence of GCRV increased, and it has been found to occur frequently mainly in large grass carp farms in the Yangtze River and Pearl River basins. In 2002, a powerful pathogenic GCRV-991 has been isolated from Changsha, Hunan province [17]. Subsequently, some other GCRV isolates, GCRV-JX2007 and GCRV-JX2008, have been isolated from diseased grass carp in Liantang Town, Nanchang County, Jiangxi Province in September 2007 and September 2008, respectively [19]. A virulent reovirus strain, GCRV-HZ08, has been isolated from diseased grass carps in Huzhou, Zhejiang Province in 2008 [14]. In 2009, the hemorrhagic disease occurred in the one- and two-year-old grass carps in Nanchang city, Jiangxi Province, and a virulent strain GCRV-JX09-02 had been isolated [16]. Research shows that this type of strain is the main epidemic strain of the GCRV in Nanchang. HGDRV (formerly named as GCRV-104) has been isolated from diseased grass carp in Hubei [12], and it is known to be a new genotype of the GCRV. In Guangdong, a reovirus had been isolated from diseased grass carp and named as the grass carp reovirus Guangdong 108 strain (GCRV-GD108) [11].

GCHD has always been the most difficult disease to control in grass carp farming in China. In 2010, GCRV-JX09-01 has been isolated from hemorrhagic grass carp in Nanchang, Jiangxi Province [13]. In 2011, GCHD has occurred in a fishing farm in Hubei, with an incidence rate of only 50% and a mortality rate of approximately 80%. In a fishing farm in Foshan, Guangdong, there have been epidemic outbreaks in five ponds, and the water temperature has been found to be obviously low, with the average water temperature being less than 20 °C. Furthermore, the morbidity and mortality rates have been observed to exceed 70% and 95%, respectively [24]. In 2012, a GCHD outbreak has been observed in Jiangsu Province and Guangdong. The mortality rate has been shown to be over 90%. In 2014, GCRV-096 has been isolated from diseased grass carp in Xiaogan, Hubei Province [25].

In 2016, both adult grass carp and fingerling in Jiangxi have been found to be infected with the GCRV, with a relatively high positive rate [22]. Although good results have been achieved in the recent years by using vaccine immunization, morbidity and death continue to occur during the onset season each year. Moreover, no obvious characteristic pattern in the geographical distribution of the GCRV genotypes has been observed (Fig. 5.1).
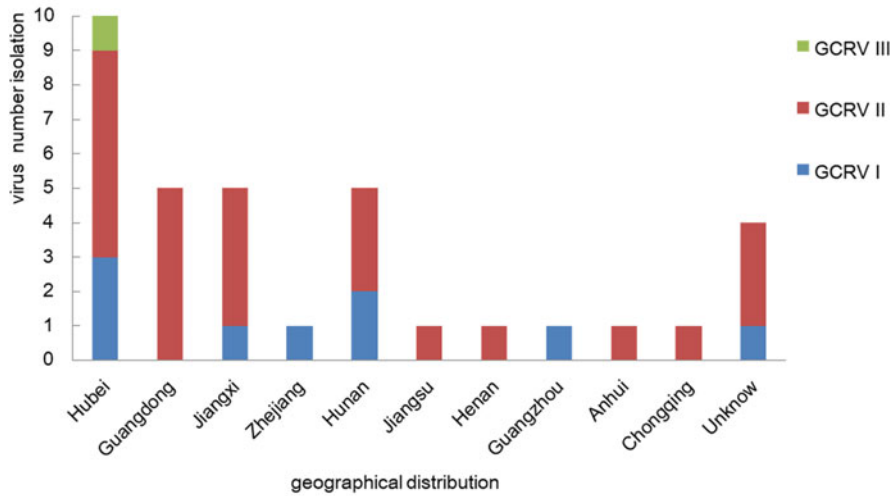
Fig. 5.1 Geographic distribution of different genotypes of GCRV isolates

Table 5.2 Susceptibility and symptoms of different fishes to GCRV infection

Fishes	Susceptibility	Hemorrhagic Symptom
Grass carp (*Ctenopharyngodon idella*)	+	+
Black carp (*Mylopharyngodon piceus*)	+	+
Silver carp (*Hypophthalmichthys molitrix*)	+	−
Variegated carp (*Aristichthys nobilis*)	−	+
Crucian carp (*Carassius auratus*)	−	−
Hemiculter bleekeri blcckeri	+	−
Megalobrama amblycephala	−	−
Carp (*Cyprinus carpio*)	−	−
Loach (*Misgurnus anguillicaudatus*)	−	−
Gobiocypris rarus	+	+
Pseudorasbora parva	+	+

+: postive −: negative

5.3   Host Range and Age

Aquareoviruses infect a variety of aquatic animals. Generally, viruses exhibit low pathogenicity towards their host species. However, the GCRV is the most pathogenic species in the genus *Aquareovirus*. It can infect many kinds of fish, such as grass carp, silver carp, black carp, *Gobiocypris rarus*, and *Pseudorasbora parva* [32–35], and cause fatal epidemics of hemorrhagic disease (Table 5.2).

Previous studies have shown that GCHD can be a cause for black carp and *Pseudorasbora parva* with hemorrhagic symptoms [32]. Ding et al. have shown that grass carp, black carp, variegated carp, crucian carp, and *Hemiculter bleekeri* are

morbid and die from being infected with the GCRV [33]. Among them, grass carp, black carp, and variegated carp display symptoms of hemorrhagic disease, while crucian carp and *Hemiculter bleekeri* show no bleeding symptoms. However, *Megalobrama amblycephala*, silver carp, common carp (*Cyprinus carpio*), and loach have been found to show no mortality; the virus species have been detected from these fish species using enzyme-linked immunosorbent assay (ELISA). Comprehensive analyses have indicated that the virus species isolated from black carp is the same as that in grass carp, and the artificial infection findings are consistent with that of ELISA, indicating that black carp is susceptible to the GCRV. Although silver carp and *Hemiculter bleekeri* show no symptoms of hemorrhagic disease, the presence of specific viral antigens can be detected. It has been shown that the GCRV can multiply in these two fishes but with low virulence. Variegated carp, crucian carp, common carp, loach, and *Megalobrama amblycephala* have been found to be not susceptible to the GCRV.

Artificial infection of the GCRV in *Gobiocypris rarus* can quickly lead to symptoms of hemorrhagic disease, and GCRV can be isolated from *Gobiocypris rarus*. Moreover, the GCRV can be passaged in *Gobiocypris rarus* [34]. After several passages, the virulence increases, which indicates that *Gobiocypris rarus* is sensitive to the GCRV infection, and the mortality rate is as high as 100%. However, due to the small scales and thin skin of *Gobiocypris rarus*, muscle plaque hyperemia can be observed at the onset of the disease, followed by appearance of increased and enlarged hyperemia clots and slow swimming. Finally, the diseased fish has been found to die within a day while the incubation period was 5d and the onset peak was 6–8d after infection. According to the different symptoms of GCHD, the infection can be divided into three types: muscle hemorrhagic type, red fins and gills and hemorrhagic type, and enteritis type. However, the main symptoms of the artificial infection in *Gobiocypris rarus* are mainly manifested as punctate and plaque hemorrhages in the muscle, gill cover, mouth, and other external organs. A small part of the infection manifests as congested internal organs, such as the intestine. At this time, congestion has also been observed in the fin base, mouth, gill cover, anus, and other tissues. In addition, the symptoms of the artificial infection are similar to those of GCHD. Furthermore, the disease is particularly harmful to grass carp, and infects approximately 85% of fingerling and yearling populations, which has resulted in large economic losses in China each year. The GCRV has been found to infect only the one- or two-year-old grass carp species, and for the two-year-old grass carp species, the incidence of infection is relatively low. Hemorrhagic disease has not been observed in adult or sexually mature grass carp. The GCRV-861 strain has been found to infect the sexually mature *Gobiocypris rarus* and cause hemorrhagic disease. It has often been observed to be accompanied by gonadal envelope plaque hyperemia, with the entire envelope appearing purplish red in color.

5.4 Clinical Features and Epidemic Potential of GCHD

At present, grass carps infected with the GCRV develop typical signs of the disease. In the early stage of the disease, they exhibit symptoms such as darkened skin, lone appearance, slow response, and reduced or no food intake. In later stages, some typical symptoms appear, such as exophthalmia, hyperemia, or hemorrhages in the skin, muscle, mouth, upper jaw, head, fin base, gills, intestinal tract, and eyes. The disease can be divided into three types according to the bleeding site: red fins and gills and hemorrhagic type, muscle hemorrhagic type, and enteritis type (Fig. 5.2). First, the muscle hemorrhagic disease type is characterized by severe congestion or bleeding in the muscles. Second, the red fins and gills, and hemorrhagic disease type shows congestion or bleeding in the gills, head, mouth, and orbit. Last, the enteritis disease type is characterized by the intestinal congestion or bleeding. These three typical patterns of congestion or bleeding can appear alone or in combination. Furthermore, these clinical signs are similar to those of bacterial enteritis. However, the intestines of fish infected by bacteria develop ulcers, while the intestines of fish infected only by the virus are found to be smooth and elastic [36]. In warm seasons, virus-infected fish can also be infected with bacteria. Therefore, the clinical signs of

Fig. 5.2 Clinical features of grass carp hemorrhagic disease. (**a**) Red fins and red gills hemorrhagic type; (**b**) Muscle hemorrhagic type; (**c**) Enteritis type
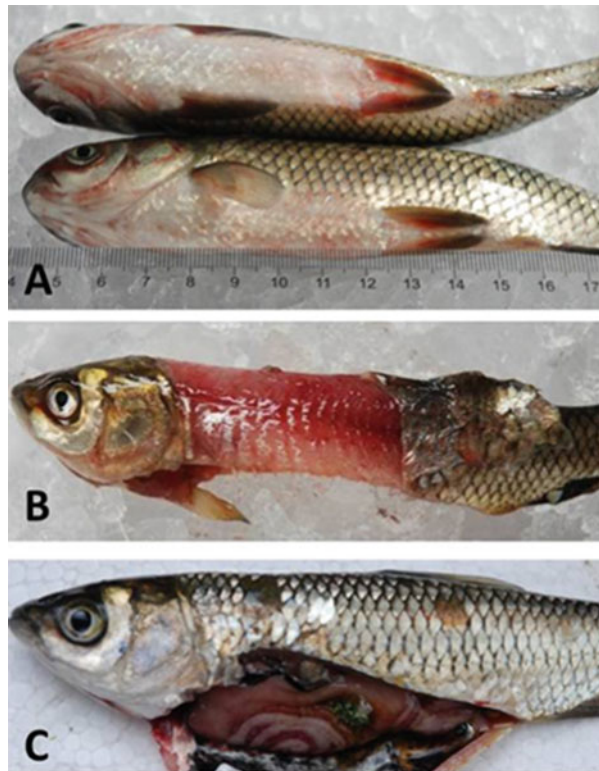
bacterial infection may conceal those of the viral infection, and hence, it is important to distinguish between bacterial and viral infections.

GCHD is widespread, with a long onset season and high mortality. The GCHD epidemic displays a typical seasonal pattern. In China, the disease outbreak appears to occur mainly from June to September, especially in August. These viruses are susceptible to infecting fish at water temperatures between 20 °C and 30 °C, with an epidemic peak between 25 °C and 28 °C. This may be related to the optimal temperature for the enzymes involved in the GCRV replication, which is approximately 28 °C. When the water temperature is lower than 20 °C, the proliferation of the GCRV is inhibited or the virus is even not infectious (the virus still has antigenicity). At this time, the grass carps infected with the GCRV would produce specific antibodies. After a rise in the water temperature, the fish will generally be resistant to the GCRV, and GCHD will not occur. Therefore, GCHD generally culminates into a large-scale outbreak in the south where the temperature is higher than the north, and it is not endemic in the north [37]. Additionally, a high-density rearing pond is more prone to infection compared with other regions.

5.5   Virus Transmission

Studies have shown that healthy grass carp can be infected using virus immersion, suggesting that GCHD is mainly transmitted horizontally in water. Using the immersion method to infect grass carp and black carp, hemorrhage symptoms have been observed to appear and viruses can be detected [33]. Wang has used immersion or hypertonic immersion to infect *Gobiocypris rarus* with hemorrhagic virus, and the mortality rate of the hemorrhagic disease in *Gobiocypris rarus* has been found to increase greatly. Horizontal transmission of the Atlantic halibut reovirus (AHRV) and long-distance spreading via movement of infected fry has already been observed [38]. Blindheim has indicated that the AHRV is only detected in farmed halibut fry but not in wild halibut [38].

Viruses may also be transmitted vertically through fish eggs. In 2013, in one of the disease outbreaks at a brood fish and hatchery site, the inlet water and live feed *Artemia nauplii* have been found to be negative for the AHRV, considering that outbreaks of a disease arise in successive batches of fry originating from the same group of brood fish, Renate Hvidsten Skoge et al. hypothesize that the AHRV can also be transmitted vertically through fish eggs [39]. They have managed to detect virus transmission from brood fish to offspring via eggs using a new real-time RT-PCR assay.

5.6   Molecular Epidemiology

The GCRV has been first isolated in China in 1983 and assigned to the *Aquareovirus C* species group [7, 8]. In 2002, the whole genome of GCRV-873 strain was sequenced for the first time [40], which is also the most thoroughly studied GCRV

strain and has long been regarded as the standard strain. To date, a number of GCRV strains have been isolated from diseased grass carps worldwide [9–25], including GCRV-873, GCRV-875, GCRV-HZ08, GCRV-GD108, GCRV-109, and HGDRV (GCRV-104). Among them, full-length gene sequences of some of the GCRV isolates have been reported [12, 40–43].

To our knowledge, there exist few studies on the serotype and genotype of the GCRV. Furthermore, there are no uniform criteria for virus genotyping. One of the virus genotyping criteria is based on nucleotide sequence analysis. The phylogenetic relationships between the aforementioned isolates categorized them into three groups based on their VP6 proteins. In addition, Zeng has indicated that there are three genotypes of the GCRV in China, and it shared 95% identity to the same genotype [10]. The similarity among the three genotypic groups has been shown to be less than 20%, with the representative isolates GCRV-873 (GCRV I), GCRV-HZ08 (GCRV II), and GCRV-104 (GCRV III) [44]. However, related studies have also analyzed the genetic sequence variation characteristics and phylogenetic relationships of 25 GCRV isolates based on VP4, VP6, and VP7 proteins. The genes encoding the major outer capsid proteins VP4, VP6, and VP7 of the GCRV are conservative. Moreover, there are many variable and informative sites across the nucleotide sequences of VP4, VP6, and VP7 in the different GCRV isolates. It has been believed that these 25 GCRV isolates can be divided into 3 genotypic groups, with the exception of the AGCRV, and no obvious relationship between the GCRV evolution and geographical distribution has been observed [18]. GCRV-096, GCRV-JX01, GCRV-873, GCRV-875, GCRV-876, and GCRV-991 have been attributed to GCRV I. GCRV-HZ08, GCRV-GD108, GCRV-918, GCRV-HuNan794, GCRV-HeNan988, GCRV-106, GCRV-ZS11, GCRV-QC11, GCRV-HN12, GCRV-HS11, GCRV-YX11, GCRV-JS12, GCRV-QY12, GCRV-JX02, and GCRV-097 have been attributed to GCRV II. GCRV-104 has been attributed to GCRV III.

Zeng has used the established multiplex PCR amplification method to detect the GCRV pathogens and analyzed 86 suspected GCHD samples collected from the main grass carp breeding area in 16 cities in China from 2009 to 2011 [45]. The analysis has revealed that the positive rates of genotypes I, II, and III are 9.3%, 45.3%, and 2.3%, respectively. The positive rate of co-infection of GCRV I and II has been found to be 5.8% and that of GCRV II and III as 2.3%. However, the co-infection rate of GCRV I and III has not been detected. Preliminary epidemiological data analysis by multiplex PCR has indicated that type II is the most common genotype, and the phenomenon of combined infection of different genotypes exists in the general grass carp population.

Fan has developed a universal detection method for the three genotypes of GCRV based on RT-PCR, and 49 suspected GCHD samples were collected from the main grass carp breeding areas in China from 2015 to 2017 [46]. The analyses have shown that all the tested samples are positive for the GCRV. The positive rates of genotypes I, II, and III have been found to be 8.2%, 85.7%, and 2%, respectively. The positive rate of co-infection of GCRV I and II has been determined to be 4.1%. However, no co-infection of other genotypes has been detected.
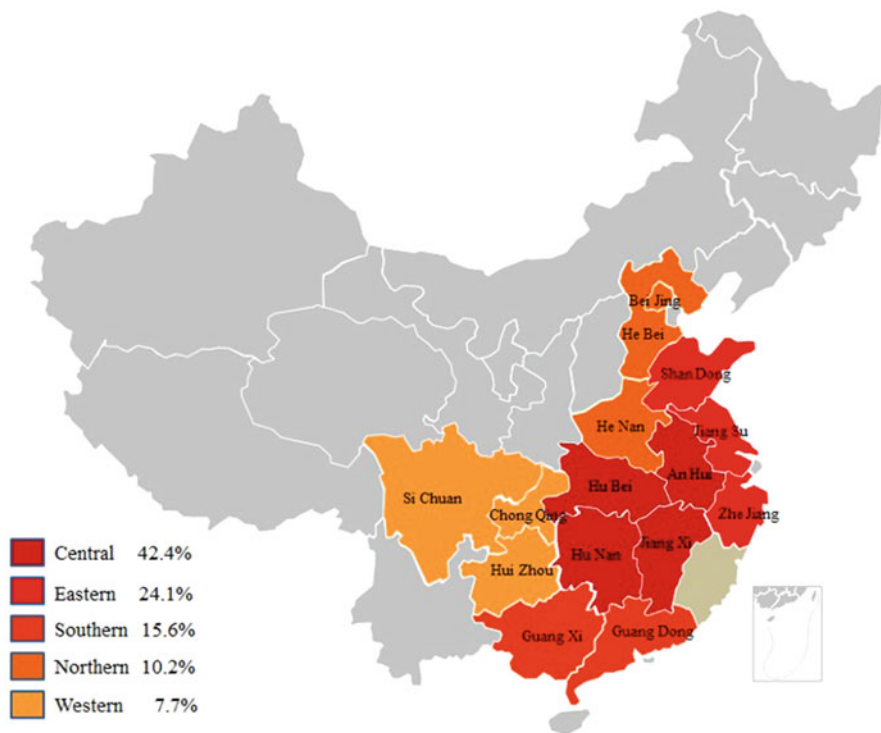
Fig. 5.3 Map of China showing the epidemiological regions (colorful) where GCRV was identified between 2012 and 2016 in China. The number of GCRV isolates in each region is represented as a percentage of the total isolates

High proportions of grass carp aquaculture sites have been continually affected by the GCRV throughout China. However, despite the long-standing historical presence of the GCRV, the molecular epidemiology of the GCRV infection in various regions of China has rarely been assessed. Therefore, molecular epidemiology and genetic diversity analyses of the GCRV are urgently needed for vaccine development and evaluation, as well as for clarification of the ecology and evolution of the GCRV. We have conducted research to describe the epidemiology of the GCRVs by evaluating nucleotide and amino acid sequence identities and assessing the phylogenetic relationships between 2012 and 2016 based on a formal investigation and published data. During the period of 5 years in an epidemiological survey, all 698 grass carp samples with hemorrhagic disease have been found to be GCRV-positive and spread across 16 provinces (Fig. 5.3). Furthermore, 42.4% of the GCRV isolations have been found to occur at collection sites located in the central region of China, which is known to be the most productive region for grass carp aquaculture. By comparing the entire dataset accumulated over 5 years, it is clear that the GCRV detection in all 5 years has peaked during the summer months (Fig. 5.4).
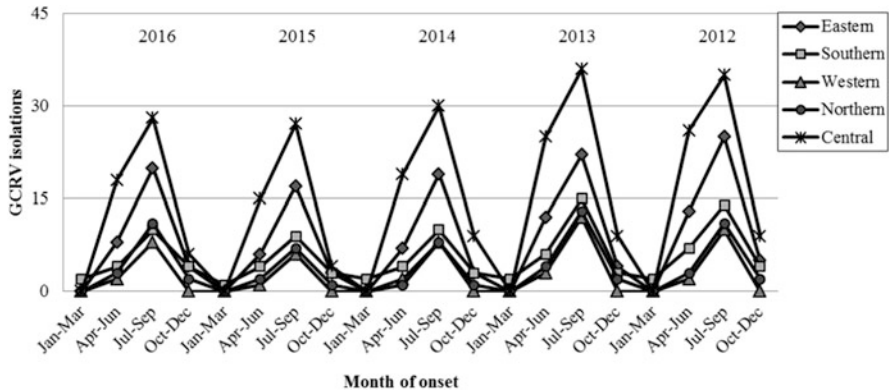
Fig. 5.4 Number of GCRV isolates identified annually in distinct regions in China between 2012 and 2016

Specific amplification bands have been produced from all the GCRV isolates using primers for GCRV II; whereas, no bands have been observed using primers for GCRV I and GCRV III. The genetic relationships among the full-length VP2 sequences of the three GCRV types have been illustrated, which clearly grouped all the GCRV types detected in this study into a single clade denoted as GCRV II (Fig. 5.5). Compared with the previously published GCRV II VP2 sequences, a nucleotide sequence identity between 83.66% and 95.42% has been observed. The numbers of GCRV isolates used in this study are indicated in Table 5.3. All analyses have suggested that all the GCRV isolates used in this study are genetically similar to GCRV II, and GCRV II is currently a prevalent strain in China. Our study confirms that the GCRV isolates obtained from various regions of China are highly homologous, and there is no specific geographic or temporal relationship. This clearly suggests that virus transmission occurs from farm to farm and is likely to be enhanced by commercial trade. Therefore, understanding the genotype and relationship among these isolates will be helpful for the future development of the GCRV vaccines and may have implications for understanding GCRV dissemination throughout China. Moreover, continual monitoring of the GCRV genotypes is also important for understanding the effects of commercial trade on virus transmission.

5.7 In Vitro GCRV Infection

Some studies have shown that the GCRV can infect multiple fish cell lines, such as *Ctenopharyngodon idella* kidney (CIK), CP-80, CF, GCB, GCO, PSF, and CAB cell lines [16, 17, 47–50]. However, various degrees of sensitivity have been confirmed for different infected fish cell lines, among which the CIK cell line is the most sensitive. At present, most of the in vitro research is conducted on CIK cells
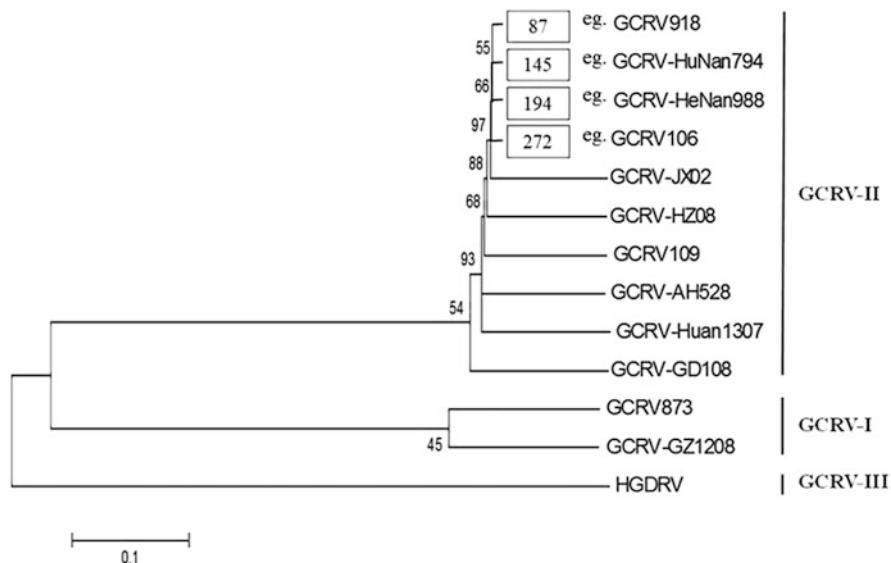
Fig. 5.5 Phylogenetic relationships of 698 GCRV isolates from 16 provinces in China. The tree was generated based on VP2 complete sequences. The complete list of GenBank accession numbers for GCRV used in this analysis is shown in Table 5.3. The numbers of GCRV isolates in this study were indicated in the boxes

Table 5.3 GenBank accession numbers for the VP2 complete sequence of GCRV isolates used in this study

Virus strain (Abbreviation)	Accession number
Grass carp reovirus 873 (GCRV-873)	AAG10436.1
Grass carp reovirus GZ1208 (GCRV-GZ1208)	KU240075.1
Grass carp reovirus GD108 (GCRV-GD108)	ADT79734.1
Grass carp reovirus JX02 (GCRV-JX02)	KM880066.1
Grass carp reovirus Huan1307 (GCRV-Huan1307)	KU254567.1
Grass carp reovirus 109 (GCRV-109)	KF712476.1
Grass carp reovirus HuNan794 (GCRV-HuNan794)	KC238677.1
Grass carp reovirus AH528 (GCRV-AH528)	KR180369.1
Grass carp reovirus HeNan988 (GCRV-HeNan988)	KC847321.1
Grass carp reovirus 918 (GCRV-918)	KC201178.1
Grass carp reovirus 106 (GCRV-106)	KC201167.1
Grass carp reovirus HZ08 (GCRV-HZ08)	ADJ75336.1
Hubei grass carp disease reovirus (HGDRV)	AFG73673.1

[47]. However, the cell infection characteristics for the three different genotypic GCRV isolates have been observed to vary.

Fang has reported that GCRV I species, such as GCRV-873 and GCRV-991, can cause a cytopathic effect (CPE) in the CIK and FHM cell lines. Nevertheless, the

EPC cell line is not sensitive to these species [48]. The CIK cell line is the most sensitive to GCRV I species and can produce a typical CPE, which usually consists of a large number of cells that are suspended in the medium forming plaques, with the cells appearing in a broken fishing net structure. As the number of passages of the GCRV strains increases, the virulence and yield of the virus increase gradually. After three consecutive passages, the virus titer of the strains tends to stabilize [51]. Deng believes that the GCRV is not strictly specific to a host under in vitro culture conditions. However, evaluating the time taken for a CPE to appear, grass carp cells generally have been found to take 2–3 days. Crucian carp and blunt snout bream cells have been observed to take 5–7 days, while no CPE has been observed in the mudfish cells [47].

Although no typical CPE has been observed after GCRV II infection in cell lines, the virus can still proliferate in cells [15, 52]. Li has simultaneously infected PSF, GSB, L8824, EPC, CO, CIB, CF, KS, KB, and CCB cell lines by inoculating the cells with GCRV-HZ08 strain at an optimal inoculation concentration. It has been demonstrated that the GCRV-HZ08 strain can proliferate in the GSB, L8824, PSF, CF, CO, CIB, and KS cells. However, among these seven cell lines, the virus proliferated better in GSB, L8824, and PSF cells, with the titers reaching 1.14×10^7, 5.90×10^6, and 6.30×10^4 copies/μL, respectively. Finally, it has been determined that GSB, L8824, and PSF cells are more sensitive for the proliferation of GCRV II compared with other cell lines [49].

Fan has indicated that GCRV-104 can be propagated in the CIK cell line showing a typical CPE, which involves shrinking cells, invisible cell boundaries, and a degree of cell fusion. Furthermore, the cell monolayer is destroyed [12]. After three consecutive passages, the CPE has been observed to become more consistent.

Since virus replication is related to the activity of RNA polymerase, factors affecting the activity of RNA polymerase will affect the virus infectivity. A study has found that the GCRV with multiple consecutive passages at different temperatures can cause a CPE in sensitive cell lines, but the virus infectivity is the highest at 28 °C. Therefore, the temperature of the virus-infected cell culture should be approximately 28 °C [51, 53]. However, slight changes in pH caused by cell metabolism and atmospheric air have shown no significant effect on virus replication [51, 52].

5.8 Conclusions and Future Considerations

In China, a GCHD outbreak appears to be seasonal, occurring mainly in the summer with an epidemic peak between 25 °C and 30 °C. According to the genetic sequence differences among the existing GCRV isolates, the GCRV in China is currently divided into three genotypic groups, namely GCRV I (representative strain GCRV-873), GCRV II (representative strain GCRV-HZ08), and GCRV III (representative strain GCRV-104). Moreover, there are many types of GCRV strains. Recent studies have shown that GCRV II is currently prevalent in southern China. Owing to the

numerous types of GCRV strains, the epidemic strains in different regions are different, and multiple strains coexist in the same region. Therefore, timely and accurate epidemiological investigation of the GCRV is necessary to control the GCHD outbreak.

References

1. Fang Q, Zhu ZY (2003) Advances in aquareovirus research. Virol Sin 18(1):82–86
2. Winton JR, Lannan CN, Fryer JL, Hedrick RP, Meyers TR, Plumb JA, Yamamoto T (1987) Morphological and biochemical properties of four members of a novel group or reoviruses isolated from aquatic animals. J Gen Virol 68:353–364
3. Plumb JA, Bowser PR, Grizzle JM, Mitchell AJ (1979) Fish viruses: a double-stranded RNA virus icosahedral virus from a North American cyprinid. J Fish Res Board Can 36:1390–1394
4. Mao SJ, Shao JZ, Hang Q (1989) On pathogen of hemorrhage of grass carp. J Fish China 13 (1):1–4
5. Fang Q, Ke LH (1989) Growth characteristics and high titer culture of grass carp hemorrhage virus (GCHV)-873 in vitro. Virol Sin 3:315–319
6. Ke LH, Fang Q, Cai YQ (1990) Characteristics of a novel isolate of grass carp hemorrhagic virus. Acta Hydrobiologica Sinica 14(2):153–159
7. Attoui H, Mertens P, Becnel J, Belaganahalli S, Zhou H (2011) Family Reoviridae. In: Virus taxonomy, ninth report of the International Committee for the Taxonomy of Viruses
8. Rangel AAC, Rockemann DD, Hetrick FM, Samal SK (1999) Identification of grass carp hemorrhage virus as a new genogroup of aquareovirus. J Gen Virol 80(9):2399
9. Pei C, Ke F, Chen ZY, Zhang QY (2014) Complete genome sequence and comparative analysis of grass carp reovirus strain 109 (GCReV-109) with other grass carp reovirus strains reveals no significant correlation with regional distribution. Arch Virol 159:2435–2440
10. Wang Q, Zeng W, Liu C, Zhang C, Wang Y, Shi C, Wu S (2012) Complete genome sequence of a reovirus isolated from grass carp, indicating different genotypes of GCRV in China. J Virol 86:12466
11. Ye X, Tian YY, Deng GC, Chi YY, Jiang XY (2012) Complete genomic sequence of a reovirus isolated from grass carp in China. Virus Res 163:275–283
12. Fan Y, Rao S, Zeng L, Ma J, Zhou Y, Xu J, Zhang H (2013) Identification and genomic characterization of a novel fish reovirus, Hubei grass carp disease reovirus, isolated in 2009 in China. J Gen Virol 94:2266–2277
13. Zeng WW, Wang Q, Liu YK, Zhang LS, Liu BQ, Shi CB, Wu SQ (2011) Isolation and identification of new GCRV strain and primary study on its immunogenicity. Acta Hydrobiologica Sinica 35(5):790–795
14. Zhang C, Wang Q, Shi CB, Zeng WW, Liu YK, Wu SQ (2010) Isolation and identification of a grass carp reovirus isolate GCRV HZ08. J Fish Sci China 17(6):1257–1263
15. Hao GJ, Shen JY, Pan XY, Xu Y, Yao JY, Yin WL (2011) Isolation and identification of a strain of grass carp reovirus in Huzhou. Prog Fish Sci 32(1):47–52
16. Liu YK, Wang Q, Zeng WW, Shi CB, Zhang C, Chen DY, Wu SQ (2011) Isolation and identification of grass carp reovirus strain JX-0902. J Fish Sci China 5:1077–1083
17. Fang Q, Xiao TY, Ding QQ, Li L, Zhang HY, Zhu ZY (2002) Virological properties of GCRV991 strain. Virol Sin 17(2):178–181
18. Yan XY, Wang Y, Xiong LF, Jian JC, Wu ZH (2014) Phylogenetic analysis of newly isolated grass carp reovirus. Springer Plus 3(1):190
19. Xu Y, Hao GJ, Shen JY, Zheng SJ, Pan XY, Yao JY, Yin WL (2010) Isolation and identification of two grass carp reovrius strains in Jiangxi province. Freshw Fish 40(3):44–49

20. Wang Y (2011) cDNA cloning, expression of vp5 and vp7 genes and subcecullar localization of VP5 and VP7 proteins in grass carp reovirus. Guangdong Ocean University
21. Yan NN, Su JG, Lei CZ (2015) Cloning and analysis of partial coding sequences of grass carp reovirus 097 strain genome segments L3, M5 and S8. J Domest Anim Ecol 3:25–28
22. Tian FY, Zeng WW, Zhang XY, Xu JH, Xie SH, Hua Q, Liu WZ, Yin XH, Meng X, Liu B, Ou YM (2016) Molecular epidemiological analysis of grass carp reovirus (GCRV) in Jiangxi in 2016. Jiangxi Fish Sci Technol 6:19–23
23. Li X (2016) Isolation, identification of grass carp reovirus GZ1208 and analysis of its complete genome. Shanghai Ocean University
24. Yang Y (2013) Epidemiologic survey of grass carp(*Ctenopharyngodon idella*) reovirus in South China and establishment of duplex real-time RT-PCR. Sichuan Agricultural University
25. Zheng SC, Xie JG, Wang Y, Cai SH, Jian JC, Wu ZH, Yan XY (2014) Construction of yeast expression vector and bioinformatics analysis of vp7 gene in GCRV 096. Journal of Guangdong Ocean University
26. Ni DS (1994) Recent developments and prospects of fish disease science in China. Mod Fish Inf 9(3):1–4
27. Chen BS, Jiang Y (1984) Morphological and physicochemical characterization of the hemorrhagic virus of grass carp. Kexue Tongbao 29:832–835
28. Grass carp haemorrhagic disease research collaboration group (Wuhan Institute of Virology, Chinese Academy of Sciences and Yangtze River Fisheries Institute, Chinese Academy of Fishery Sciences) (1983) Electron microscopy of grass carp haemorrhagic disease virus. Freshw Fish 3:39
29. Zeng LB, Zuo WG (1991) Genome SDS-PAGE analysis and nucleic acid identification of grass carp hemorrhage virus strain 854. Freshw Fish 5:17–18
30. Zeng LB, He L (1992) Studies on the purification and physical-chemical characteristics of the grass carp hemorrhage virus strain 854. Freshw Fish 2:3–5
31. Zeng LB, He L, Zuo WG (1998) Physical-chemical and biological characteristics and genome structure of grass carp hemorrhage virus-854. J Fish China 22(3):279–282
32. Section of Virus Study, Third Laboratory, Institute of Hydrobiology, Academia Sinica (1978) Studies on the causative agent of hemorrhage of the grass carp (*Ctenopharyngodon idellus*). Acta Hydrobiol Sin 6(3):321–329
33. Ding QQ, Yu LF, Ke LH, Cai YQ (1991) Study on infecting other fishes with grass carp hemorrhage virus. Virol Sin 6(4):371–373
34. Wang TH, Liu PL, Chen HX, Liu HQ, Yi YL, Guo W (1994) Preliminary study on the susceptibility of *Gobiocypris Rarus* to hemorrhagic virus of grass carp (GCHV). Acta Hydrobiol Sin 18(2):144–149
35. Chen LX, Fu SH, Wang DG, Chen T, Zhang HY (1998) A study on the biological characteristics of grass carp hemorrhage virus. J Hunan Agric Univ 24(6):468–470
36. Guo QL, Jiang Y (1993) Histopathological studies of the hemorrhage disease of grass carp infected by two types of grass carp reovirus. Trans Res Fish Dis 1:7–11
37. Li X, Zeng WW, Wang Q, Wang YY, Li YY, Shi CB, Wu SQ (2016) Progress on grass carp reovirus. Prog Vet Med 37(7):94–101
38. Blindheim S, Nylund A, Watanabe K, Plarre H, Erstad B, Nylund S (2015) A new aquareovirus causing high mortality in farmed Atlantic halibut fry in Norway. Arch Virol 160:91–102
39. Skoge RH, Nylund A, Solheim K, Plarre H (2019) Complete genome of Atlantic halibut reovirus (AHRV) associated with mortality in production of Atlantic halibut (*Hippoglossus hippoglossus*) fry. Aquaculture 509:23–31
40. Attoui H, Fang Q, Jaafar FM, Cantaloube JF, Biagini P, Micco P, Lamballerie X (2002) Common evolutionary origin of aquareoviruses and orthoreoviruses revealed by genome characterization of golden shiner reovirus, grass carp reovirus, striped bass reovirus and golden ide reovirus(genus Aquareovirus, family Reoviridae). J Gen Virol 83:1941–1951
41. Wu ML, Li HY, Jiang H, He JX, Hou GJ, Jiang YY (2018) Genomic characterization and phylogenetic analysis of grass carp reovirus AH528 strain. Prog Fish Sci 39(5):36–43

42. Zeng WW, Wang Q, Wang YY (2016) Immunogenicity of a cell culture-derived inactivated vaccine against a common virulent isolate of grass carp reovirus. Fish Shellfish Immunol 54:473–480
43. Wang T, Li J, Lu L (2013) Quantitative in vivo and in vitro characterization of co-infection by two genetically distant grass carp reoviruses. J General Virol 94(Pt_6):1301–1309
44. Wang Q, Zeng WW, Yin L, Wang YY, Liu C, Li YY, Zheng SC, Shi CB (2016) Comparative study on physical-chemical and biological characteristics of grass carp reovirus from different genotypes. J World Aquacult Soc 47(6):862–872
45. Zeng WW, Wang Q, Wang YY, Zhang LS, Liu BQ, Shi CB, Wu SQ (2013) Establishment of multiplex PCR for detection of grass carp reovirus and its application. J Fish Sci China 20 (2):419–426
46. Fan YD, Ma J, Zhou Y, Jiang N, Liu WZ, Zeng LB (2018) Establishment and application of a universal RT-PCR assay for detection of different genotype grass carp reovirus. Freshw Fish 48 (6):9–16
47. Deng CX, Yang XQ, Chen HX (1985) Susceptibility to grass carp reovirus (GCRV) of several fish cell lines. Acta Hydrobiol Sin 9(4):351–358
48. Fang Q, Ding QQ, Wang YP, Zhu ZY (2003) Partial characteristic comparison between two aquareovirus isolates. Virol Sin 18(5):464–467
49. Mao SJ, Shao JZ (1989) Studies on the reproduction of pathogenic virus of grass carp hemorrhage in fish cell. J Hangzhou Univ 16(4):471–475
50. Li X, Zeng WW, Wang Q, Wang YY, Li YY, Song XJ, Huang QW, Shi CB, Wu SQ (2016) The study on the proliferation of GCRV II in different fish cell lines. J Fish China 40(8):1249–1257
51. Fang Q, Xiao TY, Li L, Zou GP, Zhang HY, Wang YP (2002) Infection characterizations of four grass carp reovirus (GCRV) strains. Virol Sin 17(2):182–184
52. Yin L (2014) Diversity analysis on biological characteristics of three strains of grass carp reovirus from different genotype. Shanghai Ocean University
53. Fang Q, Ke LH, Cai YQ (1989) Growth characteriersitstics and high titer culture of grass carp hemorrhage virus (GCHV)-873 in vitro. Virol Sin 3:315–319

Chapter 6
Clinical Features and Diagnosis of Aquareovirus Infection

Weiwei Zeng, Yingying Wang, Qing Wang, Yahui Wang, Jiyuan Yin, and Yingying Li

Abstract Aquareoviruses can cause great losses to the aquaculture industry owing to their broad host range. They have been isolated from various marine and freshwater aquatic animals worldwide, including fish and shellfish. There are no effective antiviral therapies or vaccines available thus far for most aquareovirus diseases; therefore, accurate detection and early diagnosis of aquareovirus infections are critical for controlling these diseases. Conventional aquareovirus detection methods include virus isolation from fish cell lines, purification and electron microscopy, genomic electropherotype analysis, immunoenzyme staining, and staphylococcal coagglutination test. Currently, diagnostic methods based on nucleic acids, immunology, and genome sequencing are being developed to overcome the limitations associated with traditional methods. In this chapter, we discuss the progress in research on diagnostic strategies for detecting aquareoviruses, thereby guiding further research on these viruses and the associated disease diagnosis.

Keywords Aquaculture · Aquareoviruses · GCRV · Detection · Diagnostic methods

Abbreviations

CCK	Channel catfish kidney
CCRV	Channel catfish reovirus
CHSE	Chinook salmon embryo
CIK	*Ctenopharyngodon idella* kidney
CPE	Cytopathic effect

W. Zeng (✉)
Guangdong Provincial Key Laboratory of Animal Molecular Design and Precise Breeding, School of Life Science and Engineering, Foshan University, Foshan, China
e-mail: davy988@prfri.ac.cn

Y. Wang · Q. Wang · Y. Wang · J. Yin · Y. Li
Pearl River Fisheries Research Institute, Chinese Academy of Fishery Sciences, Guangzhou, People's Republic of China

CSRV	Chum salmon reovirus
dsRNA	Double-stranded RNA
ELISA	Enzyme-linked immunosorbent assay
EM	Electron microscopy
GCRV	Grass carp reovirus
GSRV	Golden shiner reovirus
HDGC	Hemorrhagic disease of grass carp
IgM	Immunoglobulin M
LAMP	Loop-mediated isothermal amplification
LSRV	Landlocked salmon reovirus
MCRV	Mud crab reovirus
MERV	Marbled eel reovirus
NASBA	Nucleic acid sequence-based amplification
PCR	Polymerase chain reaction
PRV	Piscine orthoreovirus
RPA	Recombinase polymerase amplification
RT-LAMP	Reverse transcription loop-mediated isothermal amplification
RT-PCR	Reverse transcription-polymerase chain reaction
SBRV	Striped bass reovirus
SDS-PAGE	Sodium dodecyl sulfate-polyacrylamide gel electrophoresis
SsRV	Scylla serrata reovirus
TRV	Turbot reovirus

6.1   Introduction

The Reoviridae, which currently consists of 15 genera, is one of the most complex members of viruses. The pathogenicity of this family varies greatly among different genera and is usually related to virus strain and host species. In all double-stranded RNA (dsRNA) virus families, Reoviridae is the largest and the best studied [1]. It has a unique position in cell biology with the discovery of the $5'$-terminal cap structure of reovirus mRNAs in 1974 [2, 3]. The Reoviridae consists of four different aquatic reoviruses, two of which can infect fish. These include the genera *Aquareovirus* and *Orthoreovirus,* where the former is characterized by a double-layered capsid and contains 11 dsRNA segments [4–6], while the latter is represented by piscine orthoreovirus (PRV) with 10 dsRNA segments [7–9]. *Cardoreovirus,* which is composed of reoviruses isolated from crabs, and *Crabreovirus,* which has 12 dsRNA segments [10–12], forms the other two types of aquareoviruses. In addition, other crustacean reoviruses, such as Eriocheir sinensis reovirus [13], Macrobrachium nipponense reovirus [14], and Scylla serrata reovirus (SsRV) [14] with 10, 12, and 13 dsRNA segments, respectively, have not yet been assigned to any genus.

Virus members of the genus *Aquareovirus* have been isolated from various marine and freshwater aquatic animals globally [8, 15–20], such as fish and shellfish [21–29], and are nonenveloped dsRNA viruses containing 11 segments [1, 30–32]. There is only one open reading frame in most segments of the aquareovirus. Five major nonstructural proteins and seven major structural proteins (VP1–VP7) are usually encoded by the genome. Typically, it is based on many factors to identify whether a species belongs to the genus *Aquareovirus*, such as RNA and amino acid sequence analysis, serological comparisons, cross-hybridization, virion morphology, re-assortment ability during mixed infections, conserved terminal sequences, genome segment number, host range, disease symptoms, and electropherotype analysis [33]. To date, aquareoviruses have been categorized into seven species (*Aquareovirus A* to *Aquareovirus G*) and several other tentative species based on RNA–RNA blot hybridization or sequence comparison analyses by the International Committee on Taxonomy of Viruses [16, 30, 32, 33]. A variety of aquareoviruses poses different threats to aquaculture [34]. Some aquareovirus species, such as the grass carp reovirus (GCRV), can cause severe hemorrhagic disease in grass carp and black carp, while others exhibit weak or even no pathogenicity, such as the channel catfish reovirus (CCRV) [35]. For most aquareoviruses, no targeted therapeutic drugs or preventive vaccines are available. Therefore, the most effective strategy would be to diagnose infection as early as possible and isolate infected aquatic animals.

Since each disease has its own specific clinical symptoms, the disease can be primarily diagnosed by its typical clinical symptoms, for example, aquareovirus-infected fish often show hemorrhage of varying degree. However, the clinical symptoms of many viral and bacterial diseases in aquatic animals are similar, thereby masking a serious aquareovirus infection. Thus, it is difficult to distinguish an aquareovirus infection from infections caused by different pathogens based solely on the clinical features. In addition, when aquatic animals become infected with aquareoviruses, they sometimes do not manifest a disease and show no clinical symptoms. Therefore, other detection methods must be used to confirm the pathogen. For example, classical whole virus detection methods, including virus isolation from fish cell lines and subsequent virus purification, electron microscopy (EM), and indirect immunofluorescence assay, have been used. For decades, various nucleic acid-based assays, which are more sensitive than the traditional methods, have been widely used for the specific detection of aquareoviruses. Moreover, some immunological methods, such as immunoenzyme staining, enzyme-linked immunosorbent assays, and western blot analysis, have been developed for aquareovirus detection.

6.2 Clinical Features and Pathology

When aquatic animals are infected with aquareoviruses, which result in disease, they usually show specific clinical symptoms. These typical clinical symptoms can be used for the initial diagnosis of the disease. Golden shiner reovirus (GSRV)-infected

fish have been observed to show punctate hemorrhages in the eyes, intestinal mucosa, dorsal muscle, and ventral surface. These fish have been found to swim near the surface without any vitality. However, GSRV infections often result in a lower mortality rate [36]. The hemorrhagic disease of grass carp (HDGC) caused by GCRV always induces clinical symptoms including spot- or plate-form hemorrhage in organs, which is usually combined with some or all of the following: swimming near the surface without any vitality, skin darkening, hemorrhage at the mouth cavity and base of the fins and gill covers, and mild or severe petechial hemorrhage throughout the musculature, intestines, and liver. In actual production, HDGC is often classified into three types according to the different clinical symptoms: "red fin and gill cover," "red intestine," and "red muscles" (Fig. 6.1). The classification of this disease is just a description of some of the symptoms, and diseased fish have one or all of these symptoms [37]. Moreover, the clinical symptoms of fish bacterial enteritis and viral enteritis are easily confused. The intestines of fish infected with either bacteria or viruses are reddish in appearance. The major difference is that the intestines of virus-infected fish are smooth and elastic, while those of bacterium-infected fish have ulcers. In addition, the typical histopathological changes in fish with HDGC include hyperemia or/and hemorrhage in the liver and spleen vessels, and necrosis and degeneration of the liver cells. During warm seasons, it is very easy for fish infected with a virus to develop a secondary bacterial infection [37].

Striped bass reovirus (SBRV)-infected fish have been found to show shedding scales and with hemorrhagic patches around the dorsolateral area. Furthermore, the swim bladder shows hemorrhaging; the liver appears pale, bloodless, and swollen,
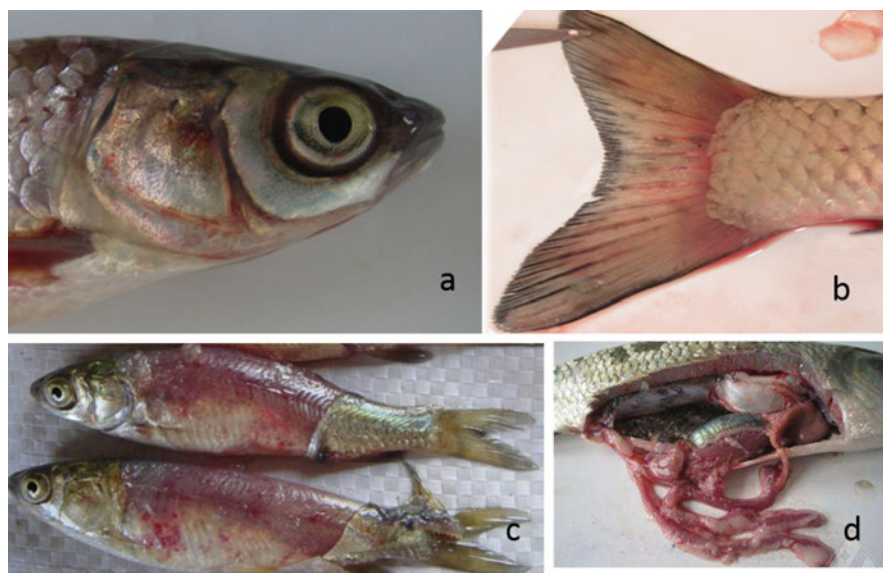
Fig. 6.1 Hemorrhage of the (**a**) gill cover (about 20 g), (**b**) fins (about 40 g), (**c**) musculature and organs (about 15 g), and (**d**) intestines (about 15 g) of grass carp infected with GCRV

and has petechia; and large amounts of membrane layers are observed attached to the body wall and liver. Frequently, diseased fish are accompanied by bacterial infections [38].

Angelfish (*Pomacanthus semicirculatus*) infected with angelfish aquareovirus has been found to exhibit erosion syndrome around the head and lateral areas. The initial symptom is superficial erosion of the head and face, which further spreads to the lateral line system and lateral flank [39]. Petechial hemorrhagic disease of marbled eels is caused by a mixed infection of adomavirus and marbled eel reovirus (MERV) [40].

6.3 Traditional Detection Methods

6.3.1 Viral Culture Method

The virus was cultured in isolated cells in vitro and was first described in the 1962s. Viral culture is considered the most reliable traditional method for aquatic animal virus detection. Cell culture is one of the most widely used methods in fish virology research and is the best way to obtain large amounts of viral material in a laboratory. After infecting permissive cell lines, the virus replicates and multiplies in large quantities in cells, causing a series of corresponding pathological changes in the cells, known as the cytopathic effect (CPE), which can be observed by light microscopy. Some virulent viruses can cause cell death and lysis, while mildly virulent viruses only cause changes in the cell genome, resulting in integration infection, or lead to pathological phenomena, such as morphological changes and increases in nuclear material. These characteristics can be used for the preliminary identification and virulence determination of some viruses.

Additionally, virus isolation is a "gold standard" for laboratory-based diagnosis of aquareovirus infections and provides unequivocal evidence of the presence of infectious viruses in clinical samples. The principle of this method is to inoculate the supernatant from the clinical samples in permissive cell lines, and syncytia, CPE, or non-syncytial phenomena are observed after several days of propagation, which can be followed by electron microscopic observation, immunoassays, or polymerase chain reaction (PCR) tests to confirm the identity of the isolated virus, if required.

The basic process of virus identification in cell culture is as follows. The cells are prepared ahead of time, ensuring that the monolayer cell density is approximately 70–85%. The clinical tissue samples are collected and homogenized in a cell culture medium or sterilized phosphate-buffered saline. After freezing the samples at −80 °C or in liquid nitrogen and thawing them three times, the homogenate is centrifuged at 5000 × g for 10 min at 4 °C to pellet cell debris. Next, we filter the supernatant through a 0.22μm filter to clean the bacterium-sized particles. Then, the filtrate is diluted with the cell culture medium at a 1:10 ratio. The diluted supernatant is then added to the monolayer cell lines. After rocking for 1–2 h at 15–28 °C, fresh cell culture medium is added, followed by incubation for several days at 15–28 °C.

Three blind passages are performed according to the aforementioned protocol, and the cells are observed daily for toxicity, contamination, or CPE, keeping non-infected cells as controls. At the same time, one or more other methods are used to evaluate viral infection and identify virus species.

Most aquareoviruses have permissive cell lines, wherein they replicate well and characteristically produce syncytia or plaque-like areas as typical CPE in monolayer cultures. Tissue homogenate filtrate obtained from the viscera of diseased channel catfish was used to isolate CCRV in the channel catfish kidney (CCK) cell line, and the CPE was observed under a light microscope at 2 days post-inoculation [4, 6, 19, 22, 41–45]. In addition, CCRV has been isolated from channel catfish ovary cells incubated at 26 °C, in which it can produce plaque-like syncytia, which is followed by cell rounding and detachment from the flask surface [35]. Turbot *Scophthalmus maximus* reovirus can cause CPE in grass carp fin and chinook salmon embryo (CHSE) cell lines after 4–5 days of incubation [23]. During a routine examination, an aquareovirus was isolated from chum salmon (*Oncorhynchus keta*) at 6 days post-inoculation, and CHSE-214 cells infected with pooled samples of the chum salmon kidney and liver were found to develop plaque-like syncytia [46]. The clinical samples of diseased salmon collected from the Coquille River in 1989 were inoculated into CHSE-214 cells and incubated at 15 °C; the syncytia was observed after several blind passages in 14 days. In contrast, the samples collected from the Eel Lake produce the same CPE at 6 days post-inoculation, and in both scenarios, the species has been identified as coho salmon aquareovirus [47]. A typical CPE in cell culture is characterized by the production of large syncytia [48]. For instance, GCRV-873, a GCRV I isolate inoculated in most of the available fish cell lines, has been shown to cause syncytia as a typical CPE [37, 49] (Fig. 6.2).

Instead of syncytia, some aquareoviruses produce a pattern of cell rounding leading to apoptosis, such as the American grass carp reovirus, a member of the *Aquareovirus G* species group [50] and GCRV-104 (HGDRV), a GCRV III isolate (Fig. 6.2) [22, 49]. However, other aquareoviruses, such as GCRV II species (including GCRV-109, GCRV-GD108, and GCRV-GZ08), infect all the available cell lines and show no CPE (Fig. 6.2) [27, 29, 51]. Another study has shown that chum salmon reovirus (CSRV) can infect rainbow trout gonad cells, and no CPE is observed [46]. Moreover, some aquareoviruses proliferate slowly when cells are inoculated with the initial tissue supernatant, causing virus isolation to fail. In the early days, some researchers tried using GF-1 FHM and EPC cell lines for PRV isolation and proliferation, but no CPE and no increase in viral titers were observed after four blind passages [52–54]. It was not until 2015 that PRV was found to be able to replicate in primary cultures of the Atlantic salmon erythrocytes, which can be visualized by EM; however, no CPE or cell lysis is observed [55]. The type of CPE produced by MERV depends on the type of cells used. For instance, syncytium is observed when MERV is inoculated into DMECF-5 and ARB8 cell lines, whereas MERV proliferation in marbled eel caudal fin (MECF) cells causes cell rounding (potential apoptosis) [56]. We have summarized the cell line susceptibility, culture temperature range, and characteristics of infected cells for various aquareoviruses in Table 6.1.
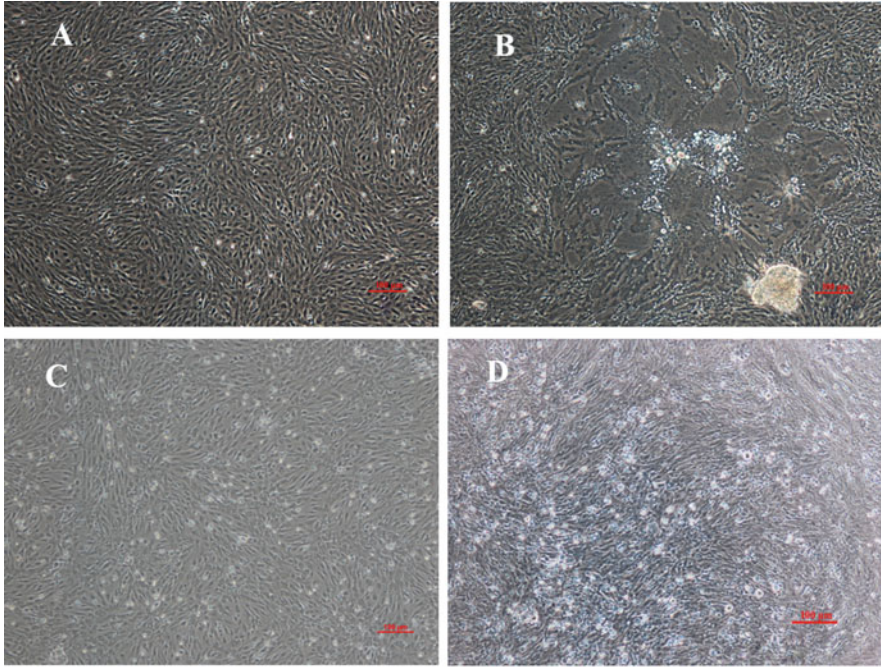
Fig. 6.2 Different CPEs in CIK (*Ctenopharyngodon idella* kidney) cells infected with GCRV-HZ08, GCRV-873, or HGDRV (GCRV-104). (**a**) Mock-infected CIK cells. (**b**) Typical CPE is observed in GCRV-873-infected CIK cells at 2 days post-infection. (**c**) A few of the apoptotic cells removed from the CIK cell monolayer infected with GCRV-HZ08 at 6 days post-infection. (**d**) Numerous pyknotic and apoptotic cells aggregate and detach from the CIK cell monolayer infected with HDGRV (GCRV-104) at 6 days post-infection

Virus isolation is a specific method for diagnosing viral infections. However, culture techniques require a week or more for completion and specialized laboratory equipment and skilled labor. Moreover, this method also involves high costs and complex operational procedures, which are not suitable for the rapid identification of viruses. Isolation techniques have also been found to be quite insensitive as a diagnostic test during several field investigations; therefore, data from virus isolation protocols are often not very useful for enacting measures to control aquatic animal viral diseases. Therefore, it would be useful to develop simple tests available for rapid diagnosis of viral infections at the onset of epidemics, in order to enforce control measures.

6.3.2 EM

EM is based on the visualization and morphological identification of virus particles in samples of diseased tissues or viruses isolated from cell cultures to diagnose the viral infection. EM is a powerful method for virus identification, and it is the most

Table 6.1 Temperature range, cell line susceptibility of infected cells of different aquareoviruses

Abbreviations of virus strain	Full name of virus strain	Temperature range (°C)	Permissive cell line
13p2	American oyster aquareovirus (13p2)	15–23	BB, AS, GE-4, WF-2, ASH, CHSE-214, CHH-1, BF-2
AFR	Angel fish reovirus	22–27	BB, BF-2, RFDF, CCO, CHSE-214
AGCRV	American grass carp reovirus	22	FHM
AHRV	Atlantic halibut reovirus		BF-2, CHSE-214
ASRV	Atlantic salmon reovirus	15–20	CHSE-214, EPC, BB, BF-2
BCRV	Black carp aquareovirus	ND	CF,CO
CRV	Chub aquareovirus	20	EPC, FHM, RTG-2, CHSE-214, CHH-1, BB
CCRV	Common carp aquareovirus	10–25	EPC, R1, CHSE-214, CO, CK, PG, CAR, FHM
CSV	Chum salmon reovirus	10–20	CHH-1, CHSE-214, STE-137, KO-6, LBF-2, BF-2, WC-1, EPC, CCB
CSR	Coho salmon reovirus		CHSE-214
CRV	Channel catfish reovirus	26	BF-2, CHH-1, BB, CHSE-214, CCO, CCK
FCRV	Fall Chinook reovirus	15	CHSE-214
FCaRV	Fancy carp aquareovirus	ND	RTG-2, CHSE-214, SSE-5, CHH-1, FHM, EPC, BF-2, EO-1, EF-1
GCRV-I	Grass carp reovirus genotype I	22–30	Most of fish cell lines
GCRV-II	Grass carp reovirus genotype II	22–30	CO, GSB, PSF, CIK
GCRV-III	Grass carp reovirus genotype III	22–30	CO, CIK
GIRV	Golden ide reovirus	20	CCB, FHM, EPC
GrRV	Grouper aquareovirus	25	BF-2, SB, GF
GSRV	Golden shiner reovirus	30	FHM, CHSE-214, BB
LSV	Landlocked salmon reovirus	15–25	AS, BF-2, BB, CCO, CHSE-214, EPC, FHM, GK, MHR, PH, PL
MERV	Marbled eel reovirus	25	DMEPF-5; ARB
JERV	Japanese eel aquareovirus	ND	EO-1, EK-1
SBR	Striped bass reovirus	15–20	CHSE-214, EPC, BB, BF-2
SMReV	Scophthalmus maximus reovirus	ND	CHSE-214, GCF, GCF, GCO;, CIK
SRV	Smelt reovirus	15–20	CHSE-214, EPC, BB
TCRV	Tenth and Chub aquareovirus	20	EPC, FHM, RTG-2, CHSE-214, CHH-1, BB

Table 6.1 (continued)

Abbreviations of virus strain	Full name of virus strain	Temperature range (°C)	Permissive cell line
TRV	Turbot reovirus	15–20	CHSE-214, EPC, BB, BF-2, GF-1
TSRV	Tasmanian aquareovirus	15–22	BF-2, EPC, CHSE-214
CAGRV	Carassius auratus gibelio reovirus	27	EPC
PLDRV	Phoxinus lagowskii Dybowskii reovirus	27	EPC
SSRV	Scylla serrata reovirus	28	HTP
WBRV	White bream reovirus	20	EPC,BF-2, RTG-2 and CHSE-214

CCK catfish kidney cell line, *CSR* Coho salmon aquareovirus, *FHM* fathead minnow, *CHSE-214* Chinook salmon embryo, *BB* brown bullhead catfish, *BF-2* bluegill fry, *CHH-1* chum salmon heart, *CCO* channel catfish ovary, *RTG-2* rainbow trout gonad, *AS* Atlantic salmon. *GE-4* guppy embryo, *WF-2* walleye fry, *ASH* Atlantic salmon heart, *RTS* rainbow trout spleen, *STE-137* steelhead trout embryo, *KO-6* kokanee salmon ovary, *LBF-2* largemouth bass, *WC-l* walleye sarcoma, *EO-1* Japanese eel ovary, *EK-1* Japanese eel kidney, *SSE-5* sockeye salmon embryo, *EPC* epithelioma papulosum cyprini, *CF* grass carp fin, *CB* carp blastoderm, *CK* grass carp kidney. *CLC* fancy carp leucocytes, *PG* Esox lucius gonad, *R1* rainbow trout liver, *IGH2* iguana heart, *GK* grouper kidney, *MHR* milkfish heart, *PH* perch heart, *PL* perch liver, *TO-2* tilapia ovary, *BHK-21* baby hamster kidney, *MA104* fetal rhesus monkey, *MDBK* bovine kidney, *Hep-2* human epidermoid carcinoma, *R1* rainbow trout liver, *CK* grass carp kidney, *PG* pike gonad, *CAR* goldish, *SB* Asian sea bass, *CEF* chicken embryo fibroblast, *bND* not determined, *RFDF* redfish dorsal fin cell line, *CCB* common carp brain, *CPE* cytopathic effect, *CIK* Ctenopharyngodon idella kidney, *EF-1:HTP* hepatopancreas testicular primary cell, *GCF* grass carp fins, *CO/GCO* grass carp ovaries, *GF* goldfish fin, *ARB* Aequidens rivulatus brain cell

widely used, highly effective, and indispensable technology in virology. Viruses are visualized by negative staining, vacuum plating, or thin sectioning of lesion tissues or cell cultures. It is mainly used to discover and identify new viruses and observe the size, shape, arrangement, structure, and processes of replication, assembly, and maturation of viruses. Additionally, it is used to observe the morphological characteristics of inclusion bodies, capsid symmetry, number and arrangement of capsid particles, position of nucleocapsid replication and assembly in cells, diameter of the helically symmetric nucleocapsid, recombined virus nucleic acids, and biological characteristics of viral proteins. Thus, they can identify and classify pathogenic viruses. EM can not only be applied in diagnostic virology, but also has continued to be valuable in elucidating mechanisms of virus attachment and replication, such as in studies of the dynamics of virus proliferation in host cells and ultrastructural pathological changes in tissues and cells caused by viruses. Generally, EM is used to detect the presence of viruses and initially identify the types of viruses, while the precise identification of species must rely on other, more specific methods.

A virus morphology study was performed with the help of EM during the first isolation and identification of aquareoviruses, which are nonenveloped, and the particles are approximately 60–80 nm in diameter and consist of two concentric
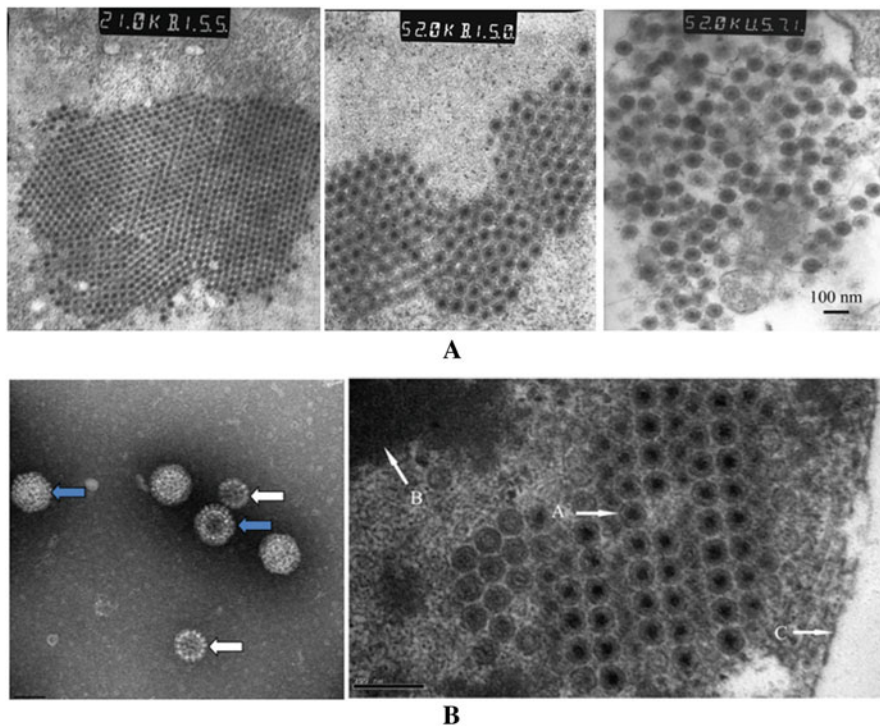
Fig. 6.3 EM of aquareoviruses. (**a**) The ultrathin sections of GCRV. A mass of icosahedral nonenveloped viruses with a diameter of approximately 70 nm is observed in the paracrystalline arrays in GCRV-infected cells. (**b**) Purified virions (left panel) and ultrathin sections (right panel) of Tasmanian Atlantic salmon reovirus (TSRV). Blue and white arrows indicate populations 1 (intact virion) and 2 (subviral particle core), respectively

icosahedral capsid layers. Since the beginning, most aquareoviruses are diagnosed and studied with EM. The observation of CCRV-730 in CIK cells using EM showed that these are double icosahedral capsid layer particles with a diameter of approximately 60–70 nm (Fig. 6.3). Characteristic nonenveloped cytoplasmic inclusion bodies of varying sizes and shapes are scattered throughout the cytoplasm at different stages of virus formation, and these inclusion bodies are composed of a granular and electron-dense matrix. CCRV-730 is morphologically similar to other aquareoviruses, such as GCRV and GSRV [43]. EM of negatively stained virions of the American oyster reovirus (13p2) revealed that the particles are approximately 79 nm in diameter with icosahedral capsid layers. Viral particles with icosahedral double capsid layers and an electron-dense core are found to be scattered in the cytoplasm of infected BF-2 cells by thin-section EM [36]. Thin-section EM of the GSRV-infected FHM cells showed the presence of icosahedral nonenveloped virions with a diameter of approximately 70 nm [36]. EM of negatively stained virions of CSRV has revealed particles 75 nm in diameter with icosahedral symmetry and a double-layered capsid; the external capsid contains 20 capsomeres and

particles are nonenveloped [46]. EM of purified CCRV has shown double capsid-layered icosahedral particles with a diameter of approximately 75 nm [35]. EM of negatively stained tenth aquareovirus, chub reovirus, SBRV, turbot reovirus (TRV), coho salmon reovirus, landlocked salmon reovirus (LSRV), and angelfish aquareovirus virions concentrated from infected cells has shown double capsid-layered spherical to icosahedral particles with a diameter of approximately 65–78 nm [38, 39, 47, 57–59].

In the past several decades, EM has been the gold standard method for virus identification. EM is not a high-throughput screening technique for virus detection, but it has been successfully used to detect viruses in both infected cell lines and clinical tissue samples. However, with the development and application of molecular biology and immunology techniques, its role in virus identification has been increasingly weakened. Immunological methods, such as immunohistochemistry and immunofluorescence, are very specific high-throughput techniques for virus detection. The principle of these methods is to utilize the specific binding reaction between antigens and antibodies, which helps to improve the success rate of virus identification. Molecular biology techniques, such as PCR, are also rapid, specific, and high-throughput screening methods, and the key aspect of these methods is to design specific primers based on known gene sequences. However, the virus is prone to mutation and the specific primers may not recognize the complementary mutated sequence, resulting in false negative results. Therefore, EM remains the most reliable method for the identification of unknown viruses, for which no primers or probes are available, especially for some of the emergent viruses. EM is and will always be essential for the characterization of new viruses.

6.3.3 Genomic Electropherotype Analysis

The genome of members of the family Reoviridae is a segmented dsRNA, and analysis of the difference in relative migration rates of these segmented dsRNAs in sodium dodecyl sulfate-polyacrylamide gel electrophoresis (SDS-PAGE) has been used to distinguish virus isolates. There is a close relationship between the electrophoretic patterns in SDS-PAGE and the species and characteristics of the viruses. Therefore, analysis of the genome by SDS-PAGE is usually used for diagnosing and distinguishing aquareovirus strains, as well as for molecular epidemiological studies.

The first comparative analysis of aquareoviruses at the molecular level was performed in 1987 [6]. In this study, SDS-PAGE was used to compare the RNA and protein electrophoretic patterns of GSRV, CCRV, CSRV, and 13p2. All viruses were found to have a genome comprising 11 dsRNA segments that are divided into three size classes, and each virus has a unique electrophoretic pattern. However, the electrophoretic patterns of isolates obtained from warm water fish (GSRV and CCRV) and cold water fish (CSRV and 13p2) appear to be similar. Moreover, CSRV and 13p2 have total molecular weights higher than that of GSRV and CCRV. In addition, a comparison of the electrophoretic patterns of tenth

aquareovirus, chub reovirus, GSRV, and CSRV in SDS-PAGE showed that these viruses have 11 dsRNA segments with different relative mobilities. However, the electrophoretic pattern of tenth aquareovirus is more similar to that of GSRV, but not exactly the same, while the electrophoretic patterns of chub reovirus and CSRV are more similar to those of other viruses.

RNA separation patterns of CSRV have been analyzed using SDS-PAGE, which showed that the genome comprised 11 dsRNA segments and categorized into three size classes [46]. The molecular weight of the three large segments is $2.5–2.3 \times 10^6$; the molecular weight of the three medium segments is $1.9–1.6 \times 10^6$; and the remaining five small segments have a molecular weight of $0.97–0.37 \times 10^6$. The total molecular weight of the viral genome has been measured as 16×10^6. In addition, analysis of the RNA separation patterns of CSRV by SDS-PAGE revealed that the 11 dsRNA segments are grouped into the large, medium, and small size classes and have an estimated molecular weight ranging from 0.4×10^6 to 2.5×10^6 [60]. SDS-PAGE analysis of the CSRV genomic RNA extracted from both virus-infected CCK cells and diseased fish tissues showed an electrophoretic pattern similar to that of SRV. As expected, the genome of CSRV consists of 11 dsRNA segments that fall into the three size classes ranging from 0.9 to 4.4 kb in length and has the typical electropherotype of the Reoviridae genome. The 11 segments are completely separated, clearly visible, and present a unique electropherotype [26]. The electrophoretic mobility of the dsRNA segments of the coho salmon reovirus CSR and coho salmon reovirus ELC has been analyzed by SDS-PAGE. The genomes of the two viruses have been observed to contain 11 dsRNA segments with similar but slightly different electropherotypes. The electrophoretic patterns of CSR and ELC are distinct from that of 13p2, but similar to the electropherotype of the chinook salmon reovirus YRC. The electrophoretic mobility of RNA and polypeptides of LSRV was examined by SDS-PAGE analysis and compared with that of other aquareoviruses. The LSRV genome contains 11 dsRNA segments with a relative mobility different from that of CSRV, GSRV, and chub reovirus. Moreover, it has been revealed that LSRV contains five structural polypeptides with molecular weights ranging from 139 to 32 kDa, which have a similar but unique pattern compared with that of GSRV, CSRV, CRV, and 13p2. SDS-PAGE analysis of the viral RNA of 17 GCRV isolates revealed that all isolates contain 11 dsRNA segments, while the genomic electrophoretic distribution of the various isolates is different. However, the 17 isolates in general can be divided into three types (Fig. 6.4), which is consistent with the division of GCRVs into three genotypic groups based on the genome sequence.

6.4 Nucleic Acid-Based Methods

Molecular biology techniques are also known as nucleic acid-based methods, including nucleic acid amplification and hybridization. These methods are based on PCR techniques for the detection of virus-specific DNA or RNA sequences. The
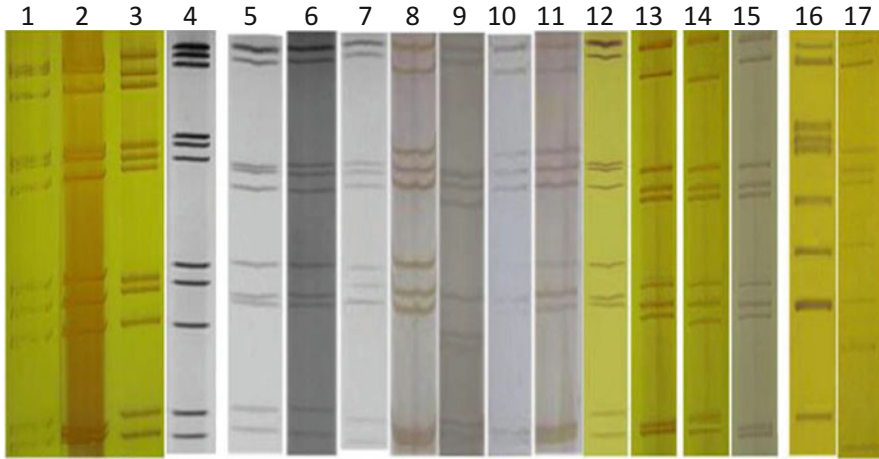
Fig. 6.4 Comparison of the genomic profiles of 17 GCRV isolates by SDS-PAGE-based electropherotype analysis. The strains in Line 1–17 are GCRV-873, JX0901, GZ1208, GX1009, GD1108, JX0902, 892, CQ1307, GX1107, JinZ1206, SD1308, GD1410, HZ08, HuNan1307, JX1206, 104 and HB1007, respectively. The genomic RNA is extracted from infected grass carp snout fibroblast cell culture

sensitivity of nucleic acid-based methods is higher than that of antigen-based immunological assays, and generally, majority of the nucleic acid-based methods are performed within 2–4 h, providing information on the aquareovirus subtypes. Nucleic acid amplification is the most commonly used method for virus detection. Currently, there are many methods for nucleic acid amplification. The classic method is PCR, which includes nested PCR, reverse transcription-polymerase chain reaction (RT-PCR), and other methods derived from PCR, such as quantitative real-time PCR (qPCR), loop-mediated isothermal amplification (LAMP), recombinase polymerase amplification (RPA), and nucleic acid sequence-based amplification (NASBA), which have been widely used in the diagnosis and detection of pathogenic diseases in aquaculture animals.

Nucleic acid hybridization methods mainly include DNA hybridization, RNA hybridization, and ribonuclease protection assay. DNA hybridization, which involves synthesizing complementary cDNA probes, is specific to the viral DNA segment and detects the virus in infected cells or tissues based on nucleic acid hybridization. The operation of this method is complex, with unstable results, thereby rendering it impractical. The ribonuclease protection assay is a novel quantitative mRNA analysis technology, which has been developed recently, and is widely used in the fields of life science and medical research [61, 62]. The principle involves the use of excess labeled RNA probes to hybridize with the target mRNA, followed by digestion of the RNA probes that do not hybridize with the target mRNA, and detection and quantification of the labeled RNA–RNA hybrids by denaturing polyacrylamide gel electrophoresis. The ribonuclease protection assay

can detect two or more kinds of mRNA simultaneously and is a sensitive, accurate, and high-throughput assay.

6.4.1   PCR

PCR is the most rapidly developed detection technology. It can detect trace samples with high sensitivity and specificity; the minimal detection amount can even reach 0.1 pg viral nucleic acid, with detection in every phase of virus infection, making it a major technology for early diagnosis and detection [63]. PCR overcomes the shortcomings of traditional methods of virus culture and immunology, such as low sensitivity, complex operation, excessive time consumption, and increased false negatives, and breaks through the limitations of molecular hybridization technology. At present, it has been successfully applied for the detection and diagnosis of viral pathogens. RT-PCR is a technique that combines the reverse transcription of RNA with cDNA PCR. First, cDNA is synthesized from RNA by reverse transcriptase, followed by target fragment amplification by DNA polymerase using the cDNA as a template, which can be used for RNA virus detection. Further, RT-PCR assays with improved sensitivity have also been developed specifically to detect aquareoviruses. RT-PCR has allowed the identification of aquareovirus RNA in both tissue specimens and cell cultures and is considered to be the most efficient and powerful method for virus identification worldwide. Researchers have developed conventional RT-PCR and nested RT-PCR, as well as double or multiple RT-PCR assays for the detection of aquareoviruses, which are summarized in Table 6.2

6.4.1.1   Conventional RT-PCR

RT-PCR was first used for GCRV detection by Li in 1997 [64]. Two pairs of PCR primers were designed according to the cloned cDNA sequences of GCHV-861 strain (GCRV II). Only one specific major product was obtained for each primer combination when the genomic dsRNA of GCHV-861 was amplified. The lengths of the expected amplified fragments were 320 and 223 bp for the two primer sets, respectively, showing a very high specificity and sensitivity. Additionally, RT-PCR can be used to detect GCHV-861 in both infected cell cultures and virus-infected fish with or without hemorrhagic clinical signs [65]. In 2010, an improved, simple, rapid, and sensitive method for detecting GCRV II species based on RT-PCR was developed in combination with an advanced RNA extraction technique using the S10 segment as the template [63]. The entire detection process can be completed within 4–5 h after RNA extraction, which is much faster than the previously reported methods. In 2018, Fan et al. developed a universal RT-PCR method for detecting the three genotypes of GCRV. A pair of degenerate primers was designed to target the multiple sequence alignment-conserved S2 segment encoding the VP2 protein of different GCRV genotype strains. The primers were used for PCR amplification

Table 6.2 RT-PCR assay primer and probe sequences and cycling conditions for detection of aquareovirus

Assay	Primer/Probe name	Sequence (5′-3′)	PCR Conditions	Amplicon (Gene)
GCRV RT-PCR (GCRV-861)	PS6-F	AGT TCT CAA AGC TGA GAC AG	94 °C 2 min, 94 °C 30s, 56 °C 30s, 72 °C 1 min (30 cycles) 72 °C 5 min	PS6: 320 bp PS9: 223 bp
	PS6-R	ACG TGC GAT TGG AAG AGC TT		
	PS9-F	ACA TCT ACT GTG CTT CAC CT		
	PS9-R	TAG TGT GTC AAT AGC GTC CA		
GCRV RT-PCR	GCRV-S6F	GTT ATT TCG ACA CTT CGC ACT CTC	94 °C 3 min, 94 °C 30s, 50–55 °C 1 min, 72 °C 90s (35cycles) 72 °C 10 min	522 bp 719 bp 365 bp 625 bp 515 bp
	GCRV-S6R1	GTC TAA GTG TTT CTG CCA GAG AGC		
	GCRV-S6F	GTT ATT TCG ACA CTT CGC ACT CTC		
	GCRV-S6R2	GCA TCG GGA AGC TTG GTG TCT		
	GCRV-S10F	GTT ATT TCT GAG CCC CCG ATC		
	GCRV-S10R1	GCG ACG AAC CCA GCT TTC ACA		
	GCRV-S10F1	GTG AGT GAC AAA GCG CAG ACC		
	GCRV-S10R	GAT GAA ACG AGA GAC CCC TAC		
	CRV-S10F2	TCT AAG GAT ATC GTC GAA CTT		
	GCRV-S10R	GAT GAA ACG AGA GAC CCC TAC		
SSRV RT-PCR	SS-1	AAG CTG ATA TAG AAT TGG CTA	42 °C 30 min, 94 °C 5 min, 94 °C 30s, 45 °C 30s, 72 °C 30s (40 cycles) 72 °C 10 min	100–200 bp
	SS-2	TCG TTA GCG AGA TCC GCA GGA		

(continued)

Table 6.2 (continued)

Assay	Primer/Probe name	Sequence (5'-3')	PCR Conditions	Amplicon (Gene)
GCRV RT-PCR (GCHV-892)	GCRV-NF GCRV-NR	ACG AGC CTT ACA GCA GCA TA CAC ATC GGC AGT ATC GTA AG	94 °C 5 min, 94 °C 45s, 55 °C 45s, 72 °C 1 min (35 cycles) 72 °C 10 min	712 bp
GCRV RT-PCR	GCRV-F GCRV-R	TCA AGA CTC CCA CGC TTG TTC TGC GTA TCG TCC AAC GGT TT	95 °C 5 min, 94 °C 45s, 54 °C 45s, 72 °C 45s (35 cycles) 72 °C 10 min	345 bp
GCRV-I,II,III RT-PCR	GCRV-F GCRV-R	TAY GTV ACM SCC MGR GGW GG AAD TGY TGY ACC ATG DYC TGC	95 °C 5 min, 94 °C 30s, 60 °C 40s, 72 °C 40s (35 cycles) 72 °C 10 min	I: 590 bp II: 590 bp or 593 bp III: 587 bp
MCRV nest-RT-PCR	MCRV-MF MCRV-MR MCRV-MNF MCRV-MNR	TTC ATT GGC ATC CTG ACT TT TTC ATT TGG TGA GCC TTT GC ACC TGA TTA TCG ACC CAA TCC CA AGC CTT TGC CTG ATG AGC CTG AA	95 °C 3 min, 94 °C 30s, 55 °C with primer M or 60 °C with primer MN 30s, 72 °C 1 min (30 cycles) 72 °C 10 min	M: 433 bp MN: 304 bp
CCRV-730 RT-PCR	PF PR	GGC GAG ACC CAG TCC TAT CGG GTG ATT GTG GCA GTT		327 bp
Carassius auratus gibelio reovirus	S6F S6R	ACG TGC GAT TGG AAG AGC TT AGT TCT CAA AGC TGA GAC AG	94 °C 3 min, 94 °C 30s, 54 °C 30s, 72 °C 60s (40 cycles) 72 °C 7 min	
Phoxinus lagowskii Dybowskii reovirus	S10F S10R	CGC GTT CGC TGA TGT AAG G CCC CGA TCA TCA CCA CGA T	94 °C 3 min, 94 °C 30s, 54 °C 30s, 72 °C 60s (40 cycles) 72 °C 7 min	
MCRV and MCDV-1 duplex-nested PCR	MR-ReoF MR-ReoR	GCAAATTGAACTACTACTACTTA GATTCCTATTGTCAACTATCTCA	95 °C3 min; 94 °C 30s, first amplification, 55 °C 30s; second	MR: 433 bp MRN:

	Primer	Sequence	Conditions	Size
	MRN-ReoNF MRN-ReoNR MD-DicF MD-DicR MDN-DicNF MDN-DicNR	ACTCATAGAGCAGTCATGGG ATATCGTCAGAATGTCGTTC GCACTGGGTACTCTTCCTG ACAACTACCAAAGCCCTAC GGATACTATGGATGATGTTTC ACAAAATACCAGATAAAGCAA	amplification, 53 °C 30s, 72 °C 1 min (30 cycles), 72 °C 10 min	304 bp MD: 686 bp MDN: 404 bp
GCRV Duplex PCR (GCRV-GD108 and GCRV873)	GCRV-L1-F GCRV-L1-R GCRV-Ctrl-F GCRV-Ctrl-R	CAA GTT TTA TGC GGC ACC GTC AAT G GAT AAC GCC ATC CGT AAC ATC GCA A TTA GGG CGG AAA GCA TAC CAG ATT- GAG ATT CCT CAT CCC ATC ACC CAC ATC CTC	94 °C 1 min; 94 °C 30s, 62 °C 30s, 72 °C 45s (35 cycles) 72 °C 10 min	L1: 258 bp Ctrl: 476 bp
Spectrum Aquareovirus RT-PCR	AQ1 (sense) AQ2 (antisense)	AWS CCK TAY ATC TAT GGC TT TTR GAG ACG AAM AKN GAS GC	94 °C 2 min, 94 °C 30s, 50 °C 30s, 72 °C 1 min (30 cycles) 72 °C 5 min	434–443 bp (segment 6)
GCRV Multiplex PCR	GCRV-P01-F GCRV-P01-R GCRV-P02-F GCRV-P02-R GCRV-P03-F	GCC ACC TTT GAG CGC GAG AC GTT AGG GCG GAA AGC ATA CCA GA GCT GAT GCT GCA GAC GGC TAA AC TAA TTG CCT GCT GCG CTG ACT GGC GGC ATG AAT ATG TAT CGA CT TAT GTG ATT ACG CGG GTC AG	95 °C 5 min, 94 °C30s,53.2 °C40s, 72 °C 40s (30 cycles) 72 °C 10 min	P01: 532 bp P02: 196 bp P03: 297 bp

(continued)

Table 6.2 (continued)

Assay	Primer/Probe name	Sequence (5'-3')	PCR Conditions	Amplicon (Gene)
	GCRV-P03-R			
TSRV RT-PCR	SpT10Fb SpT10Ra	TTC CCT CTC TAA GAC CC GCC ACC GGT AAT AGT ACG	55 °C 30 min, 94 °C 2 min, 95 °C 30s, 50 °C 30s, 68 °C 45s (35 cycles) 68 °C 7 min	280 bp (Segment 10)
TSRV hemi-nested PCR	SpT10FN SpT10Ra	AAT TGT GAT CGC GCT CTC GCC ACC GGT AAT AGT ACG	95 °C 15 min 94 °C 30s, 51 °C 30s, 72 °C 45s (35 cycles) 72 °C 7 min	141 bp (Segment 10)
Generic Aquareovirus RT-PCR	GARV-F GARV-R	TAA AGC TTG CGA CGC CTC CAT CAC TGC TCG GTG GAG GTG ACA GT	55 °C 30 min, 94 °C 2 min, 95 °C 30s, 50 °C 30s, 68 °C 45s (35 cycles) 68 °C 7 min	314 bp (Segment 2)
TSRV T10 RT-PCR	T10Fc T10Rc	GCC CGT TCC AAT ACT GTA CCG GGG AGA CCT AGT CCT CAT C	55 °C 30 min, 94 °C 2 min, 95 °C 30s, 50 °C 30s, 68 °C 45s (35 cycles) 68 °C 7 min	263 bp (Segment 10)

using the cDNA of the three genotypes of GCRV as the template, and only one specific product with a length of approximately 590 bp was obtained. Moreover, this newly developed universal RT-PCR can detect the three genotypes of GCRV simultaneously with high sensitivity and specificity [66].

A rapid, highly specific, and sensitive RT-PCR method for the detection of different aquareoviruses was described by Seng et al. [67]. It is very useful for the rapid and accurate detection of a variety of aquareovirus strains isolated from different host species and origins using specific degenerate primers. It can be used to detect aquareoviruses in low-titer virus-infected cell cultures and tissue samples from diseased fish with clinical symptoms, as well as in apparently healthy but aquareovirus-infected fish. In 2008, the detection of mud crab reovirus (MCRV) was based on the one-step and two-step RT-PCR methods, which resulted in the amplification of the predicted products of 433 and 304 bp, respectively. The lowest detection thresholds of one-step and two-step RT-PCR methods for MCRV dsRNA were 10–8 and 10–9μg, respectively. In the initial stages of infection, MCRV can be detected in all tissues and organs, except the stomach and hepatopancreas. However, MCRV can be detected in all tissues of moribund mud crabs [68]. Moreover, a pair of primers has been designed based on the S8 gene sequence, and a PCR method for the detection of CCRV-730 has been established [69]. RT-PCR has also been used to detect other aquareoviruses; for example, RT-PCR is used to screen the genetic material of PRV to monitor the prevalence of PRV infection [7, 8].

6.4.1.2 Nested RT-PCR

Nested RT-PCR, which is based on nested primers resulting in high sensitivity and specificity, has also been widely used to detect aquareoviruses. Two pairs of primers were designed based on the conserved regions of the genomes of MCRV and mud crab dicistrovirus-1, and researchers have developed a multiplex nested RT-PCR for the simultaneous detection of these two viruses. The method can detect a minimum of 10 copies of the viral genome for both viruses and shows good specificity and reliability for identifying crab viruses. Furthermore, it can also be used for the rapid diagnosis of clinical samples with suspected MCRV or mud crab dicistrovirus-1 infection, but further tests are needed to distinguish which virus is actually responsible for the infection [70].

Zainathan et al. [71] developed both conventional RT-PCR and nested RT-PCR methods for detecting aquareoviruses. At the same time, an RT-qPCR method was established for the detection of Tasmanian Atlantic salmon reovirus. This was followed by intra- and inter-laboratory comparisons of virus isolation in cell culture and PCR assays to detect and identify Tasmanian Atlantic salmon reovirus from clinical tissue samples. The methods mentioned above all have shown high specificity, while the expected sensitivity has been observed to vary across the methods, with RT-qPCR being the most sensitive, followed by virus culture and nested

RT-PCR. RT-qPCR has been found to be more sensitive than virus culture by a 1000-fold [71].

6.4.1.3 Multiplex RT-PCR

The conventional RT-PCR method has gone from single to multiplexed detection. Multiple pairs of primers are added to the same reaction system for amplification of multiple targets in a single PCR to achieve the simultaneous detection of multiple viruses. In 2004, Seng et al. designed a pair of degenerate primers for the S class-segment conserved regions of threadfin reovirus, guppy reovirus, and GCRV, which amplifies a 450 bp product and can detect threadfin reovirus, guppy reovirus, and GCRV with low titers in infected cells simultaneously by RT-PCR [67]. It can accurately diagnose aquareovirus infections in specimens from aquatic animals with dominant and recessive clinical symptoms. In 2011, Chi et al. established a dual PCR detection method to detect GCRV I and II infections. Primers were designed, followed by selection of suitable primers, according to the sequences of the 11 segments of GCRV-GD108 and GCRV prototype strains. This method can identify GCRV or GCRV-GD108 strain in a single reaction, which can improve the detection efficiency and reduce costs. Moreover, a highly sensitive and specific triple PCR method has been developed using three pairs of primers specific to the different genotypes of GCRV. This method can be applied for the simultaneous detection and differentiation of the three genotypes of GCRV from virus-infected cell cultures and clinical tissue samples. Therefore, the newly established triple PCR is suitable for diagnosis, pathogen monitoring, and molecular epidemiological investigation of HDGC [72].

6.4.2 Real-Time PCR

Real-time PCR is a new and improved PCR method developed by Higuchi et al. in 1992 and has been widely used since then, including applications in pathogen identification [73]. One of the advantages of real-time PCR is its ability to quantify specific nucleic acids in complex mixtures accurately, even at very low concentrations of the starting material. Real-time PCR is also known as quantitative PCR or qPCR. The key feature of qPCR is that the amplification of DNA is observed in real time as PCR progresses by using a fluorescent reporter. The fluorescent reporter signal strength is directly proportional to the number of amplified DNA molecules. There are two qPCR detection methods. The first is based on sequence-specific probes, such as TaqMan probes and molecular beacons. The second is based on generic non-sequence-specific double-stranded DNA-binding dyes, such as the SYBR Green. qPCR is a very sensitive and powerful DNA analysis tool.

Conventional EM, conventional PCR, and multiplex RT-PCR can only perform qualitative, but not quantitative, detection. To conduct a quantitative analysis of

viruses and improve the sensitivity of detection methods, fluorescence-based qPCR technology has been developed. qPCR has gradually replaced conventional PCR as the standard method for virus detection, and it is currently widely used for virus detection. Moreover, it has been immensely used to detect aquareoviruses. GCRV is one of the most widely studied aquareoviruses. Many researchers have established qPCR detection methods for different isolated GCRVs. Zhou et al. amplified the GCRV VP6 gene fragment by RT-PCR, cloned it into a vector to construct the recombinant plasmid pEGFP-N1-VP6, which was used as a template for TaqMan probe qPCR amplification, and generated a standard curve. This method has high sensitivity and strong specificity, and it can be used for quantitative analysis, rapid diagnosis, and quantitative detection of GCRV [11]. In 2013, Liu et al. designed primers and probes based on the conserved sequence of the S7 segment of GCRV-HZ08 strain [74]. They used the recombinant plasmid PAVX1-S7, which contains the full-length S7 segment, as the standard, constructed a standard curve, and established a TaqMan probe qPCR detection technology for GCRV-HZ08 strain, which could detect grass carp hemorrhagic disease better than conventional PCR. In the same year, Liu et al. designed primers and probes based on the conserved sequence of the S7 segment of GCRV-JX-0901 strain, constructed a standard curve, and established a TaqMan qPCR detection technology for GCRV-JX-0901 strain. This method has been shown to have good sensitivity and specificity [64]. Yin et al. designed primers and probes based on the conserved sequence of the S6 segment of GCRV I species, constructed a standard plasmid containing the PVAX1-S6 fragment, and established a standard curve. This method has been found to be sensitive, efficient, specific, and reproducible, and is suitable for rapid detection and quantitative analysis of GCRV I species. Huang et al. designed primers and TaqMan probes based on the sequence of the conserved region of the GCRV II RNA-dependent RNA polymerase. After optimization of the reaction parameters, they established a fluorescence-based qPCR method for detecting GCRV II species. The minimum detection amount was determined to be 3 copies/µL viral nucleic acid, and the sensitivity was 100 times higher than that of PCR. A one-step duplex real-time RT-PCR (rRT-PCR) assay was developed for the simultaneous detection of GCRV I/II species. The minimum threshold of this method for detecting GCRV genotypes I and II is 10 copies, exhibiting sensitivity same as that of the single-target qPCR and higher than the sensitivity of conventional RT-PCR. In addition, the newly established rRT-PCR method also has high specificity. Therefore, this method is suitable for molecular epidemiological investigation and pathogen monitoring of GCRV I and GCRV II in grass carps [75].

qPCR has also been widely used for the detection of other aquareoviruses. In order to differentiate American grass carp reovirus from rhabdoviruses that can produce similar CPE in cells, a real-time PCR assay was developed for the identification of American grass carp reovirus in cell cultures and in fish tissues by Goodwin et al. [50]. Furthermore, a qPCR method has been designed based on the alignment of the nucleotide sequences of selected segments of fall chinook aquareovirus. Primers complementary to the conserved regions of VP2 were designed, and a positive control amplicon for use in developing a standard curve

was generated using the Qiagen One-Step RT-PCR kit [24]. In addition, qPCR has been developed for the detection of PRV [76], Atlantic halibut reovirus [77], and MCRV. The qPCR methods used to detect aquareoviruses are summarized in Table 6.3.

6.4.3   LAMP

LAMP uses 4–6 primers that recognize 6–8 distinct regions of the target DNA or RNA under isothermal conditions (60–65 °C). This amplification method was developed as an alternative to PCR, with a higher specificity. LAMP or reverse transcription LAMP (RT-LAMP) was defined depending on the reverse transcriptional response and LAMP reaction either in separate tubes or simultaneously in a single tube. This method can reduce the reaction time by the use of two additional primers. There are several methods for detecting positive LAMP reactions. Owing to turbidity, we can observe the results with a naked eye. Therefore, this technique can be applied in the field as a diagnostic method, and any semiskilled individual can interpret the results. The amplified product can be observed under illumination with a UV lamp or daylight using fluorescent intercalating dyes, such as SYBR Green I, calcein, ethidium bromide, picogreen, propidium iodide, and hydroxyl naphthol blue. The electrophoresed LAMP products show a ladder-like pattern on agarose gels after electrophoresis with ethidium bromide staining.

RT-LAMP has been popular in diagnostics in human and animal medicine because of its speed, robustness, and simplicity. This method is also widely used for the detection of aquatic animal pathogens, including aquareoviruses. Zhang [78] and Zeng [79] used a one-step RT-LAMP assay to detect GCRV I and II species, respectively. A set of six primers were designed based on the sequence of the S6 segment of GCRV-873 (GCRV I) or GCRV-HZ08 (GCRV II). The assay was optimized to amplify GCRV I/II RNA by incubation at 64 °C or 62.3 °C for less than 40 min, and a simple water bath or heating block is sufficient to maintain a constant temperature. Calcein fluorescent dye can help visualize RT-LAMP products in the form of ladder-like bands by agarose gel electrophoresis. The detection limit of the RT-LAMP assay has been determined to be 7 or 10 copies of viral templates, and the sensitivity is 100 times that of conventional RT-PCR. The GCRV RT-LAMP method has great potential for the detection of GCRV both in cell cultures and fish farms.

An RT-LAMP assay for the rapid and sensitive detection of SsRV has been developed and evaluated. The RT-LAMP reaction mix was optimized at a reaction temperature of 62 °C and duration of 60 min. The sensitivity of this assay has been determined to be 0.8 fg SsRV dsRNA, which is 1000-fold higher than that of a one-step RT-PCR. Furthermore, the RT-LAMP assay has higher sensitivity than a one-step RT-PCR, as it identified nine more positive cases than the one-step RT-PCR from 55 mud crabs suspected of having an SsRV infection. No cross-reactivity was found with the DNA/RNA of the other tested viruses and SsRV-

Table 6.3 Real-time PCR assay primer and probe sequences and cycling conditions for detection of aquareovirus

Virus isolate	Primer/ Probe Name	Sequence (5'-3')	qPCR Conditions
GCRV 104	GCRV-104F GCRV-104R GCRV-104probe	GGC TAC CCT CTT TGT CT-CGC CCT CCG CAG GTA CCA CT-GC AAC GCG CGC TCG TG-GCA CTA A	50 °C 10 min, 95 °C 5 min, 95 °C 10s, 64 °C 15s, 72 °C 20s (40 cycles)
GCRV HZ08	GCRV-P1-F GCRV-P2-R GCRV-probe	CCA GGA ATC AAT AGC AAT C CCT GAT ATA ATC GCT CTT C FAM-CGA TAA CCA CCA CTA CGG CTG-Eclipse	95 °C 30s; 95 °C 5s, 60 °C 34s (45 cycles)
GCRV JX-0901	GCRV-P1-F GCRV-P2-R GCRV-probe	CCT TCG TCT AAC ATG AAC GAA GGT GGG AAT TTG AAG FAM-ACC GCA CCT TAT CCG ATG AAC A-Eclipse	95 °C 30s; 95 °C 5s, 59 °C 35s (40 cycles)
GCRV-I	GCRV-F$_1$ GCRV-F$_2$ GCRV-probe	CTC TCT GGC AGA AAC ACT TAG AC CCC GAG TAG GTA AGA GTC TTA CG FAM-CCG CCA TGA CCA TGC TAA CAC CTG ACA-BHQ1	95 °C 30s; 95 °C 5s, 60 °C 34s (40 cycles)
GCRV-II	GCRV-F GCRV-R GCRV-probe	CCG GAT ACT CAC CA GGA TCA TTT ACG TCG TAT T FAM-CGC TGA TGT AAT TGA TGCC-Eclipse	95 °C 30s, 95 °C 5s,60 °C 34s (40 cycles)
GCRV-GD108 and GCRV-873	D108L2-F D108L2-R D873S4-F D873S4-R	GTT CCT GTC GTG GCT GGT AT GCC ATT TGC AGA ACT CCA TT CTC ATG CTG CTA ACG GTG TCT GCG ACT GTG GCA CCA TCA A	95 °C 30s, 95 °C 5s,60 °C 34s (40 cycles)
GCRV-II	GCRV-F GCRV-R GCRV-probe	CCT CTA TTC GCC ACT AT TTC GCT TGT GAT GTT G FAM-CAC TGA CGC CAA CGT AGG C-BHQ	42 °C 5 min, 95 °C 1 min, 95 °C 10s,60 °C 44s (40 cycles)
AGCRV	AGCRV-F AGCRV-R	GTT ACG TGG ACC TAC ATT CC CAG CAT GTA TGG GTG AGA TC	50 °C 10 min, 95 °C 5 min, 95 °C30s,61.5 °C30s, 72 °C 60s (45 cycles) 72 °C 5 min
AHRV	AHRV-7F AHRV-7R AHRV-7probe	CCC GTA TTA GCA GTT ATC CTGTAT C CCC CAT CCT GCA CAT TCA AG	50 °C 10 min, 95 °C 5 min, 95 °C30s,58 °C30s, 72 °C 60s (40 cycles) 72 °C 5 min

Table 6.3 (continued)

Virus isolate	Primer/ Probe Name	Sequence (5′-3′)	qPCR Conditions
		GAT CCC ATG ATC GGT GAG G	
AHRV	AHRV-S11-F AHRV S11-R AHRV-S11-probe	GCTTTATGCGACGCTCTCACT GCCCCATTGTGATCCAGTTT ATTTGTATATGCCCGG	50 °C 10 min, 95 °C 5 min, 95 °C 30s, 59 °C 30s, 72 °C 60s (40 cycles) 72 °C 5 min
FCRV	qVP2-F qVP2-R	GGC GTA ATC CAG CCG C GCT AGT GAA GGG ATC GTC	95 °C 30s, 95 °C 5s, 60 °C 34s (40 cycles)
TSRV	TSRV-10F TSRV-10R TSRV-Probe	GAT CGA ACC CGT CGT GTC TAA CGG TGC TCA GCT TGT CAC A FAM- CCC GAG CCA TCT GGG CGC -TAMRA	48 °C 30 min, 95 °C 10 min, 95 °C 15s, 60 °C 60s (45 cycles)

negative animals. In addition, this method can provide results more quickly than conventional RT-PCR, and the entire assay can be performed in 60 min [80]. There are various other aquareoviruses, for which RT-LAMP methods have been established. The available RT-LAMP methods for the detection of aquareoviruses are summarized in Table 6.4.

Four primers that bind to six different regions of the target DNA provide high specificity and sensitivity in RT-LAMP, and the high amplification efficiency of LAMP is attributed to the zero time loss during thermal changes owing to its isothermal reaction conditions, with DNA being amplified 10^9–10^{10} times in 60 min. However, this method carries higher chances of contamination compared with other methods. Moreover, its applicability in field conditions will remain limited because of the complex primer designing and restricted availability of reagents.

6.4.4   Other Nucleic Acid Amplification Technologies

NASBA is a primer-dependent technology specifically designed for the detection of RNA targets. It can be used for the continuous amplification of nucleic acids in a single reaction mixture containing three enzymes, RNAse H, T7 RNA polymerase, and avian myeloblastosis virus reverse transcriptase, at one temperature. This method has been successfully applied to the detection of influenza virus, HIV, RSV, SARS, etc. It has also been used for the detection of aquareoviruses, and a NASBA assay has been developed to detect GCRV II species. Primers used for amplification in an isothermal digoxigenin-labeling NASBA assay target the viral

Table 6.4 LAMP assay primer and probe sequences and cycling conditions for detection of aquareovirus

Virus isolate	Primer/ Probe Name	Sequence (5′-3′)	Reaction conditions
GCRV-HZ08	F3 B3 FIP BIP FLP BLP	TGTGCTAGGTAACGCCTCA CGAGCAGCTATCCACAGAT AGCCACTGTTGTAAGCTTGGCTTTTT- CCAGAGGAAATGCGTTCCG GTGCGCATGCACCATCCTCCTTTTGG- TTTCGATTGGGCCTTGTT TCAGCACATCTGCTGGTAAT TCCTTGGCCCGCTTGCA	62.3 °C 40 min, 80 °C 5 min
GCRV-873	GCRV-F3 GCRV-B3 GCRV-FIP (F1c+TTTT +F2) GCRV-BIP (B1c+TTTT +B2) GCRV-LF GCRV-LB	TCT CCA CTG GTT CTC TTC CA GAA CGT TTT CGG CGA CCG TGA GAT GGG CAC CAA GCA AAG- TTTT-TGC CCA ATA CCC CAG TGT T AGG TAT CAC TTG GCG AGA CCC A- TTTT-CTG GGG GTG GTT GAA TGG ACA ACG ATG TTG CGT GAT GC TTC ACT AGC TCC AGT CCC TG	64 °C 30 min, 80 °C 5 min
GCRV-104	GCRV-F3 GCRV-B3 GCRV-FIP GCRV-BIP	CAG TGT GAT CTC GAC TTC CG AGA CCA ACG CGT CAA TCG CGG TCG TCT GAC GTA CAC CGT TTT -TTG CCG GCA TAT GGG GTA A GTT GGG TCA ATT GGC TAC GGT TTT- TAG CAC CAT GGT ACT GTT CG	63 °C 60 min, 80 °C 2 min
GCRV-HZ08 and HZ2011	GCRV-F3 GCRV-B3 GCRV-FIP GCRV-BIP	TTG CGT ACA ATG CTG ATG GA GCA AAG CAC GGT TTG TGG TAG AGG GCA CAG CTG TAC TGT TTT-CGT CGC TGT CCT GCA ATC GCC CTA TCG CTC TCC TGG ACT TTT- TAC CAG GAA CGT CCG TGA AT	65 °C 1 h, 85 °C 5 min
GCRV-873	GCRV-F GCRV-B GCRV-FIP GCRV-BIP	GCT TCA ACA TGC TCC ACC T CAA CGA CTT CGC CCT TGT TGG GAT GAG GAA TGT GCC CAA G- TTTT-CTT TGA GCG CGA GAC AAT CA TCC AAT TTC TCC AAC CCC ACG C- TTTT-TGT CGT CTC ACG TAG CAG TA	65 °C 60 min
GCRV-I, II	GCRVI-F3 GCRVI-B3 GCRVI-FIP GCRVI– BIP GCRVI- Probe GCRVII-F3 GCRVII-B3 GCRVII- FIP	CCC GTA CTG CTA CGT GAG A GCT AGT CGC GGA ATC ATC C CGA CCT CCT CAG ACG TTT GGT T-GCG AAG TCG TTG ACG CTA Biotin- CGA CGC GAT CGT GTT AGT GTC G-TCT TGA GGC GAC GGG AAT FITC- CGT ACC AGC TAC CGT CAT GG ACT CGC ATG GAT GAA AGT CG CAA CGT AGG CAC TGA ACT CA Biotin- TAC GGT GAC CCG TCT GTT GC-CAG GAT CAG GTA TGG GAC CA	LAMP:63 ºC 40 min, LFD:5–10 min

(continued)

Table 6.4 (continued)

Virus isolate	Primer/ Probe Name	Sequence (5′-3′)	Reaction conditions
	GCRVII– BIP GCRVII- Probe	TGG AAA AAT CAG CAG GTG CCG T-CGT TCA CTG TAG AGC AGG TT FITC- CTC CGG ACG CCA TGT CTA GT	
GCRV LAMP- LFD	GCRV-F GCRV-B GCRV-FIP GCRV-BIP GCRV-LF GCRV-LB GCRV-HP	TGC GCG TAT GTG TGG TAC GAC AGA CGA GGC AGA GCT (BIO)-CGT TTG GCA GAT TGC GTT AGC A-CT ACC CTT CGA CGC CTC TA GAC TAA CGC TTC CTC TTC CGC C-CA AAA CTG TTC GTA GCC GAG AGT AGC AGT CAG GCG TTG G TCC ACC TCC AGT ACT GCT TC FAM-GTC TGC ACT GCA ACT GTT TC	LAMP:63 °C 40 min, LFD: 63 °C 5 min
SsRV	SsRV-F3	CTG ATA TAG AAT TGG CTA TGC G	62 °C 1 h 85 °C 5 min 63 °C for 1 h Or 42 °C for 30 min followed by 60 min at 63 °C
	SsRV-B3	CTG TTG CCA TGC TGT AGT	
	SsRV-FIP	ATG CGC TCC AAA ACG TTT TCT TTT -TGA TGG CTT CCT TGA TTC C	
	SsRV-BIP	GAA TCC TGC GGA TCT CGC TAT TTT -GAT ATC TCC AAG TGC TGT TTG	

RNA genome S6 segment, resulting in digoxigenin-labeled RNA amplicons. Specific biotinylated DNA probes are hybridized to amplicons, followed by detection using horseradish peroxidase and a microplate reader. When testing GCRV II species and non-target-specific viruses with this new method, the diagnostic sensitivity and specificity can reach 100%, and GCRV can be detected at 14 copies/μL within 5 h. It has been shown that NASBA is a rapid, effective, and sensitive assay for GCRV detection in grass carp aquaculture [81].

Another simple, rapid, sensitive, and cost-effective isothermal DNA amplification technique is RPA [82]. A real-time reverse transcription RPA assay is based on the detection of the VP55 gene, which encodes the outer fiber protein of the virus, has been developed to detect GCRV-104 (GCRV III). The assay is completed by using a portable ESE-Quant Tube scanner—having a dimension of 17.4×18.8 cm, weighing about 1 kg, and equipped with temperature settings—for amplifying the DNA isothermally and spectral devices for detecting the amplified products by fluorescence. The assay takes about 10 min without any cross-reactions with other aquareoviruses under optimal conditions (37 °C). In resource-limited diagnostic laboratories, the reverse transcription RPA assay is a useful method for simple, rapid, and reliable detection of GCRV III strains [83].

6.4.5   Nucleic Acid Hybridization

Nucleic acid hybridization refers to the process in which complementary nucleotide sequences (DNA-DNA, DNA-RNA, or RNA-RNA) are paired with Watson–Crick bases to form noncovalent bonds, thereby producing stable homologous or heterologous double-stranded molecules, which require the design and synthesis of a gene-specific probe. Next, the specific probe is used to pair with the target sequence to form a hybrid strand. This hybridization process can be detected with the help of enzymes, fluorescent reporters, radioisotopes, or chemiluminescence agents, which are labeled onto the probe. Nucleic acid hybridization has proven to be a powerful technique in many fields of life science, including the diagnosis of diseases.

Nucleic acid hybridization has also been used for the diagnosis of diseases caused by aquareoviruses. A gene-specific probe was designed to detect and identify TRV by Lupiani et al. [84]. The whole genome of TRV was cloned into a plasmid and used for detection of TRV from virus-infected CHSE-214 cells. Using this method, PRV can be detected in CHSE-214 cells at 72 h post-infection, which is 2–3 days earlier than the appearance of a CPE.

A nucleic acid hybridization assay has been developed to detect SBRV RNA in virus-infected cells and tissue samples. The large, medium, and small RNA segments of SBRV were cloned into a plasmid. Three different cDNA clones were obtained and used to hybridize with a membrane containing total genomic RNA of SBRV, Atlantic salmon reovirus HBR, SRV, Atlantic salmon reovirus ASV, and TRV. The three cDNA clones hybridized with RNA from the four aquareoviruses belonging to the *Aquareovirus A* group (Atlantic salmon reovirus HBR, Atlantic salmon reovirus ASV, SRV, and SBRV) but not with the RNA of viruses belonging to the *Aquareovirus B* group (TRV). Furthermore, the SBRV clone did not react with RNA from cells infected with infectious pancreatic necrosis virus or infectious hematopoietic necrosis virus, or uninfected cells. The cDNA clones could detect SBRV RNA from the virus-infected CHSE-214 cells as early as 2 days post-infection, and the minimum level of detection was 5 ng of total SBRV RNA. The cDNA of SBRV has also been used as a probe to detect SBRV in artificially infected rainbow trout fingerlings. Moreover, nucleic acid hybridization has also been developed for the detection of PRV, CSRV, and other aquareoviruses [85].

6.5   Immunological Methods

Immunological methods are often used to identify pathogens based on the high specificity of the antigen–antibody reaction. Various immunological methods have been developed and widely used in human medicine and in terrestrial animal disease diagnosis. To diagnose previous exposure to a disease, immunological assays detecting circulating antibodies specific to pathogenic microbes have been used for centuries in mammals. However, the situation is slightly different for aquatic

animals, and it is not popular to use serological tests to define infection status in aquaculture. As immunoglobulin M (IgM) is the dominating isotype in the serum of fish and no isotype switching is evident, the presence of IgM does not necessarily imply recent infection. Due to the lower specificity of fish IgM than mammalian immunoglobulin G, the possibility of detecting low-affinity cross-reactive antibodies in uninfected fish increases, which may lead to false-positive results. Therefore, many immunological methods, as a complementary method to the traditional and nucleic acid-based methods, have been developed for pathogen detection and disease diagnosis in aquaculture.

Currently, immunological techniques for the detection and identification of aquareoviruses include neutralization test, enzyme-linked immunosorbent assay (ELISA), fluorescent antibody technique, western blotting, and immunohistochemistry [67]. In particular, ELISA [86, 87], discounter immunoelectrophoresis [54], staphylococcal protein A coagglutination test [88], and indirect immunofluorescence assay [51] have been developed for detecting GCRV, and antigenic serodiagnosis, using an antibody against grass carp IgM, based on western blotting has been used to detect GCRV [89, 90]. Furthermore, a bead-based assay for detecting plasma IgM directed against PRV has been developed. In this assay, recombinant PRV proteins are coated on beads to detect the structural outer capsid protein $\mu 1$ and the nonstructural protein μNS [91]. Moreover, researchers have developed an immunohistochemistry assay using an antibody targeting the PRV $\sigma 1$ protein to detect PRV [92, 93].

6.6 Conclusions and Future Considerations

The conventional histocytology method using a microscope to observe tissue morphological structures, pathological changes, and morphological characteristics of the virus for pathogen diagnosis is very intuitive and effective; however, there are some problems, such as complex operation and sample preparation, excess time consumption, and requirement of highly skilled operators. Cell culture technology forms a new method for the diagnosis of viruses and has gradually become a standard method for virus identification, making it possible to understand the pathogenic mechanisms and morphological changes. At the same time, it complements immunological methods. However, cell culture technology has the same problems as the conventional histocytological analysis, such as excess time consumption and the requirement of highly skilled labor. With the invention of molecular biological methods, such as PCR, the detection of viruses has greatly improved. Molecular biological methods have the advantages of high speed, sensitivity, and specificity; however, they need to rely on specific equipment, which limits their popularization and spontaneous application in the field. Currently, isothermal amplification technology has become one of the most popular technologies compared with conventional PCR. It does not rely on a temperature controller, and greatly shortens the reaction time. In aquareovirus research, LAMP and RPA are widely used. However,

primer designing is too complex in these methods, and they can easily produce false-positive results. Immunological methods have been widely used in the research of aquareoviruses, but only a few have been used to diagnose viral diseases. To develop antibody preparation-based technologies, an increasing number of effective commercial antibodies are prepared. Therefore, immunological technologies are vital detection methods for aquareoviruses.

In conclusion, under the premise of ensuring the benefits of high sensitivity and specificity, convenient laboratory use, and even operation and diagnosis in farms, thereby achieving riddance from large laboratory equipment, developing a highly efficient, rapid, highly sensitive, strongly specific, inexpensive, and easy to operate reagent kit should be the goal in aquareovirus detection.

Among all the presented aquareovirus diagnostic methods, which are widely used in laboratories, the conventional methods are considered "gold standard." However, most of these methods require large equipment or instruments, and excessive time. Additionally, there are certain technical requirements, which nonetheless are compensated by their high sensitivities and the production of the most reliable results. Therefore, the need for improvement in these "gold standard" methods has increased significantly. Despite a low and variable sensitivity, rapid and simple diagnostic tests are the mainstay for improved aquareovirus diagnostics, especially when diagnosis occurs in the field. Rapid and simple diagnostic tests reduce laboratory work and shift the focus on specimens designed for culture or other time-consuming methods. Furthermore, early diagnosis is greatly beneficial to control viral diseases, and therefore, more rapid and accurate methods are urgently needed in the aquaculture industry to control aquareovirus outbreaks and dissemination.

References

1. Lupiani B, Subramanian K, Samal SK (1995) Aquareoviruses. Annu Rev Fish Dis 5:175–208
2. Banerjee A (1980) 5′-terminal cap structure in eucaryotic messenger ribonucleic acids. Microbiol Rev 44(2):175–205
3. Mertens P (2004) The dsRNA viruses. Virus Res 101(1):3–13
4. Attoui H, Fang Q, Jaafar FM, Cantaloube J, Biagini P, de Micco P, de Lamballerie X (2002) Common evolutionary origin of aquareoviruses and orthoreoviruses revealed by genome characterization of golden shiner reovirus, grass carp reovirus, striped bass reovirus and golden ide reovirus (genus Aquareovirus, family Reoviridae). J Gen Virol 83(8):1941–1951
5. Lupiani B, Dopazo CP, Ledo A, Fouz B, Barja JL, Hetrick EM, Toranzo AE (1989) New syndrome of mixed bacterial and viral etiology in cultured turbot *Scophthalmus maximus*. J Aquat Anim Health 1(3):197–204
6. Winton JR, Lannan CN, Fryer JL, Kimura T (1981) Isolation of a new reovirus from chum salmon in Japan. Fish Pathol 15(3–4):155–162
7. Jing HL, Zhang LF, Fang ZZ, Xu LP, Zhang M, Wang N, Jiang YL, Lin XM (2014) Detection of grass carp reovirus (GCRV) with monoclonal antibodies. Arch Virol 159(4):649–655
8. Palacios G, Løvoll M, Tengs T, Hornig M, Hutchison S, Hui J, Kongtorp RT, Savji N, Bussetti AV, Solovyov A, Kristoffersen AB, Celone C, Street C, Trifonov V, Hirschberg DL, Rabadan R, Egholm M, Rimstad E, Lipkin WI (2010) Heart and skeletal muscle inflammation of farmed salmon is associated with infection with a novel reovirus. PLoS One 5(7):e11487

9. Rimstad E, Wessel Ø (2015) New species in the genus Orthoreovirus. http://talk.ictvonline.org/files/proposals/animal_dsrna_and_ssrna-_viruses/m/animal_rna_minus_ec_approved/5564.aspx

10. Wessel Ø, Braaen S, Alarcon M, Haatveit H, Roos N, Markussen T, Tengs T, Dahle MK, Rimstad E (2017) Infection with purified piscine orthoreovirus demonstrates a causal relationship with heart and skeletal muscle inflammation in Atlantic salmon. PLoS One 12(8):e0183781

11. Zhang YB, Gui JF (2004) Identification of two novel interferon stimulated genes from cultured CAB cells induced by UV inactivated grass carp hemorrhage virus. Dis Aquat Org 60(9):1–9

12. Zhou Y, Zeng LB, Fan YD, Xu J, Ma J, Luo XS (2011) Establishment of a TaqMan real-time assay for detecting the grass carp reovirus. J Fish China 35(5):774–779

13. Deng XX, Lü L, Ou YJ, Su HJ, Li G, Guo ZX, Zhang R, Zhang PR, Chen YG, He JG, Wang SP (2012) Sequence analysis of 12 genome segments of mud crab reovirus (MCRV). Virology 422(2):185–194

14. Chen JG, Xiong J, Yang JF, Mao ZJ, Chen XX (2011) Nucleotide sequences of four RNA segments of a reovirus isolated from the mud crab Scylla serrate provide evidence that this virus belongs to a new genus in the family Reoviridae. Arch Virol 156(3):523–528

15. Goodwin AE, Merry GE, Attoui H (2010) Detection and prevalence of the nonsyncytial American grass carp reovirus Aquareovirus G by quantitative reverse transcriptase polymerase chain reaction. J Aquat Anim Health 22(1):8–13

16. Min SQ, Hong SW, Cai YQ (1986) The preparation and application of several antisera against fish reovirus (FRV). J Fish China 10(4):383–387. (in Chinese with English abstract)

17. Racine T, Hurst T, Barry C, Shou JY, Kibenge F, Duncan R (2009) Aquareovirus effects syncytiogenesis by using a novel member of the FAST protein family translated from a noncanonical translation start site. J Virol 83(11):5951–5925

18. Rangel AAC, Rockemann DD, Hetrick FM, Samal SK (1999) Identification of grass carp haemorrhage virus as a new genogroup of aquareovirus. J Gen Virol 80(Pt 9):2399–2402

19. Seng EK, Fang Q, Lam TJ, Sin YM (2004) Development of a rapid, sensitive and specific diagnostic assay for fish Aquareovirus based of RT-PCR. J Virol Methods 118(2):111–122

20. Zhang S, Bonami JR (2012) Isolation and partial characterization of a new reovirus from the Chinese mitten crab, Eriocheir sinensis H Milne Edwards. J Fish Dis 35(10):733–739

21. Attoui H, Mertens PPC, Becnel J, Belaganahalli S, Bergoin M, Brussaard CP et al (2012) Family Reoviridae. In: King AMQ, Adams MJ, Carstens EB, Lefkowitz EJ (eds) Virus taxonomy: ninth report of the international committee on taxonomy of viruses. Academic Press, San Diego, pp 541–637

22. Fan YD, Rao SJ, Zeng LD, Ma J, Zhou Y, Xu J, Zhang H (2013) Identification and genomic characterization of a novel fish reovirus, Hubei grass carp disease reovirus, isolated in 2009 in China. J Gen Virol 94(10):2266–2277

23. Jiang YL (2009) Hemorrhagic disease of grass carp: status of outbreaks, diagnosis, surveillance, and research. Israeli J Aquacultu 61(3):188–197

24. Lupiani B, Subramanian K, Hetrick EM, Samal SK (1993) A genetic probe for the identification of the turbot aquareovirus in infected cell cultures. Dis Aquat Org 15:187–192

25. Pei C, Ke F, Chen ZY, Zhang QY (2014) Complete genome sequence and comparative analysis of grass carp reovirus strain 109 (GCReV-109) with other grass carp reovirus strains reveals no significant correlation with regional distribution. Arch Virol 159(9):2435–2440

26. Xu J, Zeng LB, Luo XS, Wang Y, Fan YD, Gong SY (2013) Reovirus infection emerged in cultured channel catfish, Ictalurus punctatus, in China. Aquaculture 372:39–44

27. Zainathan SC, Carlile G, Carson J, McColl KA, Crane MJ, Williams LM, Hoad J, Moody NJG, Aiken HM, Browning GF, Nowak BF (2015) Development and application of molecular methods (PCR) for detection of Tasmanian Atlantic salmon reovirus. J Fish Dis 38(8):739–754

28. Zeng WW, Wang Q, Wang YY, Xu DH, Wu SQ (2013) A one-step molecular biology method for simple and rapid detection of grass crap (Ctenopharyngodon idella) reovirus (GCRV) HZ08 strain. J Fish Biol 82(5):1545–1555

29. Zhang QL, Yan Y, Shen JY, Hao GJ, Shi CY, Wang QT, Liu H, Huang J (2013) Development of a reverse transcription loop-mediated isothermal amplification assay for rapid detection of grass carp reovirus. J Virol Methods 187(2):384–389

30. Attoui H, Mohd Jaafar F, Belhouchet M, de Micco P, de Lamballerie X, Brussaard CP (2006) *Micromonas pusilla* reovirus: a new member of the family Reoviridae assigned to a novel proposed genus (Mimoreovirus). J Gen Virol 87(5):1375–1383

31. Reinisch KM (2002) The dsRNA viridae and their catalytic capsids. Nat Struct Biol 9(10):714–716

32. Samal SK, Dopazo CP, McPhillips TH, Baya A, Mohanty SB, Hetrick FM (1990) Molecular characterization of rotaviruslike virus isolated from striped bass (*Morone saxatilis*). J Virol 64 (11):5235–5240

33. Ke F, He LB, Pei C, Zhang QY (2011) Turbot reovirus (SMReV) genome encoding a FAST protein with a non-AUG start site. BMC Genomics 12:323

34. DeWitte-Orr SJ, Bols NC (2007) Cytopathic effects of chum salmon reovirus to salmonid epithelial, fibroblast and macrophage cell lines. Virus Res 126(1–2):159–171

35. Amend DF, McDowell T, Hedrick RP (1984) Characteristics of a previously unidentified virus from channel catfish (*Ictalurus punctatus*). Canadian J Fish Aquat Sci 41(5):807–811

36. Plumb JA, Bowser PR, Grizzle JM, Mitchell AJ (1979) Fish viruses: a double-stranded RNA virus icosahedral virus from a North American cyprinid. J Fish Res Board Canada 36(11):1390–1394

37. Huang HW, Huang CH, Wen CM (2019) Complete genome sequence and phylogenetic analysis of a novel aquareovirus isolated from a diseased marbled eel (*Anguilla marmorata*). Arch Virol 164(10):2585–2592

38. Baya A, Toranzo AE, Nuiiez S, Barja JL, Hetrick EM (1990) Association of a Moraxella sp. and reo-like virus with mortalities of striped bass, *Morone saxatilis*. In: Perkins EO, Cheng TC (eds) Pathology in marine science. Academic Press, New York, pp 91–99

39. Walton A, Montanie H, Arcier JM, Smith VJ, Bonami JR (1999) Construction of a gene probe for detection of P virus (Reoviridae) in a marine decapod. J Virol Methods 81(1–2):183–192

40. Hsu YL, Chen BS, Wu JL (1989) Characteristics of a new reo-like virus isolated from landlocked salmon (*Oncorhynchus masou* Brevoort). Fish Pathol 24(1):37–45

41. Cusack R, Groman DG, MacKinnon AM, Kibenge FSB, Wadowska D, Brown N (2001) Pathology associated with an aquareovirus in captive juvenile Atlantic halibut *Hippoglossus hippoglossus* L and an experimental treatment strategy for a concurrent bacterial infection. Dis Aquat Org 44:7–16

42. Mikalsen AB, Haugland Ø, Rode M, Solbakk IT, Evensen Ø (2012) Atlantic salmon reovirus infection causes a CD8 T cell myocarditis in Atlantic salmon (*Salmo salar* L.). PLoS One 7(6): e37269

43. Samal SK, McPhillips TH, Dinan D, Rockemann DD (1998) Lack of restriction of growth for aquareovirus in mammalian cells. Arch Virol 143(3):571–579

44. Schachner O, Soliman H, Straif M, Schilcher F, El-Matbouli M (2014) Isolation and characterization of a novel reovirus from white bream *Blicca bjoerkna*. Dis Aquat Org 112(2):131–138

45. Vamer PW, Lewis DH (1991) Characterization of a virus associated with head and lateral line erosion syndrome in marine angelfish. J Aquat Anim Health 3(3):198–205

46. Wu ML, Cui K, Li HY, He JX, Chen HL, Jiang YY, Ren J (2016) Genomic characterization and evolution analysis of a mutant reovirus isolated from grass carp in Anhui. Arch Virol 161 (5):1385–1387

47. Winton JR, Lannan CN, Fryer JL, Hedrick RP, Meyers TR, Plumb JA, Yamamoto T (1987) Morphological and biochemical properties of four members of a novel group of reoviruses isolated from aquatic animals. J Gen Virol 68(Pt 2):353–364

48. Attoui H, Mertens PPC, Becnel J, Belaganahalli S and others (2011) Family Reoviridae. In: King AMQ, Adams MJ, Carstens EB, Lefkowitz EJ (eds) Virus taxonomy: classification and

nomenclature of viruses. Ninth report of the International Committee on Taxonomy of Viruses. Elsevier Academic Press, London, pp 541–637

49. Weng SP, Guo ZX, Sun JJ, Chan SM, He JG (2007) A reovirus disease in cultured mud crab, *Scylla serrata*, in southern China. J Fish Dis 30(3):133–139

50. Finstad ØW, Falk K, Løvoll M, Evensen Ø, Rimstad E (2012) Immunohistochemical detection of piscine reovirus (PRV) in hearts of Atlantic salmon coincide with the course of heart and skeletal muscle inflammation (HSMI). Vet Res 43(1):27

51. Wang Q, Zeng WW, Yin L, Wang YY, Liu C, Li YY, Zheng SC, Shi CB (2016) Comparative study on physical–chemical and biological characteristics of grass carp Reovirus from different genotypes. J World Aquac Soc 47(6):862–872

52. Chi SC, Hu WW, Lo BJ (1999) Establishment and characterization of a continuous cell line (GF-1) derived from grouper, *Epinephelus coioides* (Hamilton): a cell line susceptible to grouper nervous necrosis virus (GNNV). J Fish Dis 22(3):173–182

53. Kibenge MJT, Iwamoto T, Wang YW, Morton A, Godoy MG, Kibenge FSB (2013) Whole-genome analysis of piscine reovirus (PRV) shows PRV represents a new genus in family Reoviridae and its genome segment S1 sequences group it into two separate sub-genotypes. Virol J 10:230

54. Makhsous N, Jensen NL, Haman KH, Batts WN, Jerome KR, Winton JR, Greninger AL (2017) Isolation and characterization of the fall Chinook aquareovirus. Virol J 14(1):1–7

55. Winton JR, Arakawa CK, Lannan CN, Fryer JL (1989) Isolation of a reovirus from coho salmon (Oncorhynchus kisufch) in Oregon, USA. In: Ahne W, Kurstak E (eds) Viruses of lower vertebrates. Springer, Berlin, pp 257–269

56. Pao HY, Wu CY, Wen CM (2019) Persistent development of adomavirus and aquareovirus in a novel cell line from marbled eel with petechial skin haemorrhage. J Fish Dis 42(3):345–355

57. Ahne W, Kolbl O (1987) Occurrence of reoviruses in European cyprinid fishes (Tinea tinea Lin, *Leuciscus cephalus* Lin.). J Appl Ichthyol 3(3):139–141

58. Higuchi R, Dollinger G, Walsh PS, Griffith R (1992) Simultaneous amplification and detection of specific DNA sequences. Biotechnology 10(4):413–417

59. Liu BQ, Zeng WW, Wang Q, Zhang LS, Wang YY, Shi CB, Wu SQ (2012) Development of a fluorescent quantitative polymerase chain reaction technique for detection of grass carp reovirus HZ08 strain. J Fish Sci China 19(2):329–335

60. He YX, Jiang YS, Lu LQ (2013) Serodiagnosis of grass carp reovirus infection in grass carp *Ctenopharyngodon idella* by a novel Western blot technique. J Virol Methods 194(1–2):14–20

61. Prediger EA (2001) Detection and quantitation of mRNAs using ribonuclease protection assays. Methods Mol Biol 160:495–505

62. Rottman JB (2002) The ribonuclease protection assay: a powerful tool for the veterinary pathologist. Vet Pathol 39(1):2–9

63. Zhang C, Wang Q, Shi CB, Zeng WW, Liu YK, Wu SQ (2010) Molecular analysis of grass carp reovirus HZ08 genome segments 1–3 and 5–6. Virus Genes 41(1):102–104

64. Li J, Wang TH, Yi YL, Liu HQ, Lu RH, Chen HX (1997) A detection method for grass carp hemorrhagic virus (GCRV) based on a reverse transcription-polymerase chain reaction. Dis Aquat Org 29(1):7–12

65. Kongtorp RT, Taksdal T (2009) Studies with experimental transmission of heart and skeletal muscle inflammation in Atlantic salmon, *Salmo salar* L. J Fish Dis 32(3):253–262

66. Fan YD, Ma J, Zhou Y, Jiang N, Liu WZ, Zeng LB (2018) Establishment and application of a universal RT-PCR assay for detection of different genotype grass carp reovirus. Freshw Fish 48 (6):9–16

67. Shao JZ, Xiang LX, Li YN, Mao SJ (1996) Study of the detection of hemorrhagic virus by enzyme linked immunosorbent assay on nitrocellulose membrane(dot-ELISA). J Fish China 20 (1):6–12

68. Gui JF, Zhu ZY (2012) Molecular basis and genetic improvement of economically important traits in aquaculture animals. Chin Sci Bull 57(15):1751–1760

69. Yang GZ, Luo YZ, Ye XP (1991) Rapid serological diagnosis of grass carp hemorrhagic virus by coagglutination test using staphylococci protein A. J Fish China 15(1):27–33
70. Zhang LL, Luo Q, Fang Q, Wang YP (2010) An improved RT-PCR assay for rapid and sensitive detection of grass carp reovirus. J Virol Method 169(1):28–33
71. Zainathan SC, Carson J, Crane MS, Williams LM, Hoad J, Moody NJG, Gudkovs N, Leis A, Crameri S, Hyatt AD, Young J, Nowak BF (2017) Preliminary characterization of Tasmanian aquareovirus (TSRV) isolates. Arch Virol 162(3):625–634
72. Zhang D, Yang K, Su YL, Feng J, Guo ZX (2013) A duplex nested-PCR assay for detection of mud crab reovirus and mud crab dicistrovirus-1. J Fish Sci China 20(4):808–815
73. Hedrick RP, Rosemark R, Aronstein D, Winton JR, Mcdowell T, Amend DF (1984) Characteristics of a new reovirus from channel catfish (*Ictalurus punctatus*). J Gen Virol 65(9):1527–1534
74. Teige LH, Lund M, Haatveit HM, Røsæg MV, Wessel Ø, Dahle MK, Storset AK (2017) A bead based multiplex immunoassay detects piscine orthoreovirus specific antibodies in Atlantic salmon (*Salmo salar*). Fish Shellfish Immunol 63:491–499
75. Zeng WW, Wang YY, Guo YM, Sven MB, Yin JY, Li YY, Ren Y, Shi CB, Wang Q (2018) Development of a VP38 recombinant protein based indirect ELISA for detection of antibodies against grass crap reovirus genotype II. J Fish Dis 41(12):1811–1819
76. Wessel Ø, Olsen CM, Rimstad E, Dahle MK (2015) Piscine orthoreovirus (PRV) replicates in Atlantic salmon (*Salmo salar* L.) erythrocytes ex vivo. Vet Res 46:26
77. Blindheim S, Nylund A, Watanabe K, Plarre H, Erstad B, Nylund S (2015) A new aquareovirus causing high mortality in farmed Atlantic halibut fry in Norway. Arch Virol 160(1):91–102
78. Zhang QY, Ruan HM, Li ZQ, Zhang J, Gui JF (2003) Detection of grass carp hemorrhage virus (GCHV) from Vietnam and comparison with GCHV strain from China. Chin High Technol Lett 9(2):7–13
79. Zeng WW, Wang YY, Liang HR, Liu C, Song XJ, Wu SQ, Wang Q (2014) A one-step duplex rRT-PCR assay for the simultaneous detection of grass carp reovirus genotypes I and II. J Virol Methods 210:32–35
80. Chen JG, Xiong J, Cui BJ, Yang JF, Mao ZJ, Li WC, Chen XX, Zheng XJ (2011) Rapid and sensitive detection of mud crab *Scylla serrata* reovirus by a reverse transcription loop-mediated isothermal amplification assay. J Virol Methods 178(1–2):153–160
81. Zeng WW, Wang Q, Wang YY, Shi CB, Wu SQ (2013) Establishment of multiplex PCR for detection of grass carp reovirus and its application. J Fish Sci China 20(2):419–426
82. Piepenburg O, Williams CH, Stemple DL, Armes NA (2006) DNA detection using recombination proteins. PLoS Biol 4(7):e204
83. Wang Q, Xie HL, Zeng WW, Wang LC, Liu C, Wu JX, Wang YY, Li YY, Bergmann SM (2018) Development of indirect immunofluorescence assay for TCID$_{50}$ measurement of grass carp reovirus genotype II without cytopathic effect onto cells. Microb Pathog 114:68–74
84. Liu BQ, Zeng WW, Wang Q, Zhang LS, Wang YY, Shi CB, Li H, Wu SQ (2012) Development of fluorescent quantitative polymerase chain reaction for detection of crass crap reovirus JX-0901 strain and its application on virus quantitative analysis. Guangdong Agric Sci 11:139–143
85. Wang H, Zhou ST, Wen JX, Sun M, Jiang YS, Lu LQ, Xie J (2020) A real-time reverse-transcription isothermal recombinase polymerase amplification assay for the rapid detection of genotype III grass carp (*Ctenopharyngodon idella*) reovirus. J Virol Methods 277:113802
86. Blindheim S, Nylund A, Watanabe K, Plarre H, Erstad B, Nylund S (2015) A new aquareovirus causing high mortality in farmed Atlantic halibut fry in Norway. Arch Virol 160(1):91–102
87. Zeng WW, Yao W, Wang Q, Wang YY, Li YY, Sven MB, Ren Y, Shi CB, Song XJ, Huang QW, Zheng SC (2017) Molecular detection of genotype II grass carp reovirus based on nucleic acid sequence-based amplification combined with enzyme-linked immunosorbent assay (NASBA-ELISA). J Virol Methods 243:92–97
88. Ye X, Tian Y, Deng GC, Chi YY, Jiang XY (2012) Complete genomic sequence of a reovirus isolated from grass carp in China. Virus Res 163(1):275–283

89. Guo ZX, Weng SP, Li G, Chanc SM, He JG (2008) Development of an RT-PCR detection method for mud crab reovirus. J Virol Methods 151(2):237–241
90. Jaafar FM, Goodwin AE, Belhouchet M, Merry G, Fang Q, Cantaloube JF, Biagini P, Micco P, Mertens PPC, Attoui H (2008) Complete characterisation of the American grass carp reovirus genome (genus Aquareovirus: family Reoviridae) reveals an evolutionary link between aquareoviruses and coltiviruses. Virology 373(2):310–321
91. King AM et al (2012) Virus taxonomy: classification and nomenclature of viruses. Ninth report of the international committee on taxonomy of viruses, vol 9. Elsevier, Amsterdam
92. Bjørgen H, Wessel Ø, Fjelldal PG, Hansen T, Sveier H, Sæbø HR, Koppang EO (2015) Piscine orthoreovirus (PRV) in red and melanised foci in white muscle of Atlantic salmon (*Salmo salar*). Vet Res 46(1):89
93. Fauquet CM, Mayo MA, Maniloff J, Desselberger U, Ball LA (2005) Virus taxonomy: VIIIth report of the International Committee on Taxonomy of Viruses. Elsevier Academic Press, London, pp 511–516

Chapter 7
Prevention and Control of Grass Carp Hemorrhagic Disease

Check for updates

Qing Wang, Jiyuan Yin, Yingying Wang, Weiwei Zeng, and Yingying Li

Abstract Grass carp hemorrhagic disease (GCHD) is induced by the grass carp reovirus (GCRV), which reportedly causes heavy losses in grass carp production. To date, there is no specific treatment for GCHD, and most of the current treatments, such as those involving vitamins, traditional Chinese herbs, or extracts, offer only palliative care. However, vaccination is considered the most effective measure to protect grass carp from GCRV infection. Inactivated vaccines have earlier been used to prevent GCRV infection. This inactivated vaccine, which is prepared from organs of sick fish or infected cell cultures, has been shown to be mainly effective in the region from where it has been isolated and has no effect in other regions. Thereafter, a GCRV-attenuated vaccine, which is developed by attenuating the strain through serial passages in cell culture, has obtained approval and is commercially available. However, the major disadvantage of this live-attenuated vaccine is the possible safety concern in natural conditions, as it may undergo unpredictable changes in the environment. Recently, some subunit and DNA vaccines have been developed in laboratories. Numerous GCRV strains have been isolated and sequenced, and the significant differences between the new isolates and the previous representative strains have led to a reduction in the potential of the vaccine strain or are responsible for no protection against infections with the epidemic strain. Therefore, the prevention and control of GCHD, which are based on the epidemiology, should be studied.

Keywords GCHD · GCRV · Prevention · Control · Vaccination

Abbreviations

BG   Bacterial ghost
GCHD   Grass carp hemorrhagic disease

Q. Wang (✉) · J. Yin · Y. Wang · W. Zeng · Y. Li
Pearl River Fisheries Research Institute, Chinese Academy of Fishery Sciences,
Guangzhou, People's Republic of China
e-mail: wangqing@prfri.ac.cn

GCHV   Grass carp hemorrhagic virus
GCRV   Grass carp reovirus
RPS   Relative percent survival
rVP4   Recombinant VP4 protein
SWCNT   Single-walled carbon nanotube
VLP   Virus-like particle

7.1   Introduction

To date, the following four vaccine types have been investigated for the control of the grass carp reovirus (GCRV): (i) inactivated vaccine, (ii) live-attenuated vaccine, (iii) recombinant subunit vaccine, and (iv) DNA vaccine (Table 7.1 and 7.2). This chapter reviews the prevention and control measures for grass carp hemorrhagic disease (GCHD) in clinical and laboratory settings.

7.2   Inactivated Vaccines

7.2.1   *Inactivated GCRV Tissue Culture Vaccine*

The history of fish vaccine development in China is closely related to the development of the GCHD vaccine. Fish vaccine research dates back to the 1960s and begins with the preparation of inactivated vaccines using tissue homogenates from diseased grass carp, which is termed as an inactivated GCRV tissue culture vaccine [31]. In as early as 1953, Ni et al. speculated that the grass carp disease showing typical hemorrhage symptoms might be caused by a type of fish virus. However, research

Table 7.1 Information of the Vaccines with certificate and license

Name of vaccine	Department	Strain	Vaccination route	The new drug certificate/ issued year	Production license/ issued year
Inactivated cell culture vaccine against grass carp hemorrhagic disease	Zhejiang Institute of Freshwater Fisheries	ZV-8909	Injection	1992	N/A[a]
Live vaccine against grass carp hemorrhagic disease	Pearl River Fisheries Research Institute, Chinese Academy of Aquatic Sciences	GCHV-892	Injection	2010	(2011) 190986021; (2014) 190026031

[a]N/A, not applicable, the production license for inactivated cell culture vaccine was not obtained

Table 7.2 Information of the vaccines in research

Author/ years	Department	Strain	Genotype	Type of vaccine	Vaccination route	Fish weight	RPS	References
Yang XL / 1986	Yangtze River Fisheries Research Institute, Chinese Academy of Aquatic Sciences	FR-836-w	UN	Inactivated vaccine	Intraperitoneal injection; 0.3 ml/fish	UN	65%	[37]
Yang XL / 1989	Yangtze River Fisheries Research Institute, Chinese Academy of Aquatic Sciences	FR-854	UN	Inactivated vaccine	UN	UN	88.9 ± 12%	[38]
Xu SY / 1998	Pearl River Fisheries Research Institute, Chinese Academy of Aquatic Sciences	GCHV-892	UN	Attenuated vaccine	Injection; 0.2 ml/fish	UN	85%	[34]
Chen DY / 2006	Liantang Fish Disease Prevention and Treatment Center in Nanchang, Jiangxi Province	UN	UN	Inactivated tissue vaccine	Injection; 0.25 mL/fish	UN	98.03%	[4]
Li GZ / 2007	Fujian provincial Shanghang Fishery Technology Promotion Station	UN	UN	Inactivated tissue vaccine	Dorsal muscle injection; 0.25 mL/fish	UN	6.5%	[16]
He YX / 2011	Shanghai Ocean University	GCRV-873	GCRV-I	Recombinant subunit vaccine	UN	UN	UN	[12]
Shao L / 2011	Wuhan Institute of Virology, Chinese Academy of Sciences	GCRV-873	GCRV-I	Recombinant subunit vaccine	UN	UN	UN	[24]
Xu SY / 2011	Nanjing Normal University	GCRV-873	GCRV-I	DNA vaccine	Intraperitoneal injection; 30 µg /fish	60–120 g	UN	[35]
Tian YY / 2013	Pearl River Fisheries Research Institute, Chinese Academy of Aquatic Sciences	GCRV GD108	GCRV-II	Recombinant subunit vaccine	Intraperitoneal injection; 3 µg /g	25–30 g	82%	[27]

(continued)

Table 7.2 (continued)

Author/ years	Department	Strain	Genotype	Type of vaccine	Vaccination route	Fish weight	RPS	References
Li Q / 2014	Huazhong Agricultural University	GCRV-873	GCRV-I	Recombinant subunit vaccine	UN	UN	UN	[18]
Zhu B / 2015	Northwest A&F University	UN	UN	DNA vaccine	Intramuscular injection; 10 μg/fish	25.0–30.0 g	100%	[46]
Wang Y / 2015	Northwest A&F University	GCRV-097	UN	DNA vaccine	Intramuscular injection 5 μg/fish	1.1 ± 0.2 g	100%	[30]
Zeng WW / 2016	Pearl River Fisheries Research Institute, Chinese Academy of Aquatic Sciences	HuNan-1307	GCRV-II	Inactivated vaccine	Intraperitoneal injection	UN	≥80%	[41]
Hao K / 2017	Northwest A&F University	UN	UN	DNA vaccine	Intramuscular injection; 5 μg/fish	1.5–1.8 g	90%	[10]
Zhang LL / 2018	Wuhan Institute of Virology, Chinese Academy of Sciences	GCRV-873	GCRV-I	Recombinant subunit vaccine	UN	UN	UN	[45]
Hao K / 2018	Northwest A & F University	GCRV-873	GCRV-I	Recombinant subunit vaccine	Intraperitoneal injection; 20 μg/fish	2.7–3.0 g	88.89%	[11]
Hao K / 2018	Northwest A & F University	GCRV-873	GCRV-I	Recombinant subunit vaccine	Immersion; 20 mg/L	2.7–3.0 g	18.89%	[11]
Gao Y / 2018	Henan Normal University	GCRV-HN14	GCRV-II	Recombinant subunit vaccine	Intraperitoneal injection; 100 μl/fish (0.3 mg/L)	15 ± 1.5 g	60%	[9]

Author / Year	Institution	GCRV strain	GCRV-II	Vaccine type	Administration	Weight	Efficacy	Ref.
Gao Y / 2018	Henan Normal University	GCRV-HN14	GCRV-II	DNA vaccine	Intramuscular injection; 10 µg/fish	UN	UN	[8]
Gao Y / 2018	Henan Normal University	GCRV-HN14	GCRV-II	Recombinant subunit vaccine	Intramuscular injection; 100 µL (0.3 mg/mL)	15 ± 1.5 g	60%	[8]
Gao Y / 2018	Henan Normal University	GCRV-HN14	GCRV-II	Recombinant subunit vaccine	Intramuscular injection 100 µL (0.3 mg/mL)	15 ± 1.5 g	75%	[8]
Chen DD / 2018	Institute of Hydrobiology, Chinese Academy of Sciences	GCRV-HF	GCRV-II	DNA vaccine	Intramuscular injection 10 µg/100 µL	15–20 g	59.9%/23.1%	[2]
Pei C / 2019	Henan Normal University	GCRV HN14	GCRV-II	Recombinant subunit vaccine	Intraperitoneal injection; 100 µL/fish (0.3 mg/L)	15 ± 1.5 g	71–75%	[22]
Tang QQ / 2019	Anhui Agricultural University	GCRV-HF1601	GCRV-II	DNA vaccine	Intramuscular injection; 10 µg/100 µL	25–30 g	66.67%	[25]
Chen DD / 2019	Institute of Hydrobiology, Chinese Academy of Sciences	GCRV-HF	GCRV-II	DNA vaccine	Oral 2×10^9 spores/fish/d	15–20 g	30% (GC5-VP4), 36.4% (GC5-NS38)	[3]
Jiang HY / 2019	Sun Yat-sen University	GCRV-HuNan1307	GCRV-II	Recombinant subunit vaccine	Oral 1.0×10^{12} Spores/mL	23 ± 2 g	47%	[13]
Gao CX / 2020	Tianjin Agricultural University	GCRV-HuNan1307	GCRV-II	Recombinant subunit vaccine	Intraperitoneal injection; 30 µg/fish	20 ± 0.5 g	58.33–83.33%	[6]

UN, unknown, related information was not mentioned or provided in original files

on elucidation of the etiology of GCHD spanned for at least 25 years [5, 20]. To control the spread of this severe disease urgently, researchers have focused on the development of an inactivated vaccine using tissue homogenates from diseased grass carp [7]. They have collected diseased grass carp, pooled the samples, and homogenized the liver, spleen, kidney, muscle, and other parts of the fish with a blender. The mixture is diluted with 0.85% sterilized saline in ten times volume, followed by filtration through an 80 meshes screen. After centrifugation, the viral suspension is pooled and inactivated using 0.8% formalin at 37 °C for 72 h [4, 16]. The inactivated GCRV tissue culture vaccine was developed in the 1960s and successfully controlled GCHD in a few geographical regions. In 1992, three Chinese aquatic industry standards SC1001-92, SC1002-92, and SC1003-92, regarding the inactivated virus tissue culture vaccine preparation, vaccine testing methods, and vaccine injection protocol, respectively, have been issued by the Ministry of Agriculture. Tissue culture vaccines possess the advantages of easy preparation and low cost. However, as the tissue culture vaccine quality is not stable, the risk of incomplete inactivation and poor immune-protective effects under some circumstances continues to pose challenges. Therefore, it has gradually been replaced by inactivated virus cell culture vaccines.

7.2.2 Inactivated GCRV Cell Culture Vaccine

Usage of cell culture to isolate viruses constitutes the basis for in-depth studies of viral biological characteristics and vaccine development. In 1984, studies by Zuo et al. established that *Ctenopharyngodon idella* kidney (CIK) cells were sensitive to the GCRV [47]. In 1986, Yang et al. developed an inactivated cell culture vaccine using the FR-836-w strain and CIK cells. The relative percent survival (RPS) has been calculated as 77.1% ± 10.8% at 11 days post-vaccination in a laboratorial evaluation. Moreover, a satisfactory result has been obtained in the field test with the survival rate being 94.6% in the vaccinated group compared with 53.9% in the control group during an epidemic period from August to October [37]. After comparison two vaccine candidate strains in lab, the PRS from FR-854 vaccinated group was 88.9 ± 12.0%, much higher than FR-836-w group with RPS 71.3 ± 14.2% [38]. Furthermore, inactivated virus cell culture vaccines have been tested in large-scale experiments from 1987 to 1989. The average survival rate of the group via injection vaccination has been found to be 79.5% ± 5.7% compared with 48.9% ± 8.2% of the control, whereas the average survival rate of the group via immersion was 61.4 ± 16.2% compared to 40.0 ± 19.0% of the control [39]. In the following years, many scientists have focused on the inactivated grass carp hemorrhagic virus (GCHV) cell culture vaccine [36, 40]. When usage of this vaccine against GCHD obtained approval from regulatory authorities, it officially became the first certified aquatic vaccine in China (Table 7.1). The Chinese aquatic industry standards (SC7701-2007) pertaining to the inactivated virus cell culture vaccine against GCHD have been issued in 2007.

Unfortunately, the inactivated virus cell culture vaccine has not been available commercially due to the lack of a production license. In 2010, Zhang et al. published the whole genome sequence of a new isolate named GCRV-HZ08, thereby indicating a completely different genotype compared with that of the representative strain GCRV-873 [43, 44]. Furthermore, Wang et al. have compared published partial or whole genome sequences of the GCRV, and the sequential analysis of the different GCRV isolates in China has indicated that there are three distinct groups representing GCRV genotype I (GCRV-873), II (GCRV-HZ08), and III (GCRV-104) [28]. Furthermore, cross-reaction assays with rare minnows have revealed low cross-reactivity between the different genotype viruses, indicating that the present strain used for vaccine preparation may provide weak or no protection against the epidemic strain infection [29].

In recent decades, GCRV II has become the dominant genotype instead of GCRV I. Therefore, it is important to develop novel GCRV vaccines that are capable of inducing high protection combined with satisfactory safety. The following two main aspects should be addressed in the development of inactivated vaccines: (i) it is necessary to inactivate an infectious virus completely to ensure the safety of the vaccine and (ii) essential viral epitopes should be retained after inactivation, to obtain high-quality antigens [23]. Zeng et al. developed an inactivated virus cell culture vaccine using the GCRV-HuNan1307 (GCRV II) and evaluated the inactivation dynamics of the cell-associated GCRV antigen using formaldehyde or β-propiolactone (BPL) [41]. The GCRV isolate GCRV-HuNan1307 was isolated by replication in the proboscis snout fibroblasts (PSF) cell line derived from grass carp and was inactivated with 1% BPL for 60 h at 4 °C. It has been shown that the minimum dose of the inactivated virus vaccine necessary to induce immune protection is $10^{5.5}$ $TCID_{50}$/0.2 mL. The survival rate has been found to be greater than 80% after the viral challenge, which is comparable to that of grass carp immunized with a commercial live-attenuated vaccine. Moreover, the immunoprotective effects have been found to last for at least a year.

7.3 Live-Attenuated Vaccines

Research on GCRV-attenuated vaccines dates back to 1986, with the successful establishment of the PSF cell line [17]. Xu et al. cultured the virulent strain GCRV-841 on PSF cells and attenuated the virus in 53–59 generations, which subsequently demonstrated a virulence that was stable enough to fulfill the requirements for safety testing. The weakened virus prepared from 55–57 generations has been selected for vaccination, and the viral challenge test has shown 100% RPS [33]. Later, the researcher improved the attenuation technique by adding an extract obtained from eucalyptus leaves into the medium, which could successfully attenuate the GCHV-892 strain at the 19th generation and maintain stable virulence until the 29th generation. The efficacy of the attenuated virus belonging to the 25–29 generation has been tested, which shows an RPS of 100% after vaccination [32]. Furthermore,

the minimal dosage, duration of immunity, and storage condition of the live-attenuated vaccine have been determined [34]. In 1997, researchers from the Pearl River Fisheries Research Institute, Chinese Academy of Fishery Sciences, submitted an application for a new veterinary drug certificate. Owing to the strict policy for live virus registration, a successful approval and validation of the novel drug were achieved after evaluation for 13 years. In 2010, the live-attenuated vaccine (GCHV-892 strain) against GCHD was awarded with the national class I new veterinary drug certificate ((2010) No. 51), followed by issuance of the veterinary drug production license by the Chinese government in 2011 (GCHV-892 strain, (2011) 190986021; updated no.: (2014) 190026031) (Table 7.1). This live-attenuated vaccine (GCHV-892 strain) marks a milestone in aquatic vaccine research because it is the first aquatic live-attenuated vaccine developed in China, as well as the first live-attenuated vaccine against GCHD worldwide, which indicates the industrial application of aquatic vaccines.

7.4   Recombinant Subunit Vaccines

Subunit vaccines are a modification of the inactivated virus vaccines. Instead of generating antibodies against all the antigens in the pathogen, antibody against a particular antigen (or antigens) is produced. Therefore, an effective subunit vaccine identifies a specific antigen or combination of antigens [15]. The genomic RNA of GCRV II species, which contains 11 segments (S1–S11), is predicted to encode 11 proteins. These include three inner core proteins (encoded by S1, S2, and S3), two nonstructural proteins (encoded by S4 and S10), four capsid proteins (encoded by S5, S6, S9, and S11), one fiber protein (encoded by S7), and one unknown protein (encoded by S8) [21]. However, the vp38 encoded by S10 gene of GCRV-II has proved to be a structural protein with high immunogenicity [42].

Before 2010, the experiments on subunit vaccines have been performed using GCRV I isolates; for example, the GCRV-873 strain. Zhang et al. expressed recombinant VP5, a putative outer capsid protein of the GCRV, in *Escherichia coli* and demonstrated its high immunogenicity using an enzyme-linked immuno-sorbent assay [45]. He et al. demonstrated that a rabbit polyclonal antibody against the recombinant GCRV VP5 could protect against GCRV infection by neutralization experiments [12]. Shao et al. generated antibodies against the recombinant GCRV VP5 and VP7 proteins, and neutralization experiments showed that both antibodies could neutralize the GCRV [24]. However, viral challenge tests have not been conducted for the above-mentioned putative subunit vaccine candidates. Hao et al. developed a novel vaccine (BL21/InpN/vp7) based on the GCRV surface displaying a major capsid protein (VP7), using the anchoring motif of the unique N-terminal domain of the ice nucleation protein (InpN) in *Escherichia coli* BL21 (DE3) cells. Thereafter, the grass carps were immunized using both intraperitoneal injection and bath immunization. The RPS in the vaccine-injected group was determined as 88.89% compared with the bath-immunized group (18.89%) [11].

In the recent decade, GCRV II has been determined as the dominant GCRV genotype which causes severe hemorrhagic disease with high mortality in grass carp. Therefore, researchers have focused on vaccine preparation using recombinant proteins from GCRV II species. Tian et al. created a recombinant VP4 protein (rVP4), which has been inserted in the prokaryotic expression vector pET32a, and expressed an 87-kDa protein using the *Escherichia coli* BL21 (DE3) strain. Fourteen days after immunization with rVP4, the grass carps were challenged with GCRV-GD108, and it was shown that all the different doses of rVP4 (1 mg/g, 3 mg/g, and 5 mg/g) could provide protection against virus infection (47%–82%). The RPS was shown to demonstrate a value of 82% in the group immunized with 3 mg/g rVP4 [27]. Pei et al. prepared the recombinant VP56 protein expressed in the pET-32a(+) vector as a subunit vaccine to immunize grass carp. The GCRV challenge test showed an RPS of 71%–75% in the immunized group [22]. The S11 gene fragment has been speculated to encode the viral structural protein VP35. Gao et al. constructed the recombinant plasmid pET-32a-vp35 to express the recombinant VP35 protein in prokaryotic cells, which could be used as a vaccine candidate. The fish was immunized with the recombinant VP35 and challenged with 10 LD_{50} GCRV at 21 days post-immunization. The survival percentage in the immunized group was determined as 66.7% on day 15, which was significantly higher than that in the control group (16.7%) ($P < 0.01$) [9].

Baculovirus has been extensively used as a vector for exogenous gene expression, including expression in mammalian and fish cells. Li et al. constructed a recombinant baculovirus containing the GCRV VP6 gene under the control of CMV-IE promoter. Fish immunized with Bac-CMV-VP6 has been shown to produce a GCRV-specific neutralizing antibody. Additionally, the expression of two innate immune-related cytokines, interferon regulatory factor-7 and interferon-1, can be upregulated [18]. Gao et al. selected the GCRV-II S3, S6, S9, and S10 segments to construct GCRV-II viruses like particles (VLPs), using a baculovirus expression system. Multiple GCRV-II VLPs have been constructed using different combinations of recombinant baculovirus, followed by evaluation of immune effects of all VLPs. The viral challenge experiments have shown that the RPS values of the GCRV-II S3-S6-VLPs, S3-S6-S10-VLPs, and opti-S6-S9-S10-VLPs groups with adjuvant are 58.33%, 83.33%, and 79.17%, respectively, and of these, S3-S6-S10-VLPs with adjuvant have been found to offer the best immune protection for grass carps [6].

Bacillus subtilis spores have been shown to be an ideal oral vaccine delivery system for presenting heterologous antigens to the gastrointestinal tract. Two recombinant spores constructed by Chen et al. have been shown to express abundant fusion proteins of CotC-VP4 and CotC-NS38 on spores of wild type *Bacillus subtilis* GC5 isolated from grass carp. The grass carp was orally been administered with recombinant *Bacillus subtilis* spores, followed by evaluation of the immunoprotective effects. Compared with the control groups, both recombinant vaccines GC5-VP4 and GC5-NS38 have been shown to increase the survival rate of grass carp against GCRV II species infection, with an RPS of 30% and 36.4%, respectively [3]. Simultaneously, Jiang et al. used *Bacillus subtilis* spores as an oral delivery system and

successfully constructed *Bacillus subtilis* CotC-VP4 recombinant spores (CotC-VP4 spores) to evaluate its protective effect on grass carp. Grass carp orally immunized with CotC-VP4 spores has been shown to demonstrate a survival rate of 57% and an RPS of 47% after the viral challenge. Furthermore, the specific immunoglobulin M levels in the serum and the specific immunoglobulin Z levels in the intestinal mucus have been found to be significantly higher in the CotC-VP4 group than those in the naive group. Therefore, oral vaccination is of major interest owing to its noninvasive, time-saving, and easy administrable characteristics. Particularly, *Bacillus subtilis* spores are powerful platforms for oral vaccine delivery, and the combination of *Bacillus subtilis* spores with the GCRV VP4 protein presents a promising oral vaccine [13].

7.5 DNA Vaccines

DNA vaccination is a proven and effective method for conferring protection against fish viruses [1, 14, 19]. Xu et al. obtained recombinant pFastBac-β-VP7$_1$-VP7$_2$ using double VP7 genes of GCRV-873 (GCRV I) and β-actin promoter from *Megalobrama amblycephala*. After viral challenge, mortality rates were observed to be 0%, 0%, and 5% in 10 μg, 30 μg, and 60 μg vaccination groups, respectively. However, the mortality rates in the pFastBac™Dual and control groups after GCRV infection were found to be 30% and 100%, respectively [35]. The S11 and S7 segments in GCRV II species can encode proteins VP35 and VP56, respectively, and they have been hypothesized to possess good immunogenicity. The open reading frame of the S11 segment has been cloned to construct the recombinant plasmid pcDNA3.1-s11. Serum antibody titer obtained by an enzyme-linked immunosorbent assay showed a significant increase at 7 days post-immunization ($P < 0.05$) and reached a peak value at 28 days post-immunization ($P < 0.01$). The pcDNA3.1-s11 vaccine candidate has been shown to enhance the survival rate in vaccinated fish, with a survival rate of 70.4–73.3% at 14 days post-infection compared with 5–13% in the pcDNA3.1 or phosphate-buffered saline control groups [8].

To enhance the efficacy of DNA vaccines, vaccine delivery systems have been extensively studied, and many nano-sized vaccine delivery systems have been developed [26]. Zhu et al. constructed a DNA vaccine containing the major capsid protein VP7 gene of the GCRV, and they used single-walled carbon nanotubes (SWCNTs) as carriers for DNA vaccine delivery. After intramuscular administration, the serum respiratory burst activity, complement activity, lysozyme activity, superoxide dismutase activity, immune-related genes, antibody levels, and RPS were found to be significantly enhanced in fish immunized with the SWCNTs-pcDNA-vp7 vaccine. Furthermore, no mortality was observed on days 1–15 after GCRV challenge (10 mg per fish), and the RPS has been determined as 100% [46]. Similar work was conducted by Wang et al. using SWCNTs-pEGFP-vp5 DNA vaccine, wherein recombinant VP5 in the form of plasmid pEGFP-vp5 was

linked with ammonium-functionalized SWCNTs. The grass carps were vaccinated via intramuscular injection (1, 2.5, and 5 mg) and bath administration (1, 10, and 20 mg/L). The protective effect of the vaccine was observed in the bath immunization group, which at a concentration of 20 mg/L could reach an RPS similar to that observed in the injection group at a dose of 5 mg (approximately 100%) [30]. Tang et al. prepared and evaluated an oral DNA vaccine of VP5 and NS38. The DNA vaccine pcDNA3.1(+)-Bs5-10 was constructed with VP5 and NS38 via screening using a B cell linear epitope prediction server, followed by packaging into nano-scale chitosan particles. It was observed that the RPS of the naked DNA vaccine injection group and the chitosan oligosaccharide-coated DNA vaccine oral group were 66.67% and 50%, respectively, and the levels of serum anti-VP5 and anti-NS38 immunoglobulin M in these two groups were found to increase significantly after enhanced immunization ($P < 0.05$) [25].

The use of bacterial ghost (BG, nonliving bacteria) as carriers for DNA vaccine delivery has received considerable attention in veterinary and human vaccine studies. Hao et al. developed a vaccine based on *Escherichia coli* DH5a bacterial ghost (DH5a-BG), which delivered the GCRV major capsid protein gene (VP7)-encoded DNA vaccine. Grass carps were injected intramuscularly with different concentrations; the RPS was observed to be significantly enhanced in fish immunized with the DH5a-BG/pcDNA-vp7 vaccine and was found to reach 90% in the DH5a-BG/pcDNAvp7 group, compared with 42.22% in the naked pcDNA-vp7 group at the highest DNA dose (5 mg) 14 days post-infection [10].

VP4 protein is the major outer capsid protein encoded by the GCRV II S6 segment, which plays an important role in viral invasion and replication. Chen et al. vaccinated grass carps with a pcDNA3.1 based DNA vaccine consisting of the S6 segment (pC-S6; encoding VP4) or the S10 segment (pC-S10; encoding NS38) of GCRV II species. The protective effect of pC-S6 and pC-S10, in terms of RPS, has been observed to be 59.9% and 23.1%, respectively [2].

7.6 Conclusions and Future Considerations

Thus far, the most effective method to control and prevent GCHD is vaccine immunization. Although a licensed vaccine is available commercially, the significant differences between the new isolates (dominant GCRV II) and the previous representative strains (GCRV I) have posed challenges, such as provision of weak efficacy or no protection against the epidemic strains. Therefore, the development and application of vaccines should be based on long-term epidemiological surveillance. The inactivated and subunit vaccines demonstrate the advantage of safety, but the immunoprotective effects and duration of immunity offered by inactivated and subunit vaccines are inferior to those of the live-attenuated vaccines. DNA vaccines have recently gained popularity, and there is a need for strict evaluation of their biosafety before application in the field. Additionally, most vaccines under development are recommended to be administered via injections, which is not convenient

for immunizing large populations of grass carps. Therefore, a safe, efficient, and easily administrable vaccine provided via immersion or oral route should be developed in the near future.

References

1. Anderson ED, Mourich DV, Fahrenkrug SC, LaPatra S, Shepherd J, Leong JAC (1996) Genetic immunization of rainbow trout (Oncorhynchus mykiss) against infectious hematopoietic necrosis virus. Mol Mar Biol Biotechnol 5(2):114–122
2. Chen DD, Yao YY, Cui ZW, Zhang XY, Peng KS, Guo X, Wang B, Zhou YY, Lia S, Wu N, Zhang YA (2018) Comparative study of the immunoprotective effect of two DNA vaccines against grass carp reovirus. Fish Shellfish Immunol 5:66–73
3. Chen DD, Yao YY, Cui ZW, Zhang XY, Guo X, Zhou YY, Zhang YA (2019) Comparative study of the immunoprotective effect of two grass carp-sourced Bacillus subtilis spore-based vaccines against grass carp reovirus. Aquaculture 504:88–95
4. Chen DY, OuYang M (2009) The report about preparation and application of simple inactive vaccine for control of grass carp hemorrhagic disease. Acta Agric Jiangxi 21(10):143–144
5. Chen YX, Jiang YL (1983) Research of morphological structure and physicochemical properties of grass carp hemorrhagic disease virus. Chin Sci Bull 28:1138–1140
6. Gao CX (2020) Preparation and immune effect evaluation of grass carp reovirus genotype II virus-like particles [M]. Tianjin Agricultural University
7. Gao HJ, Sun MJ, Zhai ZY, Wang JB (1984) Analysis of inactivated vaccine and immune effect of grass carp hemorrhagic disease. Compendium of papers from the National Symposium on Grass Carp Disease Research. Inst Hydrobiol Chinese Acad Sci 1984:86–92
8. Gao Y (2018) Development and immune effect evaluation of three genetic engineering vaccines of grass carp reovirus [M]. Henan Normal University
9. Gao Y, Pei C, Sun XY, Zhang C, Li L, Kong XH (2018) Novel subunit vaccine based on grass carp reovirus VP35 protein provides protective immunity against grass carp hemorrhagic disease. Fish Shellfish Immunol 75:91–98
10. Hao K, Chen XH, Qi XZ, Zhu B, Wang GX, Ling F (2017) Protective immunity of grass carp induced by DNA vaccine encoding capsid protein gene (VP7) of grass carp reovirus using bacterial ghost as delivery vehicles. Fish Shellfish Immunol 64:414–425
11. Hao K, Chen XH, Qi XZ, Zhu B, Wang GX, Ling F (2018) Display of GCRV VP7 protein on the surface of Escherichia coli and its immunoprotective effects in grass carp (Ctenopharyngodon idella). Fish Shellfish Immunol 72:199–209
12. He YX, Xu HX, Yang Q, Xu D, Lu L (2011) The use of an in vitro microneutralization assay to evaluate the potential of recombinant VP5 protein as an antigen for vaccinating against grass carp reovirus. Virol J 8:132
13. Jiang HY, Bian Q, Zeng WW, Ren PL, Sun HC, Lin ZP, Tang ZL, Zhou XY, Wang Q, Wang YY, Wang YS, Wu MX, Li XR, Yu XB, Huang Y (2019) Oral delivery of Bacillus subtilis spores expressing grass carp reovirus VP4 protein produces protection against grass carp reovirus infection. Fish Shellfish Immunol 84:768–780
14. Leong JC, Anderson E, Bootland LM, Chiou PW, Johnson M, Kim C (1997) Fish vaccine antigens produced or delivered by recombinant DNA technologies. Dev Biol 90:267–277
15. Levine MM, Woodrow GC, Kaper JB, Cobon GS (1997) New generation vaccines, 2nd edn. Marcel Dekker, Inc, pp 145–176

16. Li GZ (2008) The satisfactory effect of inactivated tissue culture vaccine against grass carp hemorrhagic disease. Fishery Guide Rich 17:55
17. Li HL, Xu SY, Deng GC (1988) The establishment of proboscis snout fibroblasts (PSF) cell line derived from grass carp and its biological characteristics. J Fishery Sci China 1:1–8
18. Li Q, Liu LY, Lin L, Li ZM, Liu GX, Wu SS, Wang M, Li LJ, Yuan JF, Yuan GL, Liu XQ (2014) Immunization with recombinant baculovirus expressing the VP6 protein of grass carp reovirus induces immunity in grass carp. Virol Sin 29:261–263
19. Lorenzen N, LaPatra SE (2005) DNA vaccines for aquacultured fish. Rev Sci Tech Oie 24:201–213
20. Ni DS, Wang JG (1999) Grass carp biology and disease. Science Press, Beijing, pp 78–85
21. Pei C, Ke F, Chen ZY, Zhang QY (2014) Complete genome sequence and comparative analysis of grass carp reovirus strain 109 (GCReV-109) with other grass carp reovirus strains reveals no significant correlation with regional distribution. Arch Virol 159:2435–2440
22. Pei C, Gao Y, Sun XY, Li L, Kong XH (2019) A developed subunit vaccine based on fiber protein VP56 of grass carp reovirus providing immune protection against grass carp hemorrhagic disease. Fish Shellfish Immunol 90:12–19
23. Pereira RC, Silva AN, Souza MC, Silva MV, Neves PP, Silva AA (2015) An inactivated yellow fever 17DD vaccine cultivated in Vero cell cultures. Vaccine 33(35):4261–4268
24. Shao L, Sun X, Fang Q (2011) Antibodies against outer-capsid proteins of grass carp reovirus expressed in E. coli are capable of neutralizing viral infectivity. Virol J 8:347
25. Tang QQ, Zhang ZH, Mao YR, Lu ZY, Tao MH, Xu TT, Zeng H, Fan HM, Xu XM, Peng KS, Zhu RL, Bao CH (2019) Preparation and evaluation of a DNA vaccine oral nanoparticle oral preparation for encoding grass carp reovirus VP5 and NS38 B cell epitopes. J Anhui Agri Univ 46:389–393
26. Tian J, Yu J (2011) Poly(lactic-co-glycolic acid) nanoparticles as candidate DNA vaccine carrier for oral immunization of Japanese flounder (Paralichthys olivaceus) against lymphocystis disease virus. Fish Shellfish Immunol 30:109–117
27. Tian YY, Ye X, Zhang LL, Deng GC, Bai YQ (2013) Development of a novel candidate subunit vaccine against grass carp reovirus Guangdong strain (GCRV-GD108). Fish Shellfish Immunol 35:351–356
28. Wang Q, Zeng WW, Liu C, Zhang C, Wang YY, Shi CB, Wu SQ (2012) Complete genome sequence of a reovirus isolated from grass carp. indicating different genotypes of GCRV in China. J Virol 86:12466
29. Wang Q, Zeng WW, Liang Y, Wang YY, Liu C, Li YY, Zheng SC, Shi CB (2016) Comparative study on physical-chemical and biological characteristics of grass carp reovirus from different genotypes. J World Aquacult Soc 47(6):862–872
30. Wang Y, Liu GL, Li DL, Ling F, Zhu B, Wang GX (2015) The protective immunity against grass carp reovirus in grass carp induced by a DNA vaccination using single walled carbon nanotubes as delivery vehicles. Fish Shellfish Immunol 47:732–742
31. Wu SQ, Tao JF, Gong H, Chang OQ, Ren Y, Liu LH, Chen ZH, Lai Y (2014) Situation and tendency of the fishery vaccine development. Chin Fish Qual Stand 2014:1–13
32. Xu S, Li H, Deng G, Jiang L, Bai Y (1998) Study on attenuation of virus of hemorrhage of grass carp, *Ctenopharyngodon idella*. J Shanghai Fish Univ 7:211–216
33. Xu SY, Li HL, Deng GC (1994) Preparation of attenuated vaccine against grass carp hemorrhagic disease and its efficacy evaluation. J Fish China 13(2):110–117
34. Xu SY, Li HL, Deng GC, Jiang L, Bai YQ, Jiang JZ (1998) Study on minimum dosage, immunity duration and storage period of attenuated cell cultured vaccine against grass carp hemorrhagic disease. Freshw Fish 28(3):3–5
35. Xu SY, Liu L, Li JH, Zou Y, Ni JD, Yang YJ, Gong CL, Cao GL, Xue RY, Chen H (2011) Construction and immune efficacy studies on DNA vaccine with VP7 gene of grass carp reovirus. J Fish China 35:1694–1700

36. Yang XL, Zuo WG (1993) Inactivated vaccine obtained through cell culture for hemorrhage of grass carp (*Ctenopharyngodon idella*): the stability of vaccine and influence of adjuvants and booster immunization on the immune response. Acta Hydrobiol Sin 17(1):46–52
37. Yang XL, Du SY, Zeng LB, Qian HX, Zuo WG (1986) The preliminary research on inactivated cell-cultured vaccine against hemorrhagic disease of grass carp. Freshw Fish 3:1–5
38. Yang XL, Xia C, Zuo WG (1989) Inactive vaccine for hemorrhage of grass carp: comparison of immunogenicity and immunizing dose between two strains. J Fish China 13(2):138–144
39. Yang XL, Xia C, Zuo WG, Wu QM, Guo YJ (1992) Research on inactivated cell-cultured vaccine against hemorrhagic disease of grass carp – vaccination experiment in field. Fish Sci Rep 19(1):10–14
40. Zeng LB, Yang XL, He L, Ai XH, He JH, Zuo WG, Batch processing technology of cell cultured killed vaccine against the hemorrhage of grass carp. J Fish Sci China 5:63–68
41. Zeng WW, Wang Q, Wang YY, Zhao CC, Li YY, Shi CB, Wu SQ, Song XJ, Huang QW, Li SJ (2016) Immunogenicity of a cell culture-derived inactivated vaccine against a common virulent isolate of grass carp reovirus. Fish Shellfish Immunol 54:473–480
42. Zeng WW, Wang YY, Guo YM, Bergmann SM, Yin JY, Li YY, Ren Y, Shi CB, Wang Q (2018) Development of a VP 38 recombinant protein-based indirect ELISA for detection of antibodies against grass carp reovirus genotype II (iELISA for detection of antibodies against GCRV II). J Fish Dis 41(12):1811–1819
43. Zhang C (2010) Isolation and identification of grass carp reovirus HZ08 strain and analysis of genomic molecular characteristics [D]. Shanghai Ocean University
44. Zhang C, Wang Q, Shi CB, Zeng WW, Liu YL, Wu SQ (2010) Molecular analysis of grass carp reovirus HZ08 genome segments 1–3 and 5–6. Virus Genes 41:102–104
45. Zhang LL, Lei CF, Fan C, Fang Q (2009) Expression of outer capsid protein VP5 of grass carp reovirus and analysis of its immunogenicity. Virol Sin 24:545–551
46. Zhu B, Liu GL, Gong YX, Ling F, Wang GX (2015) Protective immunity of grass carp immunized with DNA vaccine encoding the VP7 gene of grass carp reovirus using carbon nanotubes as a carrier molecule. Fish Shellfish Immunol 42:325–334
47. Zuo WG, Qian HX, Xu YF, Du SY, Yang GY (1984) Establishment of *Ctenopharyngodon idella* kidney (CIK) cell line. Freshw Fish 2:38–39

Chapter 8
Medical Treatment of Grass Carp Hemorrhagic Disease

Hao Wang

Abstract Grass carp hemorrhagic disease caused by the grass carp reovirus (GCRV) is one of the most detrimental diseases for grass carp *Ctenopharyngodon idella* and leads to significant economic losses in the freshwater aquaculture industry. Vaccination is generally considered one of the most effective methods to control the spread of the virus. Despite successful application of several GCRV vaccines in China, they have notable limitations in clinical application, such as the mode of administration (injection, oral, or immersion), immunological memory, and cost-effectiveness. Accordingly, effective anti-GCRV drugs could compensate for the limitations of the vaccines. Recently, a small-molecule compound, (−)-epigallocatechin-3-gallate (EGCG), has been found to reduce GCRV infection based on the understanding of virus–host interactions. EGCG is mainly extracted from tea, including green tea, oolong tea, black tea, white tea, and dark tea, and has various beneficial biological functions for animal hosts. EGCG, as a core component of aquatic medicine, has been widely used as a natural medication for controlling and treating GCRV infection in China. Similarly, several natural plant extracts, such as magnolol, honokiol, and moroxydine hydrochloride, have recently been reported to possess anti-GCRV properties. In this chapter, we summarize the potential drugs that can be used against GCRV infection, including natural compounds, chemical inhibitors, and endocytosis inhibitors. Additionally, the target inhibition mechanisms of these drugs are generalized. Medical treatment strategy against GCRV infection is reasonable and feasible, and the availability of traditional medicines in Asian countries forms a basis for developing environmentally friendly aquatic drugs.

Keywords EGCG · GCRV · Aquatic medicine · Medical treatment

H. Wang (✉)
National Pathogen Collection Center for Aquatic Animals, Shanghai Ocean University, Shanghai, China
e-mail: h-wang@shou.edu.cn

Abbreviations

CIK	*Ctenopharyngodon idella* kidney
ECG	$(-)$-Epicatechin-3-gallate
EGCG	$(-)$-Epigallocatechin-3-gallate
GCRV	Grass carp reovirus
Hsp70	Heat shock protein 70
LamR	Laminin receptor
Mor	Moroxydine hydrochloride
Rib	Ribavirin

8.1 Introduction

Grass carp (*Ctenopharyngodon idella*) is one of the major economic freshwater fish in China and has recently been accounted for 10.5% of global finned fish production in 2018 (Food and Agriculture Organization of the United Nations). Since long, viral hemorrhagic disease has been considered one of the most severe diseases in the grass carp cultivation industry and listed as a notifiable disease in China since 2008 [39, 42, 60]. The grass carp reovirus (GCRV) has been classified into the genus *Aquareovirus* of the family *Reoviridae* by the International Committee on Taxonomy of Viruses in 1991. Genomic analyses have categorized the genus *Aquareovirus* into seven species (*Aquareovirus A-G*), and the GCRV belongs to *Aquareovirus C*. GCRV is a nonenveloped, double-stranded RNA (dsRNA) virus [35, 51]. Its genome encodes seven structural proteins and six nonstructural proteins [64, 67]. Similar to the other aquareoviruses, the diameter of the GCRV particle is approximately 800 Å [11]. To date, three genotypes (GCRV I, II, and III) have been identified [37, 50]. Notably, these different genotypes of the GCRVs share low similarity (less than 20%) according to the homology level of their VP6 genes. More than 20 GCRV isolates have been completely sequenced, such as GCRV-873 (GCRV I), GVRV-HZ08 (GCRV II), and GCRV-104 (GCRV III) [18, 37, 39, 69]. The epidemiological surveys of the GCRV conducted by the Chinese Ministry of Agriculture and Rural Affairs annually have shown that the GCRV is distributed all over China, and GCRV I and II have been found to be highly frequent in recent years [26]. Existing studies have suggested that the optimum temperature for the GCRV replication is approximately 28 °C and indicated that high morbidity occurs at a water temperature of approximately 25–30 °C. Although the majority of the known aquareoviruses have low virulence and have been detected in asymptomatic aquatic animals, several species, including the GCRV, are highly pathogenic under some conditions. Furthermore, there are multiple causes underlying the GCRV outbreak in China [51]. In addition to natural conditions, the mode of cultivation of grass carp is considered one of the underlying causes of the GCRV outbreak [26, 33]. For example, the cultivation of grass carp using high-density ponds is one of the main reasons for the GCRV epidemic in China.

However, due to multiple reasons (economic effect, consumption habits, and construction cost), it is difficult to apply the modern industrial aquaculture system for grass carp cultivation [39]. Moreover, it is not easy for farmers to obtain specific-pathogen-free grass carp parents and fries.

For the GCRV treatment and control, only a single commercial live-attenuated vaccine against the GCRV has been approved by the Chinese Ministry of Agriculture and Rural Affairs in 2011 [No: (2014) 190026031]. Although China has the largest aquaculture industry, there are not enough commercial vaccines available for use [58]. Extensive research on vaccines against the GCRV has been reported, including DNA vaccines, live-attenuated vaccines, inactivated GCRV vaccines, and subunit vaccines; however, only few effective vaccines have taken effect in clinical application [58]. Therefore, the multiple existing limitations should be addressed for advancements in the GCRV vaccine application. First, it is urgent to develop an automated fish vaccine syringe dispenser to make up for the inefficient artificial injection. Second, large number of commercial vaccines against the GCRV need to be launched by reducing the time taken for government approval. However, the above mentioned problems have not been addressed for a certain period. Therefore, more management technologies should be developed for the control and treatment of the GCRV. For instance, advanced viral detection techniques for GCRV are useful for protection against viruses in grass carp farming. Furthermore, in recent years, a large number of biological and chemical agents have been widely used in aquaculture to control aquatic diseases. It is well known that natural plant compounds have great potential to be developed as eco-friendly drugs for the prevention and control of viral diseases in aquaculture [73]. A large number of natural compounds extracted from plants have been widely used as traditional Chinese medical herbs in China for a long time [40, 45, 49, 52, 63, 71–73]. Therefore, it is necessary to develop natural plant compounds as anti-GCRV agents for management of viral diseases in grass carp farming. The present chapter focuses on the development of novel eco-friendly drugs against the GCRV and illustrates the effects of several chemical inhibitors and endocytosis inhibitors on GCRV infection.

8.2 Effects of Natural Compounds Against the GCRV

8.2.1 (−)-Epigallocatechin-3-Gallate (EGCG)

Extensive research has been conducted on genotype I of the GCRV using the representative GCRV-873 strain, which is the first fish virus isolated in China [19, 39]. GCRV I species, including GCRV-873, can produce significant cytopathic effects by forming large syncytia in grass carp *Ctenopharyngodon idella* kidney (CIK) cells, the classical model for investigating dsRNA viruses [75]. The GCRV I species, especially GCRV-873, contain 11 dsRNA segments and double-layered capsids. These genomic segments encode six nonstructural proteins (NS80, NS31, NS12, NS16, NS38, and NS26) and seven structural proteins (VP1–VP7) [11, 12,
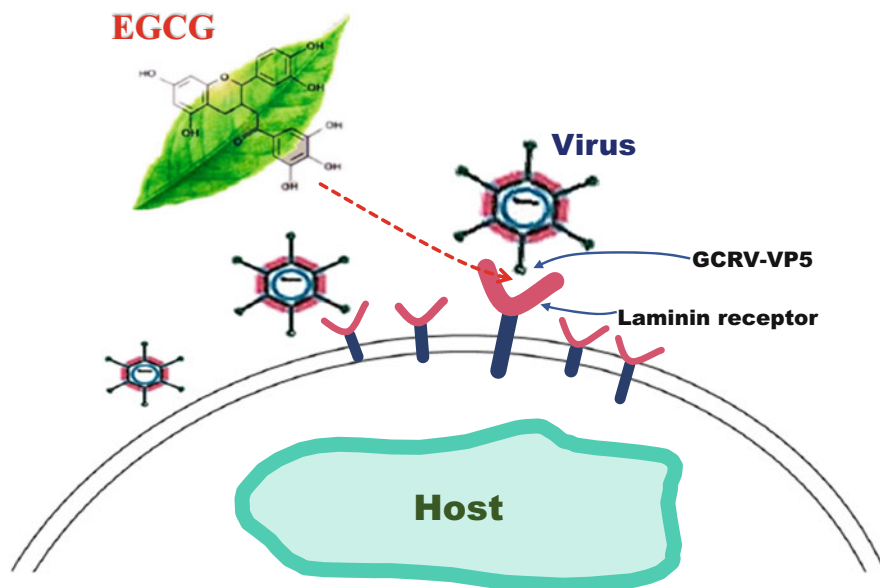
Fig. 8.1 Schematic diagram depicting the proposed mechanism by which EGCG exerts anti-GCRV. GCRV-VP5 binds to laminin receptor(LamR) present at the cell surface (attachment step). As the ligand for the LamR, EGCG's blocking effect on GCRV attachment was associated with the binding potential of GCRV particles to LamR. The natural compound EGCG is in red. EGCG: epigallocatechin-3-gallate; GCRV particles are in blue

19, 67]. Transmission electron microscopy combined with subnanometer-resolution structural analysis has demonstrated that the outer capsid of the viral particles contains 200 trimers of VP5–VP7 heterodimers [11, 12]. It is well known that the attachment of the outer capsid or envelope proteins to the receptor on the host cells is the first step in the viral infection cycle [4, 69]. Interestingly, Fang has found that the GCRV particles without VP7 can promote viral infectivity and has indicated that VP5 may be critical for viral attachment or binding cell receptors [20]. Consistently, another study has demonstrated that the GCRV VP5 can bind to the laminin receptor (LamR) protein of the host cell [1, 5, 8, 23, 55]. These findings suggest that grass carp LamR is involved in viral attachment, promoting infection by binding to the viral capsid protein VP5 of the GCRV. Thus, the grass carp LamR protein could be an ideal target for anti-GCRV drug development. Significant advances in research have revealed that EGCG is attributed to the activation of its cell surface-sensing receptor, i.e., the 37/67-kDa LamR. Consequently, EGCG, as a small-molecule compound, has the ability to bind and regulate the biological functions of LamR [1, 22, 43, 47, 48, 54, 55]. Taken together, these results indicate that EGCG may be a potential anti-GCRV drug to control grass carp hemorrhagic disease [54] (Fig. 8.1).

EGCG, the most abundant polyphenolic substance in green tea, exerts a large number of biological activities in cancer control, viral diseases, bacterial diseases, neurodegenerative diseases, etc. [34, 41, 46, 62]. The main polyphenolic compounds
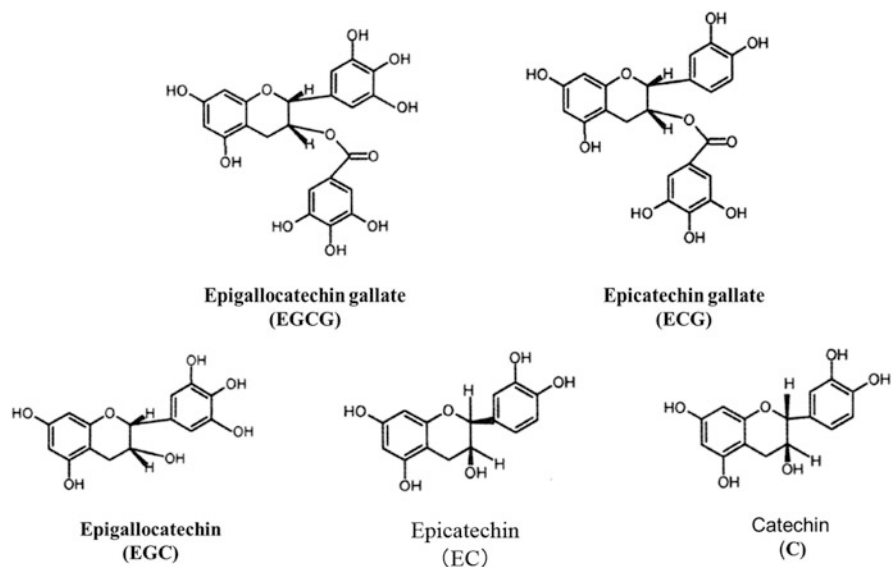
Fig. 8.2 The chemical structural formula of major catechin (EGCG, ECG, EGC, EC, and C)

in green tea, known as catechins, include (−)-epicatechin, (−)-epicatechin-3-gallate (ECG), (−)-epigallocatechin, and EGCG. EGCG accounts for approximately 59% of the total catechin component [2, 21, 62]. The EGCG structure appears as a benzenediol ring joined to a tetrahydropyran moiety, a pyrogallol ring, and a galloyl ring (Fig. 8.2).

It has been reported that EGCG can be a candidate electron donor by releasing an electron or a hydrogen atom, based on its phenolic groups [41, 47, 62]. Accordingly, EGCG typically plays a critical role in free radical scavenging, owing to its antioxidant nature [74]. In the last few decades, a large number of studies have demonstrated that EGCG exhibits strong antiviral activity against various RNA and DNA viruses [27, 36, 38, 61]. However, completely different antiviral mechanisms of action of EGCG have been reported in different viruses. As mentioned earlier, since the grass carp LamR is a receptor for the viral capsid protein VP5, EGCG shows a good inhibitory effect on GCRV I infection [54, 57]. In a recent study, the Muse Count & Viability assay has demonstrated that the viability of all tested fish cell lines, including CIK, GCO, FHM, and EPC cell lines, after treatment with various concentrations of EGCG (from 1 to 90 μg/mL) is about 80–97%. Among these four cell lines, GCO has been shown to present the best viability. In addition, the effect of EGCG, pertaining to the toxicity and immune indicators of grass carp, has previously been evaluated. Grass carp treated with 0, 50, and 100 mg/kg EGCG has shown no significant toxicity. Additionally, EGCG has shown a remarkable ability to increase serum lysozyme activity and glutathione content and decrease the malondialdehyde content in grass carp. Furthermore, the ability of EGCG to treat GCRV infection has been tested in vivo and in vitro. It has been shown that EGCG

can block GCRV infection in a dose-dependent manner in CIK cells, even at concentrations as low as 40 μg/mL EGCG (99%). Compared with the GCRV-infected grass carp not treated with EGCG, feeding on 100 mg/kg (50%) EGCG compound twice a day for a week has been shown to reduce mortality by 50%–90%. Moreover, crude extracts of green tea containing EGCG and the purified EGCG compound have shown similar results of presenting a good inhibitory effect on GCRV infection. In order to understand how EGCG may be used in anti-GCRV drug combinations, several different groups have performed pharmacokinetic studies on EGCG in grass carp. Liquid chromatography with tandem mass spectroscopy analysis has revealed that EGCG is rapidly absorbed by the plasma, kidney, and liver at 8 h post-administration. The peak concentration in the plasma, liver, and kidney has been found to be 103.67 μg/g, 151.34 μg/g, and 2.12 μg/g, respectively [76]. Similarly, another study has reported that EGCG can be detected in the serum, liver, and intestine of the grass carp in the first 15 min of oral administration, and the peak concentration in the serum has been observed to reach 512.8068 μg/mL. Interestingly, both research groups have found that ECG, as an EGCG metabolite, is present in the same set of tissues as the EGCG in the grass carp. Furthermore, since ECG has a chemical structure similar to that of EGCG, the effect of ECG on GCRV inhibition has been investigated, and the incubation of the GCRV with 20 μg/mL ECG resulted in a significant decrease in GCRV infection. Recently, Wang et al. have demonstrated that EGCG can protect mud crabs (*Scylla paramamosain*) from white spot syndrome virus infection. Additionally, they revealed that EGCG can induce the phenoloxidase and JAK-STAT pathways, resulting in enhanced immunity [56]. In addition, it has been reported that EGCG can block several novirhabdoviruses, including spring viremia of carp virus, viral hemorrhagic septicemia virus, and infectious hematopoietic necrosis virus, through the inhibition of serine protease inhibitor gene transcript 1(SERPINE1) [16].

Normally, grass carp hemorrhagic disease outbreaks are often accompanied by other aquatic bacterial and fungal infections. Furthermore, it has been shown that EGCG possesses antimicrobial activity against fungi, streptococci, and other bacteria. Moreover, EGCG has been shown to have low toxicity and enhance immunity. Consequently, EGCG, an antimicrobial agent against various pathogens, shows many potential applications as a protective agent in aquaculture.

8.2.2   Magnolol and Honokiol

Magnolol (5,5′-diallyl-2,2′-dihydroxybiphenyl) and honokiol (5,3′-diallyl-2,4-′-dihydroxybiphenyl) (Fig. 8.3) are small-molecule polyphenolic binaphthalene compounds extracted from the magnolia stem bark. Recent research has reported that both magnolol and honokiol exert beneficial effects in a dose-dependent manner on GCRV inhibition [9, 10]. Magnolol and honokiol have been found to have
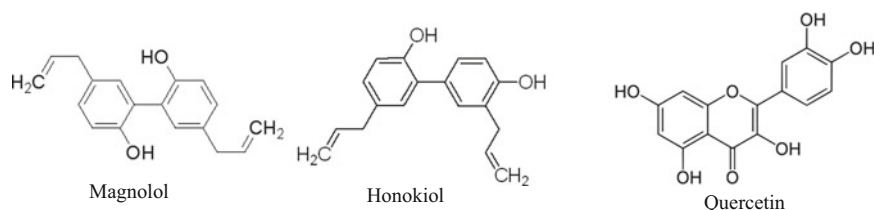
Fig. 8.3 The chemical structural formula of natural compounds against GCRV (Magnolol, Honokiol, and Quercetin)

various biological activities, including antioxidative, anti-inflammatory, antitumor, and antimicrobial activities, with no significant toxicity. Chen et al. reported that magnolol was the leading candidate screened from 30 different herbs predicted to have potential antiviral activity against GCRV infection and that magnolol significantly induced IL-1β expression without affecting the NF-κB signaling pathway in the GCRV-infected cells. Furthermore, they have demonstrated that magnolol can lead to increased resistance to GCRV infection through inhibition of the GCRV-mediated apoptosis [9].

8.2.3 Quercetin

Quercetin (2-(3,4-dihydroxyphenyl)-3,5,7-trihydroxy-4H-chromen-4-one) (Fig. 8.3) is a plant flavonoid found in high concentrations in the capers, dill, red onion, and lovage. It has been demonstrated to exert antiviral, biological, anti-fatigue, vasoprotective, antioxidative, and anti-inflammatory effects [17, 32]. Recently, Yu et al. have demonstrated that the nonstructural protein NS31 of GCRV I viruses (GCRV-JX01) can specifically induce the expression of the proviral heat shock protein 70 (Hsp70) in host cells [77]. Another study has identified that GCRV-104 (GCRV III) induces the expression of the proviral Hsp70 using a mechanism different from that GCRV I viruses [30]. Quercetin has been found to affect the expression level of Hsp70 [29, 59]. Accordingly, blocking grass carp Hsp70 with 50 μM quercetin has been shown to significantly inhibit GCRV-104 replication (Chinese Patent, application no. 202010965543.2). Additionally, no evidence shows that quercetin interferes with the physical function of Hsp70 in host cells. Therefore, these findings indicate that quercetin prevents aquareovirus replication, likely by acting as a specific suppressor of grass carp Hsp70 expression. Furthermore, due to its multiple functions, quercetin is a promising, eco-friendly, broad-spectrum antiviral agent in aquaculture.

8.3   Effect of Chemical Inhibitors Against the GCRV

8.3.1   *Heparin and Chondroitin Sulfate*

Heparin is a polysulfated glycosaminoglycan with a molecular weight ranging from 3 to 30 kDa and is found in secretory granules of mast cells [7, 44]. In addition to its use as an anticoagulant, heparin has been observed to exhibit antiviral effects against the entry and attachment of the influenza virus, hepatitis C virus, and human immunodeficiency virus [13, 14]. Recently, heparin (Fig. 8.4) has been shown to have antiviral effects against GCRV in vitro, including the GCRV I, II, and III strains. Sun et al. have reported that heparin displays an inhibitory effect on viruses at a concentration greater than 100 μg/mL, and after treatment with 20 mg/mL heparin or heparin analog, the levels of viral infection and viral protein synthesis have been shown to reduce significantly for the GCRV I and III species in vitro. However, to our knowledge, the safety and side effects of heparin application in aquaculture are unknown. A unique natural chondroitin sulfate analog has been identified as an antiviral agent against the GCRV. In comparison with heparin, the safety profiles of chondroitin sulfate have been assessed in humans and animals [25]. Therefore, it has great potential to be developed as an anti-GCRV agent.

Heparin   Chondroitin sulfate

Moroxydine hydrochloride   Ribavirin
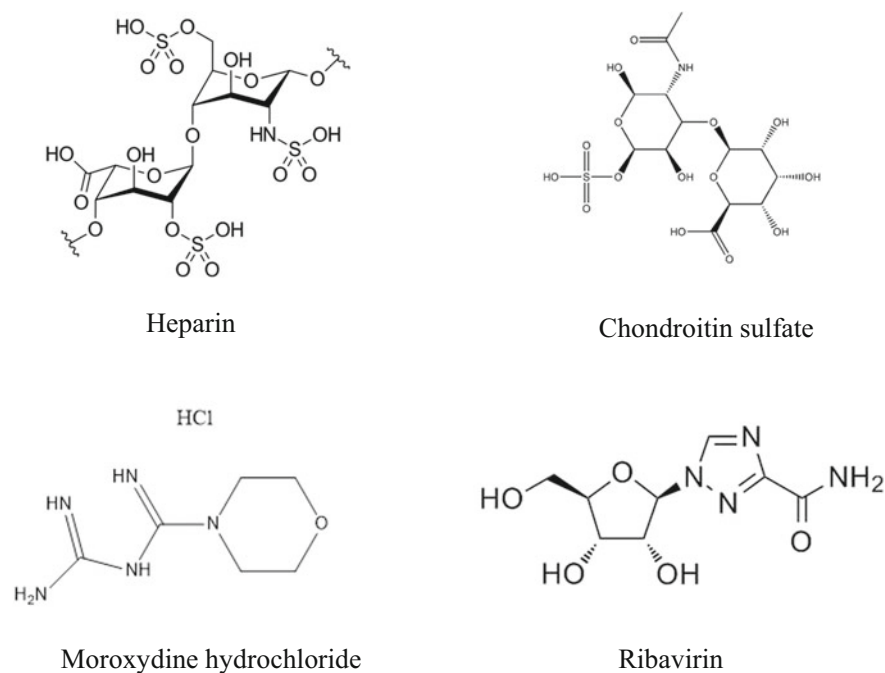
Fig. 8.4 The chemical structural formula of chemical inhibitors against GCRV (chondroitin sulfate, heparin, moroxydine hydrochloride, and ribavirin)

8.3.2   Moroxydine Hydrochloride (Mor)

Mor (Fig. 8.4) is a synthetic antiviral drug initially developed for influenza therapy in the 1950s. Mor has been reported to have multi-antiviral activities against a number of DNA and RNA viruses, including influenza, herpes simplex, varicella zoster, measles, mumps, and hepatitis C viruses. Recently, Yu et al. have reported that 6.3 mg/mL Mor can significantly inhibit the apoptosis of GCRV-infected cells, and animal testing has shown a general reduction in mortality after Mor injection within 7 days [65]. Additionally, the injection of Mor has been found to exhibit a better therapeutic effect than administration via immersion [68]. However, the possible side effects of Mor on humans are largely unknown, even though 500 mg/mL has been proven to be safe for grass carp in the abovementioned study. Moreover, it should be noted that Mor is banned in many countries. Health and food safety factors for humans are critical hurdles in development of medicines, regardless of the therapeutic efficacy of medicines. Therefore, it is unknown whether Mor therapeutics can be applied in aquaculture to control aquatic viral diseases.

8.3.3   Ribavirin (Rib)

Rib (Fig. 8.4) shows antiviral activity against a large number of RNA viruses. In a recent study, Rib has been reported to show a high antiviral activity against the GCRV in vitro and in vivo, while exhibiting an immunomodulatory activity [66]. The GCRV replication level has been observed to reduce gradually with increasing the Rib concentration, especially above the concentration of 40 μg/mL. Similar to Mor, long-term use of Rib, however, can lead to drug resistance and induce influenza virus variation in mammals and poultry. Consequently, Rib has been banned by the Food and Drug Administration, USA and Ministry of Agriculture, China. Furthermore, the applicability of Rib in controlling grass carp hemorrhagic disease remains to be evaluated.

8.4   Effects of Endocytosis Inhibitors Against the GCRV

Normally, the life cycle of a virus involves cell attachment (adsorption), penetration, uncoating, targeting, gene expression, genome replication, virion assembly, maturation, and release of new infectious virus particles [28]. Enveloped viruses entering the host cell take advantage of membrane fusion by conformational changes of specific viral envelope proteins, such as the herpes simplex virus type 1, which enters the host by fusing with the plasma membrane [3]. Due to a lacking lipid bilayer, nonenveloped viruses cannot utilize the membrane fusion functionality to penetrate the host cells [6]. Accordingly, endocytic pathways are essential for

nonenveloped virus entry into the host. It has been reported that there are several endocytosis pathways for viral entrance including macropinocytosis, clathrin-mediated endocytosis, phagocytosis, non-clathrin-mediated endocytosis, and caveolae-independent endocytic uptake. A previous study has demonstrated that the isolate GCRV-JX01 (GCRV I) penetrates CIK cells through a pH-dependent, clathrin-mediated endocytic pathway and relies on the dynamin protein [53]. Herein, endocytosis inhibitors (Fig. 8.5), including ammonium chloride, chloroquine, chlorpromazine, and dynasore, have been shown to successfully block the GCRV entry into CIK cells. Zhang et al. have shown that GCRV-873 (GCRV I) takes advantage of the caveolae/raft-mediated endocytosis for viral entry into the host. This study has confirmed that cholesterol along with methyl-β-cyclodextrin, nystatin, and genistein can strongly suppress the internalization of the GCRV particles but not the inhibitors, chlorpromazine, cholesterol, and blebb [70]. Wang et al. subsequently studied the viral endocytosis pathway used by GCRV-JX01 and indicated that both GCRV-JX01 and GCRV-104 (GCRV III) can be inhibited by chlorpromazine and pitstop2. For detailed findings on the endocytosis pathway of GCRV-873 and GCRV-JX01, please refer to Wang et al. [53] and Zhang et al. [70]. It is notable that many reoviruses can take advantage of multiple endocytic pathways into the host. According to bioinformatics analysis, GCRV-873 and GCRV-JX01 have been classified into GCRV I; however, these two isolates also present many different biological features in vitro and in vivo. For GCRV-104 (GCRV III), it has been reported that its penetration depends on macropinocytosis or the clathrin-mediated endocytic pathway, regulated by dynamin under a specific pH. It has been demonstrated that the pharmacological inhibitors, including dynasore, rottlerin, ammonium chloride, pitstop2, and chlorpromazine, but not IPA-3, methyl-β-cyclodextrin, amiloride, nystatin, latrunculin B, and bafilomycin, can block GCRV-104 infection [24].

Endocytosis is a complex and efficient cellular process essential for several functions of eukaryotic cells [15, 31]. Normally, endocytosis is critical for the regulation of nutrition delivery, cell-to-cell communication, and agonist-activated cell surface receptors. In addition, pathogens can utilize endocytosis as a pathway to enter the host. Over the past decades, pharmacological inhibitors of the endocytosis pathway have become major drug candidates for controlling viral infection [15]. Currently, no commercial endocytosis inhibitors have been applied in aquaculture for prevention and control of the GCRV. Therefore, the screening and application of pharmacological inhibitors for inhibiting viral endocytosis would be reliable, convenient, and highly cost-effective, based on our understanding of the molecular mechanisms underlying the GCRV entry dependent on endocytosis.
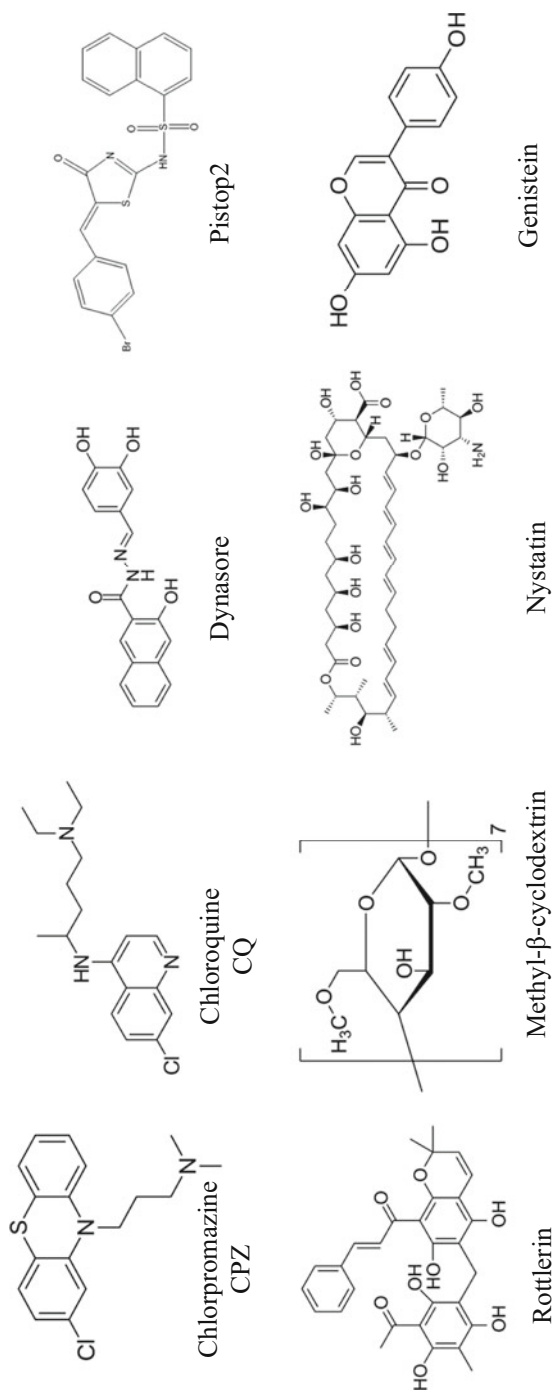
Fig. 8.5 The chemical structural formula of endocytosis inhibitors against GCRV (chlorpromazin, chloroquine, dynasore, pistop2, rottlerin, methyl-β-cyclodextrin, nystatin, and genistein)

8.5 Conclusions and Future Considerations

The GCRV is an important aquatic pathogen, and GCRV outbreaks have affected the advancement of grass carp aquaculture in China. Currently, the application of commercial vaccines, autogenous vaccines, and medical treatment strategies against the GCRV protects grass carp from viral infection. Nevertheless, further research is warranted to compensate for the limitations of vaccine therapeutics. In this chapter, we summarized the potential therapeutic compounds against the GCRV, especially the natural compound EGCG. Notably, EGCG, a small-molecule compound extracted from green tea, exhibits a broad range of antimicrobial activities against bacteria, viruses, and fungi. In addition, many studies support that EGCG has a variety of pharmacological functions in fish and other animals, such as immune enhancement and antioxidant activity. EGCG, as a multifunctional and eco-friendly compound, offers a novel and potential therapeutic option for protecting grass carp against GCRV infection. Furthermore, several chemical inhibitors and endocytosis inhibitors mentioned in this chapter have been proven to exert anti-GCRV activity in vitro. For ensuring food security and reducing environmental pollution, more research should be conducted in this respect. In conclusion, medicinal control, especially through eco-friendly compounds, shows great potential for achieving aquatic disease control in aquaculture.

References

1. Akache B, Grimm D, Pandey K, Yant SR, Xu H, Kay MA (2006) The 37/67-kilodalton laminin receptor is a receptor for adeno-associated virus serotypes 8, 2, 3, and 9. J Virol 80:9831–9836
2. Bonoli M, Pelillo M, Toschi TG, Lercker G (2003) Analysis of green tea catechins: comparative study between HPLC and HPCE. Food Chem 81:631–638
3. Bressanelli S, Stiasny K, Allison SL, Stura EA, Duquerroy S, Lescar J, Heinz FX, Rey FA (2004) Structure of a flavivirus envelope glycoprotein in its low Ph-induced membrane fusion conformation. EMBO J 23:728–738
4. Burckhardt CJ, Greber UF (2009) Virus movements on the plasma membrane support infection and transmission between cells. PLoS Pathog 5:e1000621
5. Busayarat N, Senapin S, Tonganunt M, Phiwsaiya K, Meemetta W, Unajak S, Jitrapakdee S, Lo CF, Phongdara A (2011) Shrimp laminin receptor binds with capsid proteins of two additional shrimp RNA viruses YHV and IMNV. Fish Shellfish Immunol 31:66–72
6. Chandran K, Nibert ML (2003) Animal cell invasion by a large nonenveloped virus: reovirus delivers the goods. Trends Microbiol 11:374–382
7. Chen L, Zhang Q, Yang G, Fan L, Tang J, Garrard I, Ignatova S, Fisher D, Sutherland IA (2007) Rapid purification and scale-up of honokiol and magnolol using high-capacity high-speed counter-current chromatography (vol 1142, Pg 115, 2007). J Chromatogr A 1163:337–337
8. Chen JN, He WR, Shen L, Dong H, Yu JH, Wang X, Yu SX, Li YF, Li S, Luo YZ, Sun Y, Qiu HJ (2015) The laminin receptor is a cellular attachment receptor for classical swine fever virus. J Virol 89:4894–4906

9. Chen X, Hu Y, Shan L, Yu X, Hao K, Wang GX (2017) Magnolol and honokiol from Magnolia officinalis enhanced antiviral immune responses against grass carp reovirus in *Ctenopharyngodon idella* kidney cells. Fish Shellfish Immunol 63:245–254

10. Chen X, Hao K, Yu X, Huang A, Zhu B, Wang GX, Ling F (2018) Magnolol protects *Ctenopharyngodon idella* kidney cells from apoptosis induced by grass carp reovirus. Fish Shellfish Immunol 74:426–435

11. Cheng L, Fang Q, Shah S, Atanasov IC, Zhou ZH (2008) Subnanometer-resolution structures of the grass carp reovirus core and virion. J Mol Biol 382:213–222

12. Cheng L, Zhu J, Hui WH, Zhang X, Honig B, Fang Q, Zhou ZH (2010) Backbone model of an aquareovirus virion by cryo-electron microscopy and bioinformatics. J Mol Biol 397:852–863

13. Colpitts CC, Schang LM (2014) A small molecule inhibits virion attachment to heparan sulfate- or sialic acid-containing glycans. J Virol 88:7806–7817

14. Connell BJ, Lortat-Jacob H (2013) Human immunodeficiency virus and heparan sulfate: from attachment to entry inhibition. Front Immunol 4:385

15. Dutta D, Donaldson JG (2002) Search for inhibitors of endocytosis: intended specificity and unintended consequences. Cell Logist 2(4):203–208

16. Estepa A, Coll J (2015) Inhibition of SERPINe1 reduces rhabdoviral infections in zebrafish. Fish Shellfish Immunol 47:264–270

17. Ezzati M, Yousefi B, Velaei K, Safa A (2020) A review on anti-cancer properties of Quercetin in breast cancer. Life Sci 248:12

18. Fan Y, Rao S, Zeng L, Ma J, Zhou Y, Xu J, Zhang H (2013) Identification and genomic characterization of a novel fish reovirus, Hubei grass carp disease reovirus, isolated in 2009 in China. J Gen Virol 94:2266–2277

19. Fang Q, Shah S, Liang Y, Zhou ZH (2005) 3D reconstruction and capsid protein characterization of grass carp reovirus. Sci China C Life Sci 48:593–600

20. Fang Q, Seng EK, Ding QQ, Zhang LL (2008) Characterization of infectious particles of grass carp reovirus by treatment with proteases. Arch Virol 153:675–682

21. Fassina G, Buffa A, Benelli R, Varnier OE, Noonan DM, Albini A (2002) Polyphenolic antioxidant (−)-epigallocatechin-3-gallate from green tea as a candidate anti-HIV agent. AIDS 16:939–941

22. Fujimura Y, Umeda D, Yano S, Maeda-Yamamoto M, Yamada K, Tachibana H (2007) The 67kDa laminin receptor as a primary determinant of anti-allergic effects of *O*-methylated EGCG. Biochem Biophys Res Commun 364:79–85

23. Gauczynski S, Peyrin JM, Haïk S, Leucht C, Hundt C, Rieger R, Krasemann S, Deslys JP, Dormont D, Lasmézas CI (2001) The 37-kDa/67-kDa laminin receptor acts as the cell-surface receptor for the cellular prion protein. EMBO J 20:5863–5875

24. Hao W, Liu W, Meng S, Chen D, Zeng L, Lu L, Jing XJ (2018) Inhibitor analysis revealed that clathrin-mediated endocytosis is involved in cellular entry of type III grass carp reovirus. Virol J 15:92

25. Hatano S, Watanabe H (2020) Regulation of macrophage and dendritic cell function by chondroitin sulfate in innate to antigen-specific adaptive immunity. Front Immunol 11:232

26. Jiang YL (2009) Hemorrhagic disease of grass carp: status of outbreaks, diagnosis, surveillance, and research. Isr J Aquac 61:188–197

27. Khan N, Mukhtar H (2019) Tea polyphenols in promotion of human health. Nutrients 11:39

28. Kibenge FSB, Godoy MG (2016) Reoviruses of aquatic organisms. Academic Press, pp 205–236

29. Kiyga E, Sengelen A, Adiguzel Z, Onay Ucar E (2020) Investigation of the role of quercetin as a heat shock protein inhibitor on apoptosis in human breast cancer cells. Mol Biol Rep 47:4957–4967

30. Li W, Yu F, Wang H, Hong X, Lu L (2020) Induction of pro-viral grass carp *Ctenopharyngodon idella* Hsp70 instead of Hsc70 during infection of grass carp reovirus. Fish Shellfish Immunol 98:1024–1029

31. Liu J, Sun Y, Drubin DG, Oster GF (2009) The mechanochemistry of endocytosis. PLoS Biol 7: e1000204
32. Liu X, Raghuvanshi R, Ceylan FD, Bolling BW (2020) Quercetin and its metabolites inhibit recombinant human angiotensin-converting enzyme 2 (ACE2) activity. J Agric Food Chem 68:13982–13989
33. Lu L, Xu H, He Y, Li J (2011) Protection of grass carp, Ctenopharyngon idellus (Valenciennes), through oral administration of a subunit vaccine against reovirus. J Fish Dis 34:939–942
34. Mereles D, Hunstein W (2011) Epigallocatechin-3-gallate (EGCG) for clinical trials: more pitfalls than promises? Int J Mol Sci 12:5592–5603
35. Mertens P (2004) The dsRNA viruses. Virus Res 101:3–13
36. Nagula RL, Wairkar S (2019) Recent advances in topical delivery of flavonoids: a review. J Control Release 296:190–201
37. Nibert ML, Duncan R (2013) Bioinformatics of recent aqua- and orthoreovirus isolates from fish: evolutionary gain or loss of FAST and fiber proteins and taxonomic implications. PLoS One 8:e68607
38. Prasanth MI, Sivamaruthi BS, Chaiyasut C, Tencomnao T (2019) A review of the role of green tea (*Camellia sinensis*) in antiphotoaging, stress resistance, neuroprotection, and autophagy. Nutrients 11:474
39. Rao YL, Su JG (2015) Insights into the antiviral immunity against grass carp (*Ctenopharyngodon idella*) reovirus (GCRV) in grass carp. J Immunol Res 2015:670437
40. Shang X, Pan H, Li M, Miao X, Ding H (2011) *Lonicera japonica* Thunb.: ethnopharmacology, phytochemistry and pharmacology of an important traditional Chinese medicine. J Ethnopharmacol 138:1–21
41. Steinmann J, Buer J, Pietschmann T, Steinmann E (2013) Anti-infective properties of epigallocatechin-3-gallate (EGCG), a component of green tea. Br J Pharmacol 168:1059–1073
42. Su S, Tang Y, Chang B, Zhu W, Chen Y (2020) Evolution of marine fisheries management in China from 1949 to 2019: how did China get here and where does China go next? Fish Fish 21:435–452
43. Tachibana H, Koga K, Fujimura Y, Yamada K (2004) A receptor for green tea polyphenol EGCG. Nat Struct Mol Biol 11:380–381
44. Tanaka S, Takakuwa Y (2016) A method for detailed analysis of the structure of mast cell secretory granules by negative contrast imaging. Sci Rep 6:1–8
45. Tao W, Xu X, Wang X, Li B, Wang Y, Li Y, Yang L (2013) Network pharmacology-based prediction of the active ingredients and potential targets of Chinese herbal Radix Curcumae formula for application to cardiovascular disease. J Ethnopharmacol 145:1–10
46. Thawonsuwan J, Kiron V, Satoh S, Panigrahi A, Verlhac V (2010) Epigallocatechin-3-gallate (EGCG) affects the antioxidant and immune defense of the rainbow trout, *Oncorhynchus mykiss*. Fish Physiol Biochem 36:687–697
47. Umeda D, Yano S, Yamada K, Tachibana H (2008) Green tea polyphenol epigallocatechin-3-gallate signaling pathway through 67-kDa laminin receptor. J Biol Chem 283:3050–3058
48. Wang K-S, Kuhn R, Strauss E, Ou S, Strauss J (1992) High-affinity laminin receptor is a receptor for Sindbis virus in mammalian cells. J Virol 66:4992–5001
49. Wang X, Sun H, Zhang A, Sun W, Wang P, Wang Z (2011) Potential role of metabolomics approaches in the area of traditional Chinese medicine: as pillars of the bridge between Chinese and Western medicine. J Pharm Biomed Anal 55:859–868
50. Wang Q, Zeng W, Liu C, Zhang C, Wang Y, Shi C, Wu S (2012) Complete genome sequence of a reovirus isolated from grass carp, indicating different genotypes of GCRV in China. J Virol 86:12466
51. Wang T, Li J, Lu L (2013) Quantitative in vivo and in vitro characterization of co-infection by two genetically distant grass carp reoviruses. J Gen Virol 94:1301–1309
52. Wang L, Yang R, Yuan B, Liu Y, Liu C (2015) The antiviral and antimicrobial activities of licorice, a widely-used Chinese herb. Acta Pharm Sin B 5:310–315

53. Wang H, Liu W, Yu F, Lu L (2016) Disruption of clathrin-dependent trafficking results in the failure of grass carp reovirus cellular entry. Virol J 13:25
54. Wang H, Liu WS, Yu F, Lu LQ (2016) Identification of (-)-epigallocatechin-3-gallate as a potential agent for blocking infection by grass carp reovirus. Arch Virol 161:1053–1059
55. Wang H, Yu F, Li JL, Lu LQ (2016) Laminin receptor is an interacting partner for viral outer capsid protein VP5 in grass carp reovirus infection. Virology 490:59–68
56. Wang Z, Sun B, Zhu F (2017) Epigallocatechin-3-gallate inhibit replication of white spot syndrome virus in Scylla paramamosain. Fish Shellfish Immunol 67:612–619
57. Wang H, Chen Y, Ru G, Xu Y, Lu L (2018) EGCG: potential application as a protective agent against grass carp reovirus in aquaculture. J Fish Dis 41:1259–1267
58. Wang QC, Ji W, Xu Z (2020) Current use and development of fish vaccines in China. Fish Shellfish Immunol 96:223–234
59. Wang X, Zhu Y, Zhou Q, Yan Y, Qu J, Ye H (2020) Heat shock protein 70 expression protects against sepsis-associated cardiomyopathy by inhibiting autophagy. Hum Exp Toxicol 19:960327120965758
60. Wu M, Li H, Chen X, Jiang Y, Jiang W (2020) Studies on the clinical symptoms, virus distribution, and mRNA expression of several antiviral immunity-related genes in grass carp after infection with genotype II grass carp reovirus. Arch Virol 165:1599–1609
61. Xing L, Zhang H, Qi R, Tsao R, Mine Y (2019) Recent advances in the understanding of the health benefits and molecular mechanisms associated with green tea polyphenols. J Agric Food Chem 67:1029–1043
62. Xu J, Xu Z, Zheng W (2017) A review of the antiviral role of green tea catechins. Molecules 22:1337
63. Yan L, Wang X, Liu H, Tian Y, Lian J, Yang R, Hao S, Wang X, Yang S, Li Q, Qi S, Kui L, Okpekum M, Ma X, Zhang J, Ding Z, Zhang G, Wang W, Dong Y, Sheng J (2015) The genome of dendrobium officinale illuminates the biology of the important traditional chinese orchid herb. Mol Plant 8:922–934
64. Ye X, Tian YY, Deng GC, Chi YY, Jiang XY (2012) Complete genomic sequence of a reovirus isolated from grass carp in China. Virus Res 163:275–283
65. Yu XB, Chen XH, Ling F, Hao K, Wang GX, Zhu B (2016) Moroxydine hydrochloride inhibits grass carp reovirus replication and suppresses apoptosis in *Ctenopharyngodon idella* kidney cells. Antivir Res 131:156–165
66. Yu XB, Hao K, Li J, Chen XH, Wang GX, Ling F (2018) Effects of moroxydine hydrochloride and ribavirin on the cellular growth and immune responses by inhibition of GCRV proliferation. Res Vet Sci 117:37–44
67. Yu F, Wang L, Li W, Lu LJ (2019) Identification of a novel membrane-associated protein from the S7 segment of grass carp reovirus. J Gen Virol 100:369–379
68. Yu XB, Hao K, Ling F, Zhu B, Wang GX (2020) In vivo antiviral efficacy of moroxydine hydrochloride against grass carp reovirus and the drug safety assessment. Aquac Res 51:1592–1601
69. Zhang X, Jin L, Fang Q, Hui WH, Zhou ZH (2010) 3.3 A cryo-EM structure of a nonenveloped virus reveals a priming mechanism for cell entry. Cell 141:472–482
70. Zhang F, Guo H, Zhang J, Chen Q, Fang Q (2017) Identification of the caveolae/raft-mediated endocytosis as the primary entry pathway for aquareovirus. Virology 513:195
71. Zhang D-h, Wu K-l, Zhang X, Deng S-q, Peng B (2020) In silico screening of Chinese herbal medicines with the potential to directly inhibit 2019 novel coronavirus. J Integr Med 18:152–158
72. Zhao Q, Chen X-Y, Martin C (2016) Scutellaria baicalensis, the golden herb from the garden of Chinese medicinal plants. Sci Bull 61:1391–1398
73. Zhu F (2020) A review on the application of herbal medicines in the disease control of aquatic animals. Aquaculture 526:735422

74. Zhu W, Xu J, Ge Y, Cao H, Ge X, Luo J, Xue J, Yang H, Zhang S, Cao J (2014) Epigallocatechin-3-gallate (EGCG) protects skin cells from ionizing radiation via heme oxygenase-1 (HO-1) overexpression. J Radiat Res 55:1056–1065
75. Zou G, Fang Q (1999) Study on replication and morphogenesis of the grass carp reovirus (GCRV) in CIK cells. Virol Sin 15:188–192
76. Zhang Y, Wang H, Meizhen S, Lu L (2020) (−)-Epicatechin gallate, a metabolite of (−)-epigallocatechin gallate in grass carp, exhibits antiviral activity in vitro against grass carp reovirus. Aquac Res 51(4):1673–1680
77. Yu F, Wang L, Li W, Wang H, Shun Q, Lu L (2020) Aquareovirus NS31 protein serves as a specific inducer for host heat shock 70-kDa protein. J Gen Virol 101(2):145–155

Chapter 9
Anti-Aquareovirus Immunity

Jianguo Su

Abstract In this chapter, immunity against aquareoviruses (mainly grass carp reovirus and piscine orthoreovirus) is discussed, including the innate and adaptive immunities. Innate immunity mainly involves the high-mobility group box proteins (HMGBs), toll-like receptors (TLRs), retinoic acid-inducible gene I (RIG-I)-like receptors (RLRs), nucleotide-binding domain and leucine-rich repeat containing receptors (NLRs), and other antiviral signaling molecules and their signaling pathways. In addition, TLR- and RLR-mediated grass carp antiviral signaling pathways have been described in detail. TLRs and RLRs activate and phosphorylate IFN regulatory factors (IRF)3 and IRF7, triggering type I interferon (IFN) and IFN-inducible proteins, such as myxovirus resistance (Mx) proteins and adenosine deaminase acting on RNA (ADAR) proteins, for antiviral responses. TLRs and RLRs also induce inflammatory responses via the nuclear factor κ-light-chain-enhancer of activated B cells (NF-κB) pathway. Adaptive immunity involves the humoral and cellular immune responses, including the lymphocytes, immunoglobulins (Igs), T-cell receptor (TCR), and major histocompatibility complex (MHC). In general, the relationship between innate and adaptive immunities is indiscrete and complementary. We hope that this chapter lays a foundation for future research on antiviral immunity, contributes to aquaculture in the prevention and control of aquareovirus diseases, and serves towards healthy and sustainable development of the aquaculture industry.

Keywords Aquareovirus · Innate immunity · Adaptive immunity · TLRs · RLRs

J. Su (✉)
Department of Aquatic Animal Medicine, College of Fisheries, Huazhong Agricultural University, Wuhan, China

Laboratory for Marine Biology and Biotechnology, Pilot National Laboratory for Marine Science and Technology, Qingdao, China
e-mail: sujianguo@mail.hzau.edu.cn

Abbreviations

ADAR	Adenosine deaminase acting on RNA
AP-1	Activator protein 1
BATF	Basic leucine zipper transcription factor ATF-like
BCAP	B-cell adaptor for phosphoinositide 3-kinase
CAB	*Carassius auratus* blastulae embryonic
CARD	Caspase activation and recruitment domain
CIK	*Ctenopharyngodon idella* kidney
ER	Endoplasmic reticulum
GCRV	Grass carp reovirus
HMGB	High-mobility group box
IFN	Interferon
Ig	Immunoglobulin
IKK	Inhibitor of κB kinase
IL	Interleukin
IPS-1	IFN-β promoter stimulator 1
IRF	IFN regulatory factor
ISG	IFN-stimulated gene
LGP2	Laboratory of genetics and physiology 2
LPS	Lipopolysaccharide
LRR	Leucine-rich repeat
MAMP	Microbe-associated molecular pattern
MAPK	Mitogen-activated protein kinase
MDA5	Melanoma differentiation associated gene 5
MHC I	MHC class I
MHC II	MHC class II
MHC	Major histocompatibility complex
Mx	Myxovirus resistance
MyD88	Myeloid differentiation primary response 88
NF-κB	Nuclear factor κ-light-chain-enhancer of activated B cells
NLR	Nucleotide-binding domain and leucine-rich repeat containing receptor
NOD	Nucleotide-binding oligomerization domain
PGN	Peptidoglycan
PKR	Protein kinase R
PKZ	Z-DNA binding protein kinase
Poly(I:C)	Polyinosinic:polycytidylic acid
PRR	Pattern recognition receptor
PRV	Piscine orthoreovirus
RD	Repressor domain
RIG-I	Retinoic acid-inducible gene I
RIP1	Receptor interacting protein 1
RLR	RIG-I-like receptor
RNAi	RNA interference

ROS   Reactive oxygen species
SARM1   Sterile-α- and armadillo motif-containing protein 1
SR   Scavenger receptor
STING   Stimulator of interferon gene
TBK1   TRAF family member-associated NF-κB activator binding kinase 1
TCR   T-cell receptor
TIR   Toll/IL-1 receptor
TIRAP   TIR domain-containing adaptor protein
TLR   Toll-like receptor
TM   Transmembrane
TRAM   TRIF-related adaptor molecule
TRIF   TIR domain-containing adaptor-inducing IFN-β
γC   Receptor γ chain

9.1 Introduction

Viruses belonging to the genus *Aquareovirus* have been isolated from a wide variety of aquatic animals, including shellfish and bony fish. Grass carp reovirus (GCRV), the most common aquareovirus isolated in China, causes the fatal hemorrhagic disease pandemic in cultured grass carp. GCRV is a double-stranded RNA (dsRNA) virus that belongs to the *Aquareovirus* genus in the *Reoviridae* family [59]. Many investigations have been conducted on understanding virus-induced responses in the grass carp from genomic to transcriptomic levels, as well as immunoprotection and immunogenicity of its proteins in the past decades. In general, antiviral immunity involves the innate and adaptive immunities. Innate immunity, which mainly involves the pattern recognition receptors (PRRs) that sense the presence of microbe-associated molecular patterns (MAMPs) and related signaling pathways in aquatic animals, has been researched more thoroughly than adaptive immunity.

Piscine orthoreovirus (PRV), the pathogen isolated from farmed Atlantic salmon, is classified to the genus *Orthoreovirus* in the family *Reoviridae* mainly based on its 10-segmented dsRNA genome and deduced protein characteristics. PRV is considered ubiquitous in farmed Atlantic salmon. It is an emergent virus in salmon aquaculture and associated with the heart and skeletal muscle inflammation and proven to cause erythrocyte inclusion body syndrome. Studies have shown that erythrocytes are the main targets of PRV and the main replication site of PRV during the early peak of infection. The PRV-infected red blood cells mount a strong, long-lasting innate antiviral response that lasts for several weeks, and infected red blood cells contribute to further virus dissemination to various host tissues. Trout erythrocytes express retinoic acid-inducible gene I (RIG-I) and toll-like receptor (TLR)3 after PRV induction and produce functional interferon-a (IFNa). The

transcription of type I IFNs is induced by the dsRNA receptors through the activation of IFN regulatory factors (IRFs), which mediate further antiviral responses [44].

9.2 Innate Immunity

Compared with higher mammals or human beings, fish innate immunity plays a more significant role in protection against infection of various invading pathogens. As is known, fish possess conserved PRRs that are responsible for sensing the presence of MAMPs with structural domains conserved across many microorganisms during molecular evolution. Generally, PRRs are categorized into four main classes, TLRs, RIG-I-like receptors (RLRs), nucleotide-binding domain and leucine-rich repeat containing receptors (NLRs), and C-type lectin receptors. Of these, TLRs and RLRs play crucial roles in the recognition of viral MAMPs or viruses. As such, TLRs or RLRs deliver signals to the adaptor molecules, which trigger large-scale amplification of signaling to activate IFN or nuclear factor κ-light-chain-enhancer of activated B cells (NF-κB) pathways via IRFs. Subsequently, IFNs, as well as IFN-stimulated genes (ISGs) of host cells, initiate the first antiviral response. In the following sections, we will elaborate on some of the PRRs, especially TLRs and RLRs, as well as their adaptor molecules and downstream signaling pathways.

9.2.1 High-Mobility Group Box Proteins

High-mobility group box (HMGB) proteins, the members of the high-mobility group superfamily, are self-derived immune activators that exert multiple functions in the regulation of immunity and inflammation. HMGB proteins not only can trigger inflammatory responses, but also act as a sensor of nucleic-acid-mediated immune responses. Furthermore, HMGBs are chromatin-associated proteins, which are highly conserved from invertebrates to vertebrates. Four members of HMGBs (HMGB1–4) have been identified in mammals. A highly conserved primary structure (>80% amino acid identity) is found in HMGB1–3, which comprise two DNA binding domains (HMG-box A and B) and a C-terminal acidic tail enriched with negatively charged glutamic and aspartic acid residues; HMGB4 does not have the acidic tail. However, not all members of HMGBs exist in low vertebrates or invertebrates, and the members of HMGBs vary across different species. For example, HMGB1–3 are generally present in cartilaginous fish, bony fish, and tetrapods, but no HMGB3 is present in the *Gasterosteidae* (stickleback), species *Oryzias latipes* (medaka) and *Takifugu rubripes* (fugu). Furthermore, two paralogs of each of the mammalian HMGB1, HMGB2, and HMGB3 have been characterized in the grass carp, Atlantic salmon (*Salmo salar*), goldfish (*Carassius auratus L.*), and common carp (*Cyprinus carpio*), and their expression is upregulated upon GCRV infection or recognition of viral MAMPs [26, 55, 57]. HMGBs have two members,

HMGBa and HMGBb in *Litopenaeus vannamei*, and only the *HMGB1* gene is identified in the Pacific oyster (*Crassostrea gigas*) and the Zhikong scallop (*Chlamys farreri*).

Evidence suggests that HMGB proteins can serve as universal sentinels for nucleic-acid-mediated innate immune responses. As ligands and sensors for innate immunity, HMGBs can sense immunogenic nucleic acids and evoke an immune response by delivering signals to PRRs, such as TLRs and RLRs. On the contrary, non-immunogenic oligodeoxynucleotides binding to HMGBs suppress the immune responses. In mammals, HMGB1 and HMGB3 bind DNA as well as RNA, but HMGB2 only interacts with immunogenic DNA. In grass carp, GCRV, polyinosinic: polycytidylic acid (poly(I:C)), and lipopolysaccharide (LPS) challenges evoke the nuclear export of HMGBs, with all the different HMGB family members reacting at varying degrees [26, 27, 55, 57]. Antiviral activities of HMGB1, HMGB2 and HMGB3 are exhibited through reduction of the cytopathic effect and inhibition of GCRV replication in *Ctenopharyngodon idella* kidney (CIK) cells. Moreover, all the HMGB family members not only mediate antiviral immune responses, but also are involved in responding to viral and bacterial MAMP challenges [26, 55, 57]. Some of the vital downstream molecules of TLRs and RLRs are remarkably regulated in all HMGB-overexpressing cells, especially adaptors such as Toll/IL-1 receptor (TIR) domain-containing adaptor-inducing IFN-β (TRIF, also known as TICAM1), IFN-β promoter stimulator 1 (IPS-1) and myeloid differentiation primary response 88 (MyD88). Therefore, the signals from HMGBs may be transmitted to downstream proteins through the TLR and RLR pathways.

In general, HMGB is a classic nuclear protein, they can transit from the nucleus to the cytoplasm, and ultimately, are secreted into the extracellular medium. In grass carp, under basal conditions, all the six HMGBs (HMGB1a–3a and HMGB1b–3b) exclusively localize in the nucleus. The GCRV, poly(I:C), and LPS challenges evoke the nucleocytoplasmic translocation of HMGBs to varying degrees. Among all the HMGBs, GCRV infection induces the highest nuclear export of HMGB2b and the lowest nucleocytoplasmic translocation of HMGB1b. Poly(I:C) modulates the relocation of HMGB1a, HMGB1b, and HMGB3a, while LPS evokes the intense nucleocytoplasmic shuttling of HMGB1b. However, these challenges seldom cause the nucleocytoplasmic shuttling of HMGB2a and HMGB3b. Using constructed full-length, truncated, or chimeric HMGBs, the intramolecular interaction between HMG-boxes and C-tail domains mediates the nucleocytoplasmic translocation of HMGBs, as confirmed by dynamic relocation analyses. These analyses provide experimental evidence for further elucidation of the interactions among pathogens, HMGBs, and PRRs in fish innate immunity [27].

It is well known that HMGBs act as "damage-associated molecular patterns," which are cellular "danger signals" released from injured or necrotic cells, and bind to TLRs and modulate inflammatory reactions. GCRV infection stimulates active secretion and passive release of some HMGBs that are prone to translocate from the nucleus, which is a process associated with necrosis and death of all the cells (Fig. 9.1). In infected CIK cells, replication and assembly of GCRV occurs within a viral inclusion body-like structure in the perinuclear region of the cell cytoplasm;
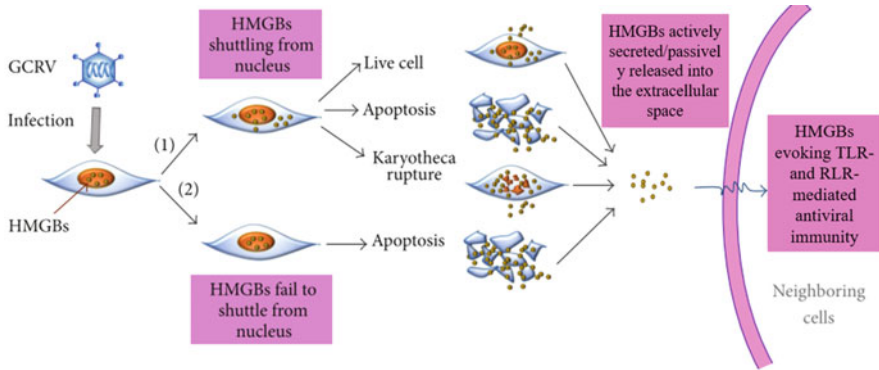
Fig. 9.1 Antiviral immune responses of GCRV infection-induced HMGBs in CIK cells. In CIK cells, there exist two pathways inducing HMGBs for their nucleocytoplasmic translocation upon GCRV infection. The first pathway leads to HMGBs shuttling from the nucleus to the cytoplasm during GCRV infection. Subsequently, cell apoptosis and nuclear membrane rupture lead to the passive release of HMGBs into the extracellular space and cell death. However, some living cells can actively secrete HMGBs, making them cross the cell membrane and enter the extracellular space. The second pathway functions when GCRV does not lead to the shuttling of HMGB2a and HMGB3b, it can cause cell necrosis or damage, thereby causing these HMGBs to be passively released into the extracellular matrix. Now, the extracellular HMGBs initiate an antiviral immune activation response mediated by TLRs and RLRs in the adjacent cells [25]

these viral inclusion bodies insulate viral particles from the contiguous cytoplasm. However, some of the HMGBs present in the cytoplasm recognize virus-derived nucleic acids and transmit signals to cytoplasmic receptors, triggering an antiviral immune response. In the case of GCRV infection not leading to the active shuttling of HMGB2a and HMGB3b, GCRV will cause cell necrosis or damage, and the HMGBs are passively released into the extracellular region. Next, the extracellular HMGBs may interact with the surface receptors of adjacent cells to act as cytokines or play proinflammatory roles. However, pathogenic stimulation or stress induces nuclear HMGB1 to shuttle to the cytoplasm, where HMGB1 is actively secreted or passively released into the extracellular matrix. HMGB1 exerts important nuclear, cytosolic, and extracellular roles in regulating autophagy under oxidative stress, starvation conditions, or chemotherapy. Studies have shown that GCRV challenge and H_2O_2 treatment induce the accumulation of reactive oxygen species (ROS) in CIK cells, which further enhances autophagy activation. However, ROS-induced autophagy, in turn, dramatically restricts GCRV replication. Simultaneously, ROS can trigger HMGB1b translocation to the cytosol, where HMGB1b interacts with beclin 1 and subsequently induces autophagy [29]. Therefore, HMGBs, as sensors of nucleic-acid-mediated immune response, can transmit signals to downstream proteins through TLRs and RLRs, display a variety of functions, and have important roles in the regulation of immune and inflammatory responses, with significant research value. Currently, most studies are based at the transcriptional level;

however, fish antibody production is urgently needed to reveal the immune-regulatory mechanisms at the protein level.

9.2.2 TLR Signaling Pathways

9.2.2.1 TLRs

The initiation of innate and adaptive immune responses is mediated by PRRs via the recognition of invading microbial pathogens. PRRs play important roles in the innate immune system in both vertebrates and invertebrates, and hence, TLRs have been extensively studied and characterized [10]. Currently, there exist TLR1–TLR10 in humans, and they can be used as receptor molecules in immune functions. Among them, TLR4 is believed to be one of the earliest discovered receptor-related proteins. Until date, 13 TLRs (TLR1–13) have been identified in mammals, and TLR11, 12, and 13 have been identified only in the murine genome. Furthermore, 20 *TLR* genes have been identified in catfish, while 21 TLRs have been identified in grass carp, including TLR1–3, TLR4-(1–4), TLR5a/5b, TLR7, TLR8a/8b, TLR9, TLR18, TLR19, TLR20a/20b, TLR21, TLR22a/22b, and TLR25. Interestingly, TLR6 and TLR10 are absent in all fish genomes based on extensive sequencing analysis. In contrast, TLR18, 19, 20, 23, 25, 26, 27, and 28 are only identified in fish and seem to be fish-specific [17, 58]. TLRs are classified into six main subfamilies TLR1, TLR3, TLR4, TLR5, TLR7, and TLR11, according to phylogenetic analysis. TLR1, TLR2, TLR6, TLR10, TLR18, TLR25, and TLR28 are contained in the TLR1 subfamily. The subfamilies TLR3–5 are monotypic. The TLR7 subfamily comprises TLR7–9, while the remaining TLR11–13, TLR19–22, and TLR26–27 are included in the TLR11 subfamily.

In teleosts and mammals, TLRs are identified as type I transmembrane protein receptors, which contain three domains: the N-terminal leucine-rich repeat (LRR) domain, transmembrane domain (TM), and TIR domain. The N-terminal LRR domain can recognize ligands, and the TIR domain functions to activate downstream signaling by interaction with and recruitment of adaptor proteins. Unlike the cytoplasmic receptors, the TLR family includes receptors residing on the cell surface or in the organelle compartments, highlighting the specialization of receptor subsets for particular tasks. In mammals, TLR1–2, TLR4–6, and TLR10–12 mainly localize on the cytomembrane, where they recognize MAMPs derived from extracellular microbes. Intracellular TLRs, including TLR3, 7, 8, 9, and 13, are found to be expressed in the endoplasmic reticulum (ER), endosomes, multivesicular bodies, and lysosomes, and they are intrinsically capable of detecting nucleic acids. In mammals, TLR3-deficient mice are shown to be resistant to poly(I:C)-dependent shock, and macrophages from these mice appear to show diminished IFN induction in response to poly(I:C), suggesting that TLR3 mediates IFN induction in response to dsRNA molecules.
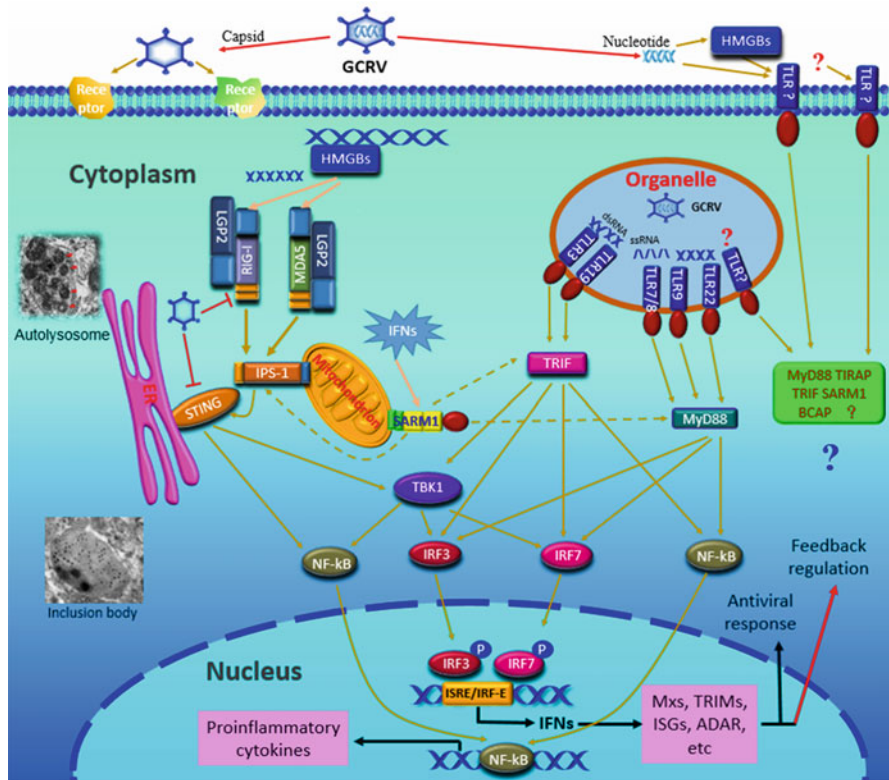
Fig. 9.2 TLR- and RLR-mediated signaling pathways in grass carps during viral infection. GCRV enters the fish and first activates HMGBs that initiate antiviral immune activation in TLR- and RLR-mediated manners. TLR3 and TLR19 recognize viral dsRNA molecules and send signals to the downstream dsRNA adaptor TRIF. TLR22 recognizes the dsRNA molecules; TLR7/8 detect ssRNA molecules; and TLR9 detects unmethylated CpG DNA molecules and transmits the signal to MyD88. RIG-I and melanoma differentiation associated gene 5 (MDA5) detect dsRNA or ssRNA of different lengths and activate the mitochondrial IPS-1; in contrast, laboratory of genetics and physiology 2 (LGP2) plays a negative/positive role at upstream of RIG-1 and MDA5. Stimulator of interferon gene (STING) localizes in the ER near IPS-1 and activates TRAF family member-associated NF-κB activator binding kinase 1 (TBK1) to induce phosphorylation of IRF3 and IRF7. The TLR and RLR adaptors induce phosphorylation and activation of IRF3 and IRF7 through some signal transduction molecules. The phosphorylated IRF3 and IRF7 interact with a combination of IFN-stimulated response elements (ISREs) and induce type I IFN to produce myxovirus resistance proteins (Mxs), TRIMs, ISG15, adenosine deaminase acting on RNA (ADAR), etc., thereby inducing immune regulation. Similarly, TLRs and RLRs can also trigger the NF-κB pathway to induce inflammatory responses

We have previously summarized the GCRV-induced signaling pathways in grass carp (Fig. 9.2). Different TLRs can sense varieties of nucleic acids originating from viral or other pathogenic genome. After recognizing the respective MAMPs, TLRs allow for homodimeric or heterodimeric interactions by changing their conformation and recruit adaptor molecules, such as TRIF, MyD88, and TRIF-related adaptor

molecule (TRAM), to their TIR domains to trigger the activation of NF-κB and IFN-I pathways. MyD88, TRIF, TIR domain-containing adaptor protein (TIRAP/Mal), TRAM, B-cell adaptor for phosphoinositide 3-kinase (BCAP), CSK-interacting membrane protein (SCIMP) and sterile-alpha and armadillo motif-containing protein 1 (SARM1) are the seven identified TIR-associated in mammals. TRAM is absent in teleosts. Among them, based on the usage of the distinct adaptor molecules, the involvement of MyD88 and TRIF in two distinct pathways has roughly been determined. With the exception of TLR3, almost all the TLRs possess the MyD88-dependent signaling pathway in mammals [13]. In this way, TLR3 recruits the adaptor molecule TRIF, which then activates the Ikke/Ikki/TBK1 complex, further phosphorylating IRF3 and inducing the expression of type I IFN. TIRAP is necessary for the TLR2/TLR4/MyD88-dependent activation of NF-κB; TRAM is critical to the TLR4/TRIF-dependent signaling pathway. In teleosts, although MyD88 is used by most TLRs, the TRIF pathway can be recruited by TLR19 and TLR3 [11].

9.2.2.2 TLR Adaptor Molecules

Several adaptors are involved in TLR signaling, including MyD88, TRIF, TIRAP, BCAP, TRAM, and SARM1. In bony fish, it is found that MyD88, TIRAP, TRIF, BCAP, and SARM1 are expressed in zebrafish embryonic cells, whereas adult fish have markedly higher expression of MyD88 than the other molecules. Moreover, MyD88, an important adaptor, plays critical roles in the TLR signaling pathway [39]. In *Miichthys miiuy*, MyD88 is broadly expressed in the brain, eye, gill, fin, intestine, heart, head kidney, muscle, liver and spleen, with the highest and lowest expression detected in the liver and kidney, respectively [38]. MyD88 expression is further elevated by stimulation with MAMPs, such as LPS, poly(I:C), and peptidoglycan (PGN), in the peripheral blood leukocytes of the Japanese flounder. MyD88 is constitutively expressed in unstimulated head kidney leukocytes of the rainbow trout, but its expression is not induced by a poly(I:C) challenge, the flagellin, and the compound R848. However, MyD88 mRNA is found to be widely expressed in all grass carp tissues, and it is highly expressed in the spleen and skin and weakly expressed in the trunk kidney and muscle. After GCRV infection, MyD88 expression in the spleen tissue first slowly increases, reaches a peak 24 h post-infection, and decreases slowly; in contrast, in the liver tissue, it increases invariably and decreases slightly at 72 h post-infection, followed by a continual increase. A similar trend of MyD88 expression, where it first increases and then decreases, has been observed after poly(I:C) stimulation in CIK cells. In conclusion, MyD88 is widely expressed in the grass carp tissues, and its amount changes significantly under the stimulation of viral dsRNA, indicating that MyD88, as a TIR domain-containing adaptor associated with the TLR signaling cascade, can participate in the innate antiviral immune responses in grass carp.

TRIF (TICAM-1) is an adaptor molecule involved in the mammalian TLR3-mediated signaling. TRIF recruits two downstream factors: receptor interacting

protein 1 (RIP1) and TBK1. RIP1 and TBK1 can activate NF-κB in mammals. However, zebrafish TRIF fails to bind to TRAF6, although mammalian TRIF is known to link TLR3 and TRAF6 to trigger the expression of relevant effector genes [30]. In the grass carp, TRIF lacks the TRAF6-binding motif and RHIM motif, as determined through comprehensive sequence analyses, and mRNA expression of IRF7 and type I IFN genes (representative downstream genes) is upregulated in TRIF-overexpressing cells. These results indicate that TRIF positively modulates the expression of IRF7 and type I IFN genes [56]. Therefore, it is likely that the piscine IFN activation pathway is different from the mammalian cognate.

It is known that TIRAP is necessary for the TLR2/TLR4/MyD88-dependent activation of NF-κB. Numerous studies indicate that TIRAP not only acts as a bridge to associate TLRs with MyD88, but also is involved in MyD88-independent signaling, ultimately culminating in the activation of mitogen-activated protein kinase (MAPK) pathways and promotion of NF-κB-mediated proinflammatory cytokine expression (for example, interleukin (IL)-6, IL-1β, and TNF-α). However, whether TIRAP functions as an adaptor or a bridging molecule in fish species still needs further validation.

TRAM, which is indispensable to the TLR4/TRIF-dependent signaling pathway, is absent in the genomes of some species (such as teleosts, amphibians, and birds), but it is present in that of mammals and reptiles.

It has already been established that zebrafish embryos express SARM1 via direct interaction with TRIF and interfere with its functioning, being a negative regulator of TRIF-dependent TLR signaling. It has been found that the expression of SARM1 can block induction of genes at downstream of TRIF but not that of genes at downstream of MyD88. Moreover, grass carp SARM1 has been shown to negatively regulate the type I IFN response and promote cell death post GCRV infection [51].

9.2.2.3 MyD88-Dependent TLR Signaling Pathway

Generally, in the MyD88-dependent pathway, the activated TLRs recruit the MyD88 adaptor molecule, which then impels IRAK1 and IRAK4 phosphorylation. This process can induce a series of activation of TRAF6, NEMO/Ikkα/Ikkβ, and IκB/NF-κB complex, which are translocated to the nucleus, finally resulting in the production of inflammatory cytokines, inducible nitric oxide synthase, and antimicrobial peptides. In teleosts, such as Ya-fish (*Schizothorax prenanti*), spotted sea bass (*Lateolabrax maculatus*), Dabry's sturgeon (*Acipenser dabryanus*), and Japanese sea bass (*Lateolabrax japonicus*), TLR1 subfamily members, including TLR2, TLR15, and TLR25, have been cloned. In addition, the expression of TLR1 subfamily members has been found to increase upon LPS, poly(I:C), and flagellin stimulation, or *Aeromonas hydrophila* and *Vibrio harveyi* infections, via the NF-κB and type I IFN signaling pathways [6, 40]. The *TLR4* gene of *Cyprinidae* displays different expression patterns following bacterial infection. In some teleosts, there are two types of TLR5, the membrane form (TLR5M) and the soluble form

(TLR5S), both of which recognize flagellin as a ligand, and TLR5S is not present in mammals [21].

The TLR7 subfamily, including TLR7–9, belongs to the group of intracellular TLRs, which are located on the organelle membranes and interact with their ligands in the lumen of intracellular vesicles [3, 54]. TLR9 may sense DNA from bacteria and viruses. Furthermore, TLR9 is the specific receptor for CpG oligodeoxynucleotides. The expression of TLR9 in teleost immunoglobulin (Ig)M$^+$ B cells indicates a responsiveness of these cells to CpGs, and association between TLR9 and CpG trigger the secretion of type 1 T helper (Th1)-promoting cytokines and IFNs, which leads to enhanced Th1-biased cellular and humoral immunity [37]. TLR7 and TLR8 sense viral ligands, recognize ssRNA, and respond to dsRNA or poly(I:C). After GCRV infection, TLR7 expression is upregulated in the grass carp spleen, but inhibited in the hepatopancreas. The expression of TLR7 in CIK cells has been found to be inhibited after GCRV infection and increased after poly(I:C) stimulation [54]. GCRV infection can upregulate TLR8 expression in the spleen and head kidney of the grass carp, while poly(I:C) stimulation can downregulate TLR8 transcription levels in the grass carp. Furthermore, GCRV replication is significantly inhibited after TLR8 knockout in CIK cells [3]. In the grass carp, MyD88 is found to be broadly expressed and its expression is upregulated by GCRV stimulation. Furthermore, MyD88 transcripts are rapidly elevated in CIK cells after challenge with poly(I:C) in vitro [34]. Therefore, the expression levels of TLR7 and TLR8 in the grass carp tissues and cells show significant changes under the stimulation of GCRV and poly(I:C), indicating that TLR7 and TLR8 can participate in the grass carp antiviral immunity via the MyD88-dependent TLR signaling pathway. Moreover, previous studies have shown that the pompano TLR7, TLR8, and TLR9 may have distinct roles in response to bacterial or viral pathogens. In mammals, TLR7, TLR8, and TLR9 induce antiviral responses by producing IFNα. Production of IFNα requires an association between MyD88 and IRF7. In addition, activated IRF7 shuttles to the nucleus and activates IFNα and ISGs. Moreover, an inhibitory interaction exists among the three TLRs: TLR8 inhibits both TLR7 and TLR9; whereas, TLR9 inhibits TLR7 but not vice versa [42].

Studies have shown that MyD88 is involved in the TLR10 and TLR11 pathways. TLR11 or TLR10/TLR1 heterodimers may play a role in NF-κB activation; on the contrary, TLR10 alone or TLR10/TLR2 heterodimer cannot activate NF-κB or IFNβ drivers. In the TLR11 subfamily, TLR22 has been determined to be dependent on MyD88 signaling pathways in the grass carp. In poikilotherm vertebrates, TLR22 localizes in the lysosomes, recognizes dsRNA, and induces IFN responses to obtain resistance against viral infection. The grass carp contains two TLR22 isoforms: TLR22a and TLR22b, both of which are induced by GCRV or poly(I:C). TLR22a and TLR22b antagonize antiviral immune responses [12]. TLR22a is involved in the innate immune responses against bacteria and viruses [35]. In goldfish, *TLR22* gene expression can be upregulated by LPS, heat-killed *Aeromonas salmonicida*, and live *Mycobacterium chelonae*. In turbot (*Scophthalmus maximus*), the upregulated *TLR22* gene expression is detected after injection of poly(I:C) or turbot reddish body iridovirus [48].

9.2.2.4   MyD88-Independent TLR Signaling Pathway

TRIF is employed as an adaptor molecule in the TLR3-mediated pathway. Upon binding TLR3, TRIF must undergo oligomerization to interact with a signaling complex (including TBK1 and an atypical inhibitor of κB kinase ε) via tumor necrosis factor receptor-associated factor 3 for further IRF3 phosphorylation. Next, TRAF6 can be recruited by TRIF to activate TGF-β-activated kinase 1 for NF-κB activation. In addition, dsRNA molecules in the cytoplasm are sensed by RIG-I and MDA5 via interactions with the adaptor mitochondrial antiviral signaling protein, which then leads to activation of the downstream molecules. Subsequently, IRF3 and IRF7 are phosphorylated, inducing the transcription of IFNs and NF-κB. Collectively, these data suggest that TRIF serves as a bridge for initiating the TLR3-mediated signaling cascade.

In teleosts, TLR3 and TLR19 recognize viral dsRNA and recruit the adaptor molecule TRIF, which then activates the Ikkε/Ikki/TBK1 complex, further phosphorylating IRF3 and leading to the expression of type I IFNs. It has been identified that teleost-specific TLR19 localizes to the endosome and recognizes dsRNA, recruits TRIF, strengthens the levels of IRF3 and phosphorylated IRF3, and suppresses the phosphorylation of IRF7. TLR19 enhances both IFN and NF-κB pathways; meanwhile, TLR3 localizes to endosome, recognizes dsRNA, and promotes IFN and NF-κB expressions. Furthermore, TLR19 has been found to play a positive role in antiviral immunity [11]. In the Japanese halibut (*Paralichthys olivaceus*), TLR3 is induced by poly(I:C) and viral hemorrhagic septicemia virus (ssRNA virus) challenge. Zebrafish TLR3 is upregulated by snakehead rhabdovirus infection and activates NF-κB. In addition, further studies have indicated that TRIF is also involved in the activation of IFN and NF-κB signaling pathways. Activation of NF-κB is dependent on its interaction with RIP1. Crucian carp TBK1 binds to IRF3, which triggers the IFN promoter. In grass carp, TRIF upregulates IRF7 and type I IFN expression and produces a significant antiviral response. PRV infection can induce the expression of TLR3 and RIG-I in trout erythrocytes; these dsRNA receptors induce type I IFNs through IRFs, which mediate further antiviral effects. Atlantic salmon red blood cells express IRFs, of which, IRF7 expression shows the highest correlation with PRV levels [44]. Therefore, grass carp and Atlantic salmon TLR3 can activate IRF7 under GCRV and PRV infection and upregulate type I IFN expression by TRIF, thereby mediating further antiviral responses.

9.2.2.5   Transcription Factors

TLRs are activated by appropriate ligands, ultimately activating several transcription factors that are critical for regulating immune defense. Several common inducible transcriptional factors, including IRFs, NF-κB, and activator protein 1 (AP-1), result in the production of IFNs, inflammatory cytokines, chemokines, and antimicrobial peptides. NF-κB is the best-known activator of immune mechanisms. These immune

mechanisms predominantly include the expression of proinflammatory cytokine-encoding genes, such as ILs, and the effector genes of piscine innate immunity, such as the acute phase gene serum amyloid A. Moreover, the activation of the TLR4 pathway leads to the activation of several intracellular signaling pathways, e.g., the NF-κB pathway. The attachment sites of NF-κB intimately interact with the binding sites of C/EBP that function in triggering inflammatory responses. NF-κB and C/EBP may eventually lead to a synergistic interaction with the promoters of a range of genes that confer innate immunity. In teleosts, NF-κB has also been shown to play an important role, as a transcription factor for many inflammation-mediated genes, in various inflammatory states.

IRFs belong to a family of mediators, which are involved in various biological processes. To date, 13 members have been identified in the IRF family in vertebrates, including 13 IRFs in teleosts as well as nine IRFs in humans and mice. Of the identified teleost IRFs, IRF11 is found to be a unique member in several teleost species [16]. Recent reports indicate that IRF10 is as a negative regulator of type I IFN production via direct interaction with IFN gene promoters, and zebrafish IRF11 is not found to be regulated by type II IFNs, as observed for zebrafish IRF1 [14]. High IRF10 expression has been observed in all grass carp tissues, with the highest levels in the thymus and gill. The fact that IRF10 expression is detected in GCRV-infected grass carp suggests that piscine IRF10 may play a role in antiviral defense [49].

AP-1 family characterizes an α-helical bZIP domain comprising a leucine zipper motif and a basic DNA binding region. bZIP proteins act as crucial transcriptional regulators that interact with AP-1-binding molecules. The basic leucine zipper transcription factor ATF-like (BATF) family, consisting of BATF1–3, belongs to the AP-1 family. BATF3 in grass carp is abundantly expressed in immune-related tissues, and the expression level changes significantly during GCRV infection. In addition, poly(I:C) challenge in CIK cells has been shown to induce higher levels of BATF3 mRNA than LPS challenge. In summary, BATF3 plays a negative regulatory role in AP-1 and NF-κB pathways [61].

9.2.3 RLR Signaling Pathways

RLRs are conserved in teleosts, and these key cytosolic PRRs detect nucleotide MAMPs of invading viruses and are crucial for dsRNA virus-triggered IFN responses. Three genes encode RLRs: *RIG-I* (alternatively known as *DDX58*), *MDA5* (also termed *IFIN1*), and *LGP2* (also known as *DHX5*). Notably, some orthologous genes of *RIG-I*, *MDA5*, and *LGP2* have been identified in teleosts in the last decade. Additionally, the functions of RIG-I, MDA5, and LGP2 have been investigated in fish species, including zebrafish (*Danio rerio*), rainbow trout (*Oncorhynchus mykiss*), Japanese halibut (*Paralichthys olivaceus*), and grass carp. Current knowledge of RLRs in teleosts will enrich our understanding of the piscine

immune system-specific diversity and molecular evolution against invading microbes in vertebrates [5].

Similar to mammals, piscine RIG-I and MDA5 contain three domains: two caspase activation and recruitment domains (CARDs) in tandem at the N-terminus, a central DExD box helicase (DExD/H-box)/ATPase domain, and a repressor domain at the C-terminal (RD; also called the C-terminal domain) [17]. RIG-I is absent in some teleosts, such as mandarin fish and large yellow croaker. LGP2, without CARD, acts as a positive/negative regulator of RIG-I and MDA5. The positive or negative role in antiviral responses depends on the different hosts, viruses, and infection phase.

The adaptor molecule IPS-1 ortholog exists in teleosts. IPS-1 is the sole adaptor involved in RIG-I- and MDA5-mediated signaling and contains the CARD and TM domains. We have preliminarily demonstrated the viral MAMP-induced RLR-mediated signaling pathways in the grass carp (Fig. 9.2). Once intracellular non-self RNA, such as a part of the viral dsRNA or ssRNA genomic fragment, is sensed by RIG-I and MDA5, they activate inhibitors of κB kinase (Ikk)-α, Ikk-β, Ikk-ε, and TBK1 to phosphorylate various transcription factors, including IRF3, NF-κB, and ATF-2. Consequently, type I IFN promoters and downstream inflammatory cytokines can be directly activated by these phosphorylated transcription factors to prevent viral infection [8].

The signaling cascade induced by RLRs activates NF-κB, MAPK, and IRF pathways. The CARDs of RIG-I and MDA5 physically interact with IPS-1, which contains an N-terminal CARD for interaction with RIG-I or MDA5 and a C-terminal TM domain for mitochondrial localization, suggesting that mitochondria play a critical role in the RLR signaling pathway. The activation of IPS-1 causes dimerization, providing a platform for the recruitment of some additional signaling proteins. However, due to a lack of the N-terminal CARDs, LGP2 cannot interact with the CARD of IPS-1. In *Mus musculus*, knockout of IPS-1 results in the absence of virus-induced NF-κB and IRF3 activation in several cell types, except the plasmacytoid dendritic cells that depend on the TLR7–9 pathways.

9.2.3.1   Expression Profiles of RLRs In Vivo and In Vitro

mRNA expression of RLRs has been extensively investigated in many fish species so far. Both in vivo and in vitro evidences indicate that RIG-I, MDA5, and LGP2 respond to poly(I:C) stimulation and viral infections. For example, RIG-I is significantly upregulated in zebrafish embryos at 24–36 h post fertilization with low-molecular weight poly(I:C) treatment. Activated RIG-I, MDA5, and LGP2 are detected in several tissues when healthy grass carp are challenged in vivo with GCRV [41]. Moreover, highly induced expression of RLRs in teleosts can be observed during pathogenic bacterial infections.

9.2.3.2 Antiviral Functions of RLRs

Each RLR plays a different role in recognizing viral MAMPs in the cytoplasm. RIG-I is an important mediator of antiviral immunity by facilitating IFN production after recognition of viruses. RIG-I distinguishes host RNA from viral RNA according to the chemical nature of the 5′ end of the RNAs. Furthermore, RIG-I recognizes short dsRNAs, and MDA5 recognizes long dsRNAs. The specific amino acids in the RDs of the RLRs distinguish and bind viral nucleic acids. In grass carp, the overexpression of RIG-I in CIK cells has demonstrated that RIG-I plays a key role in the RLR pathway, and the RD exerts an inhibitory function in the RLR signaling during GCRV infection, viral MAMP (poly(I:C)) challenge, and bacterial MAMP (LPS and PGN) stimulation. On the contrary, CARDs have been shown to play a positive role in defense against GCRV and poly(I:C) challenges [2, 52].

MDA5 has also been shown to play a critical role in the teleost antiviral immunity. MDA5 is an IFN-inducible RNA helicase with dsRNA-dependent ATPase activity and melanoma growth-suppressive properties in human melanoma cells. In grass carp, overexpression of MDA5 in CIK cells has been shown to result in the suppression of the downstream genes in transfected cells after poly(I:C), GCRV, or bacterial MAMP stimulation, and the CARD alone can mediate signaling. Furthermore, it is found that the helicase domain or RD alone negatively regulates the CARD functioning via intramolecular interaction with the CARD; however, the RD is identified to act as an enhancer during intermolecular interactions [9, 33].

LGP2 is a regulatory protein structurally similar to RIG-I and MDA5, with the exception of the absence of CARDs. It modulates the binding of RIG-I/MDA5 to viral RNAs and negatively/positively regulates the RLR signaling. Mammalian LGP2 is involved in MDA5 filament formation and MDA5-mediated viral RNA recognition. The overexpression of all the grass carp LGP2 domains has been demonstrated to provide protection against GCRV invasion in CIK cells [4, 28]. In addition, the overexpression of the black carp (*Mylopharyngodon piceus*) LGP2 greatly decreases GCRV titer in infected EPC cells [47].

However, some studies have shown that fish LGP2 can be a negative regulator of antiviral immunity. LGP2 overexpression inhibits the synthesis and phosphorylation of IRF3/7 and reduces the mRNA levels and promoter activities of IFNs and NF-κB in the resting and early phases of GCRV infection. Knockdown of LGP2 has exhibited opposite effects, with LGP2 working at upstream of RIG-I and MDA5. LGP2 binds to RIG-I and MDA5 with diverse domain preferences independent of GCRV infection [41]. Interestingly, LGP2 is also found to block K48-linked ubiquitination of RIG-I and MDA5 to suppress protein degradation. LGP2 acts as a suppressor in RLR pathways to maintain homeostasis in the resting and early phases of GCRV infection [28]. Furthermore, it is considered that LGP2 overexpression has a negative effect during the resting and early phases of viral infection but a positive effect against the viral replication.

9.2.3.3   Signaling Crosstalk Between RLRs and Other Pathways

Another molecule crucial to the activation of RLR pathways has been identified and named as STING (also known as MITA, MPYS, or ERIS). STING plays a key role in the cytosolic DNA signaling pathway that regulates IRF3 phosphorylation by TBK1. Overexpression of the C-terminal region of zebrafish STING has been shown to significantly downregulate the type I IFN expression in EPC cells. In the grass carp, STING may be involved in a broad range of innate immune responses via the TBK1-IRF3/7 signaling cascade, responding to not only a dsRNA analog in an IFN-dependent pathway, but also viral and bacterial MAMPs in an IFN-independent pathway [7]. However, it remains unclear whether fish STING interacts directly with RLRs or IPS-1, and hence, the influence of STING on the RLR signaling cascade needs to be evaluated.

IRF10 exists in several vertebrate lineages, including teleosts, reptiles, birds, and mammals (except mouse and human). It has recently been identified as a negative regulator of antiviral immunity in fish. Overexpression of zebrafish IRF10 has been shown to inhibit the type I IFN response mediated by RIG-I, MDA5, TBK1, and STING, which is likely due to the suppression of STING and IFN-stimulated response element sites in IFNs [15]. Similarly, IRF10 expression in the grass carp can be induced by GCRV infection, suggesting that IRF10 might function in antiviral defense. In addition, piscine RIG-I and MDA5 have also been found to crosstalk with NLR to activate NF-κB and antiviral responses. Zebrafish nucleotide-binding oligomerization domain (NOD)2 interacts with RIG-I, MDA5, and IPS-1, and can increase IPS-1-mediated NF-κB and IFN signaling [62]. Interestingly, the induction of IFN by NOD2 occurs through its interaction with IPS-1, demonstrating a functional overlap between NLR and RLR signaling. Another NLR protein, NLRX1/NOD9, is localized to the mitochondrion and interacts with IPS-1 to inhibit downstream signaling. Therefore, NLRs play biological roles through the mechanism underlying the activation of the NF-κB signaling pathway.

9.2.4   Other Antiviral Signaling Pathways

9.2.4.1   NLRs

NLRs are cytoplasmic PRR family members. The NLR family is typically characterized by the presence of three structural domains: an N-terminal protein–protein binding or effector domain, a central nucleotide oligomerization domain, and a C-terminal LRR domain [24, 50]. NLRs exert biological functions via two mechanisms: activation of the NF-κB and MAPK pathways, and activation of caspase-1, which results in IL-1β secretion and programmed cell death, known as the inflammasome [60].

The NLR family has been identified in fish. In grass carp, 65 NLR genes have been identified, and many members are differentially expressed in multiple tissues

post GCRV infection [50]. NOD1 and NOD2 show different expression patterns in response to LPS, PGN, and poly(I:C) stimuli, suggesting that these two NLR family members may play different roles in the defense against bacterial and viral infections [1]. NLRX1 is widely expressed in all tissues of the grass carp. NLRX1 mRNA expression levels are altered in immune system-related tissues post GCRV infection.

9.2.4.2 Scavenger Receptor, ADAR, Protein Kinase R, Z-DNA Binding Protein Kinase, and RNA Interference

Scavenger receptors (SRs) are cytomembrane receptors derived from their ability to bind and internalize modified low-density lipoproteins. SRs have now been thought as PRRs that sense polyanionic ligands other than the modified low-density lipoproteins [23]. SR-B1 expression is upregulated in the main immune system-specific tissues during the early infection period post GCRV infection. Moreover, SR-B1 can interact with the outer capsid protein of GCRV (VP5 and VP7). These results suggest that SR-B1 can be a receptor for GCRV [22]. In addition, SR-B2a has been found to mediate LPS internalization and proinflammatory responses in grass carp and green spotted pufferfish [18].

ADARs are RNA editing enzymes that target both coding and noncoding dsRNAs. There are two ADARs in grass carp. ADAR1 expression significantly increases after GCRV and poly(I:C) challenge in vivo and in vitro; ADAR2 expression is induced post GCRV challenge in the spleen and head kidney tissues and CIK cells [36, 53].

dsRNA-dependent protein kinase R (PKR) and Z-DNA binding protein kinase (PKZ) play crucial roles in the innate immune responses against viral infection. Grass carp PKR and rare minnow PKZ are significantly upregulated upon GCRV infection [31].

RNA interference (RNAi) acts against a wide range of viruses. In rare minnows, viruses can activate the piscine RNAi pathway, and perhaps, viral inclusion bodies inhibit the antiviral RNAi mechanisms at the same time, which serves as an opportunity to study in detail the antiviral mechanism of the RNAi pathway in fish [32]. In grass carp, studies have shown that chemically synthesized siRNAs can inhibit GCRV replication in CIK cells. Transfection of CIK cells with shRNA plasmids (targeting the GCRV RNA-dependent RNA polymerase gene and outer capsid protein gene), followed by a GCRV challenge, has shown that the cytopathic effect is significantly reduced in the transfected cells compared with that in the positive control cells [20]. Furthermore, shRNA has been designed for targeting different sites on the GCRV S11 gene and cloned into the interference vector pGpU6. shRNA vectors and pcDNA-NS26 have been co-transfected into CIK cells by liposome transfection, and it has been indicated that shRNA can inhibit GCRV replication.

9.3 Adaptive Immunity

Innate immunity is common to all animals, and adaptive immunity is considered a key innovation associated with the origin of vertebrates, reflecting the selective advantages related to pathogen recognition and memory. The activation of adaptive immunity depends on the innate immune system, which is the main defense system against pathogens in almost all organisms. Fish are among the earliest vertebrates to have been evolved with adaptive immunity. They also have humoral and cellular immune responses, including the lymphocytes, Igs, T-cell receptor (TCR), and major histocompatibility complex (MHC), which are associated with a highly specific immune response and memory and allow for clonal selection of T and B cells. The T and B lymphocytes have a variety of adaptive antigen receptors and survive because of long-lived immune memory cells. However, all vertebrates with jaws possess the genetic factors necessary for the proper functioning of the adaptive immune response. The composition and recombination mechanisms of the specific immunity (the causal factors of TCR and Ig diversity) are similar between fish and mammals overall.

In contrast to innate immunity, adaptive immunity is characterized by the recognition and effects of specific antigens. The defense mechanism involved in the adaptive immune response is mainly mediated by lymphocytes. Lymphocytes can be divided into T and B lymphocytes. T lymphocytes mediate cellular immune responses, directly kill infected or abnormal cells, and secrete cytokines that regulate the immune response. B lymphocytes mediate humoral immunity and produce antibodies.

The lymphocyte subsets in fish are similar to those in mammals. With the development of molecular and omics technologies, T cell genes have been cloned in some of the important cultured fish in recent years, including the main genes expressed in T cells in the Atlantic salmon, rainbow trout, and flounder, such as the genes coding for the four TCR subunits. In bony fish, the expression of the TCR gene has been confirmed in T cell lines. For example, T cell-labeled homologous genes *CD8*, *CD4*, *CD28*, *CD3e*, *TCR-z*, *TCR-g*, and *TCR-b* are expressed in the intestines of the rainbow trout. From the expression of these genes and the structural prediction of their proteins, it can be inferred that the composition and function of T cells are similar between fish and mammals [43]. In teleosts, CD154 and CD40 are two crucial co-stimulatory molecules involved in B and T cell cooperation in the thymus-dependent antibody production. Grass carp CD40 and CD154 levels significantly increase in the spleen and head kidney post GCRV challenge, which is similar to the induction of CD40 and CD154 by LPS in the zebrafish spleen. In addition, a study has revealed that the single nucleotide polymorphism markers in *CD40* correlate with the resistance of grass carp to GCRV infection [19].

Many lymphoid factors, such as IL-2, play a crucial role in the adaptive immune response. It is the most important cellular promoter of the initial T cells, regulating the activation, proliferation, and differentiation of lymphocytes. IL-4 and IL-13

are Th2 cytokines with pleiotropic functions. IL-4 interacts with two receptors: IL-4Rα/γ and IL-4Rα/IL-13Rα1. In contrast, IL-13 binds to IL-13Rα2 but also shares the receptor complex containing IL-4Rα/IL-13Rα1. Six IL-4/13 receptors have been identified in grass carp, including γC1, γC2, IL-4Rα1, IL-13Rα1, IL-13Rα2, and a soluble form of IL-4Rα2. Sequence analyses have demonstrated that these receptors share conserved characteristic domains, and possess conserved gene synteny with their human counterparts.

Igs are the central molecules of the adaptive immune system, which are produced by B lymphocytes, and possess highly diverse molecules that can recognize a large number of antigens. In the long course of animal evolution, Igs appear later in the acquired humoral immune system. Invertebrates cannot synthesize antibodies and hence, can only use innate immunity and physical barriers to defend against foreign invading microorganisms. Teleosts have three Ig isotypes: IgM, IgD, and IgZ/T. In particular, two forms of Igs have been identified in grass carp: BCR, a membrane-bound molecule that acts as an antigen receptor on the surface of B cells, and the antibody secreted by plasma cells. Igs can also reflect the close relationship between innate and adaptive immune systems. For example, TLR9 is the specific receptor for CpG oligodeoxynucleotides, and the expression of TLR9 in teleost IgM$^+$ B cells indicates a responsiveness of these cells to CpGs. Interaction between TLR9 and CpG triggers the secretion of Th1-promoting cytokines and IFNs, and enhances Th1-biased cellular and humoral immunity.

The MHC genes are recognized as an essential component of the vertebrate adaptive immune system and are responsible for the presentation of antigens. MHC II-dependent immune memory is considered a hallmark of the adaptive immune response [45]. NLRs play crucial roles in the induction of MHC I and II gene expression. CIITA is the master regulator of MHC II genes. Zebrafish NLRC5 is not only involved in the IFN-independent antiviral response, but also functions as a transcriptional regulator of MHC II genes [46].

IFNs are crucial cytokines that inhibit virus replication and modulate immune responses. Type I and type III IFNs are specialized as innate antiviral cytokines, which are grouped under the "virus-induced IFNs." Type II IFN is more likely to be a regulatory cytokine in the innate and adaptive immune responses [16].

In short, adaptive immunity has a higher degree of specificity and memory than the innate immunity. However, innate and adaptive immunities are complementary and inseparable. The former is often a prerequisite for the latter, as the innate immunity forms the conditions for the recognition of pathogens by adaptive immune responses.

9.4   Conclusions and Future Considerations

In summary, aquareoviruses cause huge losses to the aquaculture industry, especially GCRV and PRV. GCRV results in grass carp hemorrhagic disease with over 85% mortality in grass carp fingerlings, and PRV results in the heart and skeletal

muscle inflammation with 100% infection and an obviously delayed growth in fish. Therefore, to prevent these diseases, piscine immune responses should be intensively investigated. Herein, we mainly focused on the innate and adaptive immunities of the grass carp against GCRV infection. Innate immunity involves the PRRs (HMGBs, TLRs, RLRs, etc.) and their signaling pathways (type I IFN, NF-κB, AP-1, etc.). Adaptive immunity involves the humoral and cellular immunity, including the lymphocytes, Igs, and MHC. Although the grass carp possesses a powerful immune system, GCRV escapes immune surveillance. Therefore, GCRV immune evasion mechanisms should be investigated and clarified in future studies.

References

1. Chen WQ, Xu QQ, Chang MX, Nie P, Peng KM (2010) Molecular characterization and expression analysis of nuclear oligomerization domain proteins NOD1 and NOD2 in grass carp *Ctenopharyngodon idella*. Fish Shellfish Immunol 28:18–29
2. Chen L, Su J, Yang C, Peng L, Wan Q, Wang L (2012) Functional characterizations of RIG-I to GCRV and viral/bacterial PAMPs in grass carp *Ctenopharyngodon idella*. PLoS One 7:e42182
3. Chen X, Wang Q, Yang C, Rao Y, Li Q, Wan Q, Peng L, Wu S, Su J (2013) Identification, expression profiling of a grass carp TLR8 and its inhibition leading to the resistance to reovirus in CIK cells. Dev Comp Immunol 41:82–93
4. Chen X, Yang C, Su J, Rao Y, Gu T (2015) LGP2 plays extensive roles in modulating innate immune responses in *Ctenopharyngodon idella* kidney (CIK) cells. Dev Comp Immunol 49:138–148
5. Chen SN, Zou PF, Nie P (2017) Retinoic acid-inducible gene I (RIG-I)-like receptors (RLRs) in fish: current knowledge and future perspectives. Immunology 151:16–25
6. Fan H, Wang L, Wen H, Wang K, Qi X, Li J, He F, Li Y (2019) Genome-wide identification and characterization of toll-like receptor genes in spotted sea bass (*Lateolabrax maculatus*) and their involvement in the host immune response to *Vibrio harveyi* infection. Fish Shellfish Immunol 92:782–791
7. Feng X, Yang C, Zhang Y, Peng L, Chen X, Rao Y, Gu T, Su J (2014) Identification, characterization and immunological response analysis of stimulator of interferon gene (STING) from grass carp *Ctenopharyngodon idella*. Dev Comp Immunol 45:163–176
8. Feng X, Zhang Y, Yang C, Liao L, Wang Y, Su J (2015) Functional characterizations of IPS-1 in CIK cells: potential roles in regulating IFN-I response dependent on IRF7 but not IRF3. Dev Comp Immunol 53:23–32
9. Gu T, Rao Y, Su J, Yang C, Chen X, Chen L, Yan N (2015) Functions of MDA5 and its domains in response to GCRV or bacterial PAMPs. Fish Shellfish Immunol 46:693–702
10. Hopkins PA, Sriskandan S (2005) Mammalian Toll-like receptors: to immunity and beyond. Clin Exp Immunol 140:395–407
11. Ji J, Rao Y, Wan Q, Liao Z, Su J (2018) Teleost-specific TLR19 localizes to endosome, recognizes dsRNA, recruits TRIF, triggers both IFN and NF-κB pathways, and protects cells from grass carp reovirus infection. J Immunol 200:573–585
12. Ji J, Liao Z, Rao Y, Li W, Yang C, Yuan G, Feng H, Xu Z, Shao J, Su J (2020) Thoroughly remold the localization and signaling pathway of TLR22. Front Immunol 10:3003
13. Kawai T, Sato S, Ishii KJ, Coban C, Hemmi H, Yamamoto M, Terai K, Matsuda M, Inoue J, Uematsu S, Takeuchi O, Akira S (2004) Interferon-α induction through Toll-like receptors involves a direct interaction of IRF7 with MyD88 and TRAF6. Nat Immunol 5:1061–1068

14. Laghari ZA, Li L, Chen SN, Huo HJ, Huang B, Zhou Y, Nie P (2018) Composition and transcription of all interferon regulatory factors (IRFs), IRF111 in a perciform fish, the mandarin fish, *Siniperca chuatsi*. Dev Comp Immunol 81:127–140

15. Li S, Lu LF, Feng H, Wu N, Chen DD, Zhang YB, Gui JF, Nie P, Zhang YA (2014) IFN regulatory factor 10 is a negative regulator of the IFN responses in fish. J Immunol 193:1100–1109

16. Liao Z, Wan Q, Su J (2016) Bioinformatics analysis of organizational and expressional characterizations of the IFNs, IRFs and CRFBs in grass carp *Ctenopharyngodon idella*. Dev Comp Immunol 61:97–106

17. Liao Z, Wan Q, Su H, Wu C, Su J (2017) Pattern recognition receptors in grass carp *Ctenopharyngodon idella*: I. organization and expression analysis of TLRs and RLRs. Dev Comp Immunol 76:93–104

18. Lu X-J, Ning Y-J, Liu H, Nie L, Chen J (2018) A novel lipopolysaccharide recognition mechanism mediated by internalization in teleost macrophages. Front Immunol 9:2758

19. Lu XB, Chen YX, Cui ZW, Zhang XY, Lu LF, Li S, Xia XQ, Nie P, Zhang YA (2018) Characterization of grass carp CD40 and CD154 genes and the association between their polymorphisms and resistance to grass carp reovirus. Fish Shellfish Immunol 81:304–308

20. Ma J, Wang W, Zeng L, Fan Y, Xu J, Zhou Y (2011) Inhibition of the replication of grass carp reovirus in CIK cells with plasmid-transcribed shRNAs. J Virol Methods 175:182–187

21. Munoz-Flores C, Astuya A, Roa FJ, Romero A, Acosta J, Sanchez O, Toledo JR (2018) Activation of membrane-bound and soluble Toll-like Receptors 5 in *Salmo salar* depends on the MyD88 signalling pathway. Biochim Biophys Acta Gen Subj 1862:2215–2225

22. Ou M, Huang R, Luo Q, Xiong L, Chen K, Wang Y (2019) Characterisation of scavenger receptor class B type 1 in rare minnow (*Gobiocypris rarus*). Fish Shellfish Immunol 89:614–622

23. Poynter S, Lisser G, Monjo A, DeWitte-Orr S (2015) Sensors of infection: viral nucleic acid PRRs in fish. Biology 4:460–493

24. Rajendran KV, Zhang J, Liu S, Kucuktas H, Wang X, Liu H, Sha Z, Terhune J, Peatman E, Liu Z (2012) Pathogen recognition receptors in channel catfish: I. Identification, phylogeny and expression of NOD-like receptors. Dev Comp Immunol 37:77–86

25. Rao Y, Su J (2015) Insights into the antiviral immunity against grass carp (*Ctenopharyngodon idella*) reovirus (GCRV) in grass carp. J Immunol Res 2015:670437

26. Rao Y, Su J, Yang C, Peng L, Feng X, Li Q (2013) Characterizations of two grass carp *Ctenopharyngodon idella* HMGB2 genes and potential roles in innate immunity. Dev Comp Immunol 41:164–177

27. Rao Y, Su J, Yang C, Yan N, Chen X, Feng X (2015) Dynamic localization and the associated translocation mechanism of HMGBs in response to GCRV challenge in CIK cells. Cell Mol Immunol 12:342–353

28. Rao Y, Wan Q, Yang C, Su J (2017) Grass carp laboratory of genetics and physiology 2 serves as a negative regulator in retinoic acid-inducible gene I- and melanoma differentiation-associated gene 5-mediated antiviral signaling in resting state and early stage of grass carp reovirus infection. Front Immunol 8:352

29. Rao Y, Wan Q, Su H, Xiao X, Liao Z, Ji J, Yang C, Lin L, Su J (2018) ROS-induced HSP70 promotes cytoplasmic translocation of high-mobility group box 1b and stimulates antiviral autophagy in grass carp kidney cells. J Biol Chem 293:17387–17401

30. Sotolongo J, Espana C, Echeverry A, Siefker D, Altman N, Zaias J, Santaolalla R, Ruiz J, Schesser K, Adkins B, Fukata M (2011) Host innate recognition of an intestinal bacterial pathogen induces TRIF-dependent protective immunity. J Exp Med 208:2705–2716

31. Su J, Zhu Z, Wang Y (2008) Molecular cloning, characterization and expression analysis of the PKZ gene in rare minnow *Gobiocypris rarus*. Fish Shellfish Immunol 25:106–113

32. Su J, Zhu Z, Wang Y, Zou J, Wang N, Jang S (2009) Grass carp reovirus activates RNAi pathway in rare minnow, *Gobiocypris rarus*. Aquaculture 289:1–5

33. Su J, Huang T, Dong J, Heng J, Zhang R, Peng L (2010) Molecular cloning and immune responsive expression of MDA5 gene, a pivotal member of the RLR gene family from grass carp *Ctenopharyngodon idella*. Fish Shellfish Immunol 28:712–718

34. Su J, Dong J, Huang T, Zhang R, Yang C, Heng J (2011) Myeloid differentiation factor 88 gene is involved in antiviral immunity in grass carp *Ctenopharyngodon idella*. J Fish Biol 78:973–979

35. Su J, Heng J, Huang T, Peng L, Yang C, Li Q (2012) Identification, mRNA expression and genomic structure of TLR22 and its association with GCRV susceptibility/resistance in grass carp (*Ctenopharyngodon idella*). Dev Comp Immunol 36:450–462

36. Su J, Han B, Rao Y, Feng X, Su J (2016) Functional characterizations and expression profiles of ADAR2 gene, responsible for RNA editing, in response to GCRV challenge in grass carp (*Ctenopharyngodon idella*). Fish Shellfish Immunol 56:534–542

37. Su H, Liao Z, Yuan G, Su J (2017) A plasmid containing CpG ODN as vaccine adjuvant against grass carp reovirus in grass carp *Ctenopharyngodon idella*. Oncotarget 8:15

38. Tang D, Gao Y, Wang R, Sun Y, Xu T (2012) Characterization, genomic organization, and expression profiles of MyD88, a key adaptor molecule in the TLR signaling pathways in miiuy croaker (*Miichthys miiuy*). Fish Physiol Biochem 38:1667–1677

39. van der Sar AM, Stockhammer OW, van der Laan C, Spaink HP, Bitter W, Meijer AH (2006) MyD88 innate immune function in a zebrafish embryo infection model. Infect Immun 74:2436–2441

40. Voogdt CGP, Merchant ME, Wagenaar JA, van Putten JPM (2018) Evolutionary regression and species-specific codon usage of TLR15. Front Immunol 9:2626

41. Wan Q, Yang C, Rao Y, Liao Z, Su J (2017) MDA5 induces a stronger interferon response than RIG-I to GCRV infection through a mechanism involving the phosphorylation and dimerization of IRF3 and IRF7 in CIK cells. Front Immunol 8:189

42. Wang J, Shao Y, Bennett TA, Shankar RA, Wightman PD, Reddy LG (2006) The functional effects of physical interactions among Toll-like receptors 7, 8, and 9. J Biol Chem 281:37427–37434

43. Ward AE, Rosenthal BM (2014) Evolutionary responses of innate immunity to adaptive immunity. Infect Genet Evol 21:492–496

44. Wessel O, Krasnov A, Timmerhaus G, Rimstad E, Dahle MK (2018) Antiviral responses and biological concequences of piscine orthoreovirus infection in salmonid erythrocytes. Front Immunol 9:3182

45. Wilson AB (2017) MHC and adaptive immunity in teleost fishes. Immunogenetics 69:521–528

46. Wu XM, Hu YW, Xue NN, Ren SS, Chen SN, Nie P, Chang MX (2017) Role of zebrafish NLRC5 in antiviral response and transcriptional regulation of MHC related genes. Dev Comp Immunol 68:58–68

47. Xiao J, Yan J, Chen H, Li J, Tian Y, Feng H (2016) LGP2 of black carp plays an important role in the innate immune response against SVCV and GCRV. Fish Shellfish Immunol 57:127–135

48. Xing J, Zhou X, Tang X, Sheng X, Zhan W (2017) Characterization of Toll-like receptor 22 in turbot (*Scophthalmus maximus*). Fish Shellfish Immunol 66:156–162

49. Xu Q, Jiang Y, Wangkahart E, Zou J, Chang M, Yang D, Secombes CJ, Nie P, Wang T (2016) Sequence and expression analysis of interferon regulatory factor 10 (IRF10) in three diverse teleost fish reveals its role in antiviral defense. PLoS One 11:e0147181

50. Xu T, Liao Z, Su J (2020) Pattern recognition receptors in grass carp *Ctenopharyngodon idella*: II. Organization and expression analysis of NOD-like receptors. Dev Comp Immunol 110:103734

51. Yan N, Su J, Yang C, Rao Y, Feng X, Wan Q, Lei C (2015) Grass carp SARM1 and its two splice variants negatively regulate IFN-I response and promote cell death upon GCRV infection at different subcellular locations. Dev Comp Immunol 48:102–115

52. Yang C, Su J, Huang T, Zhang R, Peng L (2011) Identification of a retinoic acid-inducible gene I from grass carp (*Ctenopharyngodon idella*) and expression analysis in vivo and in vitro. Fish Shellfish Immunol 30:936–943

53. Yang C, Su J, Li Q, Zhang R, Rao Y (2012) Identification and expression profiles of ADAR1 gene, responsible for RNA editing, in responses to dsRNA and GCRV challenge in grass carp (*Ctenopharyngodon idella*). Fish Shellfish Immunol 33:1042–1049

54. Yang C, Su J, Zhang R, Peng L, Li Q (2012) Identification and expression profiles of grass carp *Ctenopharyngodon idella* tlr7 in responses to double-stranded RNA and virus infection. J Fish Biol 80:2605–2622

55. Yang C, Chen L, Su J, Feng X, Rao Y (2013) Two novel homologs of high mobility group box 3 gene in grass carp (*Ctenopharyngodon idella*): potential roles in innate immune responses. Fish Shellfish Immunol 35:1501–1510

56. Yang C, Li Q, Su J, Chen X, Wang Y, Peng L (2013) Identification and functional characterizations of a novel TRIF gene from grass carp (*Ctenopharyngodon idella*). Dev Comp Immunol 41:222–229

57. Yang C, Peng L, Su J (2013) Two HMGB1 genes from grass carp *Ctenopharyngodon idella* mediate immune responses to viral/bacterial PAMPs and GCRV challenge. Dev Comp Immunol 39:133–146

58. Zhang J, Liu S, Rajendran KV, Sun L, Zhang Y, Sun F, Kucuktas H, Liu H, Liu Z (2013) Pathogen recognition receptors in channel catfish: III phylogeny and expression analysis of Toll-like receptors. Dev Comp Immunol 40:185–194

59. Zhang A, He L, Wang Y (2017) Prediction of GCRV virus-host protein interactome based on structural motif-domain interactions. BMC Bioinformatics 18:145

60. Zhu LY, Nie L, Zhu G, Xiang LX, Shao JZ (2013) Advances in research of fish immune-relevant genes: a comparative overview of innate and adaptive immunity in teleosts. Dev Comp Immunol 39:39–62

61. Zhu D, Huang R, Fu P, Chen L, Luo L, Chu P, He L, Li Y, Liao L, Zhu Z, Wang Y (2019) Investigating the role of BATF3 in grass carp (*Ctenopharyngodon idella*) immune modulation: a fundamental functional analysis. Int J Mol Sci 20:1687

62. Zou PF, Chang MX, Li Y, Xue NN, Li JH, Chen SN, Nie P (2016) NOD2 in zebrafish functions in antibacterial and also antiviral responses via NF-kB, and also MDA5, RIG-I and MAVS. Fish Shellfish Immunol 55:173–185